

Mathematical models for the three-dimensional flow problems in the non-Newtonian fluids



By

Muhammad Awais

**Department of Mathematics
Quaid-i-Azam University
Islamabad, Pakistan
2013**

Mathematical models for the three-dimensional flow problems in the non-Newtonian fluids



By

Muhammad Awais

Supervised By

Prof. Dr. Tasawar Hayat

Department of Mathematics

Quaid-i-Azam University

Islamabad, Pakistan

2013

Mathematical models for the three-dimensional flow problems in the non-Newtonian fluids



By

Muhammad Awais

A THESIS SUBMITTED IN THE PARTIAL FULFILLMENT OF THE REQUIREMENTS FOR
THE DEGREE OF

DOCTOR OF PHILOSOPHY

IN

MATHEMATICS

Supervised By

Prof. Dr. Tasawar Hayat

Department of Mathematics

Quaid-i-Azam University

Islamabad, Pakistan

2013

Mathematical models for the three-dimensional flow problems in the non-Newtonian fluids

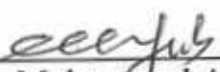
By

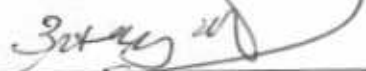
Muhammad Awais

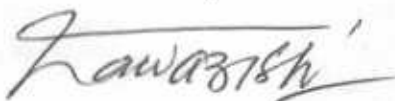
CERTIFICATE

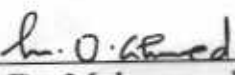
A DISSERTATION SUBMITTED IN THE PARTIAL FULFILLMENT OF THE REQUIREMENTS FOR THE DEGREE OF THE DOCTOR OF PHILOSOPHY

We accept this dissertation as conforming to the required standard

1. 
Prof. Dr. Muhammad Ayub
(Chairman)

2. 
Prof. Dr. Tasawar Hayat
(Supervisor)

3. 
Prof. Dr. Nawazish Ali Shah
(External Examiner)

4. 
Prof. Dr. Muhammad Ozair Ahmad
(External Examiner)

**Department of Mathematics
Quaid-i-Azam University
Islamabad, Pakistan
2013**

Acknowledgements

All the praises and appreciations are for the omnipotent **ALLAH**, the most merciful and generous that knows better the hidden truths of the universe and **HIS Holy Prophet Muhammad (Peace Be Upon Him)** who declared it an obligatory duty of every Muslim to seek and acquire knowledge.

First and foremost I offer my sincerest gratitude to my supervisor **Prof. Dr. Tasawar Hayat**, who has supported me throughout my research work with his patience and knowledge whilst allowing me the room to learn. I am really thankful to him for giving me valuable suggestions and extraordinary experiences throughout the work. I am indebted to him more than he knows. I would like to express my sincere gratitude to the chairman of the department **Prof. Dr Muhammad Ayub** for providing means to study, learn and research.

I am much indebted to **Dr. Muhammad Nawaz** for his valuable and sincere advice and discussions. He gave me precious time along with useful comments on my research work. I have also benefited by useful suggestions from all members of **FMG (Fluid Mechanics Group)** especially **Abdul-Qayyum**. For that I am very much thankful.

A very special thanks to my dear friends **Amjad, Tayyab, Iqtadar, Waqar, Kaleem, Tahir, Shahid, Haroon, Amjad Alvi, Omer, Omair and Adnan** for their support, care and time to listen me whenever I needed them. I can never forget their valuable company during my stay in university. Their words are just like the ointments for me.

It is my pleasure to convey my gratitude to all my **FMG** friends, colleagues, juniors and seniors including **Dr. Nawaz, Dr. Meraj, Dr. Qasim, Dr. Zahid, Dr. Ansa, Dr. Rahila, Humaira, Abdul Qayyum, Shafqat, Farooq, Fahad, Sabir, Bilal, Fakhar, Faheem, Rai Sajjad, Zaheer, Obaid, Irfan Shah, Masood, Salman, Rana Qamar, Awwais** who supported me every time during my research.

Where would I be without my family?

*I owe my heartiest thanks to my loving and affectionate **grandparents** whose prayers have accompanied me through thick and thin. My **parents** deserve special mention for their inseparable support and prayers. I would like to pay my gratitude and thanks to my loving and dear **Khala**, my wife **Sania** for love, care and support in one and the other ways, my daughter **Anaya** and niece **Sumaiya** as they always revitalized and recharged me with their love and innocence, my brother **Asim Sohail**, My sisters **Aqsa** and **Nazia** for their prayers, support and encouragement, my brother in law **Khurram Mehfooz** for his support and encouragement.*

May Allah bless all those who pray for me (Aameen)

Muhammad Awais

Date: Feb. 20, 2013

Dedicated

to

my loving family

and

my supervisor (Prof. Tasawar)

Whose prayers, love and support have helped

me in completing this degree.

Preface

Dynamics of boundary layer flows (BLF) is a topic of major interest both in sciences and engineering. Such interest of the recent researchers is generated because of importance of BLF in polymer processing and electrochemistry. In particular, the flow caused by a continuous stretching surface occurs in glass fiber and paper production, wire drawing, crystal growth, drawing of plastic films, food processing, metal spinning process, cooling of metallic plate in a cooling bath etc. Motivated by such applications, a rapidly increasing number of research papers dealing with the flow over a stretching surface have been published to understand either the sole effects of rotation, heat and mass transfer, chemical reaction, MHD, suction/blowing or their various combinations. Much attention in the reported studies has been given to the two-dimensional stretched flows of viscous fluids. Such flow analysis even in the non-Newtonian fluid mechanics is scarcely investigated. However, there is void in the literature for the three-dimensional boundary layer flows of non-Newtonian fluids over a stretching surface. Main purpose of this thesis is to fill such void through different possible combinations of heat and mass transfer, MHD and suction/injection. For non-Newtonian fluids, the boundary theory is still incomplete. Major obstacle in such completion is diversity of the rheological properties of non-Newtonian fluids. Viscoelastic effects in these fluids give rise to additional nonlinearities which offer formidable mathematical task that cannot be performed even through numerical simulations. Having these challenges in mind, the present thesis is organized as follows:

Chapter one consists of the literature survey regarding the flows of nonlinear fluids. Boundary layer equations for various non-Newtonian fluids are proposed in the three-dimensional flow situations. Advantages of homotopy analysis method (HAM) are also pointed out.

Chapter two addresses the steady three-dimensional flow of an incompressible Maxwell fluid. Boundary layer approach is adopted in the mathematical modeling. Constructed nonlinear differential system is reduced into a system containing ordinary differential equations. Series solutions are developed. Convergence of the derived series solutions is discussed in detail. Error analysis is presented for the validity of the obtained solutions. Graphical results are displayed to analyze the effects of Deborah number on the axisymmetric, two- and three-dimensional cases.

Main findings of this chapter are published in **“International Journal for Numerical Methods in Fluids, 66 (2011) 875-884”**.

Chapter three extends the flow analysis of chapter two for unsteady case. Comparison with the limiting results of the steady case is shown. The results are accepted for publication in **“Meccanica”**.

In chapter four, we have examined the mixed convection boundary layer flow of upper-convected Maxwell (UCM) fluid. The flow is induced due to a bidirectional stretching plate. Mainly the magnetic field, diffusion-thermo (Dufour) and thermal-diffusion (Soret) effects are addressed. The appropriate transformations are utilized to reduce the partial differential system into the coupled system of nonlinear ordinary differential equations. The arising problems are solved by homotopy analysis method. Results are obtained and discussed for velocity, temperature, concentration, local Nusselt and local Sherwood numbers. The main points of this chapter are published in **“ASME: Journal of Heat Transfer, 134 (2012) 044503”**.

Chapter five explores the three-dimensional flow of an Oldroyd-B fluid over a stretching surface. Mathematical modeling is developed for the boundary layer equations in the three-dimensional flow. Resulting boundary layer equations along with the subjected boundary conditions are transformed into coupled system of ordinary differential equations. Computations for the series solutions are made. Effects of Deborah number in the axisymmetric, two- and three-dimensional flows are graphically presented and analyzed. Major observations are published in **“International Journal for Numerical Methods in Fluids, DOI: 10.1002/flid.2716”**.

In chapters' six to nine, the flows of Jeffery fluid are modeled. Here, the following four problems are formulated and solved.

- a) Three-dimensional boundary layer flow over a linear stretching surface.
- b) Three-dimensional channel flow when lower wall exhibits stretching property.
- c) Three-dimensional magnetohydrodynamic shrinking flow in a rotating frame
- d) Axisymmetric flow due to rotating disk.

Convergence intervals in the series solutions are determined. Impact of key parameters entering into flow analysis is discussed in each problem. The results of chapters six, eight and nine are

already published in the journals **“Communications in Nonlinear Science and Numerical Simulations, 17 (2012) 699-707; ASME: Journal of Fluid Engineering, 133 (2011) 061201; International Journal for Numerical Methods in Fluids, DOI: 10.1002/flid.2714”**, respectively whereas the contents of chapter seven are submitted for publication in **“The European Physical Journal Plus”**.

Chapter ten presents the three-dimensional unsteady flow over a stretching surface. Constitutive relationships for the second grade fluid model have been utilized in the problem formulation. Nonlinear partial differential equations are reduced into a system of ordinary differential equations using the similarity transformations. The homotopy analysis method (HAM) has been implemented for the series solutions. Graphs are displayed for the effects of sundry parameters on the velocity field. **The findings of this chapter are published in “Zeitschrift Fur Naturforschung A, 66 (2011) 635-642”**.

The problem of unsteady three-dimensional flow, which results due to stretching of a surface, is studied in chapter eleven. Flow analysis is advanced in view of mass transfer and chemical reaction effects. The corresponding boundary value problems are computed by HAM. Conclusions for velocity and concentration fields are drawn. Comparison of present investigation is found in an excellent agreement with the existing limited studies. The observations of this chapter are published in **“Nonlinear Analysis: Modeling and Control, 17 (2012) 47-59”**.

Influence of Soret and Dufour effects in three-dimensional boundary layer flow of viscoelastic fluid bounded by a stretching surface is examined in chapter twelve. The resulting partial differential system is converted into the ordinary differential systems, which are then computed analytically using homotopic approach known as the homotopy analysis method. The flow quantities of interest are significantly influenced by the sundry parameters in the computations. The conclusions of this chapter are published in **“International Journal of Heat and Mass Transfer, 66 (2012) 2129-2136”**.

Contents

1	Introduction	6
1.1	Literature survey	6
1.2	Mathematical description of basic laws	12
1.2.1	Law of conservation of mass	12
1.2.2	Law of conservation of linear momentum	13
1.2.3	Law of conservation of energy	13
1.2.4	Equation of mass transfer	14
1.3	Three-dimensional boundary layer equations	14
1.3.1	Maxwell fluid model	14
1.3.2	Oldroyd-B fluid model	16
1.3.3	Jeffery fluid model	17
1.3.4	Second grade fluid model	18
1.3.5	Couple stress fluid model	19
1.4	Solution methodology	20
2	Flow of Maxwell fluid induced by bidirectionally stretching surface	22
2.1	Mathematical analysis	22
2.1.1	Three-dimensional flow of viscous fluid	25
2.1.2	Two-dimensional flow of Maxwell fluid	25
2.1.3	Axisymmetric flow of Maxwell fluid	25
2.1.4	Two-dimensional flow of viscous fluid	26
2.2	Homotopy solution	26

2.2.1	<i>Zeroth-order deformation problems</i>	26
2.2.2	<i>mth order deformation problems</i>	28
2.3	Process of convergence	29
2.4	Results and discussion	32
2.5	Final outcomes	35
3	Unsteady flow of Maxwell fluid over a stretching sheet	37
3.1	Mathematical analysis	37
3.2	Series solutions	39
3.2.1	<i>Zeroth-order deformation problems</i>	39
3.2.2	<i>mth order deformation problems</i>	42
3.3	Convergence analysis	43
3.4	Results and discussion	46
3.5	Conclusions	50
4	Mixed convection three-dimensional flow of Maxwell fluid with magnetic field, thermal diffusion and diffusion thermo effects	52
4.1	Mathematical analysis	52
4.2	Series solutions	56
4.2.1	<i>Zeroth-order deformation problems</i>	57
4.2.2	<i>mth order deformation problems</i>	60
4.3	Convergence	61
4.4	Discussion	64
4.5	Conclusions	72
5	Similar solutions for three-dimensional flow of an Oldroyd-B fluid over a stretching surface	74
5.1	Mathematical analysis	74
5.2	Analytic solutions	77
5.2.1	<i>Zeroth-order deformation problems</i>	77
5.2.2	<i>mth order deformation problems</i>	79

5.3	Convergence of the HAM solution	80
5.4	Results and discussion	83
5.5	Final remarks	85
6	Three-dimensional flow of Jeffery fluid over a linearly stretching sheet	87
6.1	Mathematical formulation	87
6.2	Solution methodology	89
6.2.1	<i>Zeroth-order deformation problems</i>	89
6.2.2	<i>mth order deformation problems</i>	91
6.3	Convergence procedure	92
6.4	Results and discussion	94
6.5	Conclusions	99
7	Three-dimensional channel flow of a Jeffery fluid with stretched wall	100
7.1	Mathematical formulation	100
7.2	Series solutions	104
7.2.1	<i>Zeroth-order deformation problems</i>	104
7.2.2	<i>mth order deformation problems</i>	105
7.3	Convergence of the solutions	106
7.4	Results and discussion	108
7.5	Conclusions	115
8	Magnetohydrodynamic three-dimensional rotating flow of Jeffery fluid between two porous walls	116
8.1	Mathematical formulation	116
8.2	Solution by homotopy analysis method	119
8.2.1	<i>mth order deformation problems</i>	121
8.3	Convergence of the homotopy solutions	122
8.4	Results and discussion	124
8.5	Concluding remarks	127

9 MHD axisymmetric flow of Jeffrey fluid over a rotating disk	129
9.1 Mathematical analysis	129
9.2 Solutions of the problems	131
9.3 Convergence of the series solutions	135
9.4 Results and discussion	137
9.5 Final remarks	141
10 Unsteady three-dimensional flow of second grade fluid over a stretching sur- face	143
10.1 Mathematical analysis	143
10.2 Series solutions	145
10.2.1 <i>Zeroth-order deformation problems</i>	145
10.2.2 <i>mth order deformation problems</i>	147
10.3 Convergence of the series solutions	148
10.4 Results and discussion	150
10.5 Conclusions	154
11 Mass transfer effects in an unsteady three-dimensional flow of couple stress fluid	155
11.1 Mathematical analysis	155
11.2 Series solutions	157
11.2.1 <i>Zeroth-order deformation problems</i>	157
11.2.2 <i>mth order deformation problems</i>	160
11.3 Convergence of the HAM solution	161
11.4 Results and discussion	163
11.5 Concluding remarks	167
12 Soret and Dufours effects in three-dimensional flow of viscoelastic fluid	168
12.1 Mathematical analysis	168
12.2 Series solutions	171
12.2.1 <i>Zeroth-order deformation problems</i>	171

12.2.2 <i>m</i> th order deformation problems	175
12.3 Convergence of the developed solution	176
12.4 Results and discussion	180
12.5 Concluding remarks	187

Chapter 1

Introduction

This chapter contains the survey of literature relevant to the two- and three-dimensional flows in steady and unsteady cases. Brief idea of methodology adopted and boundary layer equations are also presented.

1.1 Literature survey

Rheological characteristics of non-Newtonian fluid differ a lot than the Newtonian fluids. No doubt, the rheological properties of all the non-Newtonian fluids cannot be predicted by one constitutive equation between shear rate and rate of strain. For non-Newtonian fluids, there is always a nonlinear relationship between the stress and the rate of strain. The constitutive equations in non-Newtonian fluids are much complicated, more nonlinear and higher order in comparison to the Newtonian fluids. This is because of the elastic features in addition to the viscosity. Despite all the challenges, several researchers are involved in the discussion of such flows. For examples, Rajagopal et al. [1] presented the flow of viscoelastic fluid over a stretching surface. They have considered an incompressible second order fluid and concluded that such flow analyses are important for the applications involving polymer procession. Separation and reattachment of non-Newtonian fluid flows in a sudden expansion pipe has been analyzed by Pak et al. [2]. Rheological properties of the non-Newtonian fluids including shear-rate dependent viscosity and the viscoelasticity have been discussed. Lockett et al. [3] investigated the stability of the inelastic non-Newtonian fluid in Couette flow for concentric cylinders. Authors

have employed the finite element technique and presented the onset of toroidal vortices in the flow. Flow induced by the stretching surface has been studied by Pontrelli [4]. The homogeneous and incompressible second grade fluid has been considered and the problem is solved numerically. Hassanien et al. [5] presented the flow of power law fluid over a nonisothermal stretching surface. The heat transfer equation has been also considered with the momentum equation and outcomes of power law surface temperature and surface mass transfer rate have been presented. The Rayleigh-Stokes problem for an edge in an Oldroyd-B fluid has been investigated by Fetecau [6]. He utilized double Fourier Sine transform to compute the solutions. The well known solution for a Navier-Stokes Maxwell and second grade fluids appear as the limiting cases of his investigation. Fetecau and Fetecau [7, 8] presented the decay of potential vortex in Maxwell and Oldroyd-B fluids. Solutions in both cases are constructed by employing the Hankel transform. Various graphical and numerical results are shown to analyze the phenomena of the potential vortex. The decay of potential vortex in a generalized Oldroyd-B fluid has been studied by Fetecau et al. [9]. The authors have established the exact solutions for the velocity field and the shear stress relating to such motion in an Oldroyd-B fluid with fractional derivatives. The solutions are presented as a sum of the Newtonian solutions and the corresponding non-Newtonian contributions. They employed the Hankel and Laplace transforms for the solutions. The results for generalized Maxwell fluids and classical Maxwell or Oldroyd-B fluids can be obtained as the special cases. Effects of the fractional parameters on the decay of the vortex are also analyzed by means of the graphical illustrations. Some exact solutions for the rotating flows of a generalized Burgers' fluid in cylindrical domains have been found by Jamil and Fetecau [10]. Limiting results for the Burgers', Oldroyd-B, Maxwell, second grade and Newtonian fluids can be deduced as the special cases. Various graphical results are shown in order to reveal some relevant physical aspects of the obtained solutions. Jamil et al. [11] analyzed the unsteady helical flows of Oldroyd-B fluid. The solution by Hankel transform is presented in the form of Bessel functions. Unsteady flow of an Oldroyd-B fluid generated by constantly accelerating plate between two side walls perpendicular to the plate has been investigated by Fetecau et al. [12]. Oldroyd-B fluid model has been studied by the authors in view of the fact that it is adequate model for describing the response of polymeric liquids. The authors have concluded that the side walls have a meaningful influence on the fluid and is more

pronounced for the larger times. Tan et al. [13] presented unsteady flows of a viscoelastic fluid with the fractional Maxwell model. Analysis has been performed in a domain for which the fluid is bounded by two parallel plates. Authors have employed the fractional calculus approach to obtain the solutions. They concluded that the fractional constitutive relationship model is much handier as compared to the conventional model for describing the properties of viscoelastic fluid. Stokes first problem for a second grade fluid in a porous half-space with heat boundary has been computed by Tan and Masuoka [14]. Authors have utilized the modified Darcy's law for viscoelastic fluid and also studied the effects of viscous dissipation. Tan and Masuoka [15] presented the stability analysis of Maxwell fluid in a porous medium heated from below. They have analyzed the critical Rayleigh number, wave number and frequency and concluded that the critical Rayleigh number for over stability increases with an increase in the value of the porous parameter. Wang and Tan [16] developed the stability analysis of the Soret-driven double-diffusive convection of Maxwell fluid in a porous medium. Authors have presented the onset of the double-diffusive convection with the modified Darcy Maxwell model. Soret effects are also incorporated and analyzed by using the linear and nonlinear stability theories. Authors have concluded that the increase in the value of relaxation time enhances the instability of the system. Thermal convective instability of viscoelastic fluids in a rotating porous layer heated from below has been analyzed by Kang et al. [17]. Effects of Coriolis force are included in the analysis so the rotation effects are analyzed. Here they observed that the critical Rayleigh-Darcy number for over stability increases with increase in retardation time and Taylor-Darcy number, while decreases with increase in relaxation. Vajravelu and Rollins [18] presented the flow of non-Newtonian fluid over a stretching surface. An electrically conducting second grade fluid is analyzed when uniform magnetic field is present. Helical flow of a power law fluid in a thin annulus with permeable walls has been studied by Vajravelu et al. [19]. Influence of heat transfer on the peristaltic transport of Jeffery fluid in a vertical porous stratum has been investigated by Vajravelu et al. [20]. It is noted that the size of trapping bolus decreases with an increase in permeability parameter and bolus disappears for the larger values of permeability parameter. Peristaltic transport of Williamson fluid in asymmetric channels with permeable walls has been also studied by Vajravelu et al [21]. The asymmetry of the channel is produced by choosing a peristaltic wave train on the wall with different amplitudes and phases. The size

of the trapped bolus decreases and its symmetry disappears for large values of the permeability parameter. Unsteady flow and heat transfer in a thin film of Ostwald-de-waele liquid over a stretching surface has been analyzed by Vajravelu et al. [22]. Analysis is carried out with viscous dissipation and the temperature dependent thermal conductivity. Similarity transforms are invoked for the conversion of partial differential system into the nonlinear ordinary differential equations and the Keller-Box method is employed to compute the solution. It is revealed that the film thickness increases with an increase in the power-law index parameter as well as the injection parameter. Analytic solution for magnetohydrodynamic flow of a viscoelastic fluid in a channel with stretching walls has been investigated by Raftari and Vajravelu [23]. They incorporated the heat transfer phenomenon and employed the homotopy analysis method to compute the series solution. They made a comparison of results with the limiting numerical results and found is an excellent agreement. Series solutions of unsteady magnetohydrodynamic flows of non-Newtonian fluid caused by an impulsively stretching plate have been investigated by Xu and Liao [24]. These researchers employed the homotopy analysis method to compute the analytic solutions which are valid for the whole spatial domain of the problem. Effects of magnetic field and suction/injection on the convection heat transfer of power law fluid past a stretched sheet have been examined by Chen [25]. Surface heat flux with the power law stretched boundary has been considered. Appropriate transforms are invoked for the conversion of partial differential system into ordinary differential system which is finally solved by the central difference approach. Hayat et al [26] presented the effects of an endoscope and magnetic field on the peristalsis involving the Jeffery fluid. Exact solutions are constructed for the velocity components and pressure gradient are established under long wavelength approximation. Simultaneous effects of heat and mass transfer on the time dependent flow over a stretching surface has been analyzed by Hayat and Awais [27]. Second grade fluid in the presence of thermal diffusion and diffusion thermo effects are considered. Analytic solution for the nonlinear differential system is developed by the homotopy analysis method. Unsteady flow of a third grade fluid over a stretching surface has been presented by Hayat et al. [28]. Authors have also incorporated the Soret and Dufours effects and concluded that such effects could not be ignored for the materials having lower molecular weight. Newtonian heating and the magnetohydrodynamic effects in a flow of a Jeffery fluid over a radially stretching surface

has been analyzed by Hayat et al. [29]. It is shown that Newtonian heating acts like a boosting agent in order to increase the fluids' temperature. Hayat et al. [30] presented the effects of mass transfer on the stagnation point flow of an upper-convected Maxwell (UCM) fluid. Here corrections in the governing equations for the magnetohydrodynamic two-dimensional flow of Maxwell fluid are made. They have also plotted the graphs of the residual errors to validate the results. Important material regarding stability in second grade, third grade and temperature dependent viscosity fluids has been presented elegantly in the refs. [31 – 37].

The boundary layer flows persuaded by a stretching surface have extensive applications in engineering and several technological processes. For-instance production of sheeting material (both metal and polymer sheets), continuous casting, fibers spinning, hot rolling and glass blowing etc. Crane [38] presented pioneering research regarding two-dimensional flow over a stretching sheet. He presented the exact similarity solution for the dimensionless differential system. Afterwards various recent investigators have reconsidered the flow analysis of study [38] and show immense interest to analyze the problem for the three-dimensional flow situation. Such interest is stimulated due to the fact that in many physical situations, flow might not be one- or two-dimensional. For example in paper production, glass formation, fiber sheet and plastic manufacturing, food processing, wire drawing and coating etc. the flows are the three-dimensional and cannot be properly analyzed by considering the one- or two-dimensional flow situations. Wang [39] extended the work of Crane for the three-dimensional case. Devi et al. [40] presented the unsteady three-dimensional flow of viscous fluid caused by a stretching surface. They have also utilized the boundary layer approach in their investigation for simplification. Ariel [41] employed homotopy perturbation method to investigate the three-dimensional flow of an incompressible fluid over stretched surface. He compared the obtained results with those of Wang [39]. He also concluded that exact solutions are not possible in closed form. However, a nicely produced approximate solution requiring less effort with some decent amount of accuracy is always useful for an engineer, scientist or an applied mathematician, who can obtain a solution quickly, thereby gaining a valuable insight into the essentials of the problem. Hayat and Javed [42] found an analytic solution for the generalized three-dimensional flow over a porous stretching sheet. They also looked at the magnetohydrodynamic (MHD) effects. They employed homotopy analysis method to solve the nonlinear problem and compared their results

with those of Ariel [41]. Singh [43] analyzed the three-dimensional flow of viscous fluid with heat and mass transfer. Series solutions of unsteady free convection flow in the stagnation point region of a three-dimensional body have been investigated by Xu et al. [44]. They introduced the new similarity transform and reformulated the original momentum and energy equations. This study also concluded that unsteady flow problems can be handled by homotopy analysis method. Hayat et al. [45] examined the three-dimensional flow over a stretching surface in a viscoelastic fluid. The results for the two-dimensional and axisymmetric cases can be obtained as the limiting cases of the presented solution. Analytical solutions for the nonlinear problems are obtained by employing HAM. Hayat et al. [49] analyzed the mass transfer effects in three-dimensional flow of a viscoelastic fluid. Here the authors have analyzed the effects of generative and destructive chemical reactions on the flow. Unsteady three-dimensional boundary layer flow of micropolar fluid over a stretching surface is investigated by Ahmad et al. [47]. Hayat et al. [48] computed the homotopy solution for the unsteady three-dimensional magnetohydrodynamic flow in a porous space. They also considered the effects of mass transfer and chemical reaction.

Literature survey reveal that the investigations dealing with the three-dimensional flow by moving surfaces are further narrowed down when channel flows (bounded domains) are considered. Such flow analysis was initially considered by Borkakoti and Bharali [49]. Later on Vajravelu and Kumar [50] presented the analytical and numerical solutions of coupled non-linear system in a three-dimensional rotating flow. They employed a fourth-order Runge-Kutta integration scheme for computation of non-linear differential system. It is also found that the Coriolis force and the magnetic field acting against the pressure gradient for the larger values of rotation parameter cause reverse flow. Three-dimensional rotating flow induced by a shrinking sheet with suction has been presented by Hayat et al. [51]. Ahmer and Ali [52] developed homotopy solution for generalized three-dimensional channel flow due to uniform stretching of plate. Cross differentiation has been invoked to eliminate the pressure gradient. It is observed that the constant injection at the upper plate increases the fluid velocity and this increase in velocity has the maximum value near the lower (stretching) plate. Domairry and Aziz [53] found the approximate solution for MHD squeezing flow between two parallel disks with suction or injection using homotopy perturbation method. Flow and heat transfer of MHD viscoelastic fluid in a channel with stretching walls has been presented by Misra et

al. [54]. Hayat et al. [55] investigated the shrinking flow of second grade fluid in a rotating frame. Here the authors have computed the analytic solution by employing homotopy analysis method. Various plots of residual errors are shown in order to validate the obtained results. Mahmood and Ali [56] presented the heat transfer analysis of the three-dimensional flow in a channel of lower stretching wall. Three-dimensional squeezing flow in a rotating channel of lower stretching porous wall has been studied by Munawar et al. [57]. Authors have found the numerical results and compared them with the analytic results by homotopy analysis method. Various graphical results are presented to analyze the rheological aspects of the squeezing flows. Unsteady squeezing flow of a Jeffery fluid between two parallel disks has been analyzed by Qayyum et al. [58]. They have presented the numerical values of skin friction coefficients and a comparison with the already published work is shown. Mustafa et al. [59] investigated the heat and mass transfer phenomena in the unsteady squeezing flow between parallel plates. Physical interpretation to various embedding parameters is made through graphical and tabular results. Three-dimensional rotating flow between two porous walls with slip and heat transfer has been studied by Hayat et al. [60]. Here the authors have analyzed the thermal and concentration slip effects by using the homotopy analysis method [61 – 80].

1.2 Mathematical description of basic laws

1.2.1 Law of conservation of mass

The law of conservation of mass or the continuity equation is given by

$$\frac{\partial \rho}{\partial t} + \nabla \cdot (\rho \mathbf{V}) = 0, \quad (1.1)$$

where ρ shows the density of the fluids and \mathbf{V} as the velocity field. The above equation for incompressible fluid is reduced as

For an incompressible flow Eq. 1.1 can be expressed as

$$\nabla \cdot \mathbf{V} = 0. \quad (1.2)$$

1.2.2 Law of conservation of linear momentum

This is expressed by the following relation

$$\rho \frac{d\mathbf{V}}{dt} = \nabla \cdot \boldsymbol{\tau} + \rho \mathbf{b}, \quad (1.3)$$

in which $\boldsymbol{\tau} = -p\mathbf{I} + \mathbf{S}$ denotes the Cauchy stress tensor, p the pressure, \mathbf{I} the identity tensor, \mathbf{S} the extra stress tensor, \mathbf{b} the body force and d/dt the material time derivative. The Cauchy stress tensor $\boldsymbol{\tau}$ and the velocity field \mathbf{V} for the three-dimensional flow are

$$\boldsymbol{\tau} = \begin{bmatrix} \sigma_{xx} & \tau_{xy} & \tau_{xz} \\ \tau_{yx} & \sigma_{yy} & \tau_{yz} \\ \tau_{zx} & \tau_{zy} & \sigma_{zz} \end{bmatrix}, \quad (1.4)$$

$$\mathbf{V} = [u(x, y, z), v(x, y, z), w(x, y, z)]. \quad (1.5)$$

Scalar forms of Eq. (1.3) are

$$\rho \frac{du}{dt} = \frac{\partial(\sigma_{xx})}{\partial x} + \frac{\partial(\tau_{xy})}{\partial y} + \frac{\partial(\tau_{xz})}{\partial z} + \rho b_x, \quad (1.6)$$

$$\rho \frac{dv}{dt} = \frac{\partial(\tau_{yx})}{\partial x} + \frac{\partial(\sigma_{yy})}{\partial y} + \frac{\partial(\tau_{yz})}{\partial z} + \rho b_y, \quad (1.7)$$

$$\rho \frac{dw}{dt} = \frac{\partial(\tau_{zx})}{\partial x} + \frac{\partial(\tau_{zy})}{\partial y} + \frac{\partial(\sigma_{zz})}{\partial z} + \rho b_z. \quad (1.8)$$

In above equations b_x , b_y and b_z are the components of body force \mathbf{b} parallel to the x -, y - and z - directions respectively.

1.2.3 Law of conservation of energy

According to the energy conservation equation one has

$$\rho \frac{d\epsilon}{dt} = \boldsymbol{\tau} \cdot \mathbf{L} - \text{div } \mathbf{q} + \rho r, \quad (1.9)$$

where $\epsilon = c_p T$ is the internal energy, c_p the specific heat, T the temperature, $\mathbf{L} = \nabla \mathbf{V}$ the velocity gradient, $\mathbf{q} = -k \nabla \tau$ the heat flux vector, k the thermal conductivity and r the radiant

heating. In absence of radiative effects, Eq. (1.9) becomes

$$\rho c_p \frac{dT}{dt} = \tau \cdot \nabla \mathbf{V} + k \nabla^2 T, \quad (1.10)$$

1.2.4 Equation of mass transfer

If a fluid contains species A^* which are slightly soluble in it then there will be relative transport of species. The species A^* may be transported by advection (with the mean velocity of mixture) and by diffusion (relative to the mean motion) in each of the coordinate directions. The concentration C_A may also be affected by chemical reaction. Let \dot{N}_A be the rate at which the mass of species A^* is generated per unit volume due to some reaction and D is the coefficient of diffusing species.

The relevant boundary layer equation for concentration field is

$$u \frac{\partial C_A}{\partial x} + v \frac{\partial C_A}{\partial y} + w \frac{\partial C_A}{\partial z} = D \frac{\partial^2 C_A}{\partial z^2} + \dot{N}_A, \quad (1.11)$$

1.3 Three-dimensional boundary layer equations

1.3.1 Maxwell fluid model

The extra stress tensor \mathbf{S} in an upper-convected Maxwell (UCM) fluid can be expressed as follows:

$$\left(1 + \lambda_1 \frac{D}{Dt}\right) \mathbf{S} = \mu \mathbf{A}_1, \quad (1.12)$$

where μ designates the kinematic viscosity, λ_1 the relaxation time, D/Dt the covariant differentiation and \mathbf{A}_1 the first Rivlin-Erickson tensor for three-dimensional velocity field $\mathbf{V} = [u(x, y, z), v(x, y, z), w(x, y, z)]$ is given by

$$\begin{aligned} \mathbf{A}_1 &= \text{grad } \mathbf{V} + (\text{grad } \mathbf{V})^{\text{transpose}}, \\ &= \begin{bmatrix} 2 \frac{\partial u}{\partial x} & \frac{\partial u}{\partial y} + \frac{\partial v}{\partial x} & \frac{\partial u}{\partial z} + \frac{\partial w}{\partial x} \\ \frac{\partial u}{\partial y} + \frac{\partial v}{\partial x} & 2 \frac{\partial v}{\partial y} & \frac{\partial v}{\partial z} + \frac{\partial w}{\partial y} \\ \frac{\partial u}{\partial z} + \frac{\partial w}{\partial x} & \frac{\partial v}{\partial z} + \frac{\partial w}{\partial y} & 2 \frac{\partial w}{\partial z} \end{bmatrix}. \end{aligned} \quad (1.13)$$

and for a two rank tensor \mathbf{S} , a vector \mathbf{b} and a scalar ϕ we respectively have

$$\frac{D\mathbf{S}}{Dt} = \frac{\partial\mathbf{S}}{\partial t} + (\mathbf{V} \cdot \nabla)\mathbf{S} - (\text{grad } \mathbf{V})\mathbf{S} - \mathbf{S}(\text{grad } \mathbf{V})^{\text{transpose}}, \quad (1.14)$$

$$\frac{D\mathbf{b}}{Dt} = \frac{\partial\mathbf{b}}{\partial t} + (\mathbf{V} \cdot \nabla)\mathbf{b} - (\text{grad } \mathbf{V})\mathbf{b}, \quad (1.15)$$

$$\frac{D\phi}{Dt} = \frac{\partial\phi}{\partial t} + (\mathbf{V} \cdot \nabla)\phi. \quad (1.16)$$

Applying the operator $(1 + \lambda_1 \frac{D}{Dt})$ on Eq. (1.3), we get the following equation in the absence of body forces

$$\rho \left(1 + \lambda_1 \frac{D}{Dt}\right) \frac{d\mathbf{V}}{dt} = - \left(1 + \lambda_1 \frac{D}{Dt}\right) \nabla p + \left(1 + \lambda_1 \frac{D}{Dt}\right) (\nabla \cdot \mathbf{S}), \quad (1.17)$$

Following Harris [84], we use

$$\frac{D}{Dt} (\nabla \cdot) = \nabla \cdot \left(\frac{D}{Dt}\right) \quad (1.18)$$

and Eq. (1.17) and Eq. (1.12) thus yield

$$\rho \left(1 + \lambda_1 \frac{D}{Dt}\right) \frac{d\mathbf{V}}{dt} = - \left(1 + \lambda_1 \frac{D}{Dt}\right) \nabla p + \nabla \cdot \left(1 + \lambda_1 \frac{D}{Dt}\right) \mathbf{S}, \quad (1.19)$$

$$= - \left(1 + \lambda_1 \frac{D}{Dt}\right) \nabla p + \mu (\nabla \cdot \mathbf{A}_1) \quad (1.20)$$

In absence of pressure gradient, Eq. (1.20) takes the form

$$\rho \left(1 + \lambda_1 \frac{D}{Dt}\right) \frac{d\mathbf{V}}{dt} = \mu (\nabla \cdot \mathbf{A}_1) \quad (1.21)$$

Eq. (1.21) in component form is given by

$$\begin{aligned} \frac{\partial u}{\partial t} + u \frac{\partial u}{\partial x} + v \frac{\partial u}{\partial y} + w \frac{\partial u}{\partial z} &= \nu \left(\frac{\partial^2 u}{\partial x^2} + \frac{\partial^2 u}{\partial y^2} + \frac{\partial^2 u}{\partial z^2} \right) \\ &- \lambda_1 \left(\begin{aligned} &\frac{\partial^2 u}{\partial t^2} + 2u \frac{\partial^2 u}{\partial x \partial t} + 2v \frac{\partial^2 u}{\partial y \partial t} + 2w \frac{\partial^2 u}{\partial z \partial t} \\ &+ u^2 \frac{\partial^2 u}{\partial x^2} + v^2 \frac{\partial^2 u}{\partial y^2} + w^2 \frac{\partial^2 u}{\partial z^2} \\ &+ 2uv \frac{\partial^2 u}{\partial x \partial y} + 2vw \frac{\partial^2 u}{\partial y \partial z} + 2uw \frac{\partial^2 u}{\partial x \partial z} \end{aligned} \right), \end{aligned} \quad (1.22)$$

$$\begin{aligned} \frac{\partial v}{\partial t} + u \frac{\partial v}{\partial x} + v \frac{\partial v}{\partial y} + w \frac{\partial v}{\partial z} &= \nu \left(\frac{\partial^2 v}{\partial x^2} + \frac{\partial^2 v}{\partial y^2} + \frac{\partial^2 v}{\partial z^2} \right) \\ &- \lambda_1 \left(\begin{aligned} &\frac{\partial^2 v}{\partial t^2} + 2u \frac{\partial^2 v}{\partial x \partial t} + 2v \frac{\partial^2 v}{\partial y \partial t} + 2w \frac{\partial^2 v}{\partial z \partial t} \\ &+ u^2 \frac{\partial^2 v}{\partial x^2} + v^2 \frac{\partial^2 v}{\partial y^2} + w^2 \frac{\partial^2 v}{\partial z^2} \\ &+ 2uv \frac{\partial^2 v}{\partial x \partial y} + 2vw \frac{\partial^2 v}{\partial y \partial z} + 2uw \frac{\partial^2 v}{\partial x \partial z} \end{aligned} \right). \end{aligned} \quad (1.23)$$

Furthermore u , v , x and y are of order 1 whereas w and z are of order δ . Thus the third component of Eq. (1.21) vanishes since every term in it is of order δ . For steady flow one has

$$\begin{aligned} u \frac{\partial u}{\partial x} + v \frac{\partial u}{\partial y} + w \frac{\partial u}{\partial z} &= \nu \frac{\partial^2 u}{\partial z^2} \\ &- \lambda_1 \left(\begin{aligned} &u^2 \frac{\partial^2 u}{\partial x^2} + v^2 \frac{\partial^2 u}{\partial y^2} + w^2 \frac{\partial^2 u}{\partial z^2} \\ &+ 2uv \frac{\partial^2 u}{\partial x \partial y} + 2vw \frac{\partial^2 u}{\partial y \partial z} + 2uw \frac{\partial^2 u}{\partial x \partial z} \end{aligned} \right), \end{aligned} \quad (1.24)$$

$$\begin{aligned} u \frac{\partial v}{\partial x} + v \frac{\partial v}{\partial y} + w \frac{\partial v}{\partial z} &= \nu \frac{\partial^2 v}{\partial z^2} \\ &- \lambda_1 \left(\begin{aligned} &u^2 \frac{\partial^2 v}{\partial x^2} + v^2 \frac{\partial^2 v}{\partial y^2} + w^2 \frac{\partial^2 v}{\partial z^2} \\ &+ 2uv \frac{\partial^2 v}{\partial x \partial y} + 2vw \frac{\partial^2 v}{\partial y \partial z} + 2uw \frac{\partial^2 v}{\partial x \partial z} \end{aligned} \right), \end{aligned} \quad (1.25)$$

1.3.2 Oldroyd-B fluid model

Here the extra stress tensor is given by

$$\left(1 + \lambda_1 \frac{D}{Dt} \right) \mathbf{S} = \mu \left(1 + \lambda_2 \frac{D}{Dt} \right) \mathbf{A}_1, \quad (1.26)$$

in which λ_2 is the retardation time and conservation law of momentum in the absence of pressure gives

$$\rho \left(1 + \lambda_1 \frac{D}{Dt} \right) \frac{d\mathbf{V}}{Dt} = \mu \left(1 + \lambda_2 \frac{D}{Dt} \right) (\nabla \cdot \mathbf{A}_1). \quad (1.27)$$

Eq. (1.27) in component form under the boundary layer approximation gives

$$\begin{aligned} u \frac{\partial u}{\partial x} + v \frac{\partial u}{\partial y} + w \frac{\partial u}{\partial z} + \lambda_1 \left(\begin{aligned} &u^2 \frac{\partial^2 u}{\partial x^2} + v^2 \frac{\partial^2 u}{\partial y^2} + w^2 \frac{\partial^2 u}{\partial z^2} \\ &+ 2uv \frac{\partial^2 u}{\partial x \partial y} + 2vw \frac{\partial^2 u}{\partial y \partial z} + 2uw \frac{\partial^2 u}{\partial x \partial z} \end{aligned} \right) \\ = \nu \left[\frac{\partial^2 u}{\partial z^2} + \lambda_2 \left(\begin{aligned} &u \frac{\partial^3 u}{\partial x \partial z^2} + v \frac{\partial^3 u}{\partial y \partial z^2} + w \frac{\partial^3 u}{\partial z^3} \\ &- \frac{\partial u}{\partial x} \frac{\partial^2 u}{\partial z^2} - \frac{\partial u}{\partial y} \frac{\partial^2 v}{\partial z^2} - \frac{\partial u}{\partial z} \frac{\partial^2 w}{\partial z^2} \end{aligned} \right) \right], \end{aligned} \quad (1.28)$$

$$\begin{aligned} u \frac{\partial v}{\partial x} + v \frac{\partial v}{\partial y} + w \frac{\partial v}{\partial z} + \lambda_1 \left(\begin{aligned} &u^2 \frac{\partial^2 v}{\partial x^2} + v^2 \frac{\partial^2 v}{\partial y^2} + w^2 \frac{\partial^2 v}{\partial z^2} \\ &+ 2uv \frac{\partial^2 v}{\partial x \partial y} + 2vw \frac{\partial^2 v}{\partial y \partial z} + 2uw \frac{\partial^2 v}{\partial x \partial z} \end{aligned} \right) \\ = \nu \left[\frac{\partial^2 v}{\partial z^2} + \lambda_2 \left(\begin{aligned} &u \frac{\partial^3 v}{\partial x \partial z^2} + v \frac{\partial^3 v}{\partial y \partial z^2} + w \frac{\partial^3 v}{\partial z^3} \\ &- \frac{\partial v}{\partial x} \frac{\partial^2 u}{\partial z^2} - \frac{\partial v}{\partial y} \frac{\partial^2 v}{\partial z^2} - \frac{\partial v}{\partial z} \frac{\partial^2 w}{\partial z^2} \end{aligned} \right) \right]. \end{aligned} \quad (1.29)$$

Note that for $\lambda_2 = 0$, the above equations correspond to that of the Maxwell fluid.

1.3.3 Jeffery fluid model

Expression of extra stress tensor in Jeffery fluid is

$$\mathbf{S} = \frac{\mu}{1 + \lambda_1} \left(\mathbf{A}_1 + \lambda_2 \frac{d\mathbf{A}_1}{dt} \right), \quad (1.30)$$

where, λ_1 is the ratio of relaxation to the retardation times. Moreover

$$\frac{d\mathbf{A}_1}{dt} = \left(u \frac{\partial}{\partial x} + v \frac{\partial}{\partial y} + w \frac{\partial}{\partial z} \right) \mathbf{A}_1, \quad (1.31)$$

$$= \left(u \frac{\partial}{\partial x} + v \frac{\partial}{\partial y} + w \frac{\partial}{\partial z} \right) \begin{bmatrix} 2 \frac{\partial u}{\partial x} & \frac{\partial u}{\partial y} + \frac{\partial v}{\partial x} & \frac{\partial u}{\partial z} + \frac{\partial w}{\partial x} \\ \frac{\partial u}{\partial y} + \frac{\partial v}{\partial x} & 2 \frac{\partial v}{\partial y} & \frac{\partial v}{\partial z} + \frac{\partial w}{\partial y} \\ \frac{\partial u}{\partial z} + \frac{\partial w}{\partial x} & \frac{\partial v}{\partial z} + \frac{\partial w}{\partial y} & 2 \frac{\partial w}{\partial z} \end{bmatrix}. \quad (1.32)$$

Further the extra stresses computed from Eqs. (1.30) and (1.32) are given by

$$S_{xx} = \frac{\mu}{1 + \lambda_1} \left[2 \frac{\partial u}{\partial x} + \lambda_2 \left(u \frac{\partial}{\partial x} + v \frac{\partial}{\partial y} + w \frac{\partial}{\partial z} \right) \left(2 \frac{\partial u}{\partial x} \right) \right], \quad (1.33)$$

$$S_{xy} = S_{yx} = \frac{\mu}{1 + \lambda_1} \left[\left(\frac{\partial u}{\partial y} + \frac{\partial v}{\partial x} \right) + \lambda_2 \left(u \frac{\partial}{\partial x} + v \frac{\partial}{\partial y} + w \frac{\partial}{\partial z} \right) \left(\frac{\partial u}{\partial y} + \frac{\partial v}{\partial x} \right) \right], \quad (1.34)$$

$$S_{xz} = S_{zx} = \frac{\mu}{1 + \lambda_1} \left[\left(\frac{\partial u}{\partial z} + \frac{\partial w}{\partial x} \right) + \lambda_2 \left(u \frac{\partial}{\partial x} + v \frac{\partial}{\partial y} + w \frac{\partial}{\partial z} \right) \left(\frac{\partial u}{\partial z} + \frac{\partial w}{\partial x} \right) \right], \quad (1.35)$$

$$S_{yy} = \frac{\mu}{1 + \lambda_1} \left[2 \frac{\partial v}{\partial y} + \lambda_2 \left(u \frac{\partial}{\partial x} + v \frac{\partial}{\partial y} + w \frac{\partial}{\partial z} \right) \left(2 \frac{\partial v}{\partial y} \right) \right], \quad (1.36)$$

$$S_{yz} = S_{zy} = \frac{\mu}{1 + \lambda_1} \left[\left(\frac{\partial v}{\partial z} + \frac{\partial w}{\partial y} \right) + \lambda_2 \left(u \frac{\partial}{\partial x} + v \frac{\partial}{\partial y} + w \frac{\partial}{\partial z} \right) \left(\frac{\partial v}{\partial z} + \frac{\partial w}{\partial y} \right) \right], \quad (1.37)$$

$$S_{zz} = \frac{\mu}{1 + \lambda_1} \left[2 \frac{\partial w}{\partial z} + \lambda_2 \left(u \frac{\partial}{\partial x} + v \frac{\partial}{\partial y} + w \frac{\partial}{\partial z} \right) \left(2 \frac{\partial w}{\partial z} \right) \right]. \quad (1.38)$$

The law of conservation of momentum (in component form) for the steady flow case when body forces and pressure are absent yields

$$\rho \left(u \frac{\partial u}{\partial x} + v \frac{\partial u}{\partial y} + w \frac{\partial u}{\partial z} \right) = \frac{\partial}{\partial x} S_{xx} + \frac{\partial}{\partial y} S_{xy} + \frac{\partial}{\partial z} S_{xz}, \quad (1.39)$$

$$\rho \left(u \frac{\partial v}{\partial x} + v \frac{\partial v}{\partial y} + w \frac{\partial v}{\partial z} \right) = \frac{\partial}{\partial x} S_{yx} + \frac{\partial}{\partial y} S_{yy} + \frac{\partial}{\partial z} S_{yz}, \quad (1.40)$$

$$\rho \left(u \frac{\partial w}{\partial x} + v \frac{\partial w}{\partial y} + w \frac{\partial w}{\partial z} \right) = \frac{\partial}{\partial x} S_{zx} + \frac{\partial}{\partial y} S_{zy} + \frac{\partial}{\partial z} S_{zz}. \quad (1.41)$$

Substituting the values of extra stresses $S_{xx}, S_{xy}, S_{xz}, S_{yy}, S_{yz}$ and S_{zz} into Eqs. (1.39) – (1.41) and utilizing the order analysis one gets

$$u \frac{\partial u}{\partial x} + v \frac{\partial u}{\partial y} + w \frac{\partial u}{\partial z} = \frac{\nu}{1 + \lambda_1} \left[\frac{\partial^2 u}{\partial z^2} + \lambda_2 \left(\frac{\partial u}{\partial x} \frac{\partial^2 u}{\partial x \partial z} + \frac{\partial v}{\partial z} \frac{\partial^2 u}{\partial y \partial z} + \frac{\partial w}{\partial z} \frac{\partial^2 u}{\partial z^2} \right) \right], \quad (1.42)$$

$$u \frac{\partial v}{\partial x} + v \frac{\partial v}{\partial y} + w \frac{\partial v}{\partial z} = \frac{\nu}{1 + \lambda_1} \left[\frac{\partial^2 v}{\partial z^2} + \lambda_2 \left(\frac{\partial u}{\partial z} \frac{\partial^2 v}{\partial x \partial z} + \frac{\partial v}{\partial z} \frac{\partial^2 v}{\partial y \partial z} + \frac{\partial w}{\partial z} \frac{\partial^2 v}{\partial z^2} \right) \right], \quad (1.43)$$

1.3.4 Second grade fluid model

The extra stress tensor \mathbf{S} for a second grade fluid model is

$$\mathbf{S} = \mu \mathbf{A}_1 + \alpha_1 \mathbf{A}_2 + \alpha_2 \mathbf{A}_1^2, \quad (1.44)$$

in which the first Rivlin-Erickson tensor \mathbf{A}_1 is defined in Eq. (1.13) and the second Rivlin-Erickson tensor \mathbf{A}_2 can be computed through

$$\mathbf{A}_n = \frac{d\mathbf{A}_{n-1}}{dt} + \mathbf{A}_{n-1}\mathbf{L} + \mathbf{L}^{transpose}\mathbf{A}_{n-1}. \quad (1.45)$$

For thermodynamic second grade fluid, we have

$$\mu \geq 0, \alpha_1 \geq 0, \alpha_1 + \alpha_2 = 0. \quad (1.46)$$

The extra stresses can be computed easily from Eq. (1.44) and substituting into Eq. (1.39) – (1.41), one gets the three-dimensional boundary layer equations for the thermodynamic second grade fluid which are given by

$$\rho \left(\frac{\partial u}{\partial t} + u \frac{\partial u}{\partial x} + v \frac{\partial u}{\partial y} + w \frac{\partial u}{\partial z} \right) = \mu \frac{\partial^2 u}{\partial z^2} + \alpha_1 \left(\begin{array}{l} u \frac{\partial^3 u}{\partial x \partial z^2} + v \frac{\partial^3 u}{\partial y \partial z^2} + w \frac{\partial^3 u}{\partial z^3} \\ - \frac{\partial u}{\partial z} \frac{\partial^2 w}{\partial x^2} + \frac{\partial u}{\partial x} \frac{\partial^2 u}{\partial z^2} + \frac{\partial^2 v}{\partial z \partial x} \frac{\partial v}{\partial z} \\ + \frac{\partial v}{\partial x} \frac{\partial^2 v}{\partial z^2} - \frac{\partial u}{\partial z} \frac{\partial^2 v}{\partial y \partial z} + \frac{\partial^3 u}{\partial t \partial z^2} \end{array} \right), \quad (1.47)$$

$$\rho \left(\frac{\partial v}{\partial t} + u \frac{\partial v}{\partial x} + v \frac{\partial v}{\partial y} + w \frac{\partial v}{\partial z} \right) = \mu \frac{\partial^2 v}{\partial z^2} + \alpha_1 \left(\begin{array}{l} u \frac{\partial^3 v}{\partial x \partial z^2} + v \frac{\partial^3 v}{\partial y \partial z^2} + w \frac{\partial^3 v}{\partial z^3} \\ - \frac{\partial v}{\partial z} \frac{\partial^2 w}{\partial x^2} + \frac{\partial u}{\partial y} \frac{\partial^2 u}{\partial z^2} + \frac{\partial^2 v}{\partial z^2} \frac{\partial v}{\partial y} \\ + \frac{\partial u}{\partial z} \frac{\partial^2 u}{\partial y \partial z} - \frac{\partial v}{\partial z} \frac{\partial^2 u}{\partial x \partial z} + \frac{\partial^3 v}{\partial t \partial z^2} \end{array} \right). \quad (1.48)$$

1.3.5 Couple stress fluid model

For the couple stress fluid, the momentum equation (1.3) becomes

$$\rho \frac{d\mathbf{V}}{dt} = \nabla p + \mu \nabla^2 \mathbf{V} - \mu' \nabla^4 \mathbf{V}, \quad (1.49)$$

in which μ' represent the material constant characterizing the couple stresses. By employing the operator ∇ on the velocity field, the quantities $\nabla^2 \mathbf{V}$ and $\nabla^4 \mathbf{V}$ can be easily found which

are

$$\nabla^2 \mathbf{V} = \begin{bmatrix} \frac{\partial^2 u}{\partial x^2} + \frac{\partial^2 u}{\partial y^2} + \frac{\partial^2 u}{\partial z^2} \\ \frac{\partial^2 v}{\partial x^2} + \frac{\partial^2 v}{\partial y^2} + \frac{\partial^2 v}{\partial z^2} \\ \frac{\partial^2 w}{\partial x^2} + \frac{\partial^2 w}{\partial y^2} + \frac{\partial^2 w}{\partial z^2} \end{bmatrix}, \quad (1.50)$$

$$\nabla^4 \mathbf{V} = \begin{bmatrix} \frac{\partial^4 u}{\partial x^4} + \frac{\partial^4 u}{\partial y^4} + \frac{\partial^4 u}{\partial z^4} \\ \frac{\partial^4 v}{\partial x^4} + \frac{\partial^4 v}{\partial y^4} + \frac{\partial^4 v}{\partial z^4} \\ \frac{\partial^4 w}{\partial x^4} + \frac{\partial^4 w}{\partial y^4} + \frac{\partial^4 w}{\partial z^4} \end{bmatrix}. \quad (1.51)$$

From Eqs. (1.51) – (1.49), we write

$$\begin{aligned} \frac{\partial u}{\partial t} + u \frac{\partial u}{\partial x} + v \frac{\partial u}{\partial y} + w \frac{\partial u}{\partial z} &= \nu \left(\frac{\partial^2 u}{\partial x^2} + \frac{\partial^2 u}{\partial y^2} + \frac{\partial^2 u}{\partial z^2} \right) \\ &\quad - \nu' \left(\frac{\partial^4 u}{\partial x^4} + \frac{\partial^4 u}{\partial y^4} + \frac{\partial^4 u}{\partial z^4} \right), \end{aligned} \quad (1.52)$$

$$\begin{aligned} \frac{\partial v}{\partial t} + u \frac{\partial v}{\partial x} + v \frac{\partial v}{\partial y} + w \frac{\partial v}{\partial z} &= \nu \left(\frac{\partial^2 v}{\partial x^2} + \frac{\partial^2 v}{\partial y^2} + \frac{\partial^2 v}{\partial z^2} \right) \\ &\quad - \nu' \left(\frac{\partial^4 v}{\partial x^4} + \frac{\partial^4 v}{\partial y^4} + \frac{\partial^4 v}{\partial z^4} \right), \end{aligned} \quad (1.53)$$

in which $\nu' = \mu'/\rho$ is the couple stress viscosity. After employing the order analysis for the three-dimensional case we get

$$\frac{\partial u}{\partial t} + u \frac{\partial u}{\partial x} + v \frac{\partial u}{\partial y} + w \frac{\partial u}{\partial z} = \nu \left(\frac{\partial^2 u}{\partial z^2} \right) - \nu' \left(\frac{\partial^4 u}{\partial z^4} \right), \quad (1.54)$$

$$\frac{\partial v}{\partial t} + u \frac{\partial v}{\partial x} + v \frac{\partial v}{\partial y} + w \frac{\partial v}{\partial z} = \nu \left(\frac{\partial^2 v}{\partial z^2} \right) - \nu' \left(\frac{\partial^4 v}{\partial z^4} \right), \quad (1.55)$$

1.4 Solution methodology

It is well established argument that physical mechanism in general is always subjected to non-linearity, i.e. the governing equations are nonlinear even in the viscous fluids. Traditional perturbation method is quite attractive for the solution of such equations. But this technique requires small/large parameter in the mathematical system. Besides this, there are other methods which are known now as homotopy analysis, homotopy perturbation, Adomian decomposition etc. Among these the homotopy analysis method (HAM) is preferred due to the

reasons mentioned below.

- HAM does not require any small/large parameter in the problem.
- The convergence region can be easily controlled.
- The rate of approximations series is adjustable.
- It provides freedom to choose different sets of base functions.

Having the above mentioned advantages in mind, we will use HAM for the solutions of nonlinear mathematical models in this thesis.

Chapter 2

Flow of Maxwell fluid induced by bidirectionally stretching surface

This chapter explores the steady flow of an incompressible Maxwell fluid. The three-dimensional flow is induced due to the bidirectional stretching of a sheet. Conservation laws of mass and linear momentum are used in the problem development. The corresponding non-linear differential system is solved by the homotopy analysis method (HAM). The graphs of residual errors are plotted and the obtained results are compared with the published limiting work just to validate the results. The graphs of Deborah number are prepared to analyze the axisymmetric, two- and three-dimensional cases.

2.1 Mathematical analysis

Consider the three-dimensional flow of upper-convected Maxwell (UCM) fluid. The three-dimensional flow in the fluid is induced by the stretching wall at $z = 0$. An incompressible

UCM fluid fills the region $z > 0$ (see Fig. 2.1).

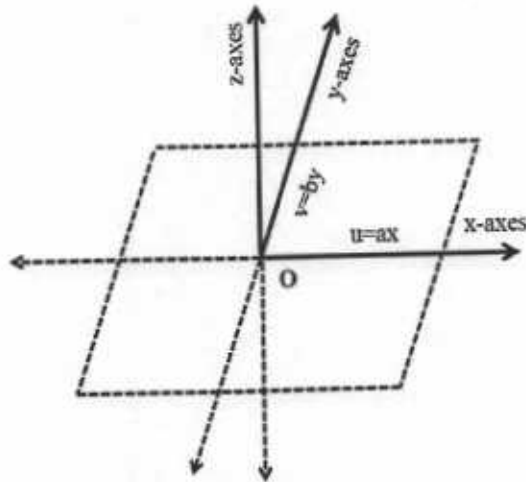


Fig. 2.1: Geometry of the problem.

The laws of conservation of mass and momentum for the present flow problem yields

$$\frac{\partial u}{\partial x} + \frac{\partial v}{\partial y} + \frac{\partial w}{\partial z} = 0, \quad (2.1)$$

$$u \frac{\partial u}{\partial x} + v \frac{\partial u}{\partial y} + w \frac{\partial u}{\partial z} = \nu \frac{\partial^2 u}{\partial z^2} - \lambda_1 \left(\begin{array}{c} u^2 \frac{\partial^2 u}{\partial x^2} + v^2 \frac{\partial^2 u}{\partial y^2} + w^2 \frac{\partial^2 u}{\partial z^2} \\ + 2uv \frac{\partial^2 u}{\partial x \partial y} + 2vw \frac{\partial^2 u}{\partial y \partial z} + 2uw \frac{\partial^2 u}{\partial x \partial z} \end{array} \right), \quad (2.2)$$

$$u \frac{\partial v}{\partial x} + v \frac{\partial v}{\partial y} + w \frac{\partial v}{\partial z} = \nu \frac{\partial^2 v}{\partial z^2} - \lambda_1 \left(\begin{array}{c} u^2 \frac{\partial^2 v}{\partial x^2} + v^2 \frac{\partial^2 v}{\partial y^2} + w^2 \frac{\partial^2 v}{\partial z^2} \\ + 2uv \frac{\partial^2 v}{\partial x \partial y} + 2vw \frac{\partial^2 v}{\partial y \partial z} + 2uw \frac{\partial^2 v}{\partial x \partial z} \end{array} \right), \quad (2.3)$$

where u , v and w are the respective velocity components along the x -, y - and z -directions, ν denote the kinematic viscosity and λ_1 the relaxation time.

The corresponding boundary conditions are

$$\begin{aligned} u &= u_w(x) = ax, \quad v = v_w(y) = by, \quad w = 0 \quad \text{at } z = 0, \\ u &\rightarrow 0, \quad v \rightarrow 0 \quad \text{as } z \rightarrow \infty, \end{aligned} \quad (2.4)$$

in which the constants $a > 0$ and $b > 0$.

Making use of the following dimensionless variables

$$\eta = \sqrt{\frac{a}{\nu}} z, \quad u = axf'(\eta), \quad v = ayg'(\eta), \quad w = -\sqrt{a\nu} \{f(\eta) + g(\eta)\} \quad (2.5)$$

in Eqs. (2.1) – (2.4) one can get

$$f''' - f'^2 + (f + g)f'' + \beta_1 [2(f + g)f'f'' - (f + g)^2 f'''] = 0, \quad (2.6)$$

$$g''' - g'^2 + (f + g)g'' + \beta_1 [2(f + g)g'g'' - (f + g)^2 g'''] = 0, \quad (2.7)$$

$$\begin{aligned} f(\eta) + g(\eta) &= 0, \quad f'(\eta) = 1, \quad g'(\eta) = c \quad \text{at } \eta = 0, \\ f'(\eta) &= 0, \quad g'(\eta) = 0 \quad \text{as } \eta \rightarrow \infty, \end{aligned} \quad (2.8)$$

where prime denotes the differentiation with respect to η . Moreover, the Deborah number β_1 and the ratio of stretching rates c are

$$\beta_1 = \lambda_1 a, \quad c = b/a. \quad (2.9)$$

It is interesting to point out that various limiting results can be deduced from the present investigation which are mentioned as follows:

2.1.1 Three-dimensional flow of viscous fluid

Problem consisting of Eqs. (2.6) and (2.7) along with the boundary conditions (2.8) can be reduced into the viscous fluid when $\beta_1 = 0$. For such case we have

$$f''' - f'^2 + (f + g)f'' = 0, \quad (2.10)$$

$$g''' - g'^2 + (f + g)g'' = 0, \quad (2.11)$$

$$\begin{aligned} f(0) + g(0) = 0, \quad f'(0) = 1, \quad g'(0) = c \quad \text{at } \eta = 0, \\ f'(\infty) = 0, \quad g'(\infty) = 0 \quad \text{as } \eta \rightarrow \infty, \end{aligned} \quad (2.12)$$

2.1.2 Two-dimensional flow of Maxwell fluid

The two-dimensional case, i.e. ($g = 0$) for the flow of an upper-convected Maxwell (UCM) fluid can be obtained by setting $c = 0$ in the Eqs. (2.6) and (2.7) i.e.

$$f''' - f'^2 + ff'' + \beta_1 [2ff'f'' - f^2f'''] = 0. \quad (2.13)$$

The associated boundary conditions take the following form

$$\begin{aligned} f(0) = 0, \quad f'(0) = 1 \quad \text{at } \eta = 0, \\ f'(\infty) = 0 \quad \text{as } \eta \rightarrow \infty. \end{aligned} \quad (2.14)$$

2.1.3 Axisymmetric flow of Maxwell fluid

The axisymmetric flow situation, i.e. ($f = g$) can be obtained by setting $c = 1.0$ in the Eqs. (2.6) and (2.7). Here we have

$$f''' - f'^2 + 2ff'' + 4\beta_1 [ff'f'' - f^2f'''] = 0 \quad (2.15)$$

with boundary conditions (2.14).

2.1.4 Two-dimensional flow of viscous fluid

The two-dimensional case, i.e. ($g = 0$) for the flow of viscous fluid can be deduced by setting $c = 0 = \beta_1$ in the Eqs. (2.6) and (2.7). Hence we obtain

$$f''' - f'^2 + f f'' = 0, \quad (2.16)$$

with the boundary conditions (2.14).

2.2 Homotopy solution

2.2.1 Zeroth-order deformation problems

In order to proceed for the homotopic solutions of the nonlinear equations (2.6) and (2.7) with the boundary conditions (2.8), the velocity distributions $f(\eta)$ and $g(\eta)$ are expressed by the set of base functions

$$\left\{ \eta^k \exp(-n\eta) \mid k \geq 0, n \geq 0 \right\} \quad (2.17)$$

in the following manner

$$f(\eta) = a_{0,0}^0 + \sum_{n=1}^{\infty} \sum_{k=1}^{\infty} a_{m,n}^k \eta^k \exp(-n\eta), \quad (2.18)$$

$$g(\eta) = A_{0,0}^0 + \sum_{n=1}^{\infty} \sum_{k=1}^{\infty} A_{m,n}^k \eta^k \exp(-n\eta), \quad (2.19)$$

where $a_{m,n}^k$ and $A_{m,n}^k$ are coefficients. The initial guesses $f_0(\eta)$, $g_0(\eta)$ and the linear operator \mathcal{L} for the problem under consideration are chosen as follows:

$$f_0(\eta) = 1 - \exp(-\eta), \quad (2.20)$$

$$g_0(\eta) = c(1 - \exp(-\eta)), \quad (2.21)$$

$$\mathcal{L}(f) = f''' - f', \quad (2.22)$$

with

$$\mathcal{L}[C_1 + C_2 \exp(\eta) + C_3 \exp(-\eta)] = 0, \quad (2.23)$$

where $C_1 - C_3$ are the constants.

The zeroth order problems are

$$(1-p)\mathcal{L}[\bar{f}(\eta, p) - f_0(\eta)] = p\hbar_f \mathcal{N}_f[\bar{f}(\eta, p), \bar{g}(\eta, p)], \quad (2.24)$$

$$(1-p)\mathcal{L}[\bar{g}(\eta, p) - g_0(\eta)] = p\hbar_g \mathcal{N}_g[\bar{f}(\eta, p), \bar{g}(\eta, p)], \quad (2.25)$$

$$\begin{aligned} \bar{f}(0, p) + \bar{g}(0, p) &= 0, \quad \bar{f}'(0, p) = 1, \quad \bar{g}'(0, p) = c, \\ \bar{f}'(\infty, p) &= 0, \quad \bar{g}'(\infty, p) = 0. \end{aligned} \quad (2.26)$$

In Eqs. (2.24) and (2.25), the nonlinear operators \mathcal{N}_f and \mathcal{N}_g are defined by the following expressions

$$\begin{aligned} \mathcal{N}_f[\bar{f}(\eta, p), \bar{g}(\eta, p)] &= \frac{\partial^3 \bar{f}}{\partial \eta^3} - \left(\frac{\partial \bar{f}}{\partial \eta} \right)^2 + \{\bar{f}(\eta, p) + \bar{g}(\eta, p)\} \frac{\partial^2 \bar{f}}{\partial \eta^2} \\ &\quad + \beta_1 \left[\begin{aligned} &2\{\bar{f}(\eta, p) + \bar{g}(\eta, p)\} \bar{f}'(\eta, p) \bar{f}''(\eta, p) \\ &-\{\bar{f}(\eta, p) + \bar{g}(\eta, p)\}^2 \bar{f}'''(\eta, p) \end{aligned} \right], \end{aligned} \quad (2.27)$$

$$\begin{aligned} \mathcal{N}_g[\bar{f}(\eta, p), \bar{g}(\eta, p)] &= \frac{\partial^3 \bar{g}}{\partial \eta^3} - \left(\frac{\partial \bar{g}}{\partial \eta} \right)^2 + \{\bar{f}(\eta, p) + \bar{g}(\eta, p)\} \frac{\partial^2 \bar{g}}{\partial \eta^2} \\ &\quad + \beta_1 \left[\begin{aligned} &2\{\bar{f}(\eta, p) + \bar{g}(\eta, p)\} \bar{g}'(\eta, p) \bar{g}''(\eta, p) \\ &-\{\bar{f}(\eta, p) + \bar{g}(\eta, p)\}^2 \bar{g}'''(\eta, p) \end{aligned} \right]. \end{aligned} \quad (2.28)$$

Here \hbar_f and \hbar_g are the auxiliary non-zero parameters and $p \in [0, 1]$ is an embedding parameter.

When $p = 0$ and $p = 1$ then

$$\bar{f}(\eta, 0) = f_0(\eta), \quad \bar{f}(\eta, 1) = f(\eta), \quad (2.29)$$

$$\bar{g}(\eta, 0) = g_0(\eta), \quad \bar{g}(\eta, 1) = g(\eta). \quad (2.30)$$

When p varies from 0 to 1 then the initial guesses $f_0(\eta)$ and $g_0(\eta)$ approach to the final solutions $f(\eta)$ and $g(\eta)$ respectively and through Taylor's series expansion one has

$$\bar{f}(\eta, p) = f_0(\eta) + \sum_{m=1}^{\infty} f_m(\eta) p^m, \quad (2.31)$$

$$\bar{g}(\eta, p) = g_0(\eta) + \sum_{m=1}^{\infty} g_m(\eta) p^m, \quad (2.32)$$

$$f_m(\eta) = \frac{1}{m!} \left. \frac{\partial^m \bar{f}(\eta, p)}{\partial p^m} \right|_{p=0}, \quad (2.33)$$

$$g_m(\eta) = \frac{1}{m!} \left. \frac{\partial^m \bar{g}(\eta, p)}{\partial p^m} \right|_{p=0}. \quad (2.34)$$

It should be noted that the convergence of series (2.31) and (2.32) strongly depends upon the auxiliary parameters \hbar_f and \hbar_g . The values of \hbar_f and \hbar_g are selected in such a way that the series (2.31) and (2.32) converge when $p = 1$. Hence Eqs. (2.31) and (2.32) become

$$f(\eta) = f_0(\eta) + \sum_{m=1}^{\infty} f_m(\eta), \quad (2.35)$$

$$g(\eta) = g_0(\eta) + \sum_{m=1}^{\infty} g_m(\eta). \quad (2.36)$$

2.2.2 m th order deformation problems

The problems at this order satisfy the following definitions

$$\mathcal{L}[f_m(\eta, p) - \chi_m f_{m-1}(\eta)] = \hbar_f \mathcal{R}_{f,m}(\eta), \quad (2.37)$$

$$\mathcal{L}[g_m(\eta, p) - \chi_m g_{m-1}(\eta)] = \hbar_g \mathcal{R}_{g,m}(\eta), \quad (2.38)$$

$$f_m(0) + g_m(0) = f'_m(0) = f'_m(\infty) = g'_m(0) = g'_m(\infty) = 0, \quad (2.39)$$

$$\chi_m = \begin{cases} 0, & m \leq 1 \\ 1, & m > 1 \end{cases}, \quad (2.40)$$

$$\begin{aligned} \mathcal{R}_{f,m}(\eta) = & f'''_{m-1} + \sum_{k=0}^{m-1} \{(f_{m-1-k} + g_{m-1-k})f''_k - f'_{m-1-k}f'_k\} \\ & + \beta_1 \sum_{k=0}^{m-1} \sum_{l=0}^k \left\{ \begin{array}{l} 2(f_{m-1-k} + g_{m-1-k})f'_{k-l}f''_l \\ -(f_{m-1-k}f_{k-l} + g_{m-1-k}g_{k-l} + 2f_{m-1-k}g_{k-l})f'''_l \end{array} \right\} \end{aligned} \quad (2.41)$$

$$\begin{aligned} \mathcal{R}_{g,m}(\eta) = & g'''_{m-1} + \sum_{k=0}^{m-1} \{(f_{m-1-k} + g_{m-1-k})g''_k - g'_{m-1-k}g'_k\} \\ & + \beta_1 \sum_{k=0}^{m-1} \sum_{l=0}^k \left\{ \begin{array}{l} 2(f_{m-1-k} + g_{m-1-k})g'_{k-l}g''_l \\ -(f_{m-1-k}f_{k-l} + g_{m-1-k}g_{k-l} + 2f_{m-1-k}g_{k-l})g'''_l \end{array} \right\} \end{aligned} \quad (2.42)$$

Employing symbolic software MATHEMATICA, the corresponding system can be solved one after the other in the order $m = 1, 2, 3, \dots$

2.3 Process of convergence

To find the adequate values of h_f and h_g so that the Eqs. (2.31) and (2.32) converge, we have prepared the curves shown in Fig. 2.2. It is seen that the suitable ranges here are $-1.6 \leq h_f \leq -0.5$ and $-1.5 \leq h_g \leq -0.3$. In the Figs. 2.3 and 2.4 the graphs are presented for an error analysis. It is anticipated that by choosing the values of h_f and h_g from their appropriate ranges, the convergent results can be obtained for 6th decimal place. Plots 2.5 and 2.6 show the residual error of f and g for different values of h_f and h_g . We have examined that $h_f = h_g = -0.85$ gives much useful results.

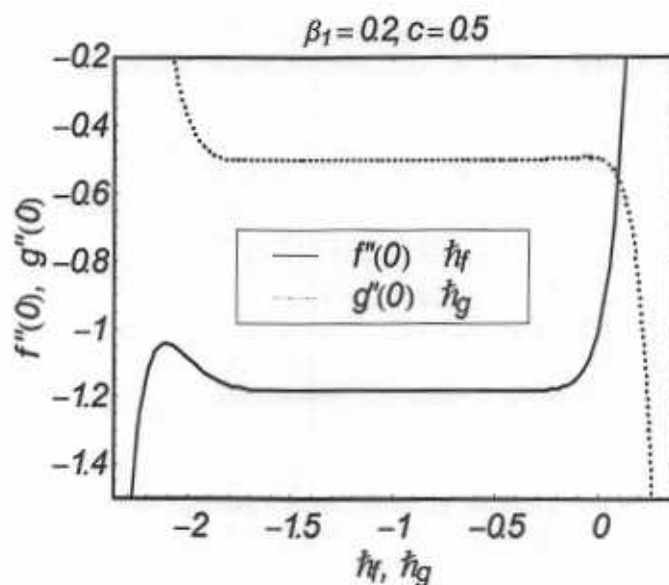


Fig. 2.2 : h curves of $f''(0)$ and $g''(0)$ at the 15th order of approximation.

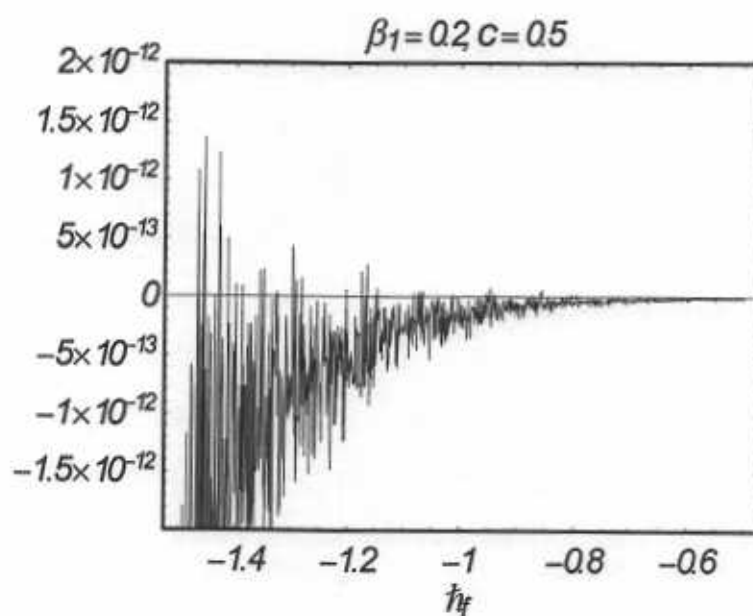


Fig. 2.3 : h curve for residual error in $f(\eta)$ at the 15th order of approximation.

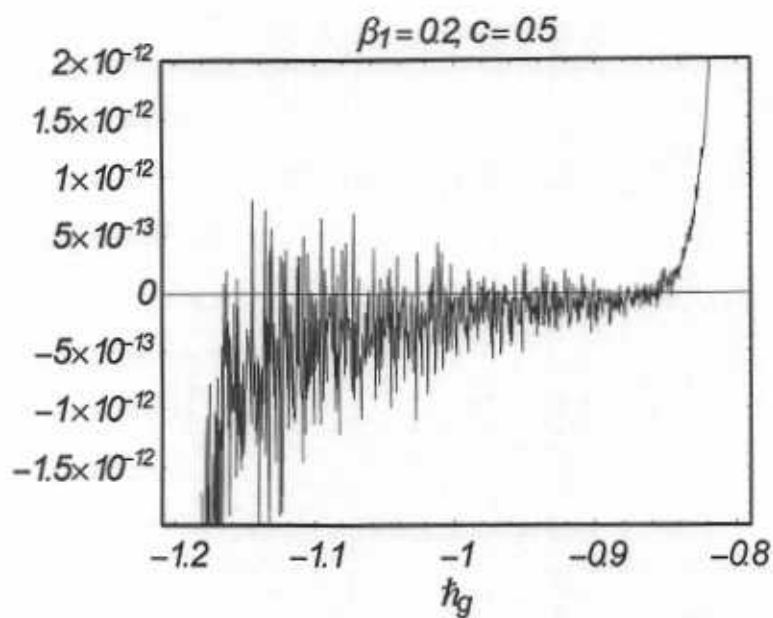


Fig. 2.4 : h curve for residual error in $g(\eta)$ at the 15th order of approximation.

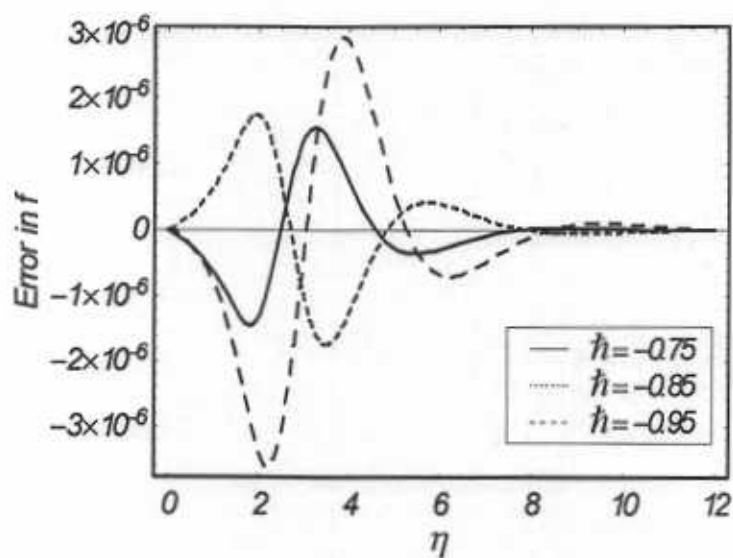


Fig. 2.5 : Comparison of residual errors in $f(\eta)$ for different values of h .

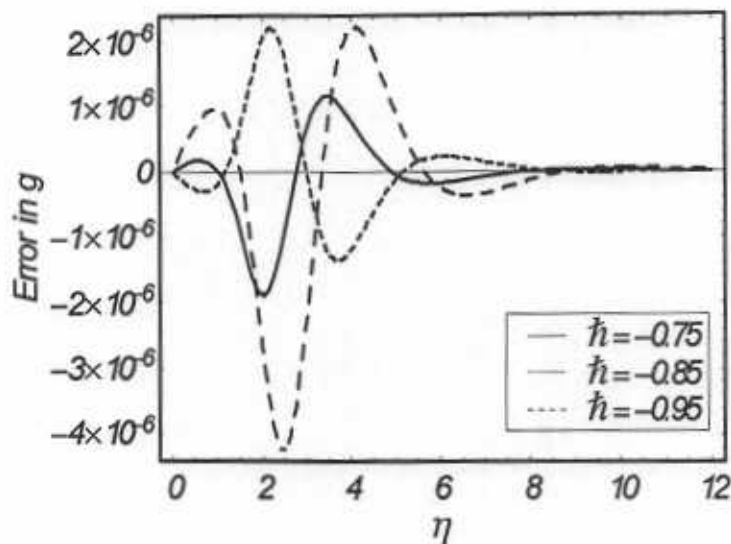


Fig. 2.6 : Comparison of residual errors in $g(\eta)$ for different values of \hbar .

2.4 Results and discussion

The aim of this section is to analyze the influence of Deborah number β_1 on f' and g' in two-dimensional, three-dimensional and axisymmetric flows. A comparative study between the present HAM solutions and the previously obtained exact and perturbation solutions for the viscous fluid case is made. The variation of Deborah number β_1 on f' for two-dimensional flow situations is portrayed in Fig. 2.7. It is observed that Deborah number β_1 retards the flow and causes a reduction in the boundary layer thickness. Figs. 2.8 and 2.9 show the effects of Deborah number β_1 on f' and g' for three-dimensional flow. It is observed that with an increase in β_1 both velocity components f' and g' decrease. It is also observed that in three-dimensional flow situation the velocity decreases rapidly when compared with the two-dimensional flow situation. Effects of β_1 on f' for an axisymmetric flow case is presented in Fig. 2.10. It is noted that the results obtained for axisymmetric flow case are quite similar to those obtained for the two- and three-dimensional flows.

Table 2.1 is made just to decide that how much order of approximations are necessary for a convergent solution. It is noted that 20th order approximations are sufficient for the convergent problem. Table 2.2 is made in order to compare the present results obtained by HAM with

the HPM and exact solutions given by Ariel [41]. It is found that present solution in a limiting sense has a good agreement with an exact solution

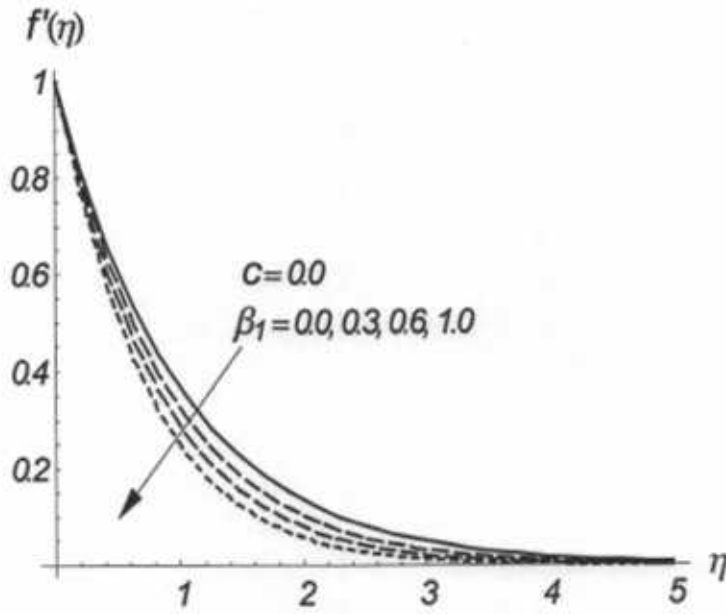


Fig. 2.7 : Influence of β_1 on f' for 2D flow.

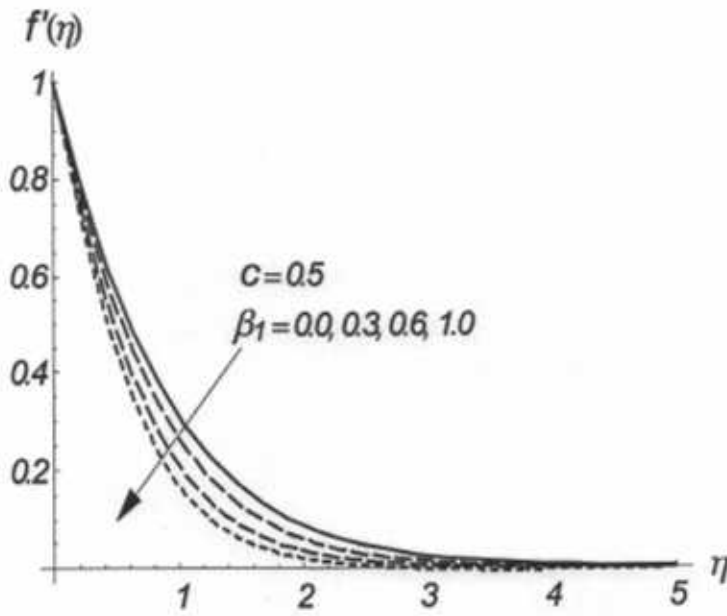


Fig. 2.8 : Influence of β_1 on f' for 3D flow.

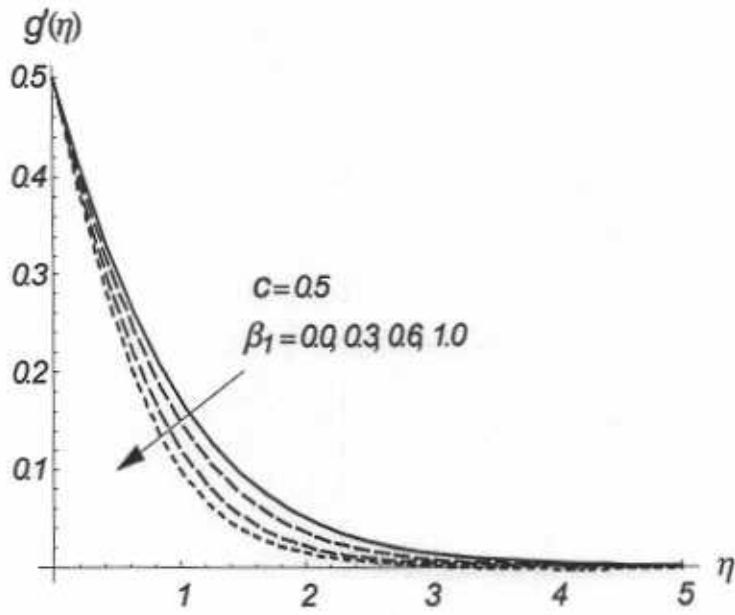


Fig. 2.9 : Influence of β_1 on g' for 3D flow.

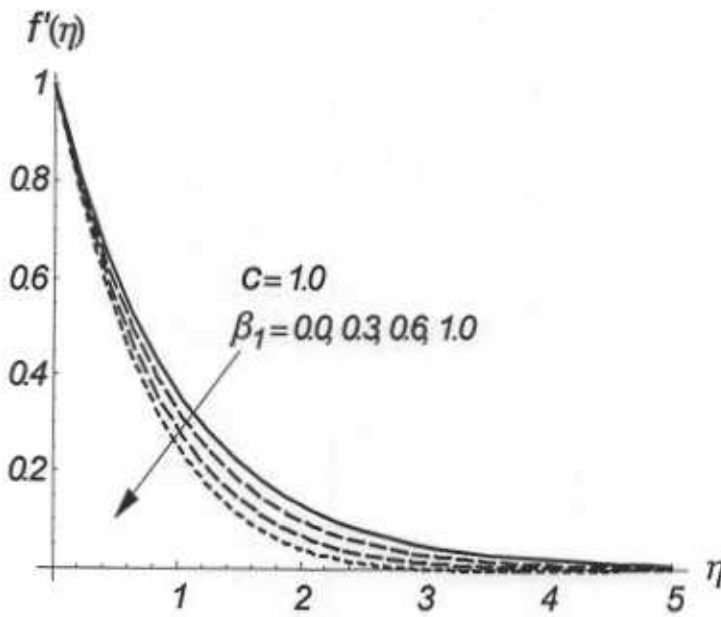


Fig. 2.10 : Influence of β_1 on f' for axisymmetric flow.

Table 2.1: Convergence of the HAM solutions for different order of approximations when $\beta_1 = 0.2$ and $c = 0.5$

order of approximation	$-f''(0)$	$-g''(0)$
1	1.153750	0.490625
2	1.182876	0.499378
5	1.181869	0.502042
10	1.182117	0.501999
15	1.182123	0.501996
20	1.182124	0.501996
25	1.182124	0.501996
30	1.182124	0.501996
40	1.182124	0.501996
50	1.182124	0.501996

Table 2.2: Illustrating the variation of $-f''(0)$ and $-g''(0)$ with c when $\beta_1 = 0$, using HAM, HPM (Ariel [41]) and exact solution (Ariel [41]).

c	$-f''(0)$			$-g''(0)$		
	HAM	HPM [41]	Exact [41]	HAM	HPM [41]	Exact [41]
0.0	1	1	1	0	0	0
0.2	1.039495	1.034587	1.039495	0.148736	0.158231	0.148736
0.4	1.075788	1.070529	1.075788	0.349208	0.360599	0.349208
0.6	1.109946	1.106797	1.109946	0.590528	0.600833	0.590528
0.8	1.142488	1.142879	1.142488	0.866682	0.874551	0.866682
1.0	1.173720	1.178511	1.173720	1.173720	1.178511	1.173720

2.5 Final outcomes

The generalized three-dimensional flow of an incompressible upper-convected Maxwell (UCM) fluid over a linearly stretching surface is examined. The main observations are listed below.

- Deborah number β_1 retards the flow.
- Results obtained for axisymmetric, two- and three-dimensional flows are qualitatively similar.

- Effects of β_1 on f' are qualitatively similar to those of g' .
- Plots of residual errors confirm the validity of the derived series solutions.
- For $g = 0 = c$, the results for two-dimensional flow of Maxwell fluid are recovered.

Chapter 3

Unsteady flow of Maxwell fluid over a stretching sheet

This chapter addresses the three-dimensional flow of Maxwell fluid bounded by a stretching sheet. The mathematical modelling has been carried out and the computations are performed by using the homotopy analysis method (HAM). The convergence of the derived series solution is shown explicitly and the error analysis has been presented. Comparison with the previously published data in steady case is shown. Various graphical results are shown in order to analyze the features of the involved key parameters.

3.1 Mathematical analysis

Let us consider the time-dependent three-dimensional boundary layer flow of a subclass of rate type fluid. Constitutive expression of UCM fluid are utilized. The fluid is bounded by the non-conducting surface situated at $z = 0$. The fluid occupies the region $z > 0$. The equations for the considered flow are

$$\frac{\partial u}{\partial x} + \frac{\partial v}{\partial y} + \frac{\partial w}{\partial z} = 0, \quad (3.1)$$

$$\frac{\partial u}{\partial t} + u \frac{\partial u}{\partial x} + v \frac{\partial u}{\partial y} + w \frac{\partial u}{\partial z} = \nu \frac{\partial^2 u}{\partial z^2} - \lambda_1 \left(\begin{array}{c} \frac{\partial^2 u}{\partial t^2} + 2u \frac{\partial^2 u}{\partial x \partial t} + 2v \frac{\partial^2 u}{\partial y \partial t} + 2w \frac{\partial^2 u}{\partial z \partial t} \\ + u^2 \frac{\partial^2 u}{\partial x^2} + v^2 \frac{\partial^2 u}{\partial y^2} + w^2 \frac{\partial^2 u}{\partial z^2} \\ + 2uv \frac{\partial^2 u}{\partial x \partial y} + 2vw \frac{\partial^2 u}{\partial y \partial z} + 2uw \frac{\partial^2 u}{\partial x \partial z} \end{array} \right), \quad (3.2)$$

$$\frac{\partial v}{\partial t} + u \frac{\partial v}{\partial x} + v \frac{\partial v}{\partial y} + w \frac{\partial v}{\partial z} = \nu \frac{\partial^2 v}{\partial z^2} - \lambda_1 \left(\begin{array}{c} \frac{\partial^2 v}{\partial t^2} + 2u \frac{\partial^2 v}{\partial x \partial t} + 2v \frac{\partial^2 v}{\partial y \partial t} + 2w \frac{\partial^2 v}{\partial z \partial t} \\ + u^2 \frac{\partial^2 v}{\partial x^2} + v^2 \frac{\partial^2 v}{\partial y^2} + w^2 \frac{\partial^2 v}{\partial z^2} \\ + 2uv \frac{\partial^2 v}{\partial x \partial y} + 2vw \frac{\partial^2 v}{\partial y \partial z} + 2uw \frac{\partial^2 v}{\partial x \partial z} \end{array} \right), \quad (3.3)$$

and the subjected boundary conditions are

$$\begin{aligned} u &= u_w(x) = \frac{ax}{1-\alpha t}, \quad v = v_w(y) = \frac{by}{1-\alpha t}, \quad w = 0 \quad \text{at } z = 0, \\ u &\rightarrow 0, \quad v \rightarrow 0, \quad \text{as } z \rightarrow \infty, \end{aligned} \quad (3.4)$$

where u , v and w denote the velocity components in x -, y - and z -directions respectively, ν the kinematic viscosity, λ_1 the relaxation time. Moreover $\alpha t < 1$ and the constants $a > 0$ and $b > 0$.

The following variables [82 and 83]

$$\eta = \sqrt{\frac{a}{\nu(1-\alpha t)}} z, \quad u = \frac{ax}{1-\alpha t} f'(\eta), \quad v = \frac{ay}{1-\alpha t} g'(\eta), \quad w = -\sqrt{\frac{a\nu}{1-\alpha t}} \{f(\eta) + g(\eta)\}. \quad (3.5)$$

satisfy the continuity equation (3.1) identically while Eqs. (3.2) – (3.4) take the following form

$$f''' - \zeta \left(f' + \frac{\eta}{2} f'' \right) - f'^2 + (f + g) f'' + \beta_1 \left(\begin{array}{l} 2(f + g) f' f'' - (f + g)^2 f''' - \zeta^2 \left(2f' + \frac{7\eta}{4} f'' + \frac{\eta^2}{4} f''' \right) \\ - \zeta \{ 2f'^2 + \eta f' f'' - (f + g) (3f''' + \eta f'''') \} \end{array} \right) = 0, \quad (3.6)$$

$$g''' - \zeta \left(g' + \frac{\eta}{2} g'' \right) - g'^2 + (f + g) g'' + \beta_1 \left(\begin{array}{l} 2(f + g) g' g'' - (f + g)^2 g''' - \zeta^2 \left(2g' + \frac{7\eta}{4} g'' + \frac{\eta^2}{4} g''' \right) \\ - \zeta \{ 2g'^2 + \eta g' g'' - (f + g) (3g''' + \eta g'''') \} \end{array} \right) = 0, \quad (3.7)$$

$$\begin{aligned} f(\eta) + g(\eta) &= 0, \quad f'(\eta) = 1, \quad g'(\eta) = c \quad \text{at } \eta = 0, \\ f'(\eta) &\rightarrow 0, \quad g'(\eta) \rightarrow 0, \quad \text{as } \eta \rightarrow \infty, \end{aligned} \quad (3.8)$$

where prime denotes differentiation with respect to η . The Deborah number β_1 , the ratio parameter c and the time-dependent parameter ζ are defined as

$$\beta_1 = \frac{\lambda_1 a}{1 - \alpha t}, \quad c = b/a, \quad \zeta = \alpha/a, \quad (3.9)$$

where $\zeta = 0$ yields the steady three-dimensional boundary layer flow of Maxwell fluid.

3.2 Series solutions

3.2.1 Zeroth-order deformation problems

The velocity distributions $f(\eta)$ and $g(\eta)$ can be presented by the set of base functions

$$\left\{ \eta^k \exp(-n\eta) \mid k \geq 0, n \geq 0 \right\} \quad (3.10)$$

in the definitions

$$f(\eta) = a_{0,0}^0 + \sum_{n=1}^{\infty} \sum_{k=1}^{\infty} a_{m,n}^k \eta^k \exp(-n\eta), \quad (3.11)$$

$$g(\eta) = b_{0,0}^0 + \sum_{n=1}^{\infty} \sum_{k=1}^{\infty} b_{m,n}^k \eta^k \exp(-n\eta), \quad (3.12)$$

in which $a_{m,n}^k$ and $b_{m,n}^k$ are the coefficients. The convenient initial guesses and linear operator are selected as follows

$$f_0(\eta) = 1 - \exp(-\eta), \quad (3.13)$$

$$g_0(\eta) = c(1 - \exp(-\eta)), \quad (3.14)$$

$$\mathcal{L}(f) = f''' - f', \quad (3.15)$$

with

$$\mathcal{L}[C_1 + C_2 \exp(\eta) + C_3 \exp(-\eta)] = 0, \quad (3.16)$$

and $C_1 - C_3$ are the constants.

The zeroth order problems are defined by

$$(1-p)\mathcal{L}[\bar{f}(\eta, p) - f_0(\eta)] = p\hbar_f \mathcal{N}_f[\bar{f}(\eta, p), \bar{g}(\eta, p)], \quad (3.17)$$

$$(1-p)\mathcal{L}[\bar{g}(\eta, p) - g_0(\eta)] = p\hbar_g \mathcal{N}_g[\bar{f}(\eta, p), \bar{g}(\eta, p)], \quad (3.18)$$

$$\begin{aligned} \bar{f}(0, p) + \bar{g}(0, p) &= 0, \quad \bar{f}'(0, p) = 1, \quad \bar{g}'(0, p) = c, \\ \bar{f}'(\infty, p) &= 0, \quad \bar{g}'(\infty, p) = 0 \end{aligned} \quad (3.19)$$

where the nonlinear operators \mathcal{N}_f and \mathcal{N}_g in Eqs. (28) and (29) are

$$\begin{aligned} \mathcal{N}_f[\bar{f}(\eta, p), \bar{g}(\eta, p)] &= \bar{f}'''(\eta, p) - \zeta \left(\bar{f}'(\eta, p) + \frac{\eta}{2} \bar{f}''(\eta, p) \right) + \{ \bar{f}(\eta, p) + \bar{g}(\eta, p) \} \bar{f}''(\eta, p) \\ &\quad - \bar{f}^{\prime 2}(\eta, p) - \beta_1 \zeta^2 \left\{ 2\bar{f}'(\eta, p) + \frac{7\eta}{4} \bar{f}''(\eta, p) + \frac{\eta^2}{4} \bar{f}'''(\eta, p) \right\} \\ &\quad - \beta_1 \zeta \left\{ \begin{array}{l} 2\bar{f}^{\prime 2}(\eta, p) + \eta \bar{f}'(\eta, p) \bar{f}''(\eta, p) \\ - \{ \bar{f}(\eta, p) + \bar{g}(\eta, p) \} \{ 3\bar{f}''(\eta, p) + \eta \bar{f}'''(\eta, p) \} \end{array} \right\} \\ &\quad + \beta_1 \left\{ \begin{array}{l} \{ \bar{f}(\eta, p) + \bar{g}(\eta, p) \}^2 \bar{f}'''(\eta, p) \\ - 2\{ \bar{f}(\eta, p) + \bar{g}(\eta, p) \} \bar{f}'(\eta, p) \bar{f}''(\eta, p) \end{array} \right\}, \end{aligned} \quad (3.20)$$

$$\begin{aligned} \mathcal{N}_g[\bar{f}(\eta, q), \bar{g}(\eta, q)] &= \bar{g}'''(\eta, q) - \zeta \left(\bar{g}'(\eta, q) + \frac{\eta}{2} \bar{g}''(\eta, q) \right) + \{ \bar{f}(\eta, q) + \bar{g}(\eta, q) \} \bar{g}''(\eta, q) \\ &\quad - \bar{g}^{\prime 2}(\eta, q) - \beta_1 \zeta^2 \left\{ 2\bar{g}'(\eta, q) + \frac{7\eta}{4} \bar{g}''(\eta, q) + \frac{\eta^2}{4} \bar{g}'''(\eta, q) \right\} \\ &\quad - \beta_1 \zeta \left\{ \begin{array}{l} 2\bar{g}^{\prime 2}(\eta, q) + \eta \bar{g}'(\eta, q) \bar{g}''(\eta, q) \\ - \{ \bar{f}(\eta, q) + \bar{g}(\eta, q) \} \{ 3\bar{g}''(\eta, q) + \eta \bar{g}'''(\eta, q) \} \end{array} \right\} \\ &\quad + \beta_1 \left\{ \begin{array}{l} \{ \bar{f}(\eta, q) + \bar{g}(\eta, q) \}^2 \bar{g}'''(\eta, q) \\ - 2\{ \bar{f}(\eta, q) + \bar{g}(\eta, q) \} \bar{g}'(\eta, q) \bar{g}''(\eta, q) \end{array} \right\}, \end{aligned} \quad (3.21)$$

where the auxiliary non-zero parameters are \hbar_f and \hbar_g and $p \in [0, 1]$ is an embedding parameter.

For $p = 0$ and $p = 1$ we have

$$\bar{f}(\eta, 0) = f_0(\eta), \quad \bar{f}(\eta, 1) = f(\eta), \quad (3.22)$$

$$\bar{g}(\eta, 0) = g_0(\eta), \quad \bar{g}(\eta, 1) = g(\eta). \quad (3.23)$$

When p varies from 0 to 1 then the initial guesses $f_0(\eta)$ and $g_0(\eta)$ approach to the final solutions $f(\eta)$ and $g(\eta)$ respectively. Through Taylor's series expansion we write

$$\bar{f}(\eta, p) = f_0(\eta) + \sum_{m=1}^{\infty} f_m(\eta) p^m, \quad (3.24)$$

$$\bar{g}(\eta, p) = g_0(\eta) + \sum_{m=1}^{\infty} g_m(\eta) p^m, \quad (3.25)$$

$$f_m(\eta) = \frac{1}{m!} \left. \frac{\partial^m \bar{f}(\eta, p)}{\partial p^m} \right|_{p=0}, \quad (3.26)$$

$$g_m(\eta) = \frac{1}{m!} \left. \frac{\partial^m \bar{g}(\eta, p)}{\partial p^m} \right|_{p=0}. \quad (3.27)$$

Note that the convergence of Eqs. (3.24) and (3.25) strongly depends upon the auxiliary parameters \hbar_f and \hbar_g . The values of \hbar_f and \hbar_g are selected in such a way that the Eqs. (3.24) and (3.25) converge when $p = 1$. Thus we write

$$f(\eta) = f_0(\eta) + \sum_{m=1}^{\infty} f_m(\eta), \quad (3.28)$$

$$g(\eta) = g_0(\eta) + \sum_{m=1}^{\infty} g_m(\eta). \quad (3.29)$$

3.2.2 m th order deformation problems

The problems at the m^{th} order are given by

$$\mathcal{L}[f_m(\eta) - \chi_m f_{m-1}(\eta)] = \hbar_f \mathcal{R}_{f,m}(\eta), \quad (3.30)$$

$$\mathcal{L}[g_m(\eta) - \chi_m g_{m-1}(\eta)] = \hbar_g \mathcal{R}_{g,m}(\eta), \quad (3.31)$$

$$f_m(0) + g_m(0) = f'_m(0) = f'_m(\infty) = g'_m(0) = g'_m(\infty) = 0, \quad (3.32)$$

$$\chi_m = \begin{cases} 0, & m \leq 1 \\ 1, & m > 1 \end{cases}, \quad (3.33)$$

$$\begin{aligned} \mathcal{R}_{f,m}(\eta) = & f'''_{m-1} - \zeta \left\{ f'_{m-1} + \frac{\eta}{2} f''_{m-1} \right\} + \sum_{k=0}^{m-1} \left\{ (f_{m-1-k} + g_{m-1-k}) f''_k - f'_{m-1-k} f'_k \right\} \\ & - \beta_1 \zeta^2 \left\{ 2f'_{m-1} + \frac{7\eta}{4} f''_{m-1} + \frac{\eta^2}{4} f'''_{m-1} \right\} - \beta_1 \zeta \sum_{k=0}^{m-1} \left\{ 2f'_{m-1-k} f'_k + \eta f'_{m-1-k} f''_k \right\} \\ & - \beta_1 \zeta \sum_{k=0}^{m-1} \left\{ f_{m-1-k} + g_{m-1-k} \right\} \left\{ 3f''_k + \eta f'''_k \right\} \\ & + \beta_1 \sum_{k=0}^{m-1} \sum_{l=0}^k \left\{ \begin{array}{l} 2(f_{m-1-k} + g_{m-1-k}) f'_{k-l} f''_l \\ -(f_{m-1-k} f_{k-l} + g_{m-1-k} g_{k-l} + 2f_{m-1-k} g_{k-l}) f'''_l \end{array} \right\}, \quad (3.34) \end{aligned}$$

$$\begin{aligned}
\mathcal{R}_{g,m}(\eta) = & g_{m-1}''' - \zeta \left\{ g'_{m-1} + \frac{\eta}{2} g''_{m-1} \right\} + \sum_{k=0}^{m-1} \{ (f_{m-1-k} + g_{m-1-k}) g''_k - g'_{m-1-k} g'_k \} \\
& - \beta_1 \zeta^2 \left\{ 2g'_{m-1} + \frac{7\eta}{4} g''_{m-1} + \frac{\eta^2}{4} g'''_{m-1} \right\} - \beta_1 \zeta \sum_{k=0}^{m-1} \{ 2g'_{m-1-k} g'_k + \eta g'_{m-1-k} g''_k \} \\
& - \beta_1 \zeta \sum_{k=0}^{m-1} \{ f_{m-1-k} + g_{m-1-k} \} \{ 3g''_k + \eta g'''_k \} \\
& + \beta_1 \sum_{k=0}^{m-1} \sum_{l=0}^k \left\{ \begin{array}{l} 2(f_{m-1-k} + g_{m-1-k}) g'_{k-l} g''_l \\ -(f_{m-1-k} f_{k-l} + g_{m-1-k} g_{k-l} + 2f_{m-1-k} g_{k-l}) g'''_l \end{array} \right\}. \quad (3.35)
\end{aligned}$$

3.3 Convergence analysis

We note that the convergence of solutions (3.30) and (3.31) depends upon \hbar_f and \hbar_g . To find the admissible values of \hbar_f and \hbar_g , the so called \hbar -curves are displayed for 15th order of approximation in Fig. 3.1. This Fig. shows that the admissible values are $-0.9 \leq \hbar_f \leq -0.5$ and $-0.9 \leq \hbar_g \leq -0.5$. In order to validate the obtained analytic results we have plotted the \hbar -curves for residual error of f and g in the Figs. 3.2 and 3.3. It is noted that the correct results upto 6th decimal place can be obtained by choosing the values of \hbar from the ranges mentioned in the Figs. 3.2 and 3.3. Table 3.1 is prepared to show the convergence of the derived series solutions. It is noted that the convergence is achieved at the 10th order of approximations. Table 3.2 is constructed in order to make a comparison of present results with the published results. It is noticed that obtained results are in an excellent agreement with the published

results.

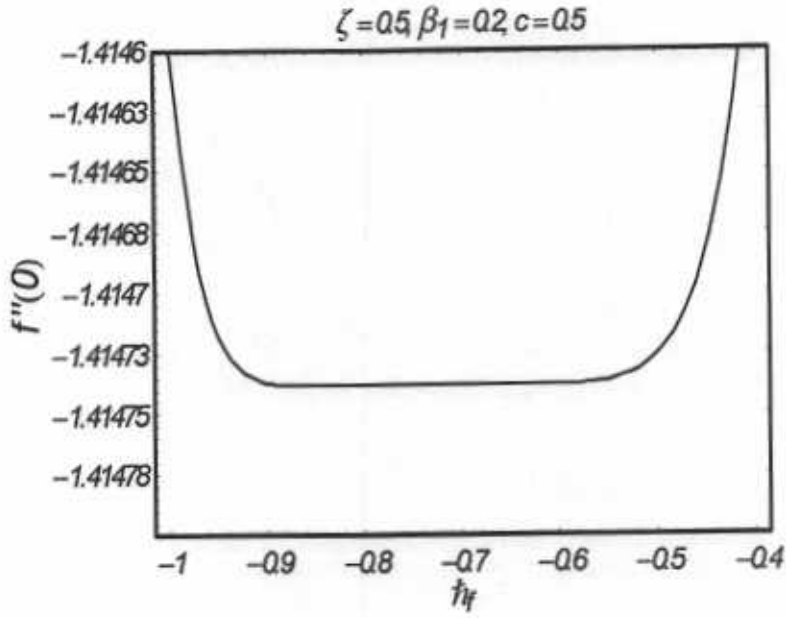


Fig. 3.1 : h curves of $f''(0)$ at the 15th order of approximation.

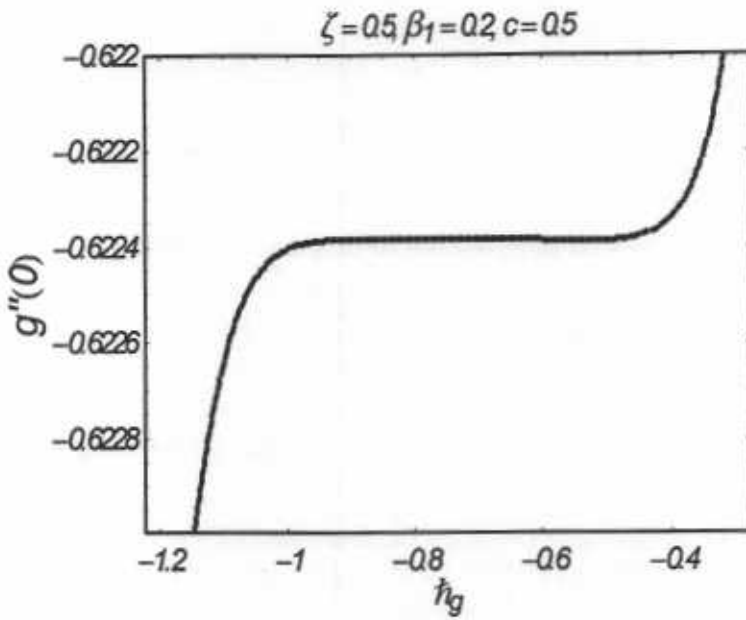


Fig. 3.2 : h curves of $g''(0)$ at the 15th order of approximation.

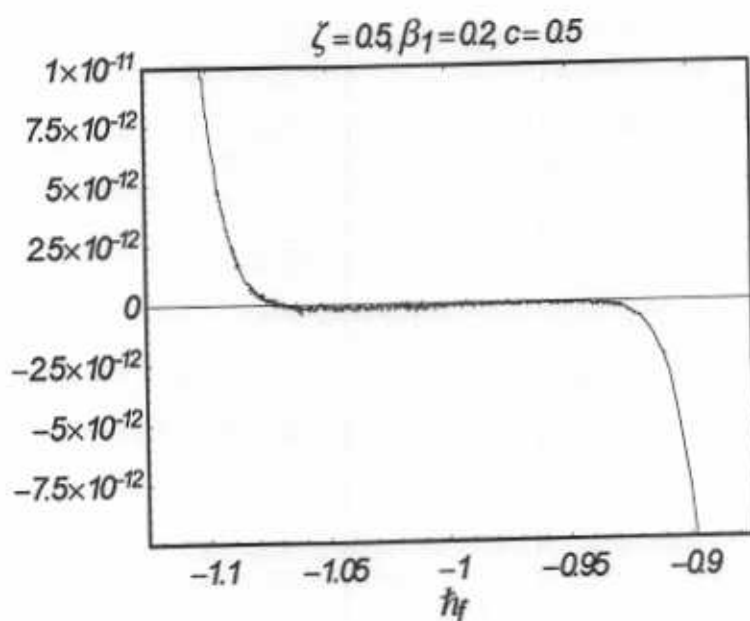


Fig. 3.3 : h curve for residual error in $f(\eta)$ at the 15th order of approximation.

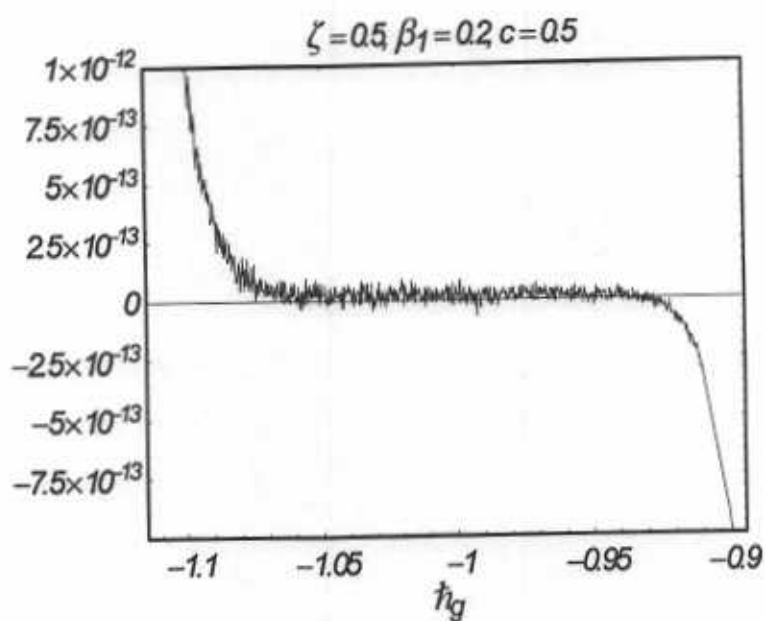


Fig. 3.4 : h curve for residual error in $g(\eta)$ at the 15th order of approximation.

Table 3.1: Convergence of the HAM solutions for different order of approximations when

$$\beta_1 = 0.2 \text{ and } \zeta = 0.5 = c$$

order of approximation	$-f''(0)$	$-g''(0)$
1	1.349513	0.597951
2	1.396291	0.616953
5	1.414430	0.622341
10	1.414737	0.622382
15	1.414737	0.622383
20	1.414737	0.622383
30	1.414737	0.622383
50	1.414737	0.622383

3.4 Results and discussion

This section describes the influence of time-dependent parameter ζ , Deborah number β_1 and the ratio parameter c on f' and g' for the case of three-dimensional flow situation. For this purpose we have constructed Figs. 3.5 – 3.10. Figs. 3.5 and 3.6 portrayed the influence of ζ on f' and g' . It is observed that both f' and g' and the associated boundary layer thickness increases when ζ is increases. The influence of Deborah parameter β_1 on f' and g' is shown in Figs. 3.7 and 3.8. From these Figs. it is analyzed that Deborah parameter β_1 retards the flow. Thus the momentum boundary layer for both components f' and g' becomes thinner with an increase in Deborah number β_1 . Since the Deborah number β_1 defines the difference between the solid and liquids (or fluids) therefore the material behaves like fluids for smaller Deborah number whereas for large value of Deborah number the material behaves like solids. This property of Deborah number is also seen in Figs. 3.7 and 3.8. Fig. 3.9 is plotted to see the influence of ratio parameter c on the velocity component f' . It is observed that an increase in c indicates a decrease in the velocity f' . From Fig. 3.10 we observed that the influence of c on g' is quite opposite to that of f' . It is because of the fact that the stretching occurs bidirectionally (stretching along $y - axis$) for the positive values of c . Thus the velocity component along $y - axis$ i.e. g' show increasing behavior near the boundary.

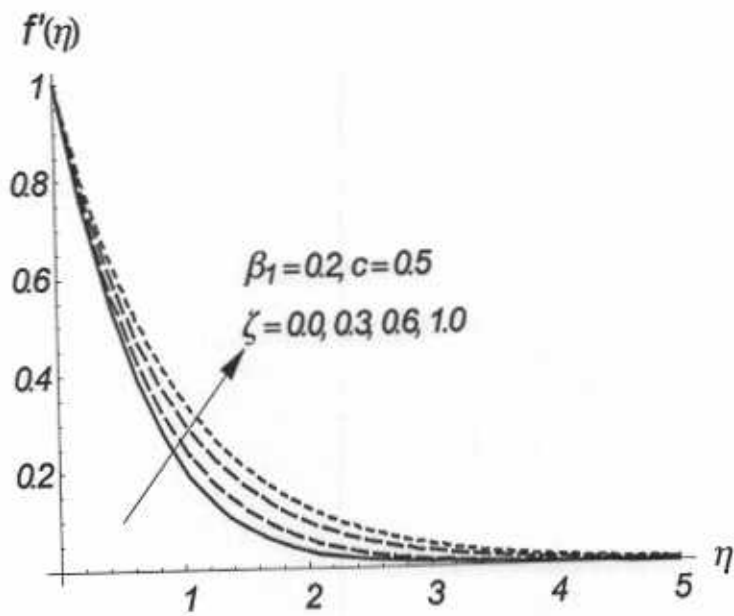


Fig. 3.5 : Influence of ζ on f' .

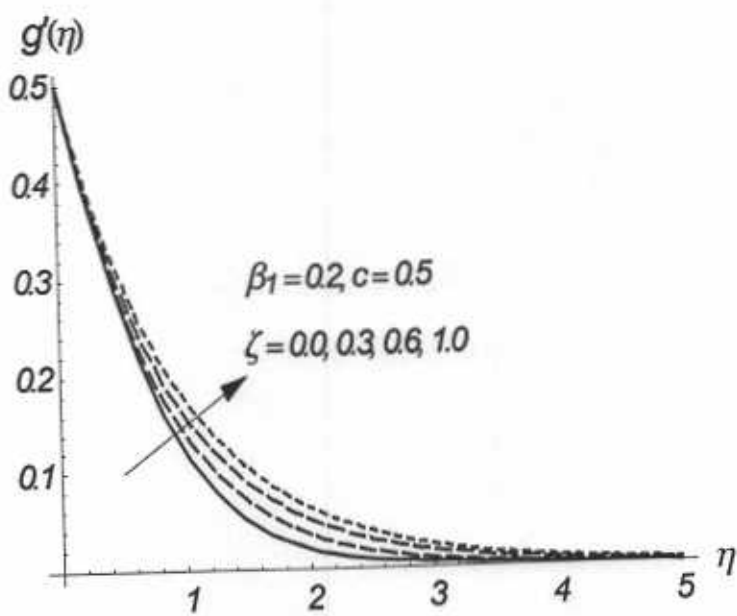


Fig. 3.6 : Influence of ζ on g' .

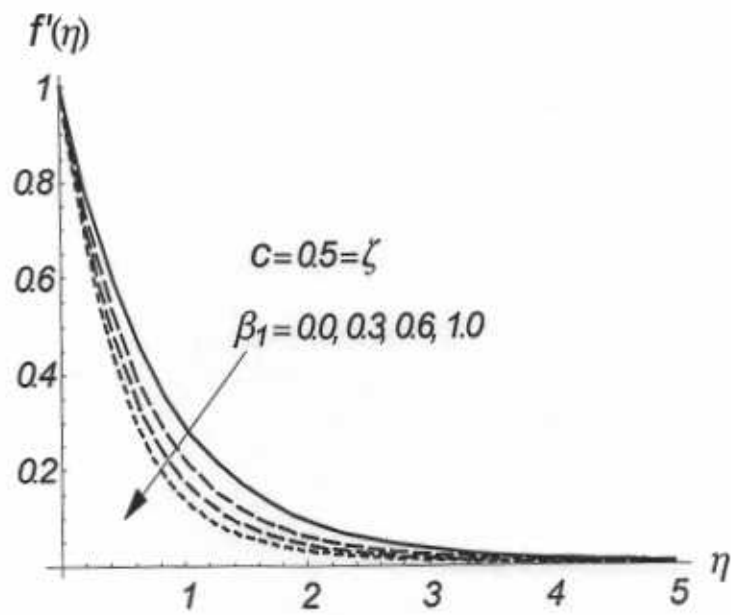


Fig. 3.7 : Influence of β_1 on f' .

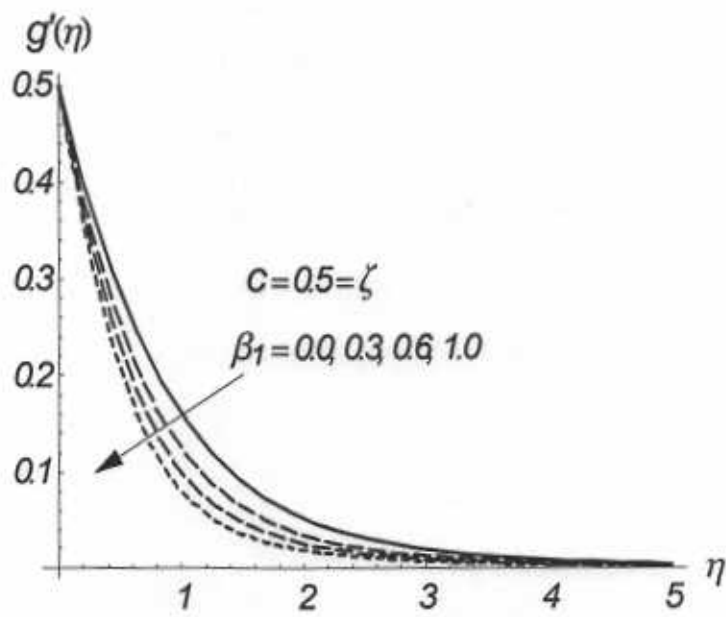


Fig. 3.8 : Influence of β_1 on g' .

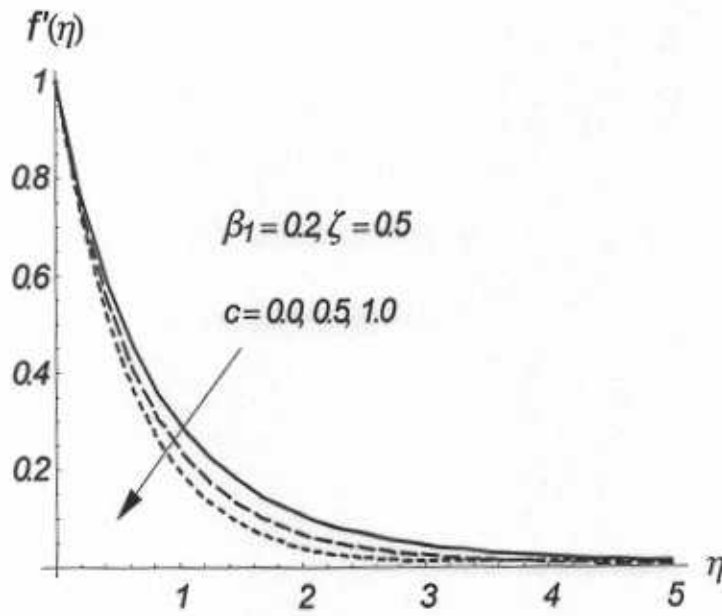


Fig. 3.9 : Influence of c on f' .

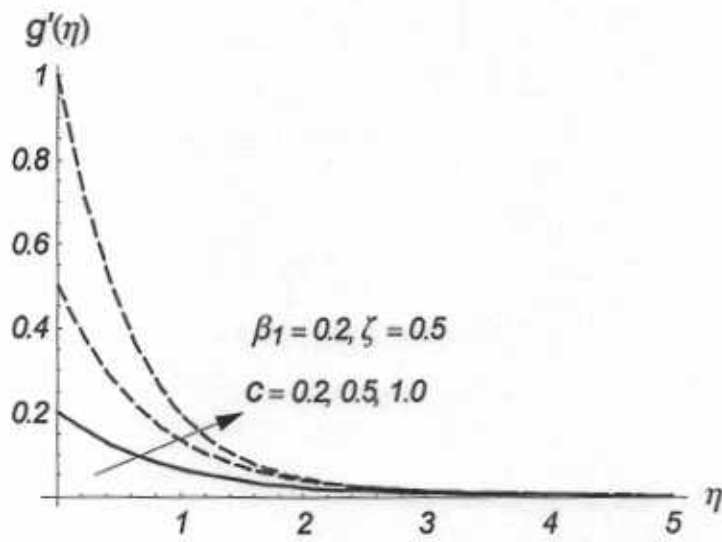


Fig. 3.10 : Influence of c on g' .

Table 3.2: Comparison of present results with the steady-state case [81] when $\zeta = 0.0$.

order of approximation	Present results		Ref. [81]	
	$-f''(0)$	$-g''(0)$	$-f''(0)$	$-g''(0)$
1	1.153750	0.490625	1.153750	0.490625
2	1.182876	0.499378	1.182876	0.499378
5	1.181869	0.502042	1.181869	0.502042
10	1.182117	0.501999	1.182117	0.501999
15	1.182123	0.501996	1.182123	0.501996
20	1.182124	0.501996	1.182124	0.501996
25	1.182124	0.501996	1.182124	0.501996
30	1.182124	0.501996	1.182124	0.501996
40	1.182124	0.501996	1.182124	0.501996
50	1.182124	0.501996	1.182124	0.501996

3.5 Conclusions

We have investigated the time-dependent three-dimensional flow of an upper convected Maxwell (UCM) fluid over an unsteady stretching surface. The results for the steady-state, two-dimensional and axisymmetric flows can be deduced as the limiting cases. Solutions for the problem are obtained by using HAM. The convergence and graphical results are displayed. The influence of time-dependent parameter and Deborah number is discussed. The main observations are pointed out below.

- Velocity fields f' and g' are increasing functions of time-dependent parameter ζ .
- Deborah number β_1 retards the flow.
- In both cases of unsteady/steady flows, f' decreases when c is increased.
- The variations of c on velocities are qualitatively similar in viscous case when compared with the case of Maxwell fluid.
- Dimensionless velocity g' increases by increasing c in both cases of steady and unsteady flows.

- The magnitude of velocities for unsteady case ($\zeta > 0$) is larger as compared to the steady-state case ($\zeta = 0$).

Chapter 4

Mixed convection three-dimensional flow of Maxwell fluid with magnetic field, thermal diffusion and diffusion thermo effects

This chapter examines the mixed convection boundary layer flow of upper-convected Maxwell (UCM) fluid. The flow is subjected to a bidirectional stretching vertical plate. Effects of applied magnetic field, diffusion-thermo (Dufour) and thermal-diffusion (Soret) are addressed. With appropriate transformations, the resulting boundary layer equations are reduced to nonlinear ordinary differential equations. The arising ordinary differential systems are solved by homotopy analysis method. Results are obtained and discussed for velocity, temperature, concentration, local Nusselt and local Sherwood numbers.

4.1 Mathematical analysis

Here we consider the phenomena of heat and mass transfer in the steady three-dimensional boundary layer flow of Maxwell fluid. The fluid is assumed to be electrically conducting in the presence of an applied magnetic field of strength B_0 . The electric and induced magnetic fields

are neglected. In addition, the mixed convection phenomenon combined with thermal-diffusion and diffusion-thermo effects is considered. The flow is induced by vertical surface stretching bidirectionally. Physical model is shown in the Fig. 4.1

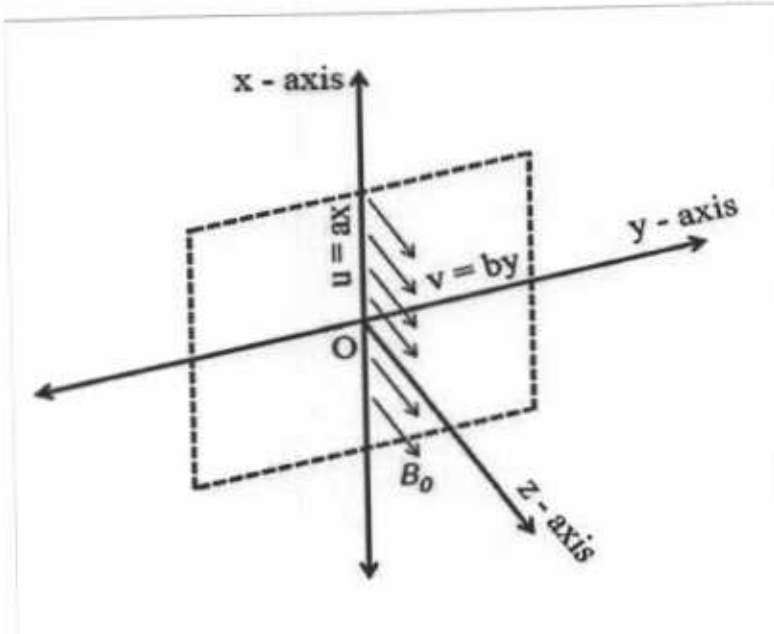


Fig. 4.1 : Geometry of the problem.

The continuity, momentum, concentration and energy equations for the present boundary layer flow become

$$\frac{\partial u}{\partial x} + \frac{\partial v}{\partial y} + \frac{\partial w}{\partial z} = 0, \quad (4.1)$$

$$\begin{aligned} \frac{\partial u}{\partial t} + u \frac{\partial u}{\partial x} + v \frac{\partial u}{\partial y} + w \frac{\partial u}{\partial z} + \lambda_1 \left(\begin{aligned} &\frac{\partial^2 u}{\partial t^2} + 2u \frac{\partial^2 u}{\partial x \partial t} + 2v \frac{\partial^2 u}{\partial y \partial t} + 2w \frac{\partial^2 u}{\partial z \partial t} \\ &+ u^2 \frac{\partial^2 u}{\partial x^2} + v^2 \frac{\partial^2 u}{\partial y^2} + w^2 \frac{\partial^2 u}{\partial z^2} \\ &+ 2uv \frac{\partial^2 u}{\partial x \partial y} + 2vw \frac{\partial^2 u}{\partial y \partial z} + 2uw \frac{\partial^2 u}{\partial x \partial z} \end{aligned} \right) \\ = \nu \frac{\partial^2 u}{\partial z^2} - \frac{\sigma B_0^2}{\rho} \left(u + \lambda_1 w \frac{\partial u}{\partial z} \right) + g^* [\beta_T (T - T_\infty) + \beta_C (C - C_\infty)], \end{aligned} \quad (4.2)$$

$$\begin{aligned} \frac{\partial v}{\partial t} + u \frac{\partial v}{\partial x} + v \frac{\partial v}{\partial y} + w \frac{\partial v}{\partial z} + \lambda_1 \left(\begin{aligned} &\frac{\partial^2 v}{\partial t^2} + 2u \frac{\partial^2 v}{\partial x \partial t} + 2v \frac{\partial^2 v}{\partial y \partial t} + 2w \frac{\partial^2 v}{\partial z \partial t} \\ &+ u^2 \frac{\partial^2 v}{\partial x^2} + v^2 \frac{\partial^2 v}{\partial y^2} + w^2 \frac{\partial^2 v}{\partial z^2} \\ &+ 2uv \frac{\partial^2 v}{\partial x \partial y} + 2vw \frac{\partial^2 v}{\partial y \partial z} + 2uw \frac{\partial^2 v}{\partial x \partial z} \end{aligned} \right) \\ = \nu \frac{\partial^2 v}{\partial z^2} - \frac{\sigma B_0^2}{\rho} \left(v + \lambda_1 w \frac{\partial v}{\partial z} \right), \end{aligned} \quad (4.3)$$

$$u \frac{\partial C}{\partial x} + v \frac{\partial C}{\partial y} + w \frac{\partial C}{\partial z} = D \frac{\partial^2 C}{\partial z^2} - K_1 C + \frac{Dk_T}{T_m} \frac{\partial^2 T}{\partial z^2}, \quad (4.4)$$

$$u \frac{\partial T}{\partial x} + v \frac{\partial T}{\partial y} + w \frac{\partial T}{\partial z} = \alpha_m \frac{\partial^2 T}{\partial z^2} + \frac{Dk_T}{C_s C_p} \frac{\partial^2 C}{\partial z^2}, \quad (4.5)$$

where u , v and w are the velocities in the x , y and z directions, respectively, ν the kinematic viscosity, λ_1 the relaxation time, ρ the density, σ the electrical conductivity, C the concentration of species, D the coefficient of diffusing species, K_1 the reaction rate, k_T the thermal-diffusion, T the temperature, C_p the specific heat at constant pressure, C_s the concentration susceptibility, α_m the thermal diffusivity, T_m the fluid mean temperature, g^* the gravitational constant and (β_T, β_C) the volumetric expansion coefficients for temperature and concentration

The boundary conditions can be written as

$$\begin{aligned} u &= u_w(x) = ax, \quad v = v_w(y) = by, \quad w = 0, \quad T = T_w(x), \quad C = C_w(x) \quad \text{at } z = 0, \\ u &\rightarrow 0, \quad v \rightarrow 0, \quad T \rightarrow T_\infty, \quad C \rightarrow C_\infty \quad \text{as } z \rightarrow \infty, \end{aligned} \quad (4.6)$$

where the wall temperature and concentration are prescribed as follows

$$T_w(x) = T_\infty + dx, \quad C_w(x) = C_\infty + ex, \quad (4.7)$$

in which C_∞ and T_∞ denote the ambient values of concentration and temperature.

Making use of the following similarity variables

$$\begin{aligned} \eta &= \sqrt{\frac{a}{\nu}} z, \quad u = ax f'(\eta), \quad v = ay g'(\eta), \quad w = -\sqrt{a\nu} \{f(\eta) + g(\eta)\}, \\ \theta(\eta) &= \frac{T - T_\infty}{T_w - T_\infty}, \quad \phi(\eta) = \frac{C - C_\infty}{C_w - C_\infty}, \end{aligned} \quad (4.8)$$

Eq. (4.1) is satisfied automatically and Eqs. (4.2) – (4.6) yield

$$f''' - M^2 f' + (M^2 \beta_1 + 1)(f + g)f'' - f'^2 + \lambda[\theta(\eta) + N\phi(\eta)] + \beta_1 [2(f + g)f'f'' - (f + g)^2 f'''] = 0, \quad (4.9)$$

$$g''' - M^2 g' + (M^2 \beta_1 + 1)(f + g)g'' - g'^2 + \beta_1 [2(f + g)g'g'' - (f + g)^2 g'''] = 0, \quad (4.10)$$

$$\phi'' + Sc(f + g)\phi' - Scf'\phi - Sc\gamma\phi + ScS_r\theta'' = 0, \quad (4.11)$$

$$\theta'' + Pr(f + g)\theta' - Prf'\theta + PrD_f\phi'' = 0, \quad (4.12)$$

$$f(0) + g(0) = 0, \quad f'(0) = 1, \quad g'(0) = c, \quad \phi(0) = 1, \quad \theta(0) = 1, \\ f'(\infty) = 0, \quad g'(\infty) = 0, \quad \phi(\infty) \rightarrow 0, \quad \theta(\infty) \rightarrow 0, \quad (4.13)$$

in which prime indicates the differentiation with respect to η and the constants $a > 0$ and $b > 0$. Furthermore the Deborah number β_1 , the ratio c , Schmidt number Sc , mixed convection parameter λ , Dufour number D_f , Soret number S_r , constant dimensionless concentration buoyancy parameter N , Prandtl number Pr , Hartman number M and the chemical reaction parameter γ are defined as

$$\beta_1 = \lambda_1 a, \quad c = \frac{b}{a}, \quad Sc = \frac{\nu}{D}, \quad \lambda = \frac{g\beta_T}{a^2} = \frac{g\beta_T(T_w - T_\infty)x^3/\nu^2}{u_w^2 x^2/\nu^2} = \frac{Gr_x}{Re_x^2}, \\ D_f = \frac{Dk_T(C_w - C_\infty)}{C_s C_p (T_w - T_\infty)\nu}, \quad S_r = \frac{Dk_T(T_w - T_\infty)}{T_m \nu (C_w - C_\infty)}, \quad N = \frac{\beta_C(C_w - C_\infty)}{\beta_T(T_w - T_\infty)}, \\ Pr = \frac{\nu}{\alpha_m}, \quad M^2 = \frac{\sigma B_0^2}{\rho a}, \quad \gamma = \frac{K_1}{a}, \quad (4.14)$$

where ($\lambda > 0$) corresponds to assisting flow, ($\lambda < 0$) corresponds to opposing flow and ($\lambda = 0$) corresponds to forced convection flow respectively.

The physical quantities of special interest are the local Nusselt (Nu_x) and local Sherwood (Sh) numbers which can be written as

$$Nu = \frac{xq_w}{k(T_w - T_\infty)}, \quad Sh = \frac{xj_w}{D(C_w - C_\infty)} \quad (4.15)$$

with

$$q_w = -k \left(\frac{\partial T}{\partial z} \right)_{\eta=0}, \quad j_w = -D \left(\frac{\partial C}{\partial z} \right)_{\eta=0}, \quad (4.16)$$

where q_w and j_w respectively denote the heat and mass fluxes. Equation (4.15) in dimensionless form becomes

$$Nu_x / Re_x^{1/2} = -\theta'(0), \quad Sh / Re_x^{1/2} = -\phi'(0) \quad (4.17)$$

4.2 Series solutions

In order to present the homotopy solutions, we select the set of base functions

$$\left\{ \eta^k \exp(-n\eta) \mid k \geq 0, n \geq 0 \right\} \quad (4.18)$$

and define

$$f(\eta) = a_{0,0}^0 + \sum_{n=1}^{\infty} \sum_{k=1}^{\infty} a_{m,n}^k \eta^k \exp(-n\eta), \quad (4.19)$$

$$g(\eta) = b_{0,0}^0 + \sum_{n=1}^{\infty} \sum_{k=1}^{\infty} b_{m,n}^k \eta^k \exp(-n\eta), \quad (4.20)$$

$$\phi(\eta) = \sum_{n=0}^{\infty} \sum_{k=0}^{\infty} c_{m,n}^k \eta^k \exp(-n\eta), \quad (4.21)$$

$$\theta(\eta) = \sum_{n=0}^{\infty} \sum_{k=0}^{\infty} b_{m,n}^k \eta^k \exp(-n\eta), \quad (4.22)$$

where $a_{m,n}^k$ and $b_{m,n}^k$ are the coefficients. The convenient initial guesses and linear operator are selected as follows

$$f_0(\eta) = 1 - \exp(-\eta), \quad (4.23)$$

$$g_0(\eta) = c(1 - \exp(-\eta)), \quad (4.24)$$

$$\theta_0(\eta) = \exp(-\eta), \quad (4.25)$$

$$\phi_0(\eta) = \exp(-\eta). \quad (4.26)$$

The auxiliary linear operators for the function f , g , ϕ and θ are of the forms

$$\mathcal{L}_f = \frac{d^3 f}{d\eta^3} - \frac{df}{d\eta}, \quad (4.27)$$

$$\mathcal{L}_g = \frac{d^3 g}{d\eta^3} - \frac{dg}{d\eta}, \quad (4.28)$$

$$\mathcal{L}_\phi = \frac{d^2 \phi}{d\eta^2} - \phi, \quad (4.29)$$

$$\mathcal{L}_\theta = \frac{d^2 \theta}{d\eta^2} - \theta, \quad (4.30)$$

with the following properties

$$\mathcal{L}_f [C_1 + C_2 \exp(\eta) + C_3 \exp(-\eta)] = 0, \quad (4.31)$$

$$\mathcal{L}_g [C_4 + C_5 \exp(\eta) + C_6 \exp(-\eta)] = 0, \quad (4.32)$$

$$\mathcal{L}_\phi [C_7 \exp(\eta) + C_8 \exp(-\eta)] = 0, \quad (4.33)$$

$$\mathcal{L}_\theta [C_{10} \exp(\eta) + C_{10} \exp(-\eta)] = 0, \quad (4.34)$$

where $c_i (i = 1 - 10)$ are the arbitrary constants.

4.2.1 Zeroth-order deformation problems

The problem at the zeroth order deformation are constructed as

$$(1 - p)\mathcal{L}_f [\bar{f}(\eta, p) - f_0(\eta)] = p\hbar_f \mathcal{N}_f [\bar{f}(\eta, p), \bar{g}(\eta, p), \bar{\phi}(\eta, p), \bar{\theta}(\eta, p)], \quad (4.35)$$

$$(1 - p)\mathcal{L}_g [\bar{g}(\eta, p) - f_0(\eta)] = p\hbar_g \mathcal{N}_g [\bar{f}(\eta, p), \bar{g}(\eta, p)], \quad (4.36)$$

$$(1 - p)\mathcal{L}_\phi [\bar{\phi}(\eta, p) - \phi_0(\eta)] = p\hbar_\phi \mathcal{N}_\phi [\bar{f}(\eta, p), \bar{g}(\eta, p), \bar{\phi}(\eta, p), \bar{\theta}(\eta, p)], \quad (4.37)$$

$$(1 - p)\mathcal{L}_\theta [\bar{\theta}(\eta, p) - \theta_0(\eta)] = p\hbar_\theta \mathcal{N}_\theta [\bar{f}(\eta, p), \bar{g}(\eta, p), \bar{\phi}(\eta, p), \bar{\theta}(\eta, p)], \quad (4.38)$$

where the nonlinear operators \mathcal{N}_f , \mathcal{N}_g , \mathcal{N}_ϕ and \mathcal{N}_θ in Eqs. (4.35 – 4.38) are

$$\begin{aligned} \mathcal{N}_f = & \bar{f}'''(\eta, p) - M^2 \bar{f}''(\eta, p) - \bar{f}'^2(\eta, p) + \lambda \{ \bar{\theta}(\eta, p) + N \bar{\phi}(\eta, p) \} \\ & + (M^2 \beta_1 + 1) \{ \bar{f}(\eta, p) + \bar{g}(\eta, p) \} \bar{f}''(\eta, p) \\ & + \beta_1 \left\{ \begin{array}{l} \{ \bar{f}(\eta, p) + \bar{g}(\eta, p) \}^2 \bar{f}'''(\eta, p) \\ -2 \{ \bar{f}(\eta, p) + \bar{g}(\eta, p) \} \bar{f}'(\eta, p) \bar{f}''(\eta, p) \end{array} \right\}, \end{aligned} \quad (4.39)$$

$$\begin{aligned} \mathcal{N}_g = & \bar{g}'''(\eta, p) - M^2 \bar{g}''(\eta, p) - \bar{g}'^2(\eta, p) \\ & + (M^2 \beta_1 + 1) \{ \bar{f}(\eta, p) + \bar{g}(\eta, p) \} \bar{g}''(\eta, p) \\ & + \beta_1 \left\{ \begin{array}{l} \{ \bar{f}(\eta, p) + \bar{g}(\eta, p) \}^2 \bar{g}'''(\eta, p) \\ -2 \{ \bar{f}(\eta, p) + \bar{g}(\eta, p) \} \bar{g}'(\eta, p) \bar{g}''(\eta, p) \end{array} \right\}, \end{aligned} \quad (4.40)$$

$$\mathcal{N}_\phi = \bar{\phi}''(\eta, p) + Sc \left(\begin{array}{l} \bar{f}(\eta, p) \bar{\phi}'(\eta, p) + \bar{g}(\eta, p) \bar{\phi}'(\eta, p) \\ -\bar{f}'(\eta, p) \bar{\phi}(\eta, p) - \gamma \bar{\phi}(\eta, p) + S_r \bar{\theta}''(\eta, p) \end{array} \right) \quad (4.41)$$

$$\mathcal{N}_\theta = \bar{\theta}''(\eta, p) + Pr \left(\begin{array}{l} \bar{f}(\eta, p) \bar{\theta}'(\eta, p) + \bar{g}(\eta, p) \bar{\theta}'(\eta, p) \\ -\bar{f}'(\eta, p) \bar{\phi}(\eta, p) + D_f \bar{\phi}''(\eta, p) \end{array} \right) \quad (4.42)$$

and the auxiliary non-zero parameters are \hbar_f , \hbar_g , \hbar_ϕ and \hbar_θ . Moreover $p \in [0, 1]$ is an embedding parameter. For $p = 0$ and $p = 1$ we have

$$\bar{f}(\eta, 0) = f_0(\eta), \quad \bar{f}(\eta, 1) = f(\eta), \quad (4.43)$$

$$\bar{g}(\eta, 0) = g_0(\eta), \quad \bar{g}(\eta, 1) = g(\eta), \quad (4.44)$$

$$\bar{\phi}(\eta, 0) = \phi_0(\eta), \quad \bar{\phi}(\eta, 1) = \phi(\eta), \quad (4.45)$$

$$\bar{\theta}(\eta, 0) = \theta_0(\eta), \quad \bar{\theta}(\eta, 1) = \theta(\eta). \quad (4.46)$$

When p varies from 0 to 1 then the initial guesses $f_0(\eta)$, $g_0(\eta)$, $\phi_0(\eta)$ and $\theta_0(\eta)$ approach to the final solutions $f(\eta)$, $g(\eta)$, $\phi(\eta)$ and $\theta(\eta)$ respectively. By Taylor's series expansions we write

$$\bar{f}(\eta, p) = f_0(\eta) + \sum_{m=1}^{\infty} f_m(\eta) p^m, \quad (4.47)$$

$$\bar{g}(\eta, p) = g_0(\eta) + \sum_{m=1}^{\infty} g_m(\eta) p^m, \quad (4.48)$$

$$\bar{\phi}(\eta, p) = \phi_0(\eta) + \sum_{m=1}^{\infty} \phi_m(\eta) p^m, \quad (4.49)$$

$$\bar{\theta}(\eta, p) = \theta_0(\eta) + \sum_{m=1}^{\infty} \theta_m(\eta) p^m, \quad (4.50)$$

$$f_m(\eta) = \left. \frac{1}{m!} \frac{\partial^m \bar{f}(\eta, p)}{\partial p^m} \right|_{p=0}, \quad (4.51)$$

$$g_m(\eta) = \left. \frac{1}{m!} \frac{\partial^m \bar{g}(\eta, p)}{\partial p^m} \right|_{p=0}, \quad (4.52)$$

$$\phi_m(\eta) = \left. \frac{1}{m!} \frac{\partial^m \bar{\phi}(\eta, p)}{\partial p^m} \right|_{p=0}, \quad (4.53)$$

$$\theta_m(\eta) = \left. \frac{1}{m!} \frac{\partial^m \bar{\theta}(\eta, p)}{\partial p^m} \right|_{p=0}. \quad (4.54)$$

Note that the convergence of equations (4.51) and (4.54) strongly depends upon the auxiliary parameters \hbar_f , \hbar_g , \hbar_ϕ and \hbar_θ . The values of \hbar_f , \hbar_g , \hbar_ϕ and \hbar_θ are selected in such a way that the equations (4.51) and (4.54) converge when $p = 1$. Thus we write

$$f(\eta) = f_0(\eta) + \sum_{m=1}^{\infty} f_m(\eta), \quad (4.55)$$

$$g(\eta) = g_0(\eta) + \sum_{m=1}^{\infty} g_m(\eta), \quad (4.56)$$

$$\phi(\eta) = \phi_0(\eta) + \sum_{m=1}^{\infty} \phi_m(\eta). \quad (4.57)$$

$$\theta(\eta) = \theta_0(\eta) + \sum_{m=1}^{\infty} \theta_m(\eta). \quad (4.58)$$

$$\begin{aligned} \mathcal{R}_{\phi,m}(\eta) = & \phi''_{m-1} + Sc \sum_{k=0}^{m-1} (f_{m-1-k} + g_{m-1-k})\phi'_k - Sc \sum_{k=0}^{m-1} f'_{m-1-k}\phi_k \\ & - Sc\gamma\phi_{m-1} + ScS_r\theta''_{m-1} \end{aligned} \quad (4.67)$$

$$\mathcal{R}_{\theta,m}(\eta) = \theta''_{m-1} + Pr \sum_{k=0}^{m-1} (f_{m-1-k} + g_{m-1-k})\theta'_k - Pr \sum_{k=0}^{m-1} f'_{m-1-k}\theta_k + Pr D_f \phi''_{m-1}. \quad (4.68)$$

4.3 Convergence

It is seen that the convergence of solutions (4.55) – (4.58) depends upon \hbar_f , \hbar_g , \hbar_ϕ and \hbar_θ . These parameters play a vital role in controlling the convergence of the obtained series solutions. To find the admissible values of \hbar_f , \hbar_g , \hbar_ϕ and \hbar_θ , we have constructed the \hbar -curves for 15th order of approximation as shown in Figs. 4.2 – 4.5. These Figs. clearly show that the admissible values are $-1.2 \leq (\hbar_f, \hbar_g, \hbar_\phi, \hbar_\theta) \leq -0.4$. Table 4.1 is presented to show the convergence of the obtained series solutions. It is noted that the obtained solutions are convergent up to 6th decimal place.

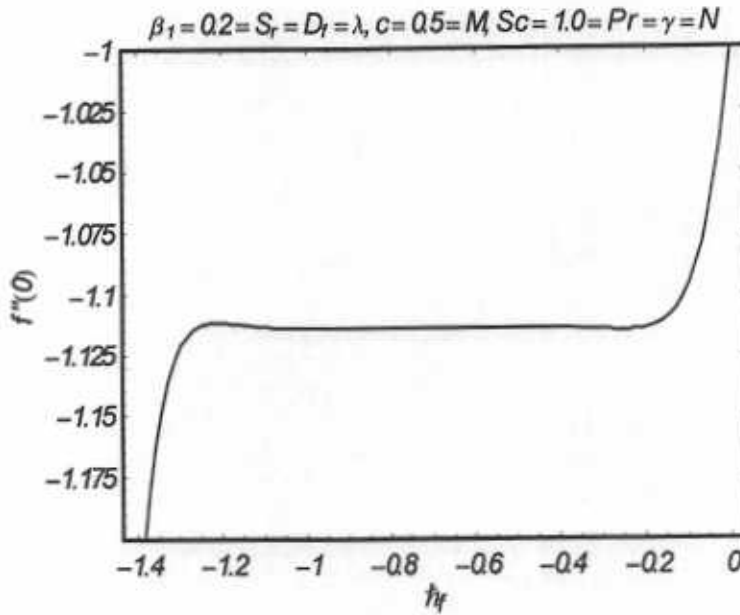


Fig. 4.2 : \hbar curves of $f''(0)$ at the 15th order of approximation.

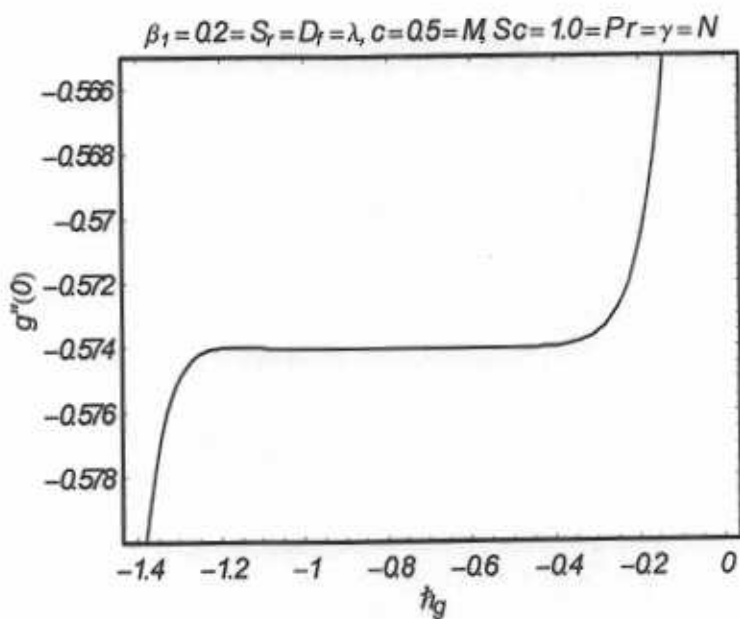


Fig. 4.3 : h curves of $g''(0)$ at the 15th order of approximation.

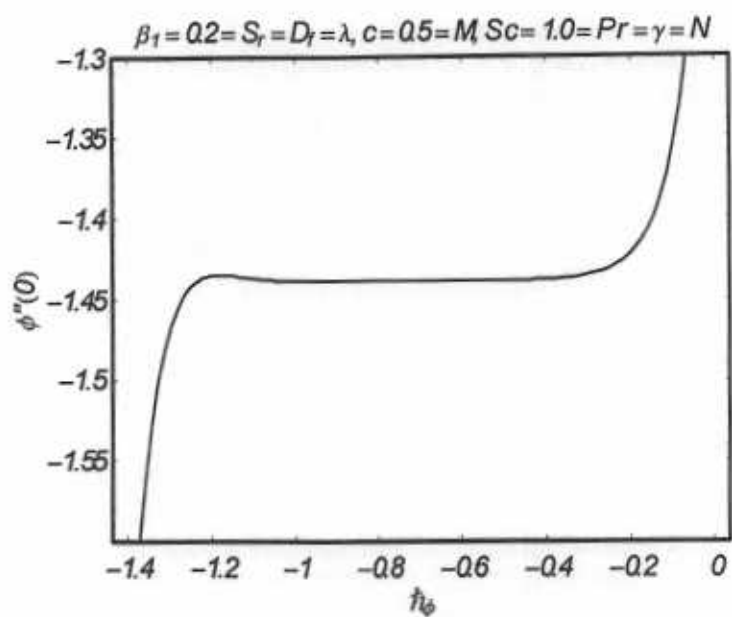


Fig. 4.4 : h curves of $\phi''(0)$ at the 15th order of approximation.

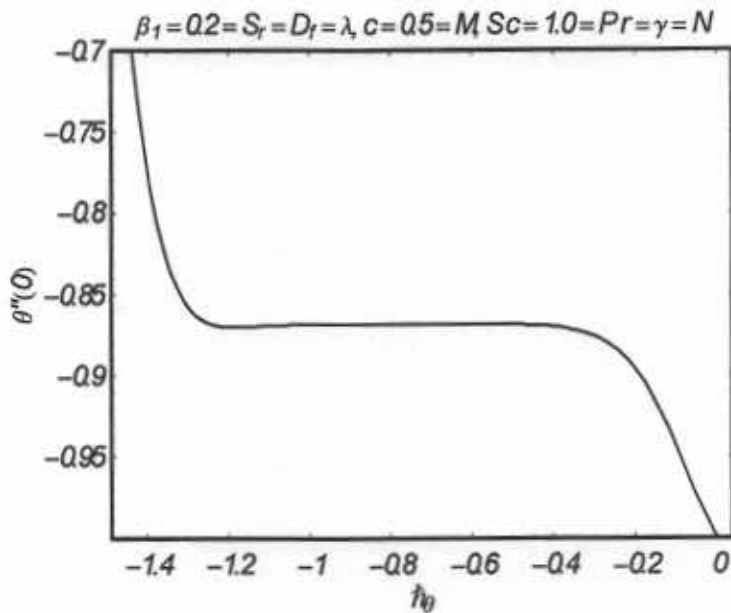


Fig. 4.5 : h curves of $\theta''(0)$ at the 15th order of approximation.

Table 4.1: Convergence of the HAM solutions for different order of approximations when $c = 0.5 = M$, $\beta_1 = 0.2 = D_f = S_r = \lambda$, $Pr = 1.0 = Sc = \gamma = N$.

approximation order	$-f''(0)$	$-g''(0)$	$-\phi'(\eta)$	$-\theta'(\eta)$
1	1.075833	0.540833	1.338333	0.988333
2	1.111655	0.562161	1.407796	0.937823
5	1.115011	0.573595	1.434085	0.873785
10	1.113760	0.574067	1.438251	0.868215
15	1.113771	0.574061	1.438296	0.868217
20	1.113772	0.574061	1.438295	0.868218
25	1.113772	0.574061	1.438295	0.868218
30	1.113772	0.574061	1.438295	0.868218
40	1.113772	0.574061	1.438295	0.868218
50	1.113772	0.574061	1.438295	0.868218

4.4 Discussion

Our interest in this section is to explain the behavior of various physical variables on the velocity, concentration and temperature fields. These parameters include the Deborah number β_1 , the ratio c , the Schmidt number Sc , the chemical reaction parameter γ , Prandtl number Pr , mixed convection parameter λ , Hartman number M , Dufour number D_f , Soret number S_r and concentration buoyancy parameter N . Since our main focus here is related to mixed convection phenomenon when both thermal-diffusion and diffusion thermo effects are present. Therefore, we kept the other quantities fixed and analyze the effects of M , N , λ , S_r , D_f , γ , Sc and Pr . Thus Figs. 4.6 – 4.17 have been plotted. The variations of M , λ and N on f' for three-dimensional flow are shown in the Figs. 4.6 – 4.9. From Fig. 4.6 it is noted that magnetic field M opposes the flow. Physically when magnetic field is applied to fluid then its apparent viscosity increases to the point of becoming a viscoelastic solid. Importantly, the yield stress of the fluid can be controlled very accurately by varying the magnetic field intensity. The outcome of which is that the fluid's ability to transmit force can be controlled with the help of an electromagnet which gives rise to its many possible control-based applications including MHD power generation, electromagnetic casting of metals, MHD ion propulsion etc. Fig. 4.7 elucidates the effects of concentration buoyancy parameter N on f' . Physically buoyancy is a force exerted by a fluid that increases the up thrust. Since the pressure at the depth of fluid in any domain is greater when compared to the pressure at the upper portion inducing a force that try to move an object upward. Magnitude of this force is equal to the difference in the pressure between the top and the bottom of the column and is also equivalent to the weight of the fluid that would otherwise occupy the region. Thus an increase in buoyancy increases the up thrust force causing an increase in fluid velocity. As noted in Fig. 4.7 that the effects of buoyancy force is found to be more pronounced for a fluid with a small Prandtl number Pr . Since fluid with smaller Pr is more susceptible to the effects of buoyancy force. Fig. 4.8 plots the effects of $(\lambda < 0)$ on f' for the case of opposing flow. From this Fig. it is obvious that $(\lambda < 0)$ retards the flow. The influence of λ on f' for the case of assisting flow is plotted in Fig. 4.9. Since for assisting flow $(\lambda > 0)$ means positive value of gravitational force which acts as a quantity which speed up the flow. Thus the fluid velocity increases for the positive values of λ .

Fig. 4.10 shows the simultaneous effects of S_r and D_f (when S_r increases and D_f decreases

by keeping their product constant) on ϕ . It is observed that concentration field ϕ and concentration boundary layer increase. From Fig. 4.11, opposite results are found when S_r decreases and D_f increases by keeping their product constant. The effects of γ on ϕ in the destructive and generative chemical reactions are shown in the Figs. 4.12 and 4.13. It is noted that the effects of generative and destructive chemical reactions on ϕ are quite opposite. Moreover it is also noted that the magnitude for $\gamma > 0$ is smaller than $\gamma < 0$. Fig. 4.14 presents the effects of Schmidt number Sc on the concentration field ϕ . It is noted that concentration field ϕ decreases rapidly with an increase in Sc . Figs. 4.15 and 4.16 show the simultaneous effects of S_r and D_f (when S_r increases and D_f decreases by keeping their product constant) on θ . It is noted that the obtained results are quite opposite to those observed for concentration field. Fig. 4.17 elucidates the variation of Prandtl number Pr on the temperature profile. It is observed that Pr causes a reduction in the temperature profile and a thermal boundary layer. This is in view of the fact that larger Prandtl number yields weaker thermal diffusivity and thinner boundary layer.

Table 4.2 explains the local Sherwood number $Re_x^{-1/2} Sh$ and the local Nusselt number $Re_x^{-1/2} Nu_x$ for M , D_f , S_r , λ and N . It is noted that magnitude of local Sherwood number increases for large values of λ , N and D_f whereas it decreases for large values of M and S_r . Also local Nusselt number increases for large values of λ , N and S_r . Such magnitude decreases when M and D_f are increased

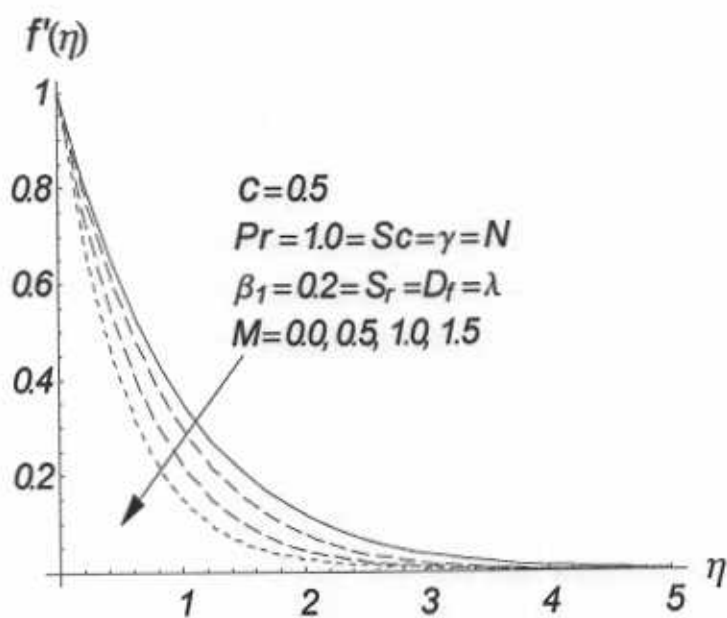


Fig. 4.6 : Influence of M on f' .

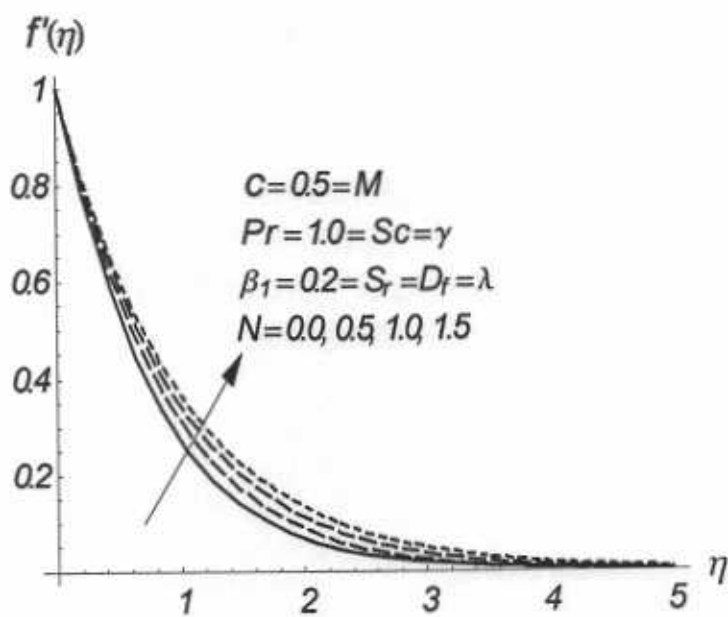


Fig. 4.7 : Influence of N on f' .

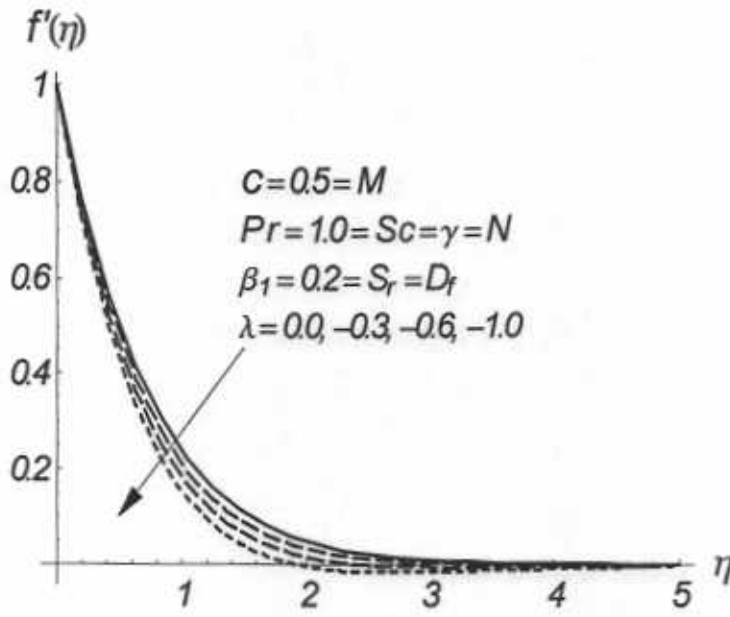


Fig. 4.8 : Influence of $\lambda < 0$ on f' .

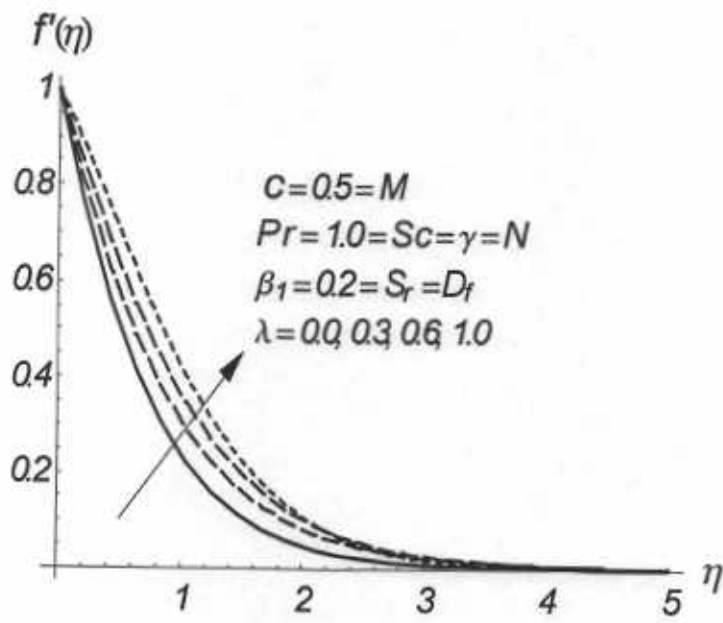


Fig. 4.9 : Influence of $\lambda > 0$ on f' .

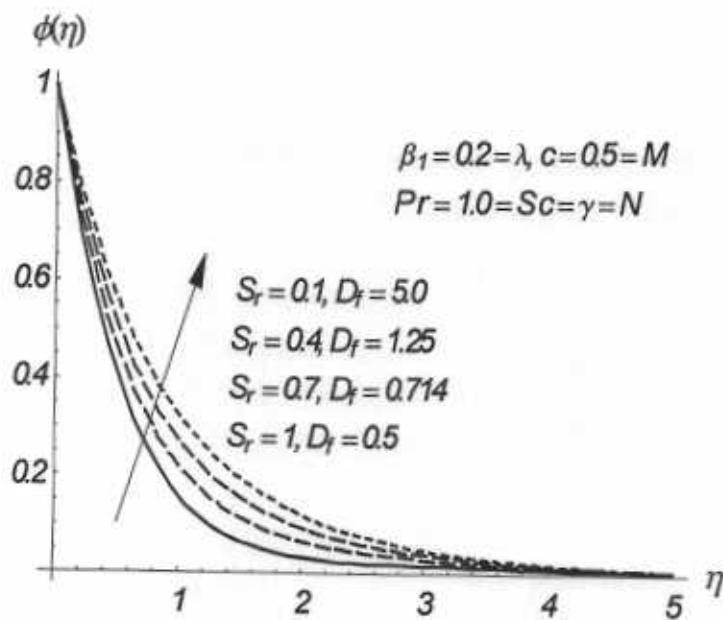


Fig. 4.10 : Influence of S_r and D_f on ϕ .

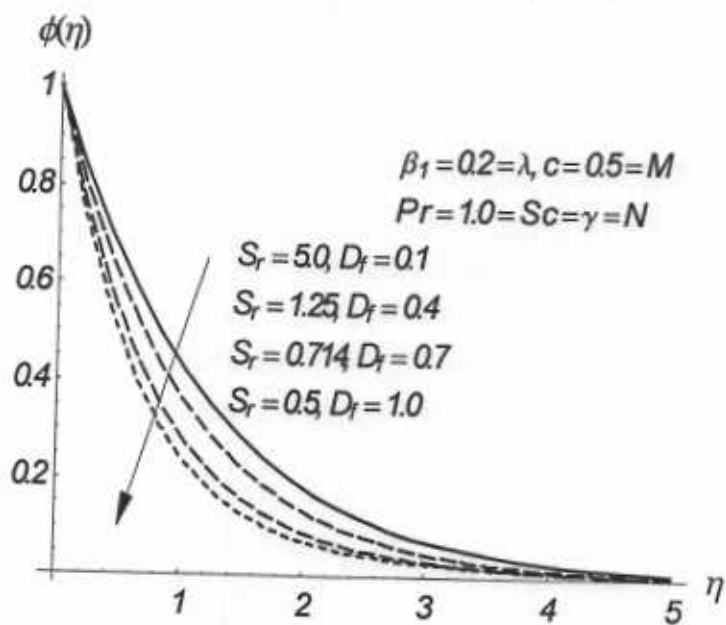


Fig. 4.11 : Influence of S_r and D_f on ϕ .

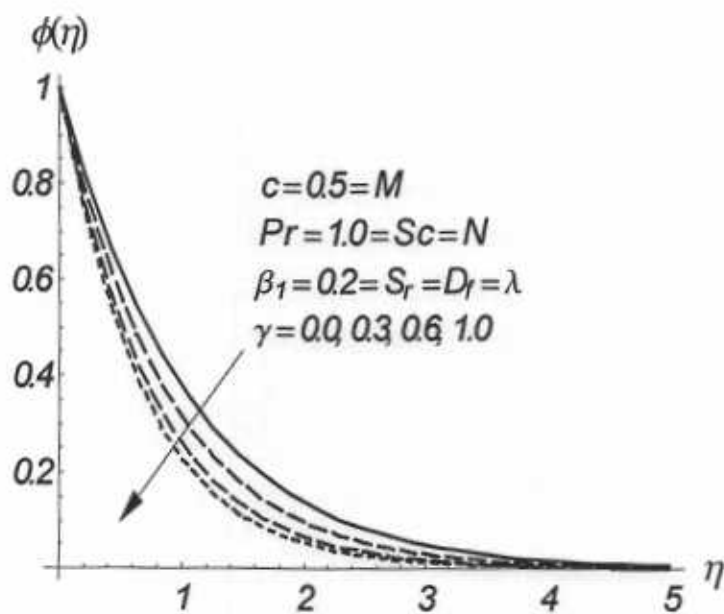


Fig. 4.12 : Influence of $\gamma > 0$ on ϕ .

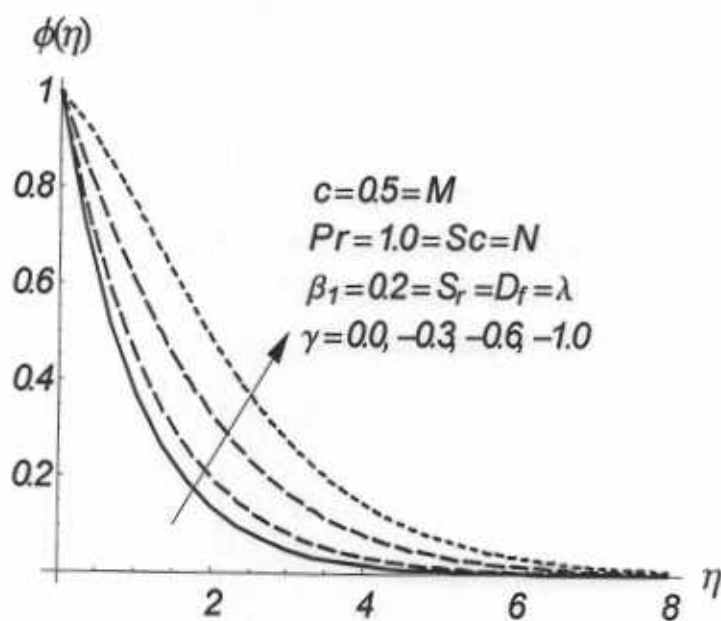


Fig. 4.13 : Influence of $\gamma < 0$ on ϕ .

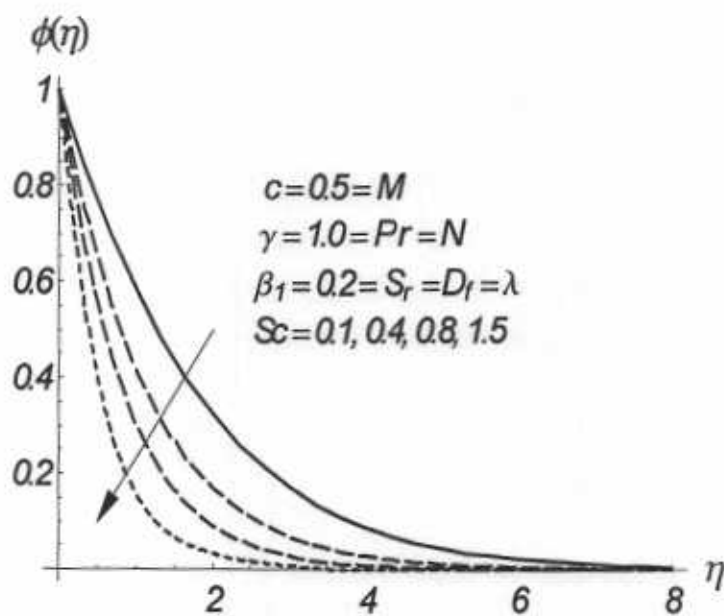


Fig. 4.14 : Influence of Sc on ϕ .

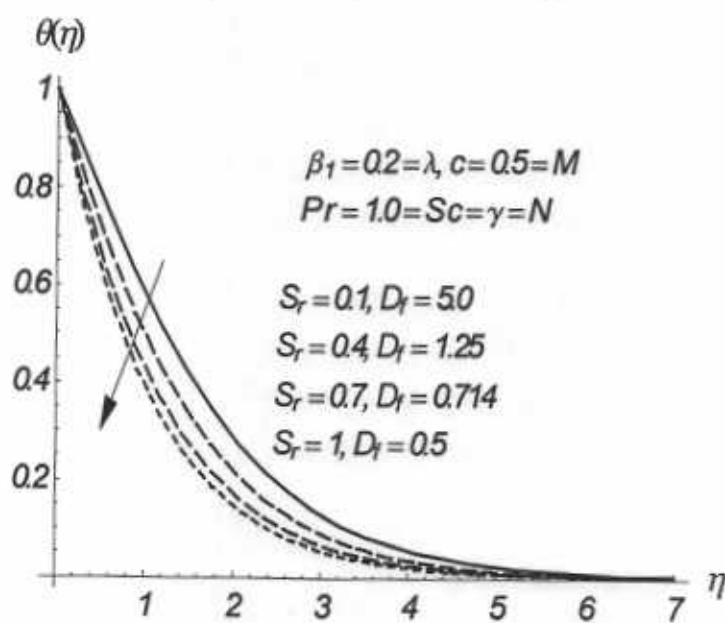


Fig. 4.15 : Influence of S_r and D_f on θ .

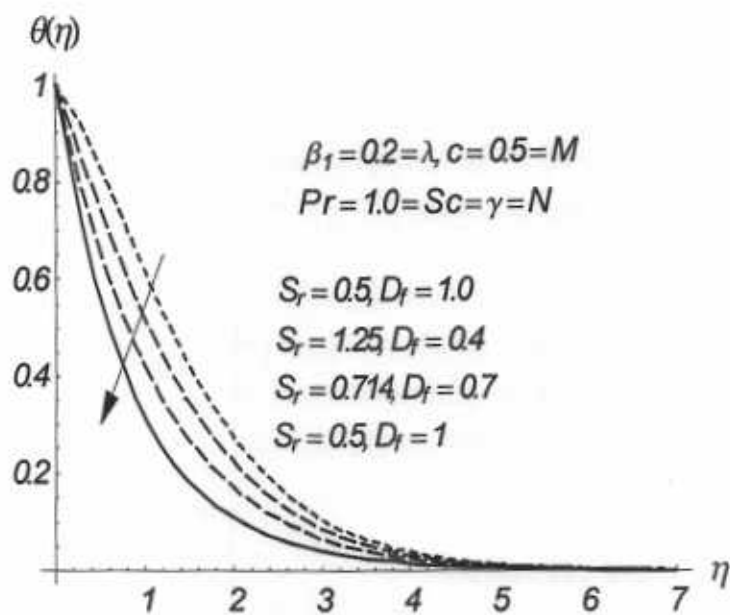


Fig. 4.16 : Influence of S_r and D_f on θ .

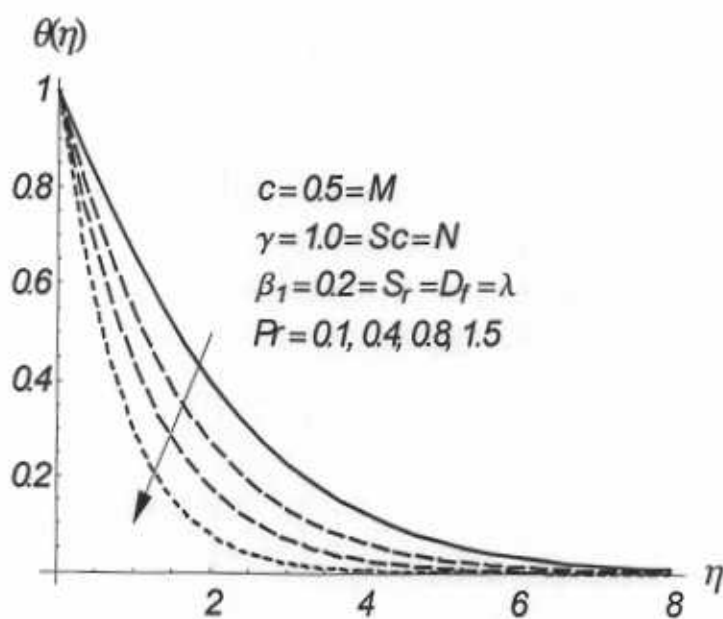


Fig. 4.17 : Influence of Pr on θ .

Table 4.2: Values of local Sherwood number $Re_x^{-1/2} Sh$ and the local Nusselt number $Re_x^{-1/2} Nu_x$ for some values of M , λ , N , D_f and S_r when $c = 0.5$, $\beta_1 = 0.2$ and $Sc = 1.0 = Pr = \gamma$.

M	λ	N	S_r	D_f	$-\phi'(\eta)$	$-\theta'(\eta)$
0.0	0.2	1.0	0.2	0.2	1.44935	0.89620
0.5					1.43829	0.86821
1.0					1.41122	0.79528
0.5	0.2				1.43829	0.86821
	0.4				1.45102	0.89943
	0.6				1.46252	0.92544
	0.2	0.2			1.43400	0.85773
		0.6			1.43616	0.86304
		1.0			1.43829	0.86821
		1.5			1.43829	0.86821
		1.0	0.1	0.2	1.47501	0.86163
			0.2	0.1	1.42332	0.96740
			0.3	0.07	1.37276	1.00012
			0.2	0.1	1.42332	0.96740
			0.1	0.2	1.47501	0.86163
			0.07	0.3	1.49176	0.75679

4.5 Conclusions

Mixed convection three dimensional flow of an upper-convected Maxwell (UCM) fluid with magnetic field, thermal-diffusion and diffusion-thermo effects is explored. The concluding remarks of the presented study are given below.

- It is noted that the magnetic field M opposes the flow.
- An upthrust can be generated by buoyancy which results an increase in fluid velocity.
- Opposite results are obtained in the cases of opposing ($\lambda < 0$) and assisting ($\lambda > 0$) flows.

- Generative ($\gamma < 0$) and destructive ($\gamma > 0$) chemical reactions has opposite results.
- Schmidt number Sc and Prandtl number Pr show a decrease in concentration and temperature profiles.
- Simultaneous effects of Soret S_r and Dufour D_f numbers on the temperature and concentration are quite opposite.

Chapter 5

Similar solutions for three-dimensional flow of an Oldroyd-B fluid over a stretching surface

This chapter deals with the three-dimensional stretched flow of an Oldroyd-B fluid. The governing equations for the three-dimensional flow are modelled and simplified by order analysis. Similarity transforms are invoked to convert the nonlinear partial differential system into coupled system of ordinary differential equations. Computations for the analytic solutions are made through implementation of the homotopy analysis method (HAM). Main emphasis is given to the Deborah number effects in the axisymmetric, two- and three-dimensional flow situations.

5.1 Mathematical analysis

We investigate the three-dimensional flow of an Oldroyd-B fluid. The fluid occupies the region $z > 0$ and bounded by a flat surface situated at $z = 0$ which is stretching linearly to generate

the motion. The governing boundary layer equations for the current analysis are given by

$$\frac{\partial u}{\partial x} + \frac{\partial v}{\partial y} + \frac{\partial w}{\partial z} = 0, \quad (5.1)$$

$$\begin{aligned} u \frac{\partial u}{\partial x} + v \frac{\partial u}{\partial y} + w \frac{\partial u}{\partial z} + \lambda_1 \left(\begin{aligned} &u^2 \frac{\partial^2 u}{\partial x^2} + v^2 \frac{\partial^2 u}{\partial y^2} + w^2 \frac{\partial^2 u}{\partial z^2} \\ &+ 2uv \frac{\partial^2 u}{\partial x \partial y} + 2vw \frac{\partial^2 u}{\partial y \partial z} + 2uw \frac{\partial^2 u}{\partial x \partial z} \end{aligned} \right) \\ = \nu \left[\frac{\partial^2 u}{\partial z^2} + \lambda_2 \left(\begin{aligned} &u \frac{\partial^3 u}{\partial x \partial z^2} + v \frac{\partial^3 u}{\partial y \partial z^2} + w \frac{\partial^3 u}{\partial z^3} \\ &- \frac{\partial u}{\partial x} \frac{\partial^2 u}{\partial x^2} - \frac{\partial u}{\partial y} \frac{\partial^2 u}{\partial y^2} - \frac{\partial u}{\partial z} \frac{\partial^2 u}{\partial z^2} \end{aligned} \right) \right], \quad (5.2) \end{aligned}$$

$$\begin{aligned} u \frac{\partial v}{\partial x} + v \frac{\partial v}{\partial y} + w \frac{\partial v}{\partial z} + \lambda_1 \left(\begin{aligned} &u^2 \frac{\partial^2 v}{\partial x^2} + v^2 \frac{\partial^2 v}{\partial y^2} + w^2 \frac{\partial^2 v}{\partial z^2} \\ &+ 2uv \frac{\partial^2 v}{\partial x \partial y} + 2vw \frac{\partial^2 v}{\partial y \partial z} + 2uw \frac{\partial^2 v}{\partial x \partial z} \end{aligned} \right) \\ = \nu \left[\frac{\partial^2 v}{\partial z^2} + \lambda_2 \left(\begin{aligned} &u \frac{\partial^3 v}{\partial x \partial z^2} + v \frac{\partial^3 v}{\partial y \partial z^2} + w \frac{\partial^3 v}{\partial z^3} \\ &- \frac{\partial v}{\partial x} \frac{\partial^2 v}{\partial x^2} - \frac{\partial v}{\partial y} \frac{\partial^2 v}{\partial y^2} - \frac{\partial v}{\partial z} \frac{\partial^2 v}{\partial z^2} \end{aligned} \right) \right], \quad (5.3) \end{aligned}$$

$$\begin{aligned} u &= u_w(x) = ax, \quad v = v_w(y) = by, \quad w = 0 \quad \text{at } z = 0, \\ u &\rightarrow 0, \quad v \rightarrow 0 \quad \text{as } z \rightarrow \infty, \end{aligned} \quad (5.4)$$

where u, v and w represent the velocity components, ν the kinematic viscosity, (λ_1, λ_2) the relaxation and retardation times respectively and the constants $a > 0$ and $b > 0$.

We write the following similarity transforms

$$\eta = \sqrt{\frac{a}{\nu}} z, \quad u = axf'(\eta), \quad v = ayg'(\eta), \quad w = -\sqrt{a\nu} \{f(\eta) + g(\eta)\}, \quad (5.5)$$

where f and g are the dimensionless velocity components. Using these variables, continuity

equation (5.1) is satisfied automatically and Eqs. (5.2) – (5.4) take the following forms

$$f''' - f'^2 + (f + g)f'' + \beta_1 [2(f + g)f'f'' - (f + g)^2 f'''] + \beta_2 [(f'' + g'')f'' - (f + g)f'''] = 0, \quad (5.6)$$

$$g''' - g'^2 + (f + g)g'' + \beta_1 [2(f + g)g'g'' - (f + g)^2 g'''] + \beta_2 [(f'' + g'')g'' - (f + g)g'''] = 0, \quad (5.7)$$

$$\begin{aligned} f(\eta) + g(\eta) &= 0, \quad f'(\eta) = 1, \quad g'(\eta) = c \quad \text{at } \eta = 0, \\ f'(\eta) &= 0, \quad g'(\eta) = 0, \quad \text{as } \eta \rightarrow \infty. \end{aligned} \quad (5.8)$$

In the aforementioned equations, prime presents the differentiation with respect to η . Moreover β_1 and β_2 are the Deborah numbers in terms of relaxation and retardation times respectively and c is the ratio parameter. These are given by

$$\beta_1 = \lambda_1 a, \quad \beta_2 = \lambda_2 a, \quad c = b/a, \quad (5.9)$$

It is noted that $c = 0 = g$ yields the following two-dimensional case given by

$$f''' - f'^2 + ff'' + \beta_1 [2ff'f'' - f^2 f'''] + \beta_2 [f'^2 - ff'''] = 0, \quad (5.10)$$

$$\begin{aligned} f(\eta) &= 0, \quad f'(\eta) = 1 \quad \text{at } \eta = 0, \\ f'(\eta) &= 0 \quad \text{as } \eta \rightarrow \infty \end{aligned} \quad (5.11)$$

and the axisymmetric flow i.e. ($f = g$) is deduced when $c = 1$. Hence we have

$$f''' - f'^2 + 2ff'' + 4\beta_1 [ff'f'' - f^2 f'''] + 2\beta_2 [f'^2 - ff'''] = 0 \quad (5.12)$$

with the boundary conditions 5.11.

5.2 Analytic solutions

5.2.1 Zeroth-order deformation problems

Our aim is to solve the nonlinear equations (5.6) and (5.7) subject to the boundary conditions (5.8). Thus we have selected the following base functions

$$\{\eta^k \exp(-n\eta) \mid k \geq 0, n \geq 0\} \quad (5.13)$$

and the velocity distributions $f(\eta)$ and $g(\eta)$ are

$$f(\eta) = a_{0,0}^0 + \sum_{n=1}^{\infty} \sum_{k=1}^{\infty} a_{m,n}^k \eta^k \exp(-n\eta), \quad (5.14)$$

$$g(\eta) = A_{0,0}^0 + \sum_{n=1}^{\infty} \sum_{k=1}^{\infty} A_{m,n}^k \eta^k \exp(-n\eta), \quad (5.15)$$

where $a_{m,n}^k$ and $A_{m,n}^k$ are the coefficients. The initial guesses $f_0(\eta)$, $g_0(\eta)$ and the linear operator \mathcal{L} are selected as

$$f_0(\eta) = 1 - \exp(-\eta), \quad (5.16)$$

$$g_0(\eta) = c(1 - \exp(-\eta)), \quad (5.17)$$

$$\mathcal{L}(f) = f''' - f', \quad (5.18)$$

with the following property

$$\mathcal{L}[C_1 + C_2 \exp(\eta) + C_3 \exp(-\eta)] = 0, \quad (5.19)$$

where $C_1 - C_3$ are the constants.

The problems at the zeroth order are

$$(1-p)\mathcal{L}[\bar{f}(\eta, p) - f_0(\eta)] = p\hbar_f \mathcal{N}_f[\bar{f}(\eta, p), \bar{g}(\eta, p)], \quad (5.20)$$

$$(1-p)\mathcal{L}[\bar{g}(\eta, p) - g_0(\eta)] = p\hbar_g \mathcal{N}_g[\bar{f}(\eta, p), \bar{g}(\eta, p)], \quad (5.21)$$

$$\begin{aligned}\bar{f}(0, p) + \bar{g}(0, p) &= 0, \bar{f}'(0, p) = 1, \bar{g}'(0, p) = c, \\ \bar{f}'(\infty, p) &= 0, \bar{g}'(\infty, p) = 0,\end{aligned}\tag{5.22}$$

where the nonlinear operators \mathcal{N}_f and \mathcal{N}_g are defined as

$$\begin{aligned}\mathcal{N}_f[\bar{f}(\eta, p), \bar{g}(\eta, p)] &= \frac{\partial^3 \bar{f}}{\partial \eta^3} - \left(\frac{\partial \bar{f}}{\partial \eta}\right)^2 + \{\bar{f}(\eta, p) + \bar{g}(\eta, p)\} \frac{\partial^2 \bar{f}}{\partial \eta^2} \\ &+ \beta_1 \left[\begin{aligned} &2\{\bar{f}(\eta, p) + \bar{g}(\eta, p)\} \bar{f}'(\eta, p) \bar{f}''(\eta, p) \\ &-\{\bar{f}(\eta, p) + \bar{g}(\eta, p)\}^2 \bar{f}'''(\eta, p) \end{aligned} \right] \\ &+ \beta_2 \left[\begin{aligned} &\bar{f}''(\eta, p) \bar{f}''(\eta, p) + \bar{g}''(\eta, p) \bar{f}''(\eta, p) \\ &-\{\bar{f}(\eta, p) + \bar{g}(\eta, p)\} \bar{f}''''(\eta, p) \end{aligned} \right],\end{aligned}\tag{5.23}$$

$$\begin{aligned}\mathcal{N}_g[\bar{f}(\eta, p), \bar{g}(\eta, p)] &= \frac{\partial^3 \bar{g}}{\partial \eta^3} - \left(\frac{\partial \bar{g}}{\partial \eta}\right)^2 + \{\bar{f}(\eta, p) + \bar{g}(\eta, p)\} \frac{\partial^2 \bar{g}}{\partial \eta^2} \\ &+ \beta_1 \left[\begin{aligned} &2\{\bar{f}(\eta, p) + \bar{g}(\eta, p)\} \bar{g}'(\eta, p) \bar{g}''(\eta, p) \\ &-\{\bar{f}(\eta, p) + \bar{g}(\eta, p)\}^2 \bar{g}'''(\eta, p) \end{aligned} \right] \\ &+ \beta_2 \left[\begin{aligned} &\bar{f}''(\eta, p) \bar{g}''(\eta, p) + \bar{g}''(\eta, p) \bar{g}''(\eta, p) \\ &-\{\bar{f}(\eta, p) + \bar{g}(\eta, p)\} \bar{g}''''(\eta, p) \end{aligned} \right]\end{aligned}\tag{5.24}$$

and (\hbar_f, \hbar_g) are the auxiliary non-zero parameters which are useful in controlling the convergence of the series solutions. Moreover $p \in [0, 1]$ is an embedding parameter. It is noted that when $p = 0$ and $p = 1$ then

$$\bar{f}(\eta, 0) = f_0(\eta), \quad \bar{f}(\eta, 1) = f(\eta),\tag{5.25}$$

$$\bar{g}(\eta, 0) = g_0(\eta), \quad \bar{g}(\eta, 1) = g(\eta).\tag{5.26}$$

Furthermore when p varies from 0 to 1 then the initial guesses $f_0(\eta)$ and $g_0(\eta)$ approach to final solutions $f(\eta)$ and $g(\eta)$ respectively and through Taylor's series expansion we write

$$\bar{f}(\eta, p) = f_0(\eta) + \sum_{m=1}^{\infty} f_m(\eta) p^m,\tag{5.27}$$

$$\bar{g}(\eta, p) = g_0(\eta) + \sum_{m=1}^{\infty} g_m(\eta) p^m,\tag{5.28}$$

$$f_m(\eta) = \frac{1}{m!} \left. \frac{\partial^m \bar{f}(\eta, p)}{\partial p^m} \right|_{p=0}, \quad (5.29)$$

$$g_m(\eta) = \frac{1}{m!} \left. \frac{\partial^m \bar{g}(\eta, p)}{\partial p^m} \right|_{p=0}. \quad (5.30)$$

Note that the convergence of series (5.27) and (5.28) depends upon the auxiliary parameters \hbar_f and \hbar_g . The values of \hbar_f and \hbar_g are selected in such a way that the equations (5.27) and (5.28) converge at $p = 1$. Hence we write

$$f(\eta) = f_0(\eta) + \sum_{m=1}^{\infty} f_m(\eta), \quad (5.31)$$

$$g(\eta) = g_0(\eta) + \sum_{m=1}^{\infty} g_m(\eta). \quad (5.32)$$

5.2.2 *m*th order deformation problems

The problems at this order satisfy the following definitions

$$\mathcal{L}[f_m(\eta, p) - \chi_m f_{m-1}(\eta)] = \hbar_f \mathcal{R}_{f,m}(\eta), \quad (5.33)$$

$$\mathcal{L}[g_m(\eta, p) - \chi_m g_{m-1}(\eta)] = \hbar_g \mathcal{R}_{g,m}(\eta), \quad (5.34)$$

$$f_m(0) + g_m(0) = f'_m(0) = f'_m(\infty) = g'_m(0) = g'_m(\infty) = 0, \quad (5.35)$$

$$\chi_m = \begin{cases} 0, & m \leq 1 \\ 1, & m > 1 \end{cases}, \quad (5.36)$$

$$\begin{aligned}
\mathcal{R}_{f,m}(\eta) &= f_{m-1}''' + \sum_{k=0}^{m-1} \{(f_{m-1-k} + g_{m-1-k})f_k'' - f_{m-1-k}'f_k'\} \\
&+ \beta_1 \sum_{k=0}^{m-1} \sum_{l=0}^k \left\{ \begin{array}{l} 2(f_{m-1-k} + g_{m-1-k})f_{k-l}'f_l'' \\ -(f_{m-1-k}f_{k-l} + g_{m-1-k}g_{k-l} + 2f_{m-1-k}g_{k-l})f_l''' \end{array} \right\} \\
&+ \beta_2 \sum_{k=0}^{m-1} \{(f_{m-1-k}'' + g_{m-1-k}'')f_k'' - (f_{m-1-k} + g_{m-1-k})f_k'''\}, \quad (5.37)
\end{aligned}$$

$$\begin{aligned}
\mathcal{R}_{g,m}(\eta) &= g_{m-1}''' + \sum_{k=0}^{m-1} \{(f_{m-1-k} + g_{m-1-k})g_k'' - g_{m-1-k}'g_k'\} \\
&+ \beta_1 \sum_{k=0}^{m-1} \sum_{l=0}^k \left\{ \begin{array}{l} 2(f_{m-1-k} + g_{m-1-k})g_{k-l}'g_l'' \\ -(f_{m-1-k}f_{k-l} + g_{m-1-k}g_{k-l} + 2f_{m-1-k}g_{k-l})g_l''' \end{array} \right\} \\
&+ \beta_2 \sum_{k=0}^{m-1} \{(f_{m-1-k}'' + g_{m-1-k}'')g_k'' - (f_{m-1-k} + g_{m-1-k})g_k'''\}. \quad (5.38)
\end{aligned}$$

5.3 Convergence of the HAM solution

To find the suitable values of \hbar_f and \hbar_g so that the Eqs. (5.31) and (5.32) converge, the so called \hbar -curves are displayed in Fig. 5.1. This Fig. shows that the proper ranges here are $-1.6 \leq \hbar_f \leq -0.5$ and $-1.5 \leq \hbar_g \leq -0.3$. In Figs. 5.2 and 5.3 the \hbar -curves for error analysis are sketched. It is seen that $\hbar_f = \hbar_g = -0.85$ give better approximation when compared with the others.

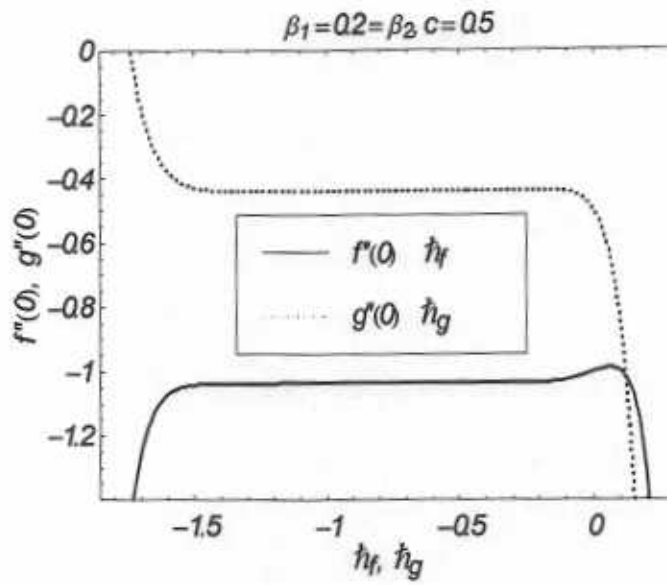


Fig. 5.1 : h curves of $f''(0)$ and $g''(0)$ at the 15th order of approximation.

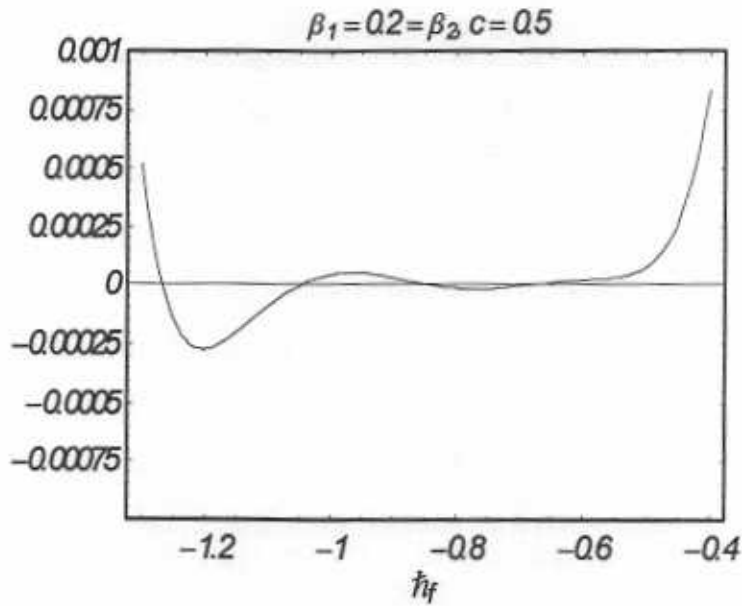


Fig. 5.2 : h curve for residual error in $f(\eta)$ at the 15th order of approximation.

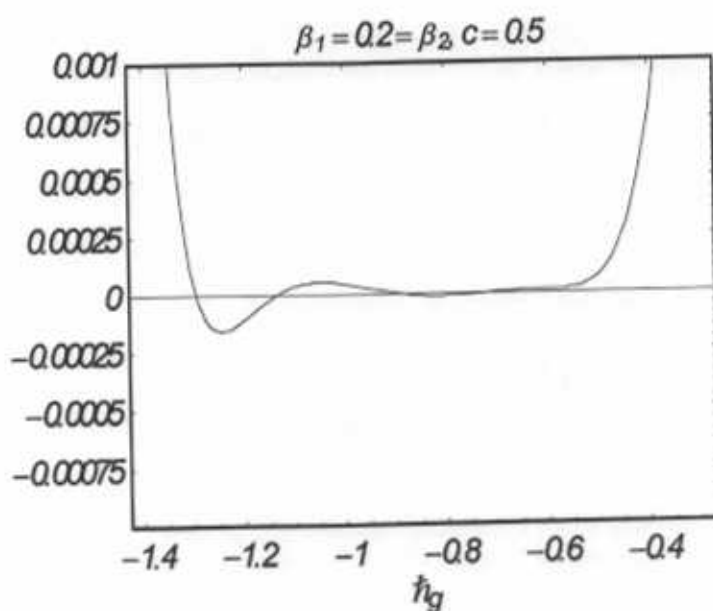


Fig. 5.3 : h curve for residual error in $g(\eta)$ at the 15th order of approximation.

Table 5.1: Convergence of the HAM solutions for different order of approximations when $\beta_1 = 0.2 = \beta_2$ and $c = 0.5$

Order of approximation	$-f''(0)$	$-g''(0)$
1	1.01666	0.43166
2	1.03522	0.43385
5	1.03448	0.43779
10	1.03474	0.43747
15	1.03473	0.43743
20	1.03473	0.43742
25	1.03473	0.43742
30	1.03473	0.43742
40	1.03473	0.43742
50	1.03473	0.43742

5.4 Results and discussion

In this section we have plotted the graphs for different values of β_2 on f' and g' for two-dimensional, three-dimensional and axisymmetric flow situations whereas the graphs for β_1 in such situations are not presented here because it is already mentioned in chapter 1. Fig. 5.4 presents the effects of Deborah number β_2 on f' . It is noted that velocity profile increases with an increase in β_2 . Since β_2 is proportional to retardation time λ_2 . Physically an increase in retardation time of any material enhances the flow. It is also observed that the effects of β_2 on f' are quite opposite to the effects of β_1 on f' (as shown in chapter 1). The effects of β_2 on f' and g' for the case of three-dimensional flow situations are portrayed in Figs. 5.5 and 5.6. The obtained results are qualitatively similar to the case of two-dimensional flow. Fig. 5.7 elucidates the effects of β_2 on f' for an axisymmetric flow. It is observed that the obtained results in this case are similar to those obtained for the two- and three-dimensional flow situations. It is because of the fact that axisymmetry will only makes the flow symmetric about axes and will not disturb the flow behavior. Table 5.2 presents a comparative study of present results with those given in [81]. It is observed that obtained results are in a good agreement with the published results [81].

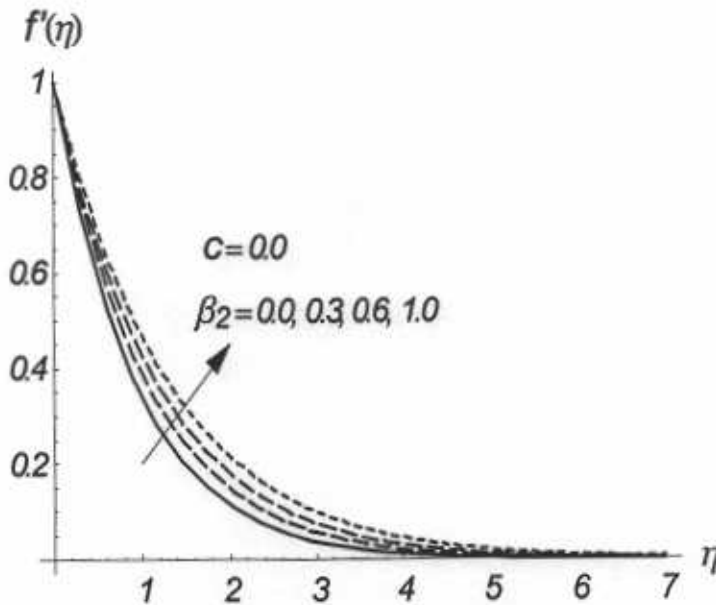


Fig. 5.4 : Influence of β_2 on f' for 2D flow.

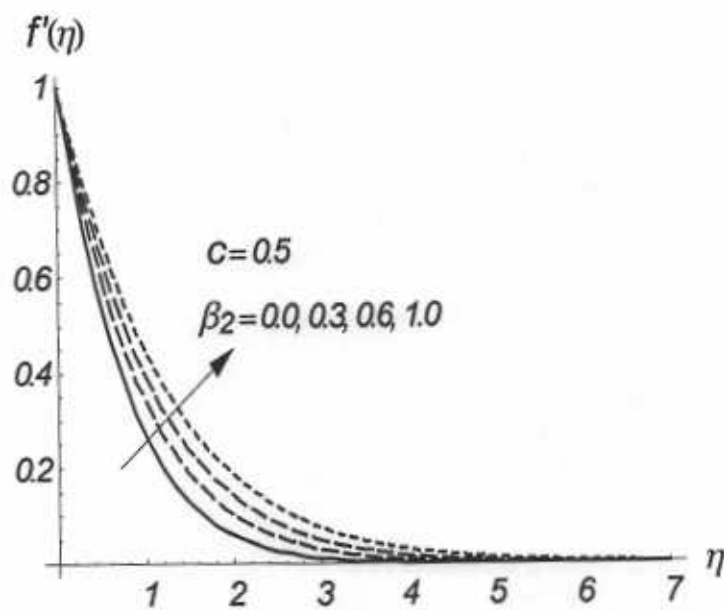


Fig. 5.5 : Influence of β_2 on f' for 3D flow.

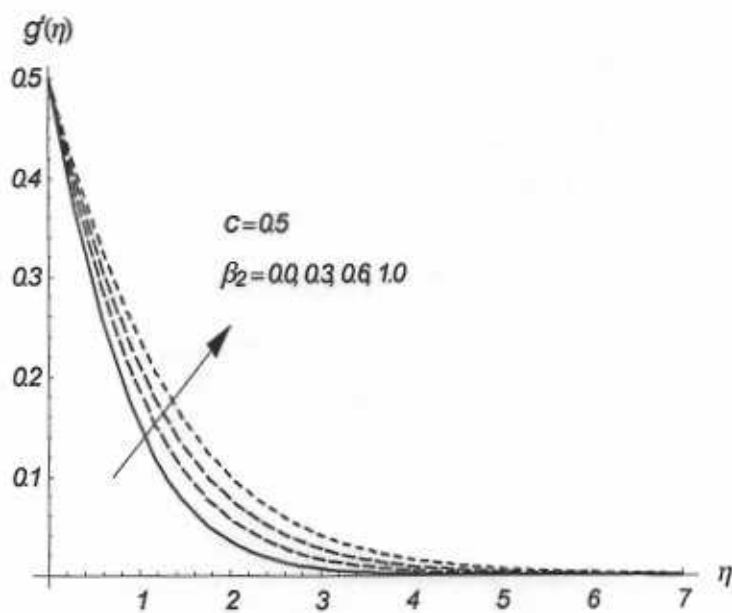


Fig. 5.6 : Influence of β_2 on g' for 3D flow.

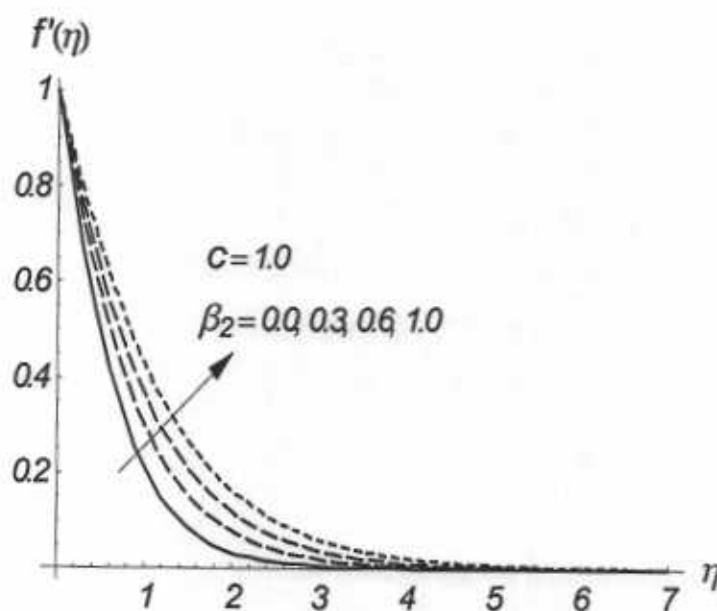


Fig. 5.7 : Influence of β_2 on f' for axisymmetric flow.

Table 5.2: Comparison of values of $-f''(0)$ and $-g''(0)$ for UCM fluid case ($\beta_2 = 0$) with those of Hayat and Awais [81] when $\beta_1 = 0.2$ and $c = 0.5$.

Order of approximation	Present results		Hayat and Awais [81]	
	$-f''(0)$	$-g''(0)$	$-f''(0)$	$-g''(0)$
1	1.153750	0.490625	1.153750	0.490625
5	1.181869	0.502042	1.181869	0.502042
10	1.182117	0.501999	1.182117	0.501999
15	1.182123	0.501996	1.182123	0.501996
20	1.182124	0.501996	1.182124	0.501996
30	1.182124	0.501996	1.182124	0.501996
50	1.182124	0.501996	1.182124	0.501996

5.5 Final remarks

The three-dimensional flow of an Oldroyd-B fluid over a stretching sheet is examined. Limiting results for the two dimensional and axisymmetric flows can be deduced for the cases of upper convected Maxwell (UCM) and viscous fluids.

- Deborah number β_2 enhances the flow.
- The effects of β_1 on f' are quite opposite to those of β_2 .
- Residual errors have been plotted to show the validity.
- Results for the flow of Maxwell fluid can be reduced by setting $\beta_2 = 0$.

Chapter 6

Three-dimensional flow of Jeffery fluid over a linearly stretching sheet

This chapter models the three-dimensional flow of Jeffery fluid over a linearly stretching surface. Transformation method has been utilized for the reduction of partial differential equations into the coupled nonlinear system of ordinary differential equations. The solutions of the nonlinear system is presented by homotopy analysis method. The reported graphical results are analyzed and a comparative study is made to validate the present results.

6.1 Mathematical formulation

Here we studied an incompressible flow of a Jeffery fluid over a flat surface located at $z = 0$. The fluid fills the space $z > 0$ and the motion of the fluid is caused by stretching of a surface. The continuity and momentum equations subject to boundary layer approximations give

$$\frac{\partial u}{\partial x} + \frac{\partial v}{\partial y} + \frac{\partial w}{\partial z} = 0, \quad (6.1)$$

$$u \frac{\partial u}{\partial x} + v \frac{\partial u}{\partial y} + w \frac{\partial u}{\partial z} = \frac{\nu}{1 + \lambda_1} \left[\frac{\partial^2 u}{\partial z^2} + \lambda_2 \left(\frac{\partial u}{\partial z} \frac{\partial^2 u}{\partial x \partial z} + \frac{\partial v}{\partial z} \frac{\partial^2 u}{\partial y \partial z} + \frac{\partial w}{\partial z} \frac{\partial^2 u}{\partial z^2} \right) \right. \\ \left. + u \frac{\partial^3 u}{\partial x \partial z^2} + v \frac{\partial^3 u}{\partial y \partial z^2} + w \frac{\partial^3 u}{\partial z^3} \right], \quad (6.2)$$

$$u \frac{\partial v}{\partial x} + v \frac{\partial v}{\partial y} + w \frac{\partial v}{\partial z} = \frac{\nu}{1 + \lambda_1} \left[\frac{\partial^2 v}{\partial z^2} + \lambda_2 \left(\frac{\partial u}{\partial z} \frac{\partial^2 v}{\partial x \partial z} + \frac{\partial v}{\partial z} \frac{\partial^2 v}{\partial y \partial z} + \frac{\partial w}{\partial z} \frac{\partial^2 v}{\partial z^2} \right) \right. \\ \left. + u \frac{\partial^3 v}{\partial x \partial z^2} + v \frac{\partial^3 v}{\partial y \partial z^2} + w \frac{\partial^3 v}{\partial z^3} \right] \quad (6.3)$$

and the associated boundary conditions are

$$u = u_w(x) = ax, \quad v = v_w(y) = by, \quad w = 0 \quad \text{at } z = 0, \\ u \rightarrow 0, \quad v \rightarrow 0 \quad \text{as } z \rightarrow \infty, \quad (6.4)$$

where u , v and w are the velocities in the x , y and z directions respectively, ν denote the kinematic viscosity, λ_1 the ratio of relaxation and retardation times, λ_2 the retardation time and the constants $a > 0$ and $b > 0$.

If prime denotes the differentiation with respect to η then setting

$$\eta = \sqrt{\frac{a}{\nu}} z, \quad u = axf'(\eta), \quad v = ayg'(\eta), \quad w = -\sqrt{a\nu} \{f(\eta) + g(\eta)\} \quad (6.5)$$

Eq. (6.1) is satisfied automatically and Eqs. (6.2) – (6.4) yield

$$f''' + (1 + \lambda_1) [(f + g)f'' - (f')^2] + \beta_2 [(f'')^2 - (f + g)f'''' - g'f'''] = 0, \quad (6.6)$$

$$g''' + (1 + \lambda_1) [(f + g)g'' - (g')^2] + \beta_2 [(g'')^2 - (f + g)g'''' - f'g'''] = 0, \quad (6.7)$$

$$f(\eta) + g(\eta) = 0, \quad f'(\eta) = 1, \quad g'(\eta) = c \quad \text{at } \eta = 0, \\ f'(\eta) = 0, \quad g'(\eta) = 0 \quad \text{as } \eta \rightarrow \infty, \quad (6.8)$$

where the Deborah number β_2 and the ratio parameter c are

$$\beta_2 = \lambda_2 a, \quad c = b/a. \quad (6.9)$$

It is worth mentioning to note that the resulting problems for three-dimensional flow of viscous fluid can be deduced when $\beta_2 = 0 = \lambda_1$ [41]. These problems corresponds to two-dimensional

flow of Jeffery fluid when $g = 0 = c$. For $c = 1.0$, we recover the axisymmetric flow (i.e. $f = g$) of a Jeffery fluid. Two-dimensional flow in viscous fluid is obtained when $c = 0 = g = \beta_2 = \lambda_1$.

6.2 Solution methodology

6.2.1 Zeroth-order deformation problems

In order to proceed for the series solution, let us consider the base functions of the form

$$\left\{ \eta^k \exp(-n\eta) \mid k \geq 0, n \geq 0 \right\} \quad (6.10)$$

where the velocity distributions $f(\eta)$ and $g(\eta)$ are expressed as

$$f(\eta) = a_{0,0}^0 + \sum_{n=1}^{\infty} \sum_{k=1}^{\infty} a_{m,n}^k \eta^k \exp(-n\eta), \quad (6.11)$$

$$g(\eta) = A_{0,0}^0 + \sum_{n=1}^{\infty} \sum_{k=1}^{\infty} A_{m,n}^k \eta^k \exp(-n\eta), \quad (6.12)$$

in which $a_{m,n}^k$ and $A_{m,n}^k$ are coefficients. The initial guesses $f_0(\eta)$, $g_0(\eta)$ and the linear operator \mathcal{L} for the considered problem are selected as follows:

$$f_0(\eta) = 1 - \exp(-\eta), \quad (6.13)$$

$$g_0(\eta) = c(1 - \exp(-\eta)), \quad (6.14)$$

$$\mathcal{L}(f) = f''' - f', \quad (6.15)$$

with

$$\mathcal{L}[C_1 + C_2 \exp(\eta) + C_3 \exp(-\eta)] = 0, \quad (6.16)$$

where $C_1 - C_3$ are the constants.

The zeroth order deformation problems are

$$(1-p)\mathcal{L}[\bar{f}(\eta, p) - f_0(\eta)] = p\hbar_f \mathcal{N}_f[\bar{f}(\eta, p), \bar{g}(\eta, p)], \quad (6.17)$$

$$(1-p)\mathcal{L}[\bar{g}(\eta, p) - g_0(\eta)] = p\hbar_g \mathcal{N}_g[\bar{f}(\eta, p), \bar{g}(\eta, p)], \quad (6.18)$$

$$\begin{aligned} \bar{f}(0, p) + \bar{g}(0, p) &= 0, \bar{f}'(0, p) = 1, \bar{g}'(0, p) = c, \\ \bar{f}'(\infty, p) &= 0, \bar{g}'(\infty, p) = 0. \end{aligned} \quad (6.19)$$

In Eqs. (6.17) and (6.18), the nonlinear operators \mathcal{N}_f and \mathcal{N}_g are defined as

$$\begin{aligned} \mathcal{N}_f[\bar{f}(\eta, p), \bar{g}(\eta, p)] &= \frac{\partial^3 \bar{f}}{\partial \eta^3} + (1 + \lambda_1) \left[\{\bar{f}(\eta, p) + \bar{g}(\eta, p)\} \frac{\partial^2 \bar{f}}{\partial \eta^2} - \left(\frac{\partial \bar{f}}{\partial \eta} \right)^2 \right] \\ &+ \beta_2 \left[\begin{aligned} &\bar{f}''(\eta, p) \bar{f}'''(\eta, p) - \bar{g}'(\eta, p) \bar{f}''''(\eta, p) \\ &- \{\bar{f}(\eta, p) + \bar{g}(\eta, p)\} \bar{f}''''(\eta, p) \end{aligned} \right], \end{aligned} \quad (6.20)$$

$$\begin{aligned} \mathcal{N}_g[\bar{f}(\eta, p), \bar{g}(\eta, p)] &= \frac{\partial^3 \bar{g}}{\partial \eta^3} + (1 + \lambda_1) \left[\{\bar{f}(\eta, p) + \bar{g}(\eta, p)\} \frac{\partial^2 \bar{g}}{\partial \eta^2} - \left(\frac{\partial \bar{g}}{\partial \eta} \right)^2 \right] \\ &+ \beta_2 \left[\begin{aligned} &\bar{g}''(\eta, p) \bar{g}'''(\eta, p) - \bar{f}'(\eta, p) \bar{g}''''(\eta, p) \\ &- \{\bar{f}(\eta, p) + \bar{g}(\eta, p)\} \bar{g}''''(\eta, p) \end{aligned} \right]. \end{aligned} \quad (6.21)$$

In Eqs. (6.17) and (6.18), the \hbar_f and \hbar_g are the auxiliary non-zero parameters whereas $p \in [0, 1]$ is an embedding parameter. It is noted that when $p = 0$ and $p = 1$ then

$$\bar{f}(\eta, 0) = f_0(\eta), \quad \bar{f}(\eta, 1) = f(\eta), \quad (6.22)$$

$$\bar{g}(\eta, 0) = g_0(\eta), \quad \bar{g}(\eta, 1) = g(\eta). \quad (6.23)$$

The initial guesses $f_0(\eta)$ and $g_0(\eta)$ approach to final solutions $f(\eta)$ and $g(\eta)$ respectively when p varies from 0 to 1 and through Taylor's series expansion we write

$$\bar{f}(\eta, p) = f_0(\eta) + \sum_{m=1}^{\infty} f_m(\eta) p^m, \quad (6.24)$$

$$\bar{g}(\eta, p) = g_0(\eta) + \sum_{m=1}^{\infty} g_m(\eta) p^m, \quad (6.25)$$

$$f_m(\eta) = \frac{1}{m!} \left. \frac{\partial^m \bar{f}(\eta, p)}{\partial p^m} \right|_{p=0}, \quad (6.26)$$

$$g_m(\eta) = \frac{1}{m!} \left. \frac{\partial^m \bar{g}(\eta, p)}{\partial p^m} \right|_{p=0}. \quad (6.27)$$

The convergence of series (6.24) and (6.25) strongly depends upon the auxiliary parameters \hbar_f and \hbar_g . The values of \hbar_f and \hbar_g are chosen in such a way that the series (6.24) and (6.25) converge when $p = 1$. Thus Eqs. (6.24) and (6.25) are reduced as follows

$$f(\eta) = f_0(\eta) + \sum_{m=1}^{\infty} f_m(\eta), \quad (6.28)$$

$$g(\eta) = g_0(\eta) + \sum_{m=1}^{\infty} g_m(\eta). \quad (6.29)$$

6.2.2 *m*th order deformation problems

The *m*th order problems are given by

$$\mathcal{L}[f_m(\eta, p) - \chi_m f_{m-1}(\eta)] = \hbar_f \mathcal{R}_{f,m}(\eta), \quad (6.30)$$

$$\mathcal{L}[g_m(\eta, p) - \chi_m g_{m-1}(\eta)] = \hbar_g \mathcal{R}_{g,m}(\eta), \quad (6.31)$$

$$f_m(0) + g_m(0) = f'_m(0) = f'_m(\infty) = g'_m(0) = g'_m(\infty) = 0, \quad (6.32)$$

$$\chi_m = \begin{cases} 0, & m \leq 1 \\ 1, & m > 1 \end{cases}, \quad (6.33)$$

$$\begin{aligned} \mathcal{R}_{f,m}(\eta) = & f'''_{m-1} + (1 + \lambda_1) \sum_{k=0}^{m-1} \{(f_{m-1-k} + g_{m-1-k})f''_k - f'_{m-1-k}f'_k\} \\ & + \beta_2 \sum_{k=0}^{m-1} \{f''_{m-1-k}f''_k - g'_{m-1-k}f'''_k - (f_{m-1-k} + g_{m-1-k})f'''_k\}, \end{aligned} \quad (6.34)$$

$$\begin{aligned} \mathcal{R}_{g,m}(\eta) = & g'''_{m-1} + (1 + \lambda_1) \sum_{k=0}^{m-1} \{(f_{m-1-k} + g_{m-1-k})g''_k - g'_{m-1-k}g'_k\} \\ & + \beta_2 \sum_{k=0}^{m-1} \{g''_{m-1-k}g''_k - f'_{m-1-k}g'''_k - (f_{m-1-k} + g_{m-1-k})g'''_k\}. \end{aligned} \quad (6.35)$$

6.3 Convergence procedure

In order to find the convergent solutions for the velocity components f and g we have plotted the h_f and h_g -curves at the 15th order of approximation (see Fig. 6.1). These curves give the admissible ranges of the auxiliary parameters h_f and h_g . It is noted that the admissible values are $-1.5 \leq (h_f, h_g) \leq -0.4$. In order to validate the obtained results we have plotted the h -curves for the residual errors in f and g (see Figs. 6.2 and 6.3). It is noticed the obtained solutions are convergent upto 6th decimal place (see Table 6.1).

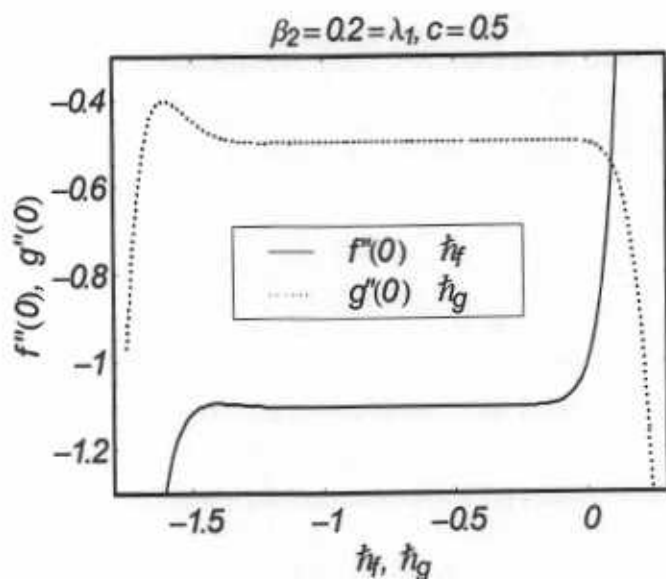


Fig. 6.1 : h curves of $f''(0)$ and $g''(0)$ at the 15th order of approximation.

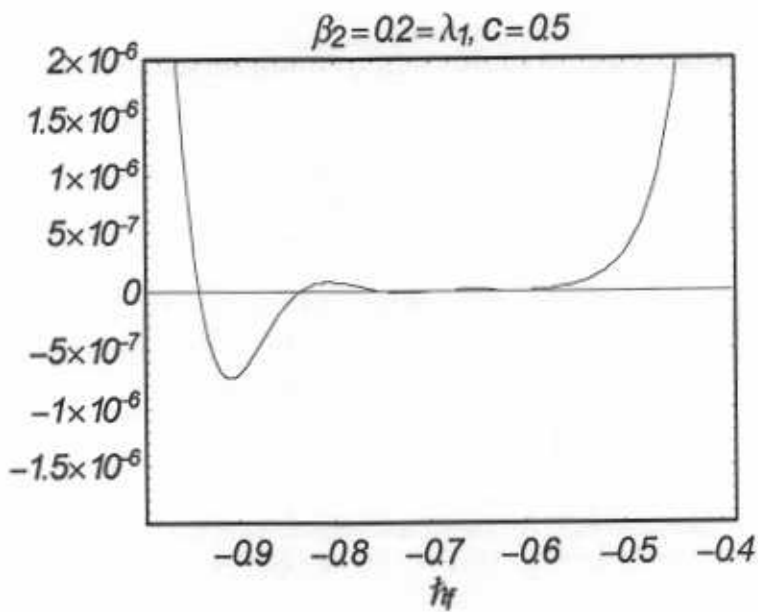


Fig. 6.2 : h curve for residual error in $f(\eta)$ at the 15th order of approximation.

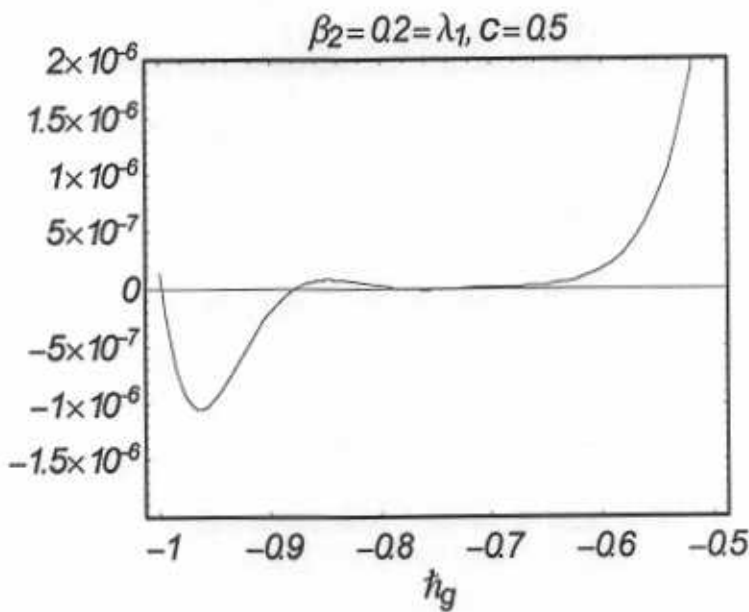


Fig. 6.3 : h curve for residual error in $g(\eta)$ at the 15th order of approximation.

Table 6.1: Convergence of the series solutions for different order of approximations when $\beta = 0.2 = \lambda_1$ and $c = 0.5$

order of approximation	$-f''(0)$	$-g''(0)$
1	1.058333	0.495833
2	1.084270	0.495468
5	1.101755	0.497607
10	1.102571	0.498116
15	1.102582	0.498118
20	1.102582	0.498118
25	1.102582	0.498118
30	1.102582	0.498118
40	1.102582	0.498118
50	1.102582	0.498118

6.4 Results and discussion

Here Figs. 6.4 – 6.11 have been prepared to predict the effects of physical parameters such as Deborah number β_2 and ratio of relaxation and retardation times λ_1 on f' and g' for axisymmetric, two-and three-dimensional flows respectively. The variation of β_2 on f' for two-dimensional flow is shown in the Fig. 6.4. This Fig. illustrates that f' and associated boundary layer are increasing functions of β_2 . Since β_2 is dependent on λ_2 (retardation time) and the fluid velocity increases with an increase in retardation time. This fact is quite obvious from Fig. 6.4. On the other hand it is noted from Fig. 6.5 that the velocity field f' and boundary layer thickness decrease with an increase in λ_1 for two-dimensional flow. It is because of the fact that λ_1 being the viscoelastic parameter exhibit both viscous and elastic characteristics. Thus the fluid will always retard whenever viscosity or elasticity will increase. Figs. 6.6 – 6.9 show the effects of β_2 and λ_1 on f' and g' for the case of three-dimensional flow. It is observed that the results obtained in three-dimensional case are quite similar to the two-dimensional case. Since the surface is stretched uniformly in the x - and y -directions so the behaviors of β_2 and λ_1 on g' (second component of velocity) are also qualitatively similar to that of f' (first component of velocity). Figs. 6.10 and 6.11 give the effects of β_2 and λ_1 on f' for the case of

axisymmetric flow. The obtained results are qualitatively similar to those obtained for two- and three-dimensional flows. Table 6.2 is made in order to compare the present results obtained by HAM with HPM and exact solution given by Ariel [41]. It is found that present solution has a good agreement with an exact solution in the limiting situations

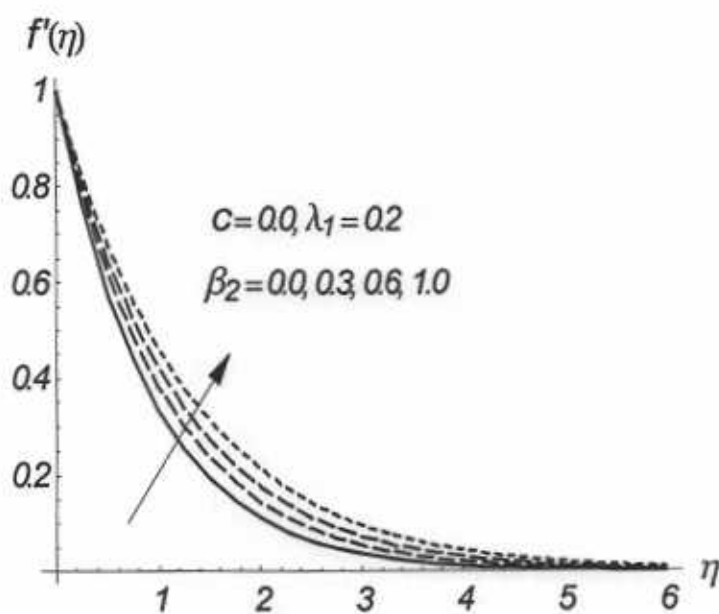


Fig. 6.4 : Influence of β_2 on f' for 2D flow.

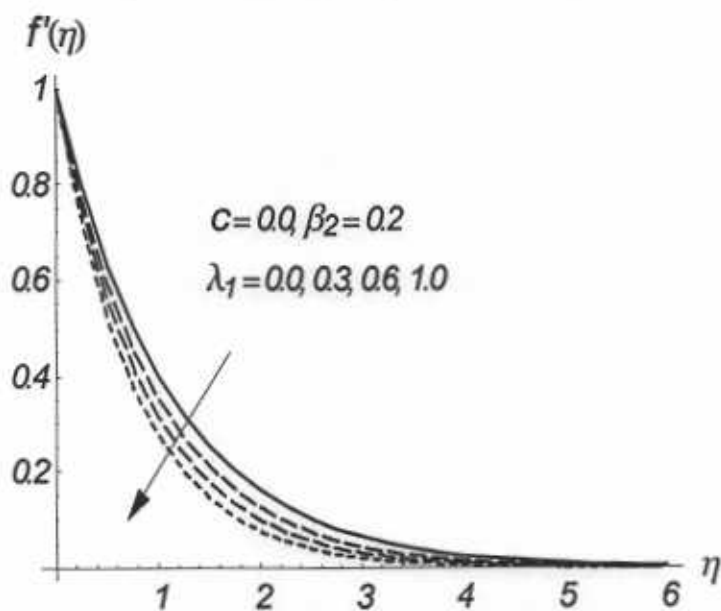


Fig. 6.5 : Influence of λ_1 on f' for 2D flow.

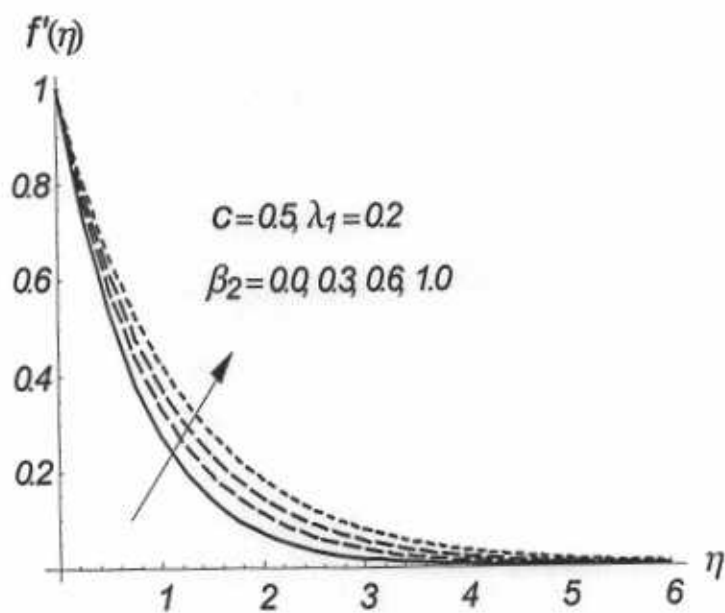


Fig. 6.6 : Influence of β_2 on f' for 3D flow.

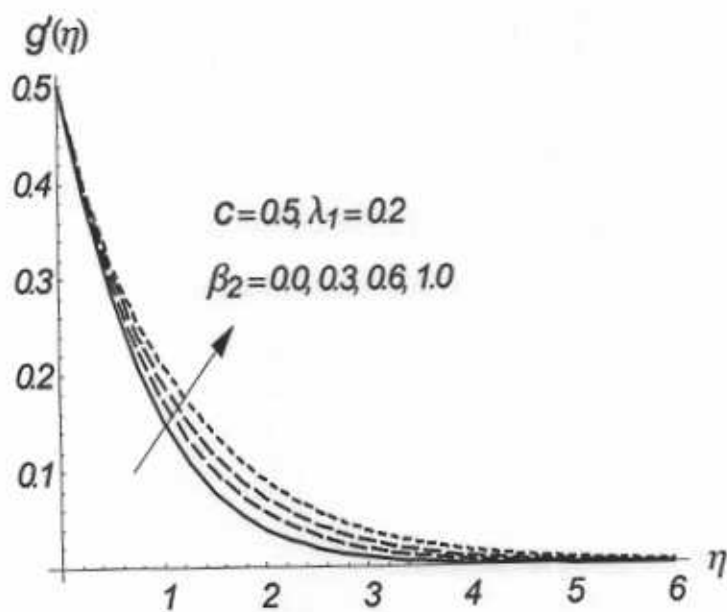


Fig. 6.7 : Influence of β_2 on g' for 3D flow.

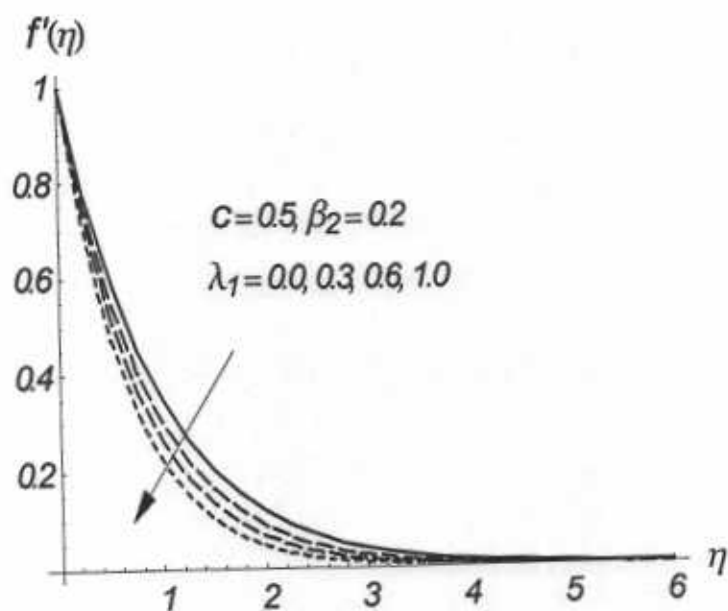


Fig. 6.8 : Influence of λ_1 on f' for 3D flow.

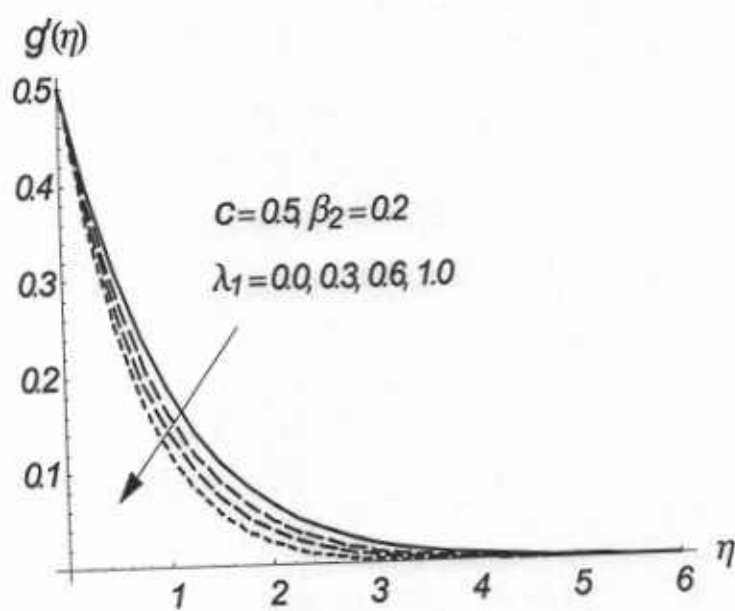


Fig. 6.9 : Influence of λ_1 on g' for 3D flow.

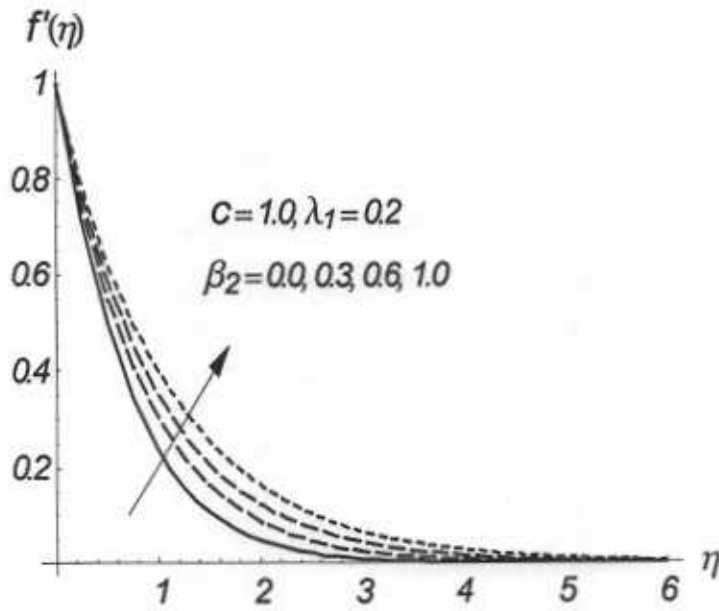


Fig. 6.10 : Influence of β_2 on f' for axisymmetric flow.

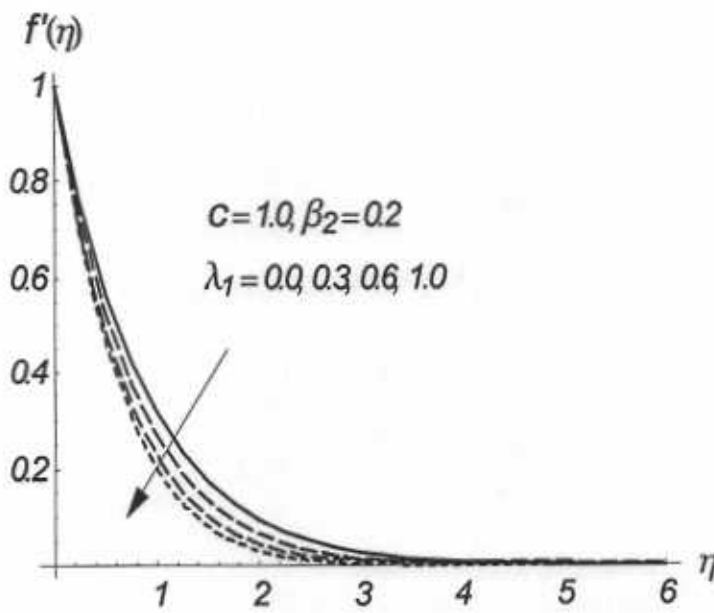


Fig. 6.11 : Influence of λ_1 on f' for axisymmetric flow.

Table 6.2: Illustrating the variation of $-f''(0)$ and $-g''(0)$ with c when $\beta_2 = 0 = \lambda_1$, using HAM, HPM (Ariel [41]) and exact solution (Ariel [41]).

c	$-f''(0)$			$-g''(0)$		
	HAM	HPM [41]	Exact [41]	HAM	HPM [41]	Exact [41]
0.0	1	1	1	0	0	0
0.2	1.039495	1.034587	1.039495	0.148736	0.158231	0.148736
0.4	1.075788	1.070529	1.075788	0.349208	0.360599	0.349208
0.6	1.109946	1.106797	1.109946	0.590528	0.600833	0.590528
0.8	1.142488	1.142879	1.142488	0.866682	0.874551	0.866682
1.0	1.173720	1.178511	1.173720	1.173720	1.178511	1.173720

6.5 Conclusions

The three-dimensional flow of a Jeffery fluid over a stretching surface is analyzed. The final outcomes are mentioned below.

- It is noted that the velocity field increases by increasing β_2 .
- Effects of β_2 and λ_1 are quite opposite on velocity components.
- Results obtained are qualitatively similar for axisymmetric, two- and three-dimensional flows.
- Obtained solutions are convergent upto 6th decimal place.
- Two-dimensional case ($g = 0$) can be deduced by setting $c = 0$.
- $\beta_2 = 0 = \lambda_1$ gives the results of viscous fluid.

Chapter 7

Three-dimensional channel flow of a Jeffery fluid with stretched wall

Three-dimensional channel flow of an incompressible Jeffery fluid is investigated in this chapter. The flow is induced due to a stretching property of lower wall. Mathematical modelling is performed and the resulting problems are computed by homotopy analysis method. Graphical results for various pertinent parameters are plotted and analyzed. Tables are constructed to show the convergence of the obtained solutions and to validate the present solutions through comparison with the published limiting results.

7.1 Mathematical formulation

Consider the three-dimensional channel flow of an incompressible Jeffery fluid. The fluid is bounded by two parallel plates distant H apart. The lower plate at $z = 0$ whereas the upper

plate subjected to uniform injection in the channel is at $z = H$ (see Fig. 7.1).

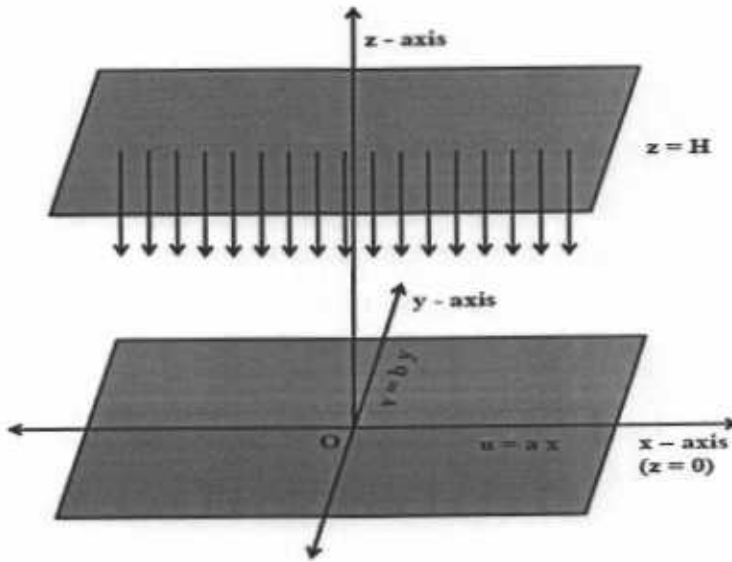


Fig. 7.1 : Geometry of the problem.

The motion in the fluid is generated due to the bidirectional stretching of plate in the x - and y - directions. The laws of conservation of mass and momentum for the present flow problem give

$$\frac{\partial u}{\partial x} + \frac{\partial v}{\partial y} + \frac{\partial w}{\partial z} = 0, \quad (7.1)$$

$$u \frac{\partial u}{\partial x} + v \frac{\partial u}{\partial y} + w \frac{\partial u}{\partial z} = -\frac{1}{\rho} \frac{\partial p}{\partial x} + \frac{\nu}{1 + \lambda_1} \left[\frac{\partial^2 u}{\partial x^2} + \frac{\partial^2 u}{\partial y^2} + \frac{\partial^2 u}{\partial z^2} \right] + \frac{\nu \lambda_2}{1 + \lambda_1} \left[\begin{aligned} & \left(u \frac{\partial}{\partial x} + v \frac{\partial}{\partial y} + w \frac{\partial}{\partial z} \right) \left(\frac{\partial^2 u}{\partial x^2} + \frac{\partial^2 u}{\partial y^2} + \frac{\partial^2 u}{\partial z^2} \right) \\ & + 2 \frac{\partial u}{\partial x} \frac{\partial^2 u}{\partial x^2} + 2 \frac{\partial v}{\partial x} \frac{\partial^2 u}{\partial x \partial y} + 2 \frac{\partial w}{\partial x} \frac{\partial^2 u}{\partial x \partial z} \\ & + \left(\frac{\partial u}{\partial y} \frac{\partial}{\partial x} + \frac{\partial v}{\partial y} \frac{\partial}{\partial y} + \frac{\partial w}{\partial y} \frac{\partial}{\partial z} \right) \left(\frac{\partial u}{\partial y} + \frac{\partial v}{\partial x} \right) \\ & + \left(\frac{\partial u}{\partial z} \frac{\partial}{\partial x} + \frac{\partial v}{\partial z} \frac{\partial}{\partial y} + \frac{\partial w}{\partial z} \frac{\partial}{\partial z} \right) \left(\frac{\partial u}{\partial z} + \frac{\partial w}{\partial x} \right) \end{aligned} \right], \quad (7.2)$$

$$\begin{aligned}
u \frac{\partial v}{\partial x} + v \frac{\partial v}{\partial y} + w \frac{\partial v}{\partial z} &= -\frac{1}{\rho} \frac{\partial p}{\partial y} + \frac{\nu}{1 + \lambda_1} \left[\frac{\partial^2 v}{\partial x^2} + \frac{\partial^2 v}{\partial y^2} + \frac{\partial^2 v}{\partial z^2} \right] \\
&+ \frac{\nu \lambda_2}{1 + \lambda_1} \left[\begin{aligned} &\left(u \frac{\partial}{\partial x} + v \frac{\partial}{\partial y} + w \frac{\partial}{\partial z} \right) \left(\frac{\partial^2 v}{\partial x^2} + \frac{\partial^2 v}{\partial y^2} + \frac{\partial^2 v}{\partial z^2} \right) \\ &+ \left(\frac{\partial u}{\partial x} \frac{\partial}{\partial x} + \frac{\partial v}{\partial x} \frac{\partial}{\partial y} + \frac{\partial w}{\partial x} \frac{\partial}{\partial z} \right) \left(\frac{\partial v}{\partial y} + \frac{\partial v}{\partial z} \right) \\ &+ 2 \frac{\partial u}{\partial y} \frac{\partial^2 v}{\partial x \partial y} + 2 \frac{\partial v}{\partial y} \frac{\partial^2 v}{\partial y^2} + 2 \frac{\partial w}{\partial y} \frac{\partial^2 v}{\partial y \partial z} \\ &+ \left(\frac{\partial u}{\partial z} \frac{\partial}{\partial x} + \frac{\partial v}{\partial z} \frac{\partial}{\partial y} + \frac{\partial w}{\partial z} \frac{\partial}{\partial z} \right) \left(\frac{\partial v}{\partial z} + \frac{\partial v}{\partial y} \right) \end{aligned} \right], \quad (7.3)
\end{aligned}$$

$$\begin{aligned}
u \frac{\partial w}{\partial x} + v \frac{\partial w}{\partial y} + w \frac{\partial w}{\partial z} &= -\frac{1}{\rho} \frac{\partial p}{\partial z} + \frac{\nu}{1 + \lambda_1} \left[\frac{\partial^2 w}{\partial x^2} + \frac{\partial^2 w}{\partial y^2} + \frac{\partial^2 w}{\partial z^2} \right] \\
&+ \frac{\nu \lambda_2}{1 + \lambda_1} \left[\begin{aligned} &\left(u \frac{\partial}{\partial x} + v \frac{\partial}{\partial y} + w \frac{\partial}{\partial z} \right) \left(\frac{\partial^2 w}{\partial x^2} + \frac{\partial^2 w}{\partial y^2} + \frac{\partial^2 w}{\partial z^2} \right) \\ &+ \left(\frac{\partial u}{\partial x} \frac{\partial}{\partial x} + \frac{\partial v}{\partial x} \frac{\partial}{\partial y} + \frac{\partial w}{\partial x} \frac{\partial}{\partial z} \right) \left(\frac{\partial w}{\partial z} + \frac{\partial w}{\partial y} \right) \\ &+ \left(\frac{\partial u}{\partial y} \frac{\partial}{\partial x} + \frac{\partial v}{\partial y} \frac{\partial}{\partial y} + \frac{\partial w}{\partial y} \frac{\partial}{\partial z} \right) \left(\frac{\partial v}{\partial z} + \frac{\partial w}{\partial y} \right) \\ &+ 2 \frac{\partial u}{\partial z} \frac{\partial^2 w}{\partial x \partial y} + 2 \frac{\partial v}{\partial z} \frac{\partial^2 w}{\partial y \partial z} + 2 \frac{\partial w}{\partial z} \frac{\partial^2 w}{\partial z^2} \end{aligned} \right] \quad (7.4)
\end{aligned}$$

and the boundary conditions are

$$\begin{aligned}
u &= ax, & v &= by, & w &= 0 & \text{at } z &= 0, \\
u &= 0, & v &= 0, & w &= -V_0, & \text{as } z &= H,
\end{aligned} \quad (7.5)$$

in which u, v and w denote the velocities in the x, y and z directions, respectively, $a > 0$ and $b > 0$ are the constants and V_0 is the constant injection velocity at the upper plate. Introducing

$$\eta = \frac{z}{H}, \quad u = axf'(\eta), \quad v = ayg'(\eta), \quad w = -aH(f(\eta) + g(\eta)) \quad (7.6)$$

continuity equation (7.1) is satisfied automatically and by eliminating pressure after cross differentiation Eqs. (7.2) – (7.5) become

$$f'''' - \text{Re}(1 + \lambda_1) [(f' - g') f'' - (f + g) f'''] + \beta_2 [(2f'' - g'') f''' - (2g' + f') f'''' - (f + g) f'''''] = 0, \quad (7.7)$$

$$g'''' - \text{Re}(1 + \lambda_1) [(g' - f') g'' - (f + g) g'''] + \beta_2 [(2g'' - f'') g''' - (2f' + g') g'''' - (f + g) g'''''] = 0, \quad (7.8)$$

$$\begin{aligned} f' = 1, \quad g' = c, \quad f + g = 0, \quad \text{at } \eta = 0, \\ f' = 0, \quad g' = 0, \quad f + g = \xi, \quad \text{at } \eta = 1, \end{aligned} \quad (7.9)$$

where prime denotes differentiation with respect to η . Moreover the Deborah number β_2 , the Reynolds number Re , the dimensionless injection parameter ξ and the stretching ratio c are defined as

$$\beta_2 = \lambda_2 a, \quad \text{Re} = \frac{H^2 a}{\nu}, \quad \xi = \frac{V_0}{aH}, \quad c = \frac{b}{a}. \quad (7.10)$$

Note that for $\beta_2 = 0 = \lambda_1$ one can obtain the results for viscous flow i.e.

$$f'''' - \text{Re} [(f' - g') f'' - (f + g) f'''] = 0, \quad (7.11)$$

$$g'''' - \text{Re} [(g' - f') g'' - (f + g) g'''] = 0, \quad (7.12)$$

with the similar boundary conditions (7.9). When $c = 0.0$ the system reduces to two-dimensional case ($g = 0$) which is given below

$$f'''' - \text{Re}(1 + \lambda_1) [f' f'' - f f'''] + \beta_2 [2f'' f''' - f' f'''' - f f'''''] = 0 \quad (7.13)$$

and for $c = 1.0$, we have axisymmetric flow i.e. ($f = g$). In such situation, Eqs. (7.7) and (7.8) are reduced to

$$f'''' - \text{Re}(1 + \lambda_1) [2f f'''] + \beta_2 [f'' f''' - 3f' f'''' - 2f f'''''] = 0, \quad (7.14)$$

7.2 Series solutions

7.2.1 Zeroth-order deformation problems

Let the initial approximations for f and g are

$$f_0(\eta) = \eta + \left(\frac{3\xi}{2} - 2\right)\eta^2 + (1 - \xi)\eta^3 \quad (7.15)$$

$$g_0(\eta) = c\eta + \left(\frac{3\xi}{2} - 2c\right)\eta^2 + (c - \xi)\eta^3 \quad (7.16)$$

and the corresponding linear operator is

$$\mathcal{L} = \frac{d^4}{d\eta^4}, \quad (7.17)$$

with the following property

$$\mathcal{L}[C_1 + C_2\eta + C_3\eta^2 + C_4\eta^3] = 0, \quad (7.18)$$

in which $C_1 - C_4$ are the constants. The zeroth order problems are

$$(1 - p)\mathcal{L}[\bar{f}(\eta, p) - f_0(\eta)] = p\mathcal{H}_f\mathcal{N}_f[\bar{f}(\eta, p), \bar{g}(\eta, p)], \quad (7.19)$$

$$(1 - p)\mathcal{L}[\bar{g}(\eta, p) - g_0(\eta)] = p\mathcal{H}_g\mathcal{N}_g[\bar{f}(\eta, p), \bar{g}(\eta, p)], \quad (7.20)$$

$$\begin{aligned} \bar{f}'(0, p) = 0, \quad \bar{g}'(0, p) = 0, \quad \bar{f}(0, p) + \bar{g}(0, p) = 0, \\ \bar{f}'(1, p) = 0, \quad \bar{g}'(1, p) = 0, \quad \bar{f}(1, p) + \bar{g}(1, p) = 0 \end{aligned} \quad (7.21)$$

and the nonlinear operators \mathcal{N}_f and \mathcal{N}_g are

$$\begin{aligned} \mathcal{N}_f[\bar{f}(\eta, p), \bar{g}(\eta, p)] = & \bar{f}'''' - \text{Re}(1 + \lambda_1) [(\bar{f}' - \bar{g}')\bar{f}'' - (\bar{f} + \bar{g})\bar{f}'''] \\ & + \beta_2 [(2\bar{f}'' + \bar{g}'')\bar{f}'' - (2\bar{g}' + \bar{f}')\bar{f}'' - (\bar{f} + \bar{g})\bar{f}'''], \end{aligned} \quad (7.22)$$

$$\begin{aligned} \mathcal{N}_g[\bar{f}(\eta, p), \bar{g}(\eta, p)] = & \bar{g}'''' - \text{Re}(1 + \lambda_1) [(\bar{g}' - \bar{f}')\bar{g}'' - (\bar{f} + \bar{g})\bar{g}'''] \\ & + \beta_2 [(2\bar{g}'' + \bar{f}'')\bar{g}'' - (2\bar{f}' + \bar{g}')\bar{g}'' - (\bar{f} + \bar{g})\bar{g}'''], \end{aligned} \quad (7.23)$$

where \hbar_f and \hbar_g are the auxiliary non-zero parameters and $p \in [0, 1]$ is an embedding parameter. When $p = 0$ and $p = 1$ then

$$\bar{f}(\eta, 0) = f_0(\eta), \quad \bar{f}(\eta, 1) = f(\eta), \quad (7.24)$$

$$\bar{g}(\eta, 0) = g_0(\eta), \quad \bar{g}(\eta, 1) = g(\eta). \quad (7.25)$$

When p varies from 0 to 1 then $f_0(\eta)$ tends to $f(\eta)$ and $g_0(\eta)$ tends to $g(\eta)$ respectively. Moreover the Taylor's series expansion gives

$$\bar{f}(\eta, p) = f_0(\eta) + \sum_{m=1}^{\infty} f_m(\eta) p^m, \quad (7.26)$$

$$\bar{g}(\eta, p) = g_0(\eta) + \sum_{m=1}^{\infty} g_m(\eta) p^m, \quad (7.27)$$

$$f_m(\eta) = \frac{1}{m!} \left. \frac{\partial^m \bar{f}(\eta, p)}{\partial p^m} \right|_{p=0}, \quad (7.28)$$

$$g_m(\eta) = \frac{1}{m!} \left. \frac{\partial^m \bar{g}(\eta, p)}{\partial p^m} \right|_{p=0}. \quad (7.29)$$

It is noted that the convergence of Eqs. (7.26) and (7.27) depends strongly upon the auxiliary parameters \hbar_f and \hbar_g . The values of \hbar_f and \hbar_g are selected in such a way that the Eqs. (7.26) and (7.27) converge when $p = 1$. Thus we write

$$f(\eta) = f_0(\eta) + \sum_{m=1}^{\infty} f_m(\eta), \quad (7.30)$$

$$g(\eta) = g_0(\eta) + \sum_{m=1}^{\infty} g_m(\eta). \quad (7.31)$$

7.2.2 *m*th order deformation problems

The *m*th order deformation problems can be written as

$$\mathcal{L}[f_m(\eta, p) - \chi_m f_{m-1}(\eta)] = \hbar_f \mathcal{R}_{f,m}(\eta), \quad (7.32)$$

$$\mathcal{L}[g_m(\eta, p) - \chi_m g_{m-1}(\eta)] = \hbar_g \mathcal{R}_{g,m}(\eta), \quad (7.33)$$

$$\begin{aligned} f'_m(0) &= g'_m(0) = f_m(0) + g_m(0) = 0, \\ f'_m(1) &= g'_m(1) = f_m(1) + g_m(1) = 0, \end{aligned} \quad (7.34)$$

$$\chi_m = \begin{cases} 0, & m \leq 1 \\ 1, & m > 1 \end{cases}, \quad (7.35)$$

$$\begin{aligned} \mathcal{R}_{f,m}(\eta) &= f'''_{m-1} - \text{Re}(1 + \lambda_1) \sum_{k=0}^{m-1} \{ (f'_{m-1-k} - g'_{m-1-k}) f''_k - (f_{m-1-k} + g_{m-1-k}) f'''_k \} \\ &+ \beta_2 \sum_{k=0}^{m-1} \left\{ \begin{aligned} &(2f''_{m-1-k} - g''_{m-1-k}) f'''_k - (2g'_{m-1-k} + f'_{m-1-k}) f''''_k \\ &- (f_{m-1-k} + g_{m-1-k}) f''''_k \end{aligned} \right\}, \end{aligned} \quad (7.36)$$

$$\begin{aligned} \mathcal{R}_{g,m}(\eta) &= g'''_{m-1} - \text{Re}(1 + \lambda_1) \sum_{k=0}^{m-1} \{ (g'_{m-1-k} - f'_{m-1-k}) g''_k - (f_{m-1-k} + g_{m-1-k}) g'''_k \} \\ &+ \beta_2 \sum_{k=0}^{m-1} \left\{ \begin{aligned} &(2g''_{m-1-k} - f''_{m-1-k}) g'''_k - (2f'_{m-1-k} + g'_{m-1-k}) g''''_k \\ &- (f_{m-1-k} + g_{m-1-k}) g''''_k \end{aligned} \right\}. \end{aligned} \quad (7.37)$$

Employing symbolic software MATHEMATICA, the corresponding system can be solved one after the other in the order $m = 1, 2, 3, \dots$

7.3 Convergence of the solutions

It is noted that the convergence of solutions (7.30) and (7.31) depends upon \hbar_f and \hbar_g . In order to find the meaningful values of \hbar_f and \hbar_g , the so called \hbar -curves are displayed for 15th order of approximation in the Figs. 7.2 and 7.3. These Figs. show that the admissible values are $-0.7 \leq (\hbar_f, \hbar_g) \leq -0.2$. Table 7.1 shows that 25th order approximations are sufficient in the present problem for a convergent solution. Table 7.2 presents a comparative study of present results with those obtained in Ref. [52]. It is observed that obtained results are in a nice agreement with the already published results.

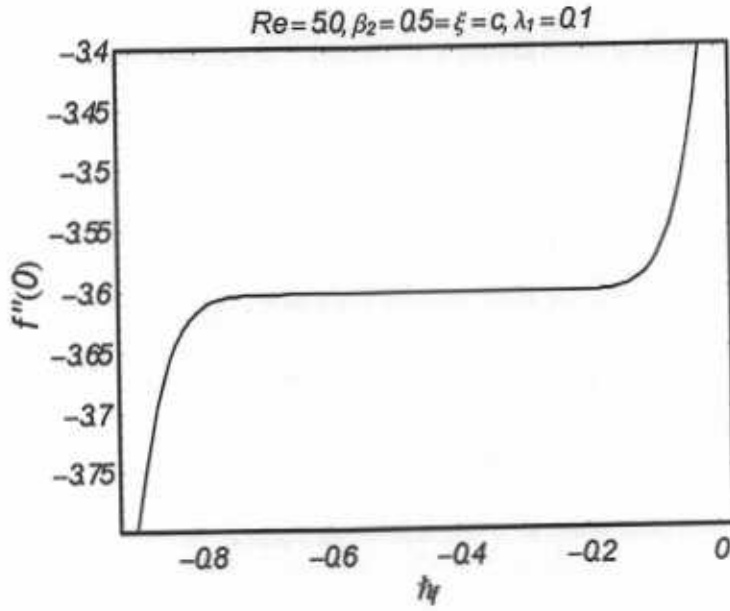


Fig. 7.2 : h curve of $f''(0)$ at the 15th order of approximation.

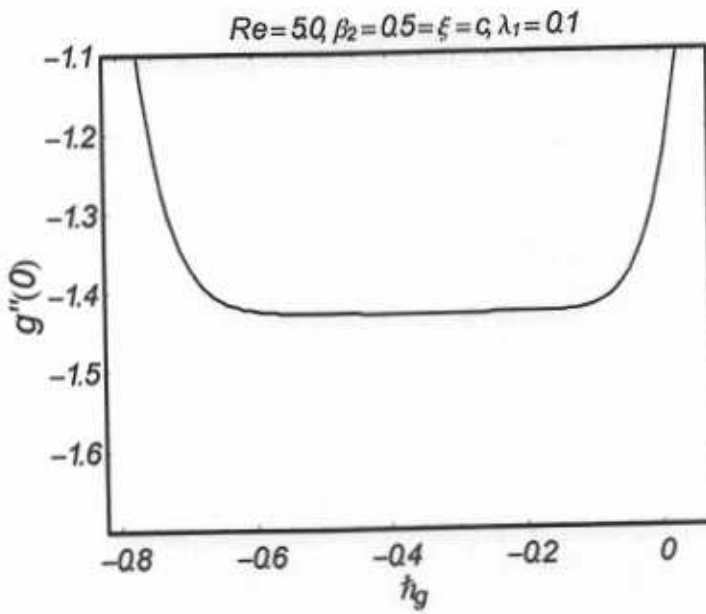


Fig. 7.3 : h curve of $g''(0)$ at the 15th order of approximation.

Table 7.1: Convergence of the HAM solutions for different order of approximations when $Re = 5.0$, $\beta_2 = 0.5$, $\lambda_1 = 0.1$, $c = 0.5$ and $\xi = 0.5$.

order of approximation	$-f''(0)$	$-g''(0)$
1	3.346830	1.300491
5	3.544026	1.410712
10	3.597077	1.442177
15	3.601718	1.446013
20	3.601715	1.446499
25	3.601711	1.446511
30	3.601711	1.446512
40	3.601711	1.446512
50	3.601711	1.446512

7.4 Results and discussion

Impact of different emerging parameters including ratio c , Deborah number β_2 and ratio parameter λ_1 on the velocity components f' and g' are explored in this section. Three-dimensional plots of velocity components are also presented. We have plotted Figs. 7.4 – 7.14. Figs. 7.4 and 7.5 portray the influence of ratio parameter c on the dimensionless velocity components f' and g' . It is shown that velocity components increase near the stretching wall by increasing ratio parameter c . However the velocity components decrease near the porous wall. In principle, this is due to the fact that the flow over stretched surfaces can be controlled by an increase or decrease in the stretching velocity of the boundaries. Figs. 7.6 and 7.7 plot the influence of Deborah number β_2 on the velocity components f' and g' . These Figs. elucidate that velocity components show increasing behavior near the stretching wall but obviously to satisfy mass conservation constraint an increase in fluid velocity in the vicinity of stretching sheet is compensated by a decrease in fluid velocity in the upper half of channel. Influence of λ_1 on the velocity components f' and g' are plotted in the Figs. 7.8 and 7.9. It is noticed from these Figs. that λ_1 retards the flow near the stretching surface whereas the velocity components increase near the porous wall. This is because of the fact that λ_1 being the viscoelastic parameter exhibits both viscous and elastic characteristics. Thus the fluid always retard whenever viscosity or elasticity increases. It is also noted that injection has dominant behavior near the porous wall. Thus the velocity components finally increases near the porous wall due to injection. Figs.

7.10 and 7.11 present the effects of injection parameter ξ on the velocity components f' and g' . It is observed that both components of velocity increase rapidly with an increase in ξ . The three-dimensional plot of velocity components u , v and w are shown in the Figs. 7.12 – 7.14. It is found that velocity components u and v are increasing near the stretching wall but there is a decrease towards the porous wall. This is quite obvious from the no slip condition that induced motion is maximum near the stretched boundaries and vanishes far away from the stretched surface (as shown in Figs. 7.12 and 7.13). Fig. 7.14 shows the three-dimensional plot of velocity component w with η and H . It is noticed that with an increase in channel width H the velocity decreases.

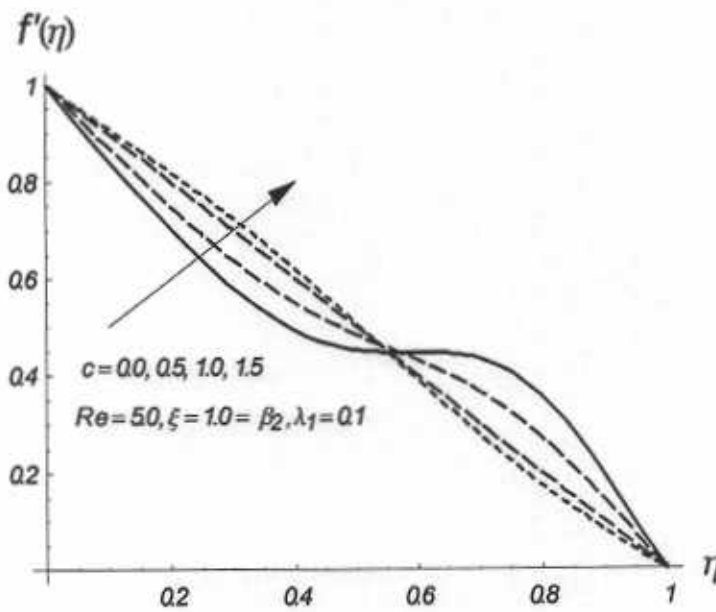


Fig. 7.4 : Influence of c on f' .

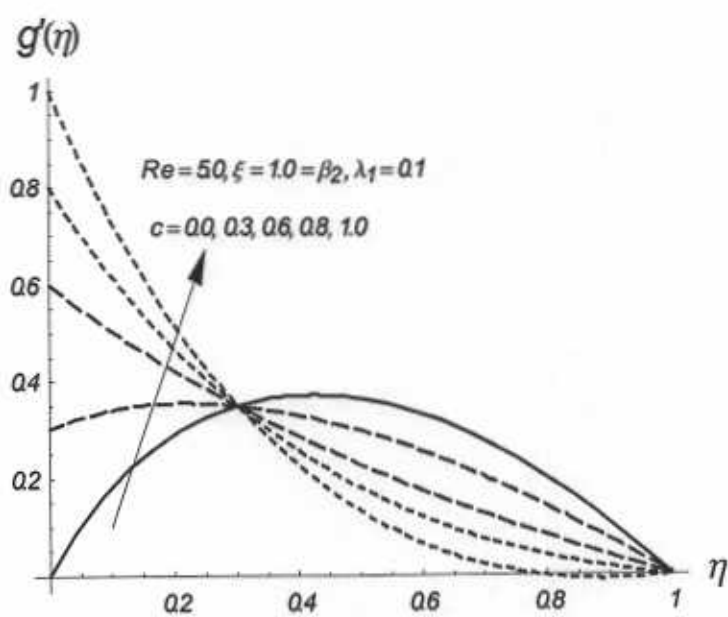


Fig. 7.5 : Influence of c on g' .

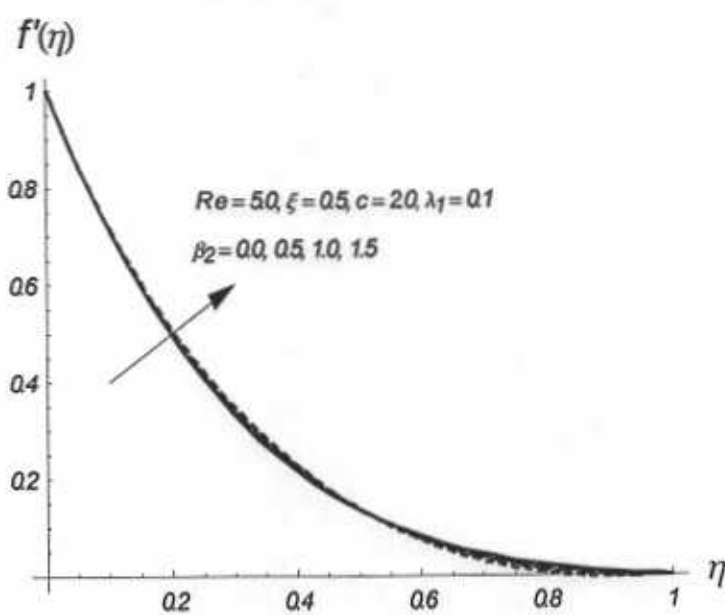


Fig. 7.6 : Influence of β_2 on f' .

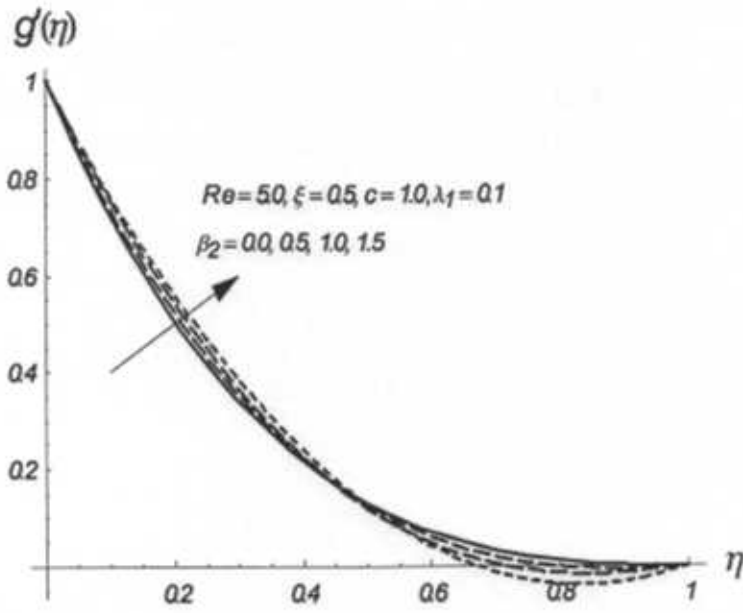


Fig. 7.7 : Influence of β_2 on g' .

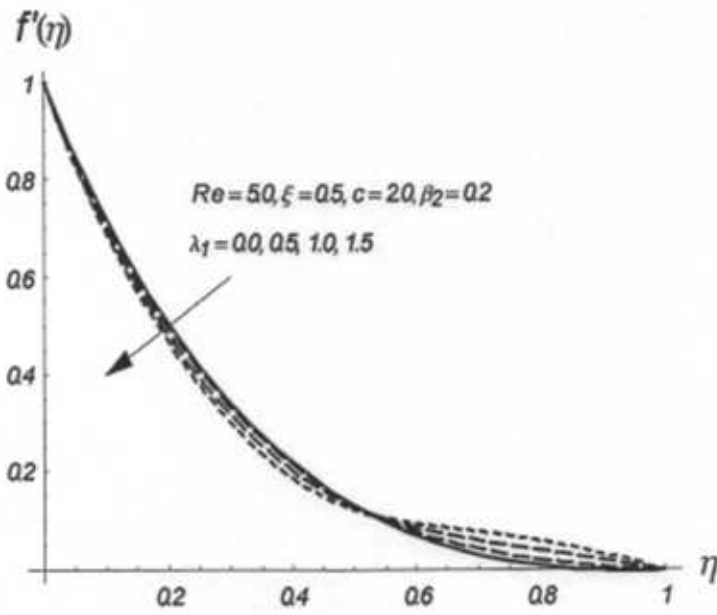


Fig. 7.8 : Influence of λ_1 on f' .

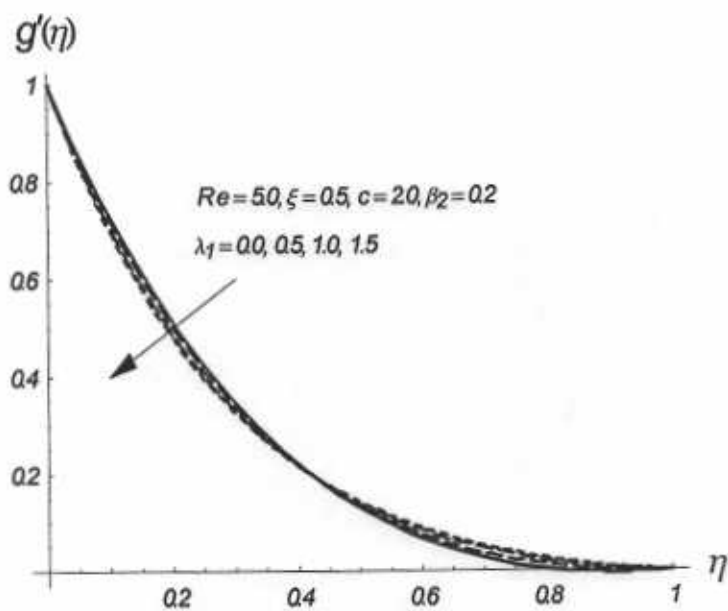


Fig. 7.9 : Influence of λ_1 on g' .

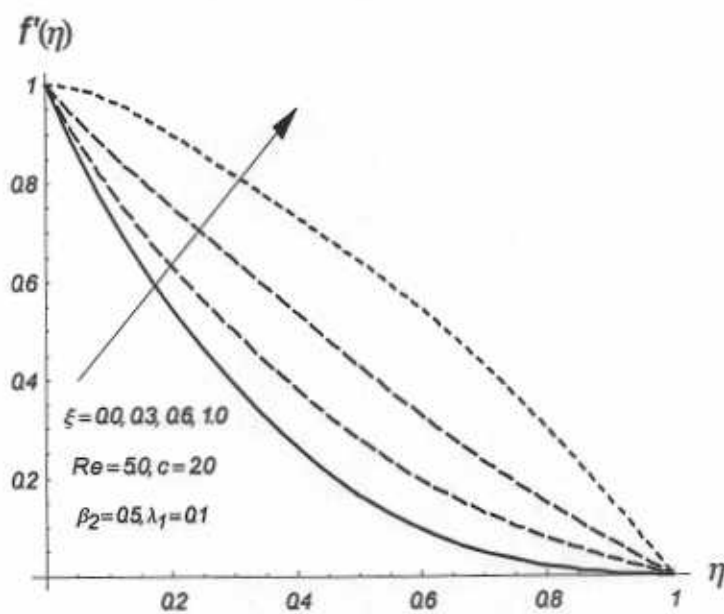


Fig. 7.10 : Influence of ξ on f' .

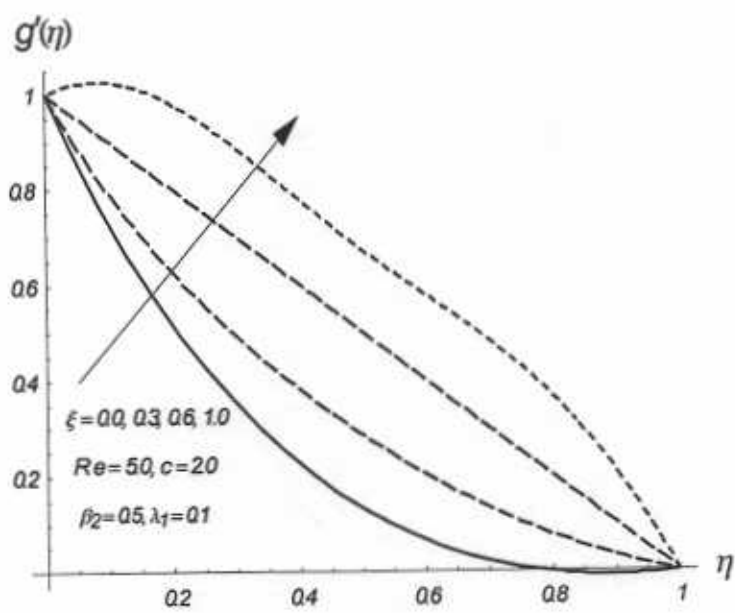


Fig. 7.11 : Influence of ξ on g' .

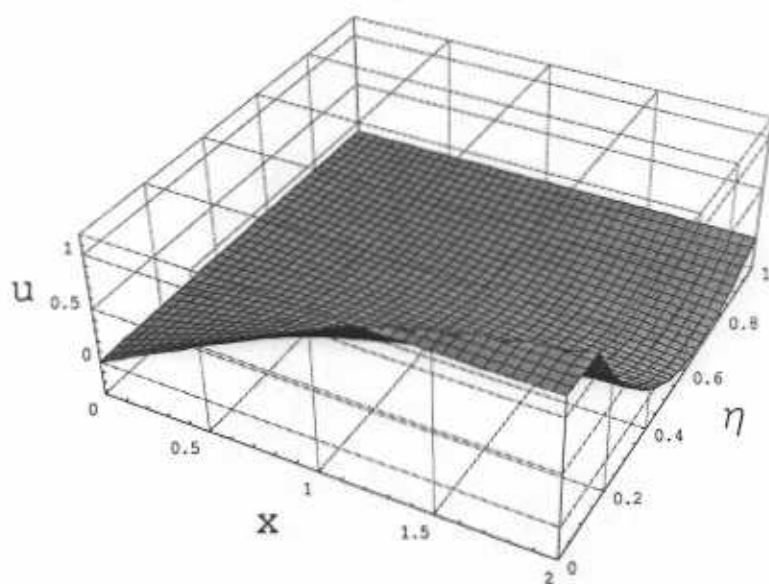


Fig. 7.12 : 3D plot of u with x and η .

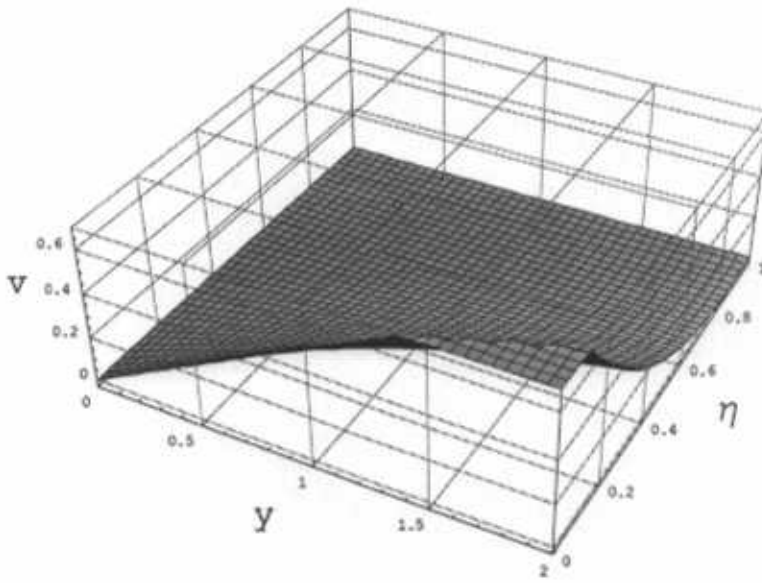


Fig. 7.13 : 3D plot of v with y and η .

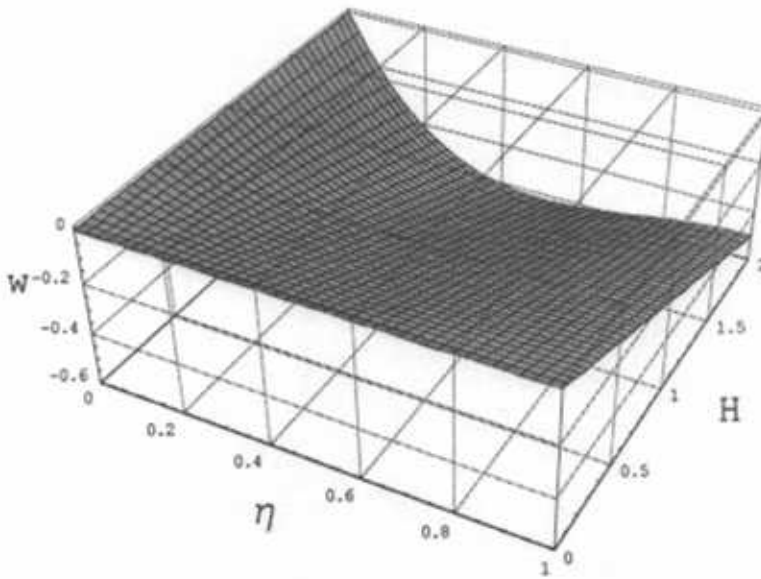


Fig. 7.14 : 3D plot of w with η and H .

Table 7.2: Comparison of values of $-f''(0)$ and $-g''(0)$ for viscous fluid ($\beta_2 = 0 = \lambda_1$) [52] when $Re = 5.0$, $c = 0.5$ and $\xi = 0.5$.

Order of approximation	Present results		Ahmer and Asif [52]	
	$-f''(0)$	$-g''(0)$	$-f''(0)$	$-g''(0)$
5	2.987025	0.5037159	2.98703	0.503716
10	2.990508	0.5037637	2.99051	0.503764
15	2.990524	0.5037629	2.99052	0.503763
20	2.990525	0.5037629	2.99053	0.503763
25	2.990525	0.5037629	2.99053	0.503763

7.5 Conclusions

Three-dimensional channel flow of Jeffery fluid between two walls is analyzed. The presented solutions lead to the following main points.

- Effects of β_2 and λ_1 are quite opposite.
- Velocity decreases with an increase in channel width
- Injection enhances the velocity.
- Increase in channel width cause a reduction in the velocity.
- $\beta_2 = 0 = \lambda_1$ gives the results of viscous fluid.

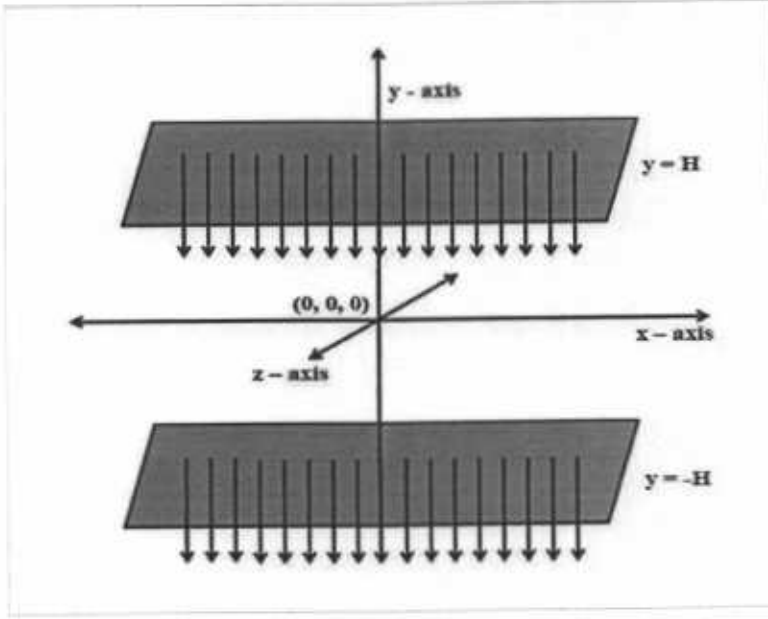
Chapter 8

Magnetohydrodynamic three-dimensional rotating flow of Jeffery fluid between two porous walls

Three-dimensional shrinking flow of Jeffery fluid in a rotating system is modeled here. The fluid is electrically conducting in the presence of a uniform applied magnetic field and the induced magnetic field is neglected. The similarity transformations reduce the non-linear partial differential equations into the ordinary differential equations. Series solutions are derived. Convergence of the obtained solutions is checked. Graphs are plotted and discussed for various parameters of interest.

8.1 Mathematical formulation

Consider the magnetohydrodynamic (MHD) steady flow of a Jeffery fluid between two porous plates distant $2H$ apart. The lower and upper plates correspond to suction and blowing respectively. The fluid is rotating under the action of Coriolis and centrifugal forces with constant angular velocity Ω about the y -axis (see Fig. 8.1).



The laws of conservation of mass and momentum for the present flow situation are given by

$$\frac{\partial u}{\partial x} + \frac{\partial v}{\partial y} + \frac{\partial w}{\partial z} = 0, \quad (8.1)$$

$$u \frac{\partial u}{\partial x} + v \frac{\partial u}{\partial y} + 2\Omega w = -\frac{1}{\rho} \frac{\partial p^*}{\partial x} + \frac{\nu}{1 + \lambda_1} \left(\frac{\partial^2 u}{\partial x^2} + \frac{\partial^2 u}{\partial y^2} \right) - \frac{\sigma B_0^2 u}{\rho} + \frac{\nu \lambda_2}{1 + \lambda_1} \left(\begin{aligned} &2 \frac{\partial u}{\partial x} \frac{\partial^2 u}{\partial x^2} + 2u \frac{\partial^3 u}{\partial x^3} + 2v \frac{\partial^3 u}{\partial x^2 \partial y} + 2 \frac{\partial v}{\partial x} \frac{\partial^2 u}{\partial x \partial y} \\ &+ \frac{\partial u}{\partial y} \frac{\partial^2 u}{\partial x \partial y} + u \frac{\partial^3 u}{\partial x \partial y^2} + v \frac{\partial^3 v}{\partial y \partial x^2} + \frac{\partial v}{\partial y} \frac{\partial^2 u}{\partial y^2} \\ &+ v \frac{\partial^3 u}{\partial y^3} + \frac{\partial u}{\partial y} \frac{\partial^2 v}{\partial x^2} + \frac{\partial v}{\partial y} \frac{\partial^2 v}{\partial x \partial y} + v \frac{\partial^3 v}{\partial y^2 \partial x} \end{aligned} \right), \quad (8.2)$$

$$u \frac{\partial v}{\partial x} + v \frac{\partial v}{\partial y} = -\frac{1}{\rho} \frac{\partial p^*}{\partial y} + \frac{\nu}{1 + \lambda_1} \left(\frac{\partial^2 v}{\partial x^2} + \frac{\partial^2 v}{\partial y^2} \right) + \frac{\nu \lambda_2}{1 + \lambda_1} \left(\begin{aligned} &\frac{\partial u}{\partial x} \frac{\partial^2 u}{\partial x \partial y} + u \frac{\partial^3 u}{\partial x^2 \partial y} + \frac{\partial u}{\partial x} \frac{\partial^2 v}{\partial x^2} + u \frac{\partial^3 v}{\partial x^3} \\ &+ \frac{\partial v}{\partial x} \frac{\partial^2 u}{\partial y^2} + v \frac{\partial^3 u}{\partial y^2 \partial x} + \frac{\partial v}{\partial x} \frac{\partial^2 v}{\partial x \partial y} + v \frac{\partial^3 v}{\partial y \partial x^2} \\ &+ 2 \frac{\partial u}{\partial y} \frac{\partial^2 v}{\partial x \partial y} + 2u \frac{\partial^3 v}{\partial x \partial y^2} + 2 \frac{\partial v}{\partial y} \frac{\partial^2 v}{\partial y^2} + 2v \frac{\partial^3 v}{\partial y^3} \end{aligned} \right), \quad (8.3)$$

$$\begin{aligned}
u \frac{\partial w}{\partial x} + v \frac{\partial w}{\partial y} - 2\Omega u = \frac{\nu}{1 + \lambda_1} \left(\frac{\partial^2 w}{\partial x^2} + \frac{\partial^2 w}{\partial y^2} \right) - \frac{\sigma B_0^2 w}{\rho} \\
+ \frac{\nu \lambda_2}{1 + \lambda_1} \left(\frac{\partial u}{\partial x} \frac{\partial^2 w}{\partial x^2} + u \frac{\partial^3 w}{\partial x^3} + \frac{\partial v}{\partial x} \frac{\partial^2 w}{\partial x \partial y} + v \frac{\partial^3 w}{\partial x^2 \partial y} \right. \\
\left. + \frac{\partial u}{\partial y} \frac{\partial^2 w}{\partial x \partial y} + u \frac{\partial^3 w}{\partial x \partial y^2} + \frac{\partial v}{\partial y} \frac{\partial^2 w}{\partial y^2} + v \frac{\partial^3 w}{\partial y^3} \right), \quad (8.4)
\end{aligned}$$

with the appropriate boundary conditions

$$\begin{aligned}
u &= -ax, & v &= -V_0, & w &= 0, & \text{at } y &= -H, \\
u &= 0, & v &= V_0, & w &= 0, & \text{at } y &= H,
\end{aligned} \quad (8.5)$$

where u , v and w are the velocity components along x -, y - and z - directions, ν is the kinematic viscosity, p^* the modified pressure which includes the centrifugal force effects, $a > 0$ the dimensional constant, λ_1 the ratio of relaxation to retardation time, λ_2 the retardation time, ρ the density, σ the electrical conductivity, B_0 the constant magnetic field and V_0 the uniform suction/injection velocity.

The Eqs. (8.1) – (8.4) can be written in a simpler form by defining the following transformations

$$\eta = \frac{y}{h}, \quad u = -axf'(\eta), \quad v = ahf(\eta), \quad w = axg(\eta). \quad (8.6)$$

Now continuity equation (8.1) is clearly satisfied and Eqs. (8.2) – (8.3) after eliminating the pressure yield

$$f'''' - (1 + \lambda_1) [M^2 f'' - 2K^2 g' - \text{Re}(f' f'' - f f''')] + \beta_2 (f f'''' + f' f'''' - 2f'' f''') = 0, \quad (8.7)$$

$$g'' - (1 + \lambda_1) [M^2 g + 2K^2 f' - \text{Re}(f' g - f g')] + \beta_2 (f g''' - f'' g') = 0, \quad (8.8)$$

$$\begin{aligned}
f &= -\xi, & f' &= 1, & g &= 0, & \text{at } \eta &= -1, \\
f &= \xi, & f' &= 0, & g &= 0, & \text{at } \eta &= 1,
\end{aligned} \quad (8.9)$$

in which prime shows the differentiation with respect to η . The suction/ blowing parameter ξ , the Reynolds number Re , the Hartman number M , the rotation parameter K and the Deborah

number β_2 are defined as follows

$$\xi = \frac{V_0}{aH}, \quad \text{Re} = \frac{aH^2}{\nu}, \quad M^2 = \frac{\sigma B_0^2 H^2}{\mu}, \quad K^2 = \frac{\Omega H^2}{\nu}, \quad \beta_2 = \lambda_2 a. \quad (8.10)$$

8.2 Solution by homotopy analysis method

Let the initial approximations for f and g and auxiliary linear operators are

$$f_0(\eta) = \frac{1}{4} + \frac{(-1 + 6\xi)}{4}\eta - \frac{\eta^2}{4} + \frac{(1 - 2\xi)}{4}\eta^3, \quad (8.11)$$

$$g_0(\eta) = 1 - \eta^2, \quad (8.12)$$

with the following auxiliary linear operator

$$\mathcal{L}_f = \frac{d^4 f}{d\eta^4}, \quad (8.13)$$

$$\mathcal{L}_g = \frac{d^2 g}{d\eta^2}. \quad (8.14)$$

The above operators satisfy

$$\mathcal{L}_f[C_1\eta^3 + C_2\eta^2 + C_3\eta + C_4] = 0, \quad (8.15)$$

$$\mathcal{L}_g[C_5\eta + C_6] = 0, \quad (8.16)$$

where C_i ($i = 1 - 6$) are the constants.

We construct the zeroth order problems as follows:

$$(1 - p)\mathcal{L}_f[\bar{f}(\eta; p) - f_0(\eta)] = p\hbar_f \mathcal{N}_f[\bar{f}(\eta; p), \bar{g}(\eta; p)], \quad (8.17)$$

$$(1 - p)\mathcal{L}_g[\bar{g}(\eta; p) - g_0(\eta)] = p\hbar_g \mathcal{N}_g[\bar{g}(\eta; p), \bar{f}(\eta; p)], \quad (8.18)$$

$$\begin{aligned} \bar{f}(-1; p) &= -\xi, & \bar{f}'(-1; p) &= 1, & \bar{f}(1; p) &= \xi, & \bar{f}'(1; p) &= 0, \\ \bar{g}(-1; p) &= 0, & \bar{g}(1; p) &= 0, \end{aligned} \quad (8.19)$$

$$\begin{aligned}
\mathcal{N}_f [\bar{f}(\eta; p), \bar{g}(\eta; p)] &= \frac{\partial^4 \bar{f}(\eta; p)}{\partial \eta^4} - M^2 (1 + \lambda_1) \frac{\partial^2 \bar{f}(\eta; p)}{\partial \eta^2} + 2K^2 (1 + \lambda_1) \frac{\partial \bar{f}(\eta; p)}{\partial \eta} \\
&+ \operatorname{Re}(1 + \lambda_1) \left(\frac{\partial \bar{f}(\eta; p)}{\partial \eta} \frac{\partial^2 \bar{f}(\eta; p)}{\partial \eta^2} - \bar{f}(\eta; p) \frac{\partial^3 \bar{f}(\eta; p)}{\partial \eta^3} \right) \\
&+ \beta_2 \left(\bar{f}(\eta; p) \frac{\partial^5 \bar{f}(\eta; p)}{\partial \eta^5} + \frac{\partial \bar{f}(\eta; p)}{\partial \eta} \frac{\partial^4 \bar{f}(\eta; p)}{\partial \eta^4} - 2 \frac{\partial^2 \bar{f}(\eta; p)}{\partial \eta^2} \frac{\partial^3 \bar{f}(\eta; p)}{\partial \eta^3} \right), \quad (8.20)
\end{aligned}$$

$$\begin{aligned}
\mathcal{N}_g [\bar{g}(\eta; p), \bar{f}(\eta; p)] &= \frac{\partial^2 \bar{g}(\eta; p)}{\partial \eta^2} - M^2 (1 + \lambda_1) \bar{g}(\eta; p) - 2K^2 (1 + \lambda_1) \frac{\partial \bar{f}(\eta; p)}{\partial \eta} \\
&+ \operatorname{Re}(1 + \lambda_1) \left(\frac{\partial \bar{f}(\eta; p)}{\partial \eta} \bar{g}(\eta; p) - \bar{f}(\eta; p) \frac{\partial \bar{g}(\eta; p)}{\partial \eta} \right) \\
&+ \beta_2 \left(\bar{f}(\eta; p) \frac{\partial^3 \bar{g}(\eta; p)}{\partial \eta^3} + \frac{\partial \bar{g}(\eta; p)}{\partial \eta} \frac{\partial^2 \bar{f}(\eta; p)}{\partial \eta^2} \right), \quad (8.21)
\end{aligned}$$

where \hbar_f and \hbar_g are the auxiliary non-zero parameters and $p \in [0, 1]$ is an embedding parameter.

For $p = 0$ and $p = 1$ we have

$$\bar{f}(\eta, 0) = f_0(\eta), \quad \bar{f}(\eta, 1) = f(\eta), \quad (8.22)$$

$$\bar{g}(\eta, 0) = g_0(\eta), \quad \bar{g}(\eta, 1) = g(\eta). \quad (8.23)$$

Note that when p varies from 0 to 1 then the initial guesses $f_0(\eta)$ and $g_0(\eta)$ approach $f(\eta)$ and $g(\eta)$ respectively and by Taylor's series expansion we have

$$\bar{f}(\eta, p) = f_0(\eta) + \sum_{m=1}^{\infty} f_m(\eta) p^m, \quad (8.24)$$

$$\bar{g}(\eta, p) = g_0(\eta) + \sum_{m=1}^{\infty} g_m(\eta) p^m, \quad (8.25)$$

$$f_m(\eta) = \frac{1}{m!} \left. \frac{\partial^m \bar{f}(\eta, p)}{\partial p^m} \right|_{p=0}, \quad (8.26)$$

$$g_m(\eta) = \frac{1}{m!} \left. \frac{\partial^m \bar{g}(\eta, p)}{\partial p^m} \right|_{p=0}, \quad (8.27)$$

where the convergence of series (8.24) and (8.25) strongly depends upon the auxiliary parameters \hbar_f and \hbar_g . These parameters are selected through such a procedure that the series (8.24) and

(8.25) converge for $p = 1$. Therefore we have

$$f(\eta) = f_0(\eta) + \sum_{m=1}^{\infty} f_m(\eta), \quad (8.28)$$

$$g(\eta) = g_0(\eta) + \sum_{m=1}^{\infty} g_m(\eta). \quad (8.29)$$

8.2.1 m th order deformation problems

Here the problems are of the following types

$$\mathcal{L}_f [f_m(\eta) - \chi_m f_{m-1}(\eta)] = \hbar_f \mathcal{R}_{f,m}(\eta), \quad (8.30)$$

$$\mathcal{L}_g [g_m(\eta) - \chi_m g_{m-1}(\eta)] = \hbar_g \mathcal{R}_{g,m}(\eta), \quad (8.31)$$

$$\begin{aligned} f_m(-1) = f'_m(-1) = f_m(1) = f'_m(1) = 0, \\ g_m(-1) = g_m(1) = 0, \end{aligned} \quad (8.32)$$

$$\chi_m = \begin{cases} 0, & m \leq 1 \\ 1, & m > 1 \end{cases}, \quad (8.33)$$

$$\begin{aligned} \mathcal{R}_{1m}(\eta) = & f_{m-1}^{(4)} - M^2 f_{m-1}'' + 2K^2 g_{m-1}' + R \sum_{k=0}^{m-1} [f'_{m-1-k} f_k'' - f_{m-1-k} f_k^{(4)}] \\ & + \beta \sum_{k=0}^{m-1} [f_{m-1-k} f_k^{(4)} + f'_{m-1-k} f_k^{(4)} - 2f_{m-1-k} f_k^{(4)}], \end{aligned} \quad (8.34)$$

$$\begin{aligned} \mathcal{R}_{2m}(\eta) = & g_{m-1}'' - M^2 g_{m-1} - 2K^2 f_{m-1}' + R \sum_{k=0}^{m-1} [g_{m-1-k} f_k' - g'_{m-1-k} f_k] \\ & + \beta \sum_{k=0}^{m-1} [f_{m-1-k} g_k''' - g'_{m-1-k} f_k''], \end{aligned} \quad (8.35)$$

$$\chi_m = \begin{cases} 0, & m \leq 1, \\ 1, & m > 1. \end{cases} \quad (8.36)$$

We notice that the above systems can be solved by means of the symbolic computation software MATHEMATICA.

8.3 Convergence of the homotopy solutions

The auxiliary parameters \hbar_f and \hbar_g in the series solutions (8.28) and (8.29) are important in controlling the convergence. For the allowed values of \hbar_f and \hbar_g , the \hbar_f and \hbar_g -curves are plotted at the center of the channel for 15th-order of approximations in Fig. 2. Here the range for the admissible values of \hbar_f and \hbar_g is $-1.0 \leq (\hbar_f, \hbar_g) \leq -0.2$. In Figs. 3 and 4 we have plotted the \hbar_f and \hbar_g -curves for residual errors of f and g in order to get the admissible range for \hbar_f and \hbar_g . We have analyzed that by choosing the values of \hbar_f and \hbar_g from this range we will get the correct result up to 6th decimal place. Our computations also indicate that the series given by Eqs. (8.28) and (8.29) converge in the whole region of η when $\hbar_f = -0.6 = \hbar_g$. Table 8.1 is prepared to show the convergence of series solutions. It is found that the convergence is achieved at 20th- order of approximations

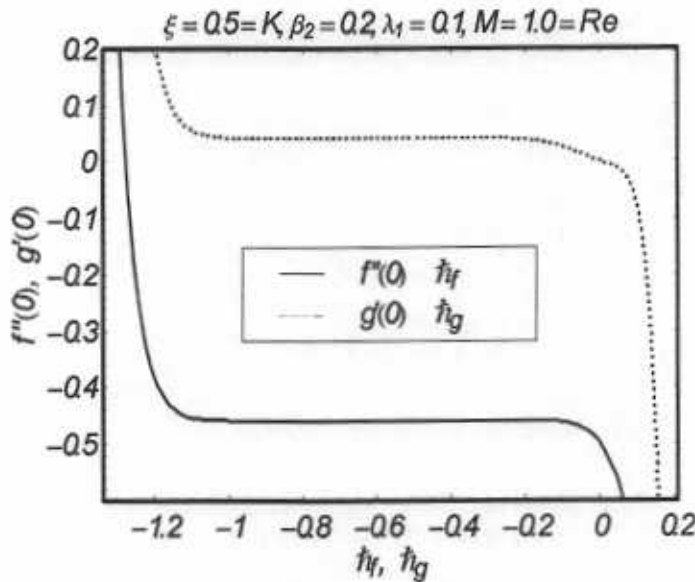


Fig. 8.2 : \hbar curve of $f''(0)$ at the 15th order of approximation.

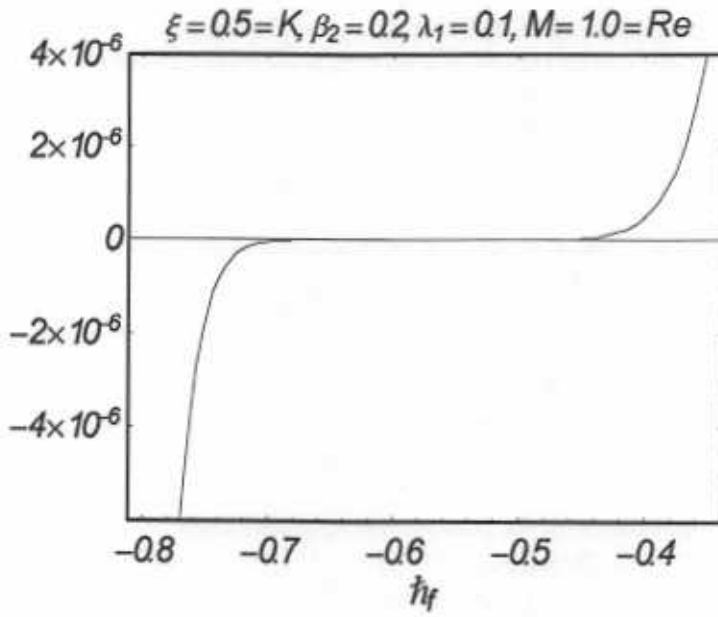


Fig. 8.3 : h curve for residual error in $f(\eta)$ at the 15th order of approximation.

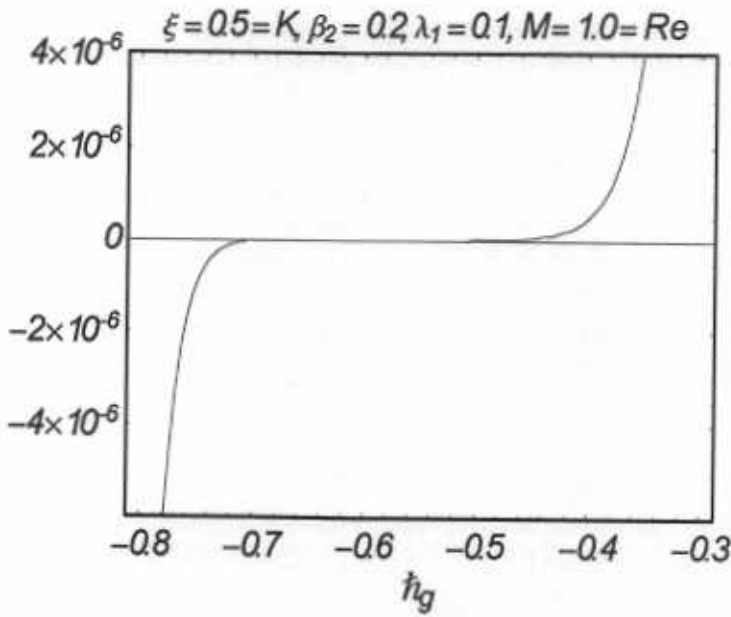


Fig. 8.4 : h curve for residual error in $g(\eta)$ at the 15th order of approximation.

Table 8.1: Convergence of the HAM solutions for different order of approximations when $Re = 5.0$, $\beta_2 = 0.5$, $\lambda_1 = 0.1$, $c = 0.5$ and $\xi = 0.5$.

Order of approximations	$-f''(0)$	$g'(0)$
1	0.4791666	0.0041666
5	0.4625018	0.0313111
10	0.4623650	0.0376506
20	0.4623255	0.0378602
40	0.4623255	0.0378602

8.4 Results and discussion

In this section we have prepared Figs. (8.5 – 8.10) in order to assess the effects of suction/injection parameter ξ , magnetic parameter M and rotation parameter K on the dimensionless velocity components f' and g . The effects of ξ on f' and g are shown in the Figs. 8.5 and 8.6. These Figs. depict that the magnitudes of f' and g increase with an increase in ξ . It is because of the fact that for the shrinking sheet the vorticity of the sheet is not confined within a boundary layer and the flow is unlikely to exist unless adequate suction is imposed on the sheet. Thus suction occurs when the fluid condenses on the surface. Therefore we can say that physically the suction plays very important role to flow the fluid smoothly in case of shrinking sheet. Figs. 8.7 and 8.8 show the effects of M on f' and g . It is observed from these Figs. that the magnitude of velocity components f' and g decreases with an increase in M . Physically when any fluid is subjected to a magnetic field then its apparent viscosity increases to the point of becoming a viscoelastic solid. Importantly, the yield stress of the fluid can be controlled very accurately by varying the magnetic field intensity. The outcome of which is that the fluid's ability to transmit force can be controlled with the help of an electromagnet, which gives rise to its many possible control-based applications including MHD power generation, electromagnetic casting of metals, MHD ion propulsion etc. The effects of rotation parameter K on f' and g are shown in the Figs. 8.9 and 8.10. These Figs. elucidate that velocity components f' and g show oscillating behavior with an increase in rotation parameter K . This physically predicts that oscillatory motion can also be engendered by increasing rotation.

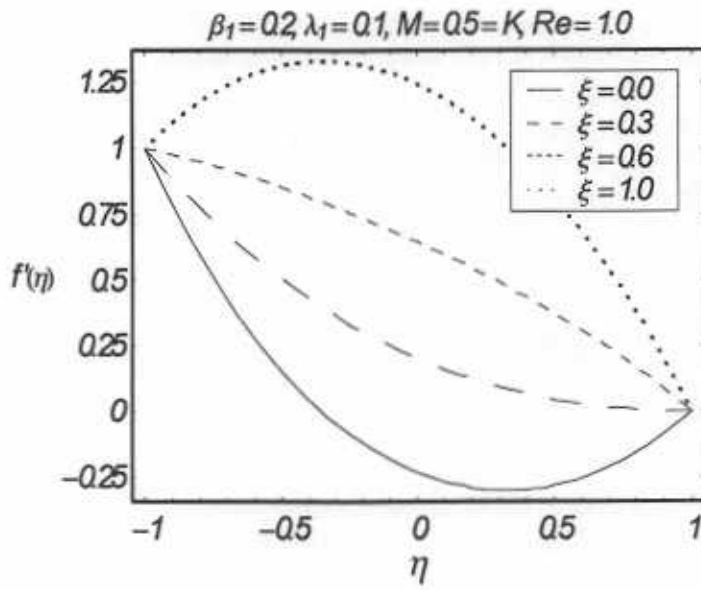


Fig. 8.5 : Influence of ξ on f' .

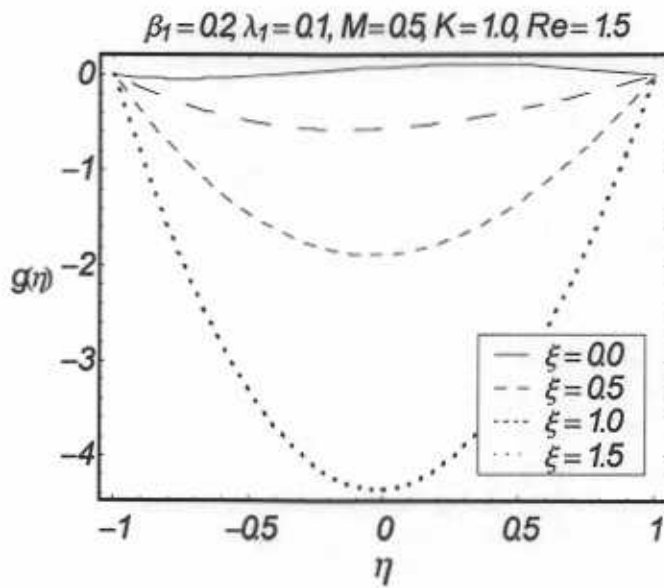


Fig. 8.6 : Influence of ξ on g .

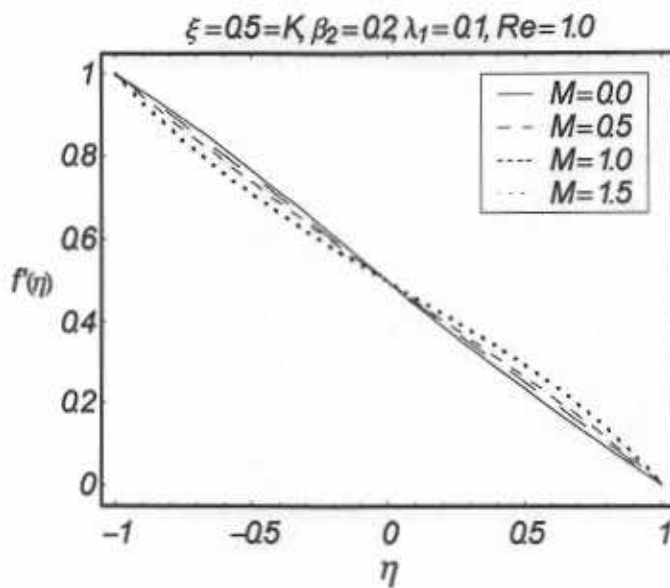


Fig. 8.7 : Influence of M on f' .

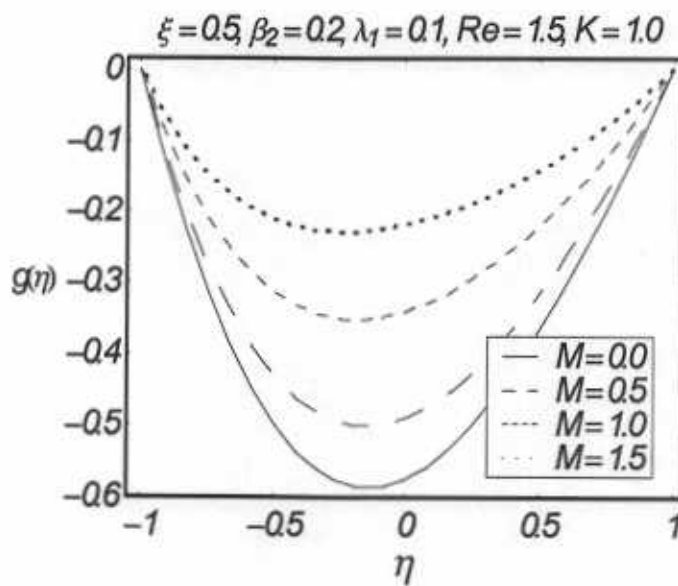


Fig. 8.8 : Influence of M on g .

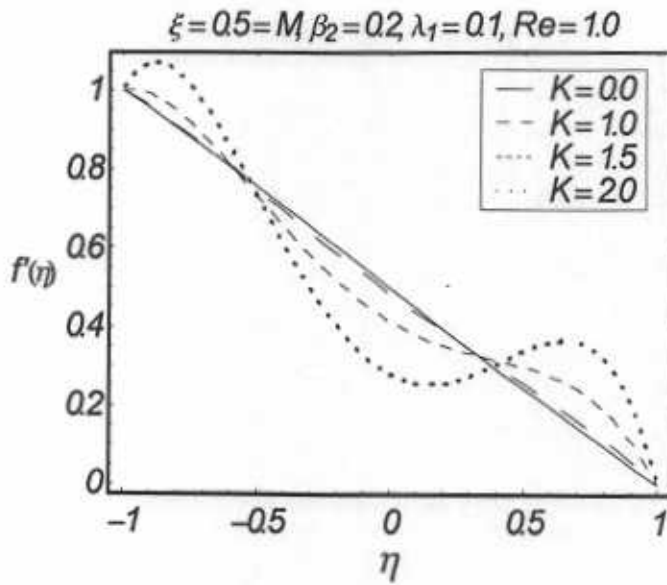


Fig. 8.9 : Influence of K on f' .

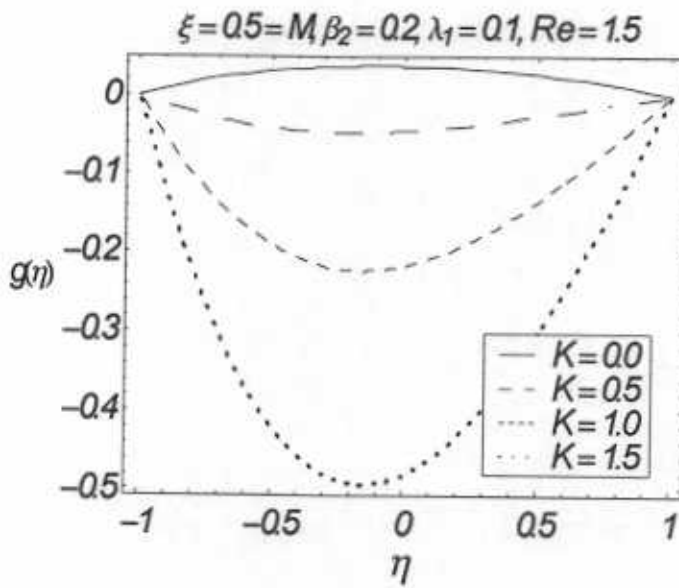


Fig. 8.10 : Influence of K on g .

8.5 Concluding remarks

Here analytic technique is employed to compute the rotating flow of a Jeffery fluid between the two porous plates. Mathematical calculations give rise to a non-linear differential system whose

series solution is computed by homotopy analysis method. Graphs are plotted to analyze the effects of various physical parameters. Main points are presented below.

- The magnitude of velocity components increases with an increase in suction/injection parameter ξ .
- It is observed that the applied magnetic field M retards the flow near the shrinking sheet.
- Oscillatory effects can be obtained by increasing rotation parameter K .
- The case of viscous fluid can be deduced by taking $\beta_2 = 0$.

Chapter 9

MHD axisymmetric flow of Jeffrey fluid over a rotating disk

This chapter examines the MHD boundary layer flow of Jeffrey fluid due to a rotating disk. Governing partial differential equations are first transformed into the coupled system of ordinary differential equations and then solved by using the homotopy analysis Method (HAM). Influence of various involved physical parameters on the dimensionless radial and azimuthal velocities is sketched and analyzed. Variation of skin friction coefficients in radial and azimuthal directions is examined for various values of pertinent parameters.

9.1 Mathematical analysis

We consider steady and axisymmetric boundary layer flow of an electrically conducting Jeffrey fluid bounded by a non-conducting infinite disk at $z = 0$ rotating with constant angular velocity Ω about the z -axis. A uniform magnetic field of strength B_0 is applied perpendicular (parallel to z -axis) to the plane of disk. Induced magnetic field is neglected under the assumption of small magnetic Reynolds number.

The boundary layer equations that govern the flow are

$$\frac{\partial u}{\partial r} + \frac{u}{r} + \frac{\partial w}{\partial z} = 0, \quad (9.1)$$

$$u \frac{\partial u}{\partial r} + w \frac{\partial u}{\partial z} - \frac{v^2}{r} = \frac{\nu}{1 + \lambda_1} \left[\frac{\partial^2 u}{\partial z^2} + \lambda_2 \left\{ \frac{\partial u}{\partial z} \frac{\partial^2 u}{\partial r \partial z} + u \frac{\partial^3 u}{\partial r \partial z^2} + \frac{\partial w}{\partial z} \frac{\partial^2 u}{\partial z^2} \right\} \right] \\ + \frac{\nu \lambda_2}{1 + \lambda_1} \left[w \frac{\partial^3 u}{\partial z^3} - \frac{1}{r} \left(\frac{\partial v}{\partial z} \right)^2 - \frac{v}{r} \frac{\partial^2 v}{\partial z^2} \right] - \frac{\sigma B_o^2}{\rho} u, \quad (9.2)$$

$$u \frac{\partial v}{\partial r} + w \frac{\partial v}{\partial z} + \frac{uv}{r} = \frac{\nu}{1 + \lambda_1} \left[\frac{\partial^2 v}{\partial z^2} + \lambda_2 \left\{ \frac{\partial u}{\partial z} \frac{\partial^2 v}{\partial r \partial z} + u \frac{\partial^3 v}{\partial r \partial z^2} + \frac{\partial w}{\partial z} \frac{\partial^2 v}{\partial z^2} \right\} \right] \\ + \frac{\nu \lambda_2}{1 + \lambda_1} \left[w \frac{\partial^3 v}{\partial z^3} + \frac{1}{r} \frac{\partial v}{\partial z} \frac{\partial u}{\partial z} + \frac{v}{r} \frac{\partial^2 u}{\partial z^2} \right] - \frac{\sigma B_o^2}{\rho} v, \quad (9.3)$$

where u , v and w are the velocity components in the r , θ and z directions respectively, ρ is the density and σ is the electrical conductivity of fluid. The appropriate boundary conditions are

$$u(r, 0) = 0, \quad v(r, 0) = r\Omega, \quad w(r, 0) \text{ at } z = 0, \\ u(r, z) = 0, \quad v(r, z) = 0 \text{ as } z \rightarrow \infty. \quad (9.4)$$

Using the following suitable transforms

$$u(r, z) = r\Omega f'(\eta), \quad v(r, z) = r\Omega g(\eta), \\ w(r, z) = -\sqrt{2\Omega\nu} f(\eta), \quad \eta = \sqrt{\frac{2\Omega}{\nu}} z, \quad (9.5)$$

Eqs. (9.2) and (9.3) become

$$f''' - \frac{1}{2}M(1 + \lambda_1)f' + \frac{(1 + \lambda_1)}{2} [2ff'' - f'^2 + g^2] \\ + \beta_2 [f''^2 - f'f''' - 2ff'''' - g'^2 - gg''] = 0, \quad (9.6)$$

$$g'' - \frac{1}{2}M(1 + \lambda_1)g + (1 + \lambda_1) [fg' - f'g] \\ + \beta_2 [2f''g' - f'g'' - 2fg''' + f'''g] = 0, \quad (9.7)$$

with the transformed boundary conditions

$$f(0) = 0, \quad f'(0) = 0, \quad f'(\infty) = 0, \\ g(0) = 1, \quad g(\infty) = 0, \quad (9.8)$$

where the dimensionless parameters

$$M = \frac{\sigma B_0^2}{\rho \Omega}, \quad \beta_2 = \Omega \lambda_2, \quad (9.9)$$

respectively denotes the Hartman number and the Deborah number. Moreover prime denotes derivative with respect to η .

The skin friction coefficients C_f and C_g in radial and azimuthal directions at the disk are

$$C_f = \frac{\tau_{rz}|_{z=0}}{\rho (\Omega r)^2}, \quad (9.10)$$

$$C_g = \frac{\tau_{\theta z}|_{z=0}}{\rho (\Omega r)^2}, \quad (9.11)$$

where τ_{rz} and $\tau_{\theta z}$ are defined as

$$\tau_{rz} = \frac{\mu}{1 + \lambda_1} \left[\frac{\partial u}{\partial z} + \lambda_2 \left\{ 3 \frac{\partial u}{\partial r} \frac{\partial u}{\partial z} + 2 \frac{\partial v}{\partial r} \frac{\partial v}{\partial z} - \frac{v}{r} \frac{\partial v}{\partial z} + \frac{\partial u}{\partial z} \frac{\partial w}{\partial z} \right\} \right], \quad (9.12)$$

$$\tau_{\theta z} = \frac{\mu}{1 + \lambda_1} \left[\frac{\partial v}{\partial z} + \lambda_2 \left\{ \frac{\partial u}{\partial z} \frac{\partial v}{\partial r} - \frac{2v}{r} \frac{\partial u}{\partial z} + \frac{3u}{r} \frac{\partial v}{\partial z} \right\} \right]. \quad (9.13)$$

Eqs. (9.12) and (9.13) in dimensionless form become

$$C_f = \left(\frac{2}{\text{Re}_r} \right)^{1/2} \frac{1}{1 + \lambda_1} [f'''(0) + 3\beta g'(0)], \quad (9.14)$$

$$C_g = \left(\frac{2}{\text{Re}_r} \right)^{1/2} \frac{1}{1 + \lambda_1} [g'(0) - \beta f''(0)], \quad (9.15)$$

where $\text{Re}_r = \Omega r^2 / \nu$ is the local rotational Reynolds number.

9.2 Solutions of the problems

Solutions $f(\eta)$ and $g(\eta)$ in the form of base functions

$$\{\eta^m \exp(-n\eta), \quad m \geq 0, \quad n \geq 0\}, \quad (9.16)$$

can be expressed as

$$f(\eta) = \sum_{m=0}^{\infty} \sum_{n=1}^{\infty} a_{m,n} \eta^m \exp(-n\eta), \quad (9.17)$$

$$g(\eta) = \sum_{m=0}^{\infty} \sum_{n=1}^{\infty} b_{m,n} \eta^m \exp(-n\eta), \quad (9.18)$$

Note that $a_{n,m}$ and $b_{n,m}$ are coefficients to be determined. The appropriate initial guesses $f_0(\eta)$, $g_0(\eta)$ and linear operators \mathcal{L}_f , \mathcal{L}_g can be chosen in the following forms

$$f_0(\eta) = 0, \quad (9.19)$$

$$g_0(\eta) = \exp(-\eta), \quad (9.20)$$

$$\mathcal{L}_f[f(\eta)] = \frac{\partial^3 f}{\partial \eta^3} - \frac{\partial f}{\partial \eta}, \quad (9.21)$$

$$\mathcal{L}_g[g(\eta)] = \frac{\partial^2 g}{\partial \eta^2} - g, \quad (9.22)$$

such that

$$\mathcal{L}_f[C_1 + C_2 \exp(\eta) + C_3 \exp(-\eta)] = 0, \quad (9.23)$$

$$\mathcal{L}_g[C_4 \exp(\eta) + C_5 \exp(-\eta)] = 0. \quad (9.24)$$

The zeroth order deformation problems are

$$(1-p)\mathcal{L}_f[\bar{f}(\eta;p) - f_0(\eta)] = p\hbar_f \mathcal{N}_f[\bar{f}(\eta;p), \bar{g}(\eta;p)], \quad (9.25)$$

$$(1-p)\mathcal{L}_g[\bar{g}(\eta;p) - g_0(\eta)] = p\hbar_g \mathcal{N}_g[\bar{f}(\eta;p), \bar{g}(\eta;p)], \quad (9.26)$$

$$\begin{aligned} \bar{f}(0;p) &= 0, \quad \left. \frac{\partial \bar{f}(\eta;p)}{\partial \eta} \right|_{\eta=0} = 0, \quad \bar{f}(\eta;p)|_{\eta=\infty} = 0, \\ \bar{g}(0;p) &= 1, \quad \bar{g}(\infty;p) = 0. \end{aligned} \quad (9.27)$$

In above expressions $p \in [0, 1]$ and $h_i \neq 0$ ($i = f, g$) are respectively the embedding and auxiliary parameters and $\bar{f}(\eta; 0) = f_0(\eta)$, $\bar{g}(\eta; 0) = g_0(\eta)$ and $\bar{f}(\eta; 1) = f(\eta)$, $\bar{g}(\eta; 1) = g(\eta)$. When p varies from 0 to 1, then $\bar{f}(\eta; p)$ varies from the initial guess $f_0(\eta)$ to $f(\eta)$ and $\bar{g}(\eta; p)$ varies from the initial guess $g_0(\eta)$ to $g(\eta)$ varies from the initial guess. We further led to define the following nonlinear operators \mathcal{N}_f and \mathcal{N}_g

$$\begin{aligned} \mathcal{N}_f [\bar{f}(\eta; p), \bar{g}(\eta; p)] &= \frac{\partial^3 \bar{f}(\eta; p)}{\partial \eta^3} - \frac{1}{2} M (1 + \lambda_1) \frac{\partial \bar{f}(\eta; p)}{\partial \eta} \\ &\frac{(1 + \lambda_1)}{2} \left[2\bar{f}(\eta; p) \frac{\partial^2 \bar{f}(\eta; p)}{\partial \eta^2} - \left(\frac{\partial \bar{f}(\eta; p)}{\partial \eta} \right)^2 + (\bar{g}(\eta; p))^2 \right] \\ &+ \beta_2 \left[\left(\frac{\partial^2 \bar{f}(\eta; p)}{\partial \eta^2} \right)^2 - \frac{\partial \bar{f}(\eta; p)}{\partial \eta} \frac{\partial^3 \bar{f}(\eta; p)}{\partial \eta^3} - 2\bar{f}(\eta; p) \frac{\partial^4 \bar{f}(\eta; p)}{\partial \eta^4} \right] \\ &- \beta_2 \left[\left(\frac{\partial \bar{g}(\eta; p)}{\partial \eta} \right)^2 + \bar{g}(\eta; p) \frac{\partial^2 \bar{g}(\eta; p)}{\partial \eta^2} \right], \end{aligned} \quad (9.28)$$

$$\begin{aligned} \mathcal{N}_g [\bar{f}(\eta; p), \bar{g}(\eta; p)] &= \frac{\partial^2 \bar{g}}{\partial \eta^2} - \frac{1}{2} M (1 + \lambda_1) \bar{g}(\eta; p) \\ &+ (1 + \lambda_1) \left[\bar{f}(\eta; p) \frac{\partial \bar{g}(\eta; p)}{\partial \eta} - \bar{g}(\eta; p) \frac{\partial \bar{f}(\eta; p)}{\partial \eta} \right] \\ &+ \beta_2 \left[2 \frac{\partial^2 \bar{f}(\eta; p)}{\partial \eta^2} \frac{\partial \bar{g}(\eta; p)}{\partial \eta} - \frac{\partial \bar{f}(\eta; p)}{\partial \eta} \frac{\partial^2 \bar{g}(\eta; p)}{\partial \eta^2} \right] \\ &- \beta_2 \left[2\bar{f}(\eta; p) \frac{\partial^3 \bar{g}(\eta; p)}{\partial \eta^3} - \frac{\partial^3 \bar{f}(\eta; p)}{\partial \eta^3} \bar{g}(\eta; p) \right]. \end{aligned} \quad (9.29)$$

With the help of Taylors theorem, one can get

$$f(\eta; q) = f_0(\eta) + \sum_{m=1}^{\infty} f_m(\eta) p^m, \quad (9.30)$$

$$g(\eta; q) = g_0(\eta) + \sum_{m=1}^{\infty} g_m(\eta) p^m, \quad (9.31)$$

where

$$f_m(\eta) = \frac{1}{m!} \left. \frac{\partial^m \bar{f}(\eta; p)}{\partial \eta^m} \right|_{p=0}, \quad (9.32)$$

$$g_m(\eta) = \frac{1}{m!} \left. \frac{\partial^m \bar{g}(\eta; p)}{\partial \eta^m} \right|_{p=0}. \quad (9.33)$$

Writing

$$f_m(\eta) = \{f_0(\eta), f_1(\eta), f_2(\eta), f_3(\eta) \dots f_m(\eta)\}, \quad (9.34)$$

$$g_m(\eta) = \{g_0(\eta), g_1(\eta), g_2(\eta), g_3(\eta) \dots g_m(\eta)\}, \quad (9.35)$$

the deformation problems at the m th order are

$$\mathcal{L}_f [f_m(\eta) - \chi_m f_{m-1}(\eta)] = \hbar_f \mathcal{R}_m^f (f_{m-1}(\eta), g_{m-1}(\eta)), \quad (9.36)$$

$$\mathcal{L}_g [g_m(\eta) - \chi_m g_{m-1}(\eta)] = \hbar_g \mathcal{R}_m^g (g_{m-1}(\eta)), \quad (9.37)$$

$$\begin{aligned} f_m(0) &= 0, \quad f'_m(0) = 0, \quad f'_m(\infty) = 0, \\ g_m(0) &= 0, \quad g'_m(\infty) = 0, \end{aligned} \quad (9.38)$$

$$\chi_m = \begin{cases} 0, & m \leq 1, \\ 1, & m > 1, \end{cases} \quad (9.39)$$

$$\begin{aligned} \mathcal{R}_m^f &= f_{m-1}'''(\eta) - \frac{1}{2} M (1 + \lambda_1) f_{m-1}'(\eta) + \frac{(1 + \lambda_1)}{2} \sum_{n=0}^{m-1} [2f_n(\eta) f_{m-n-1}''(\eta)] \\ &\quad - \frac{(1 + \lambda_1)}{2} \sum_{n=0}^{m-1} [f_n'(\eta) f_{m-n-1}'(\eta) - g_n(\eta) g_{m-n-1}(\eta)] \\ &\quad + \beta \sum_{n=0}^{m-1} [f_n''(\eta) f_{m-n-1}''(\eta) - f_n'(\eta) f_{m-n-1}'''(\eta) - 2f_n(\eta) f_{m-n-1}''''(\eta)] \\ &\quad - \beta \sum_{n=0}^{m-1} [g_n'(\eta) g_{m-n-1}'(\eta) + g_n(\eta) g_{m-n-1}''(\eta)], \end{aligned} \quad (9.40)$$

$$\begin{aligned}
\mathcal{R}_m^g &= g''_{m-1}(\eta) - \frac{1}{2}M(1 + \lambda_1)g_{m-1}(\eta) + (1 + \lambda_1) \sum_{n=0}^{m-1} [f_n(\eta)g'_{m-n-1}(\eta)] \\
&\quad - (1 + \lambda_1) \sum_{n=0}^{m-1} [f'_n(\eta)g_{m-n-1}(\eta)] + \beta \sum_{n=0}^{m-1} [2f''_n(\eta)g'_{m-n-1}(\eta) - f'_n(\eta)g''_{m-n-1}(\eta)] \\
&\quad - \beta \sum_{n=0}^{m-1} [2f_n(\eta)g'''_{m-n-1}(\eta) - f'''_n(\eta)g_{m-n-1}(\eta)]. \tag{9.41}
\end{aligned}$$

The general solutions of problems (9.30) and (9.31) are

$$f(\eta) = f^*(\eta) + C_1^m + C_2^m \exp(\eta) + C_3^m \exp(-\eta), \tag{9.42}$$

$$g(\eta) = g^*(\eta) + C_4^m \exp(\eta) + C_5^m \exp(-\eta), \tag{9.43}$$

where $f^*(\eta)$, and $g^*(\eta)$ are particular solutions.

9.3 Convergence of the series solutions

The convergence of the series solutions given by Eqs. (9.30) and (9.31) depends upon the values of auxiliary parameters \hbar_f and \hbar_g . For this purpose the \hbar_i -curves of $f''(0)$ and $g'(0)$ are plotted for 15th order of approximations in order to get the admissible ranges of \hbar_i . Figs. 1 and 2 show that the ranges for these auxiliary parameters are $-1.0 \leq (\hbar_f, \hbar_g) \leq -0.2$. Table 9.1 is constructed in order to ensure the convergence of HAM solutions. Convergence is achieved up to 20th order of approximations.

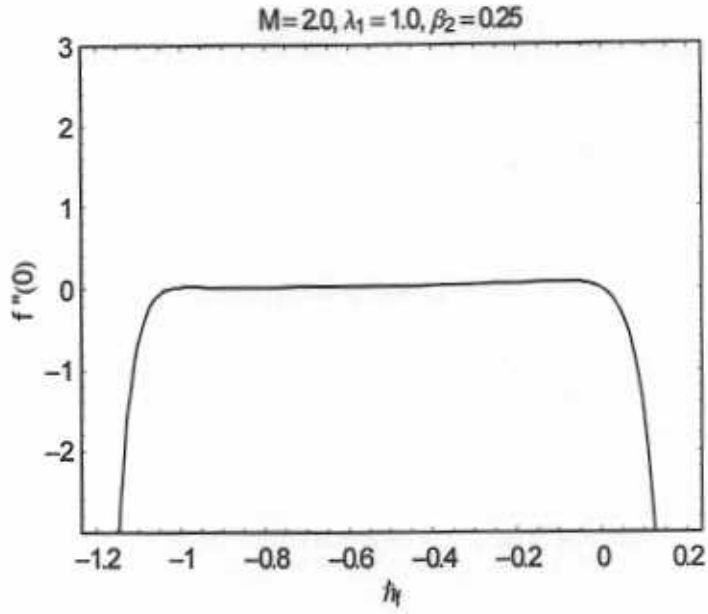


Fig. 9.1 : h curves of $f''(0)$ at the 15th order of approximation.

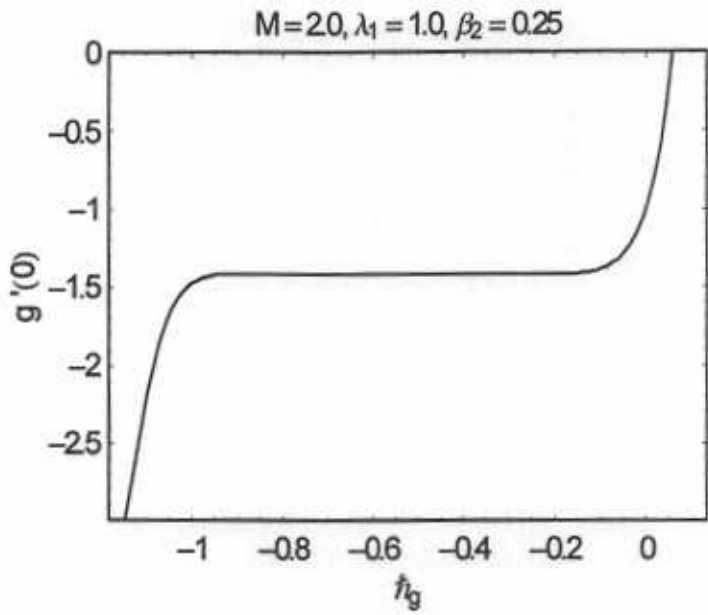


Fig. 9.2 : h curves of $g'(0)$ at the 15th order of approximation.

Table 9.1: The convergence of HAM solutions $f''(0)$ and $g'(0)$ for different order of Pade-approximations when $M = 2.0$, $\lambda_1 = 1.0$ and $\beta_2 = 0.25$.

Pade approximations $[m, m]$	$f''(0)$	$-g'(0)$
[1, 1]	0.100	1.43902
[5, 5]	0.0396	1.42205
[10, 10]	0.011	1.41458
[15, 15]	0.004	1.41443
[20, 20]	0.0020	1.41443
[21, 21]	0.0020	1.41443

9.4 Results and discussion

Here Figs. (9.3) – (9.5) are plotted to see the influence of Hartman number M , Deborah number β_2 and λ_1 (the ratio of relaxation time to retardation time) on the dimensionless radial velocity $f'(\eta)$ and Figs. 9.6 – 9.8 are sketched to study the influence of M , λ_1 and β_2 on dimensionless azimuthal velocity $g(\eta)$. Fig. 9.3 shows that dimensionless radial velocity $f'(\eta)$ decreases with an increase of Hartman number M . This shows that magnetic field decelerates the motion of fluid in radial direction. This Fig. also shows that boundary layer thickness decreases with the increase of Hartman number M . Fig. 9.4 illustrates that the dimensionless radial velocity $f'(\eta)$ has decreasing trend when Deborah number β_2 is increased. From this Fig. one can conclude that the boundary layer thickness decreases by increasing β_2 . It is noted from Fig. 9.5 that radial velocity $f'(\eta)$ is an increasing function of λ_1 . This Fig. also depicts that boundary layer thickness increases when λ_1 is increased. Fig. 9.6 indicates that the dimensionless azimuthal velocity $g(\eta)$ decreases with an increase in Hartman number M . It means that magnetic field retards the motion of fluid particles in axial direction. Fig. 9.7 depicts that the dimensionless axial velocity $g(\eta)$ and the boundary layer thickness increase with the increase of Deborah number β_2 . Fig. 9.8 illustrates that the dimensionless axial velocity $g(\eta)$ decreases when λ_1 increases and the boundary layer thickness also decreases. Table 9.2 is constructed for the variation of skin friction coefficients in radial and azimuthal directions for various values of physical parameters. From this table it can be concluded that $(\frac{Re_\infty}{2})^{1/2} C_f$ is decreasing function of M and β_2 but it increases with an increase in λ_1 . However $(\frac{Re_\infty}{2})^{1/2} C_g$

is increasing function of M and λ_1 whereas it decreases by increasing β_2 .

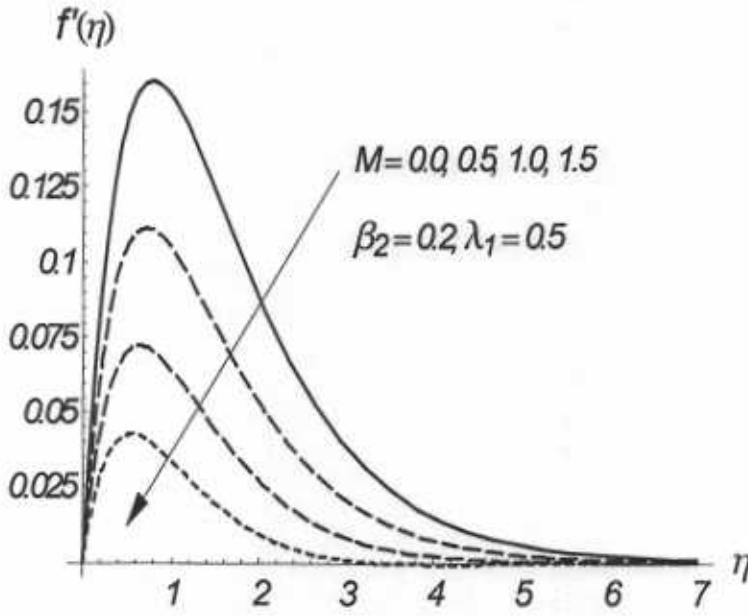


Fig. 9.3. Variation of radial velocity $f'(\eta)$ for different values of M .

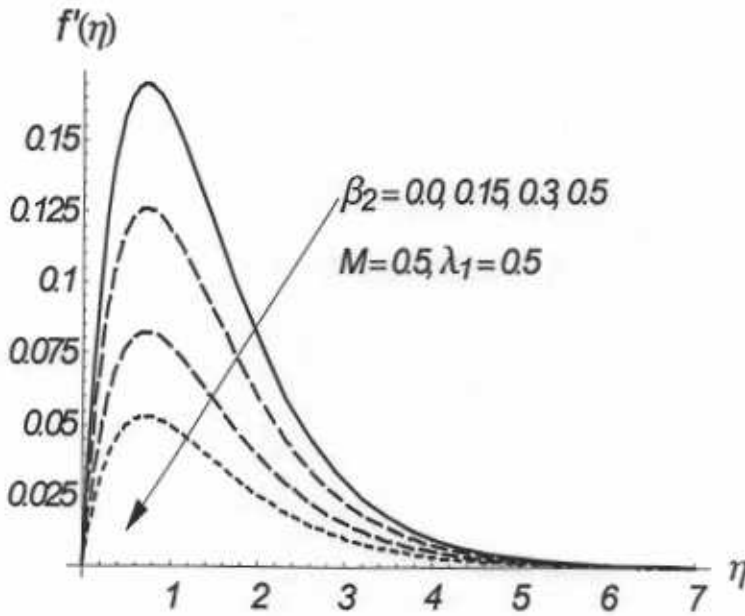


Fig. 9.4. Variation of radial velocity $f'(\eta)$ for different values of β_2 .

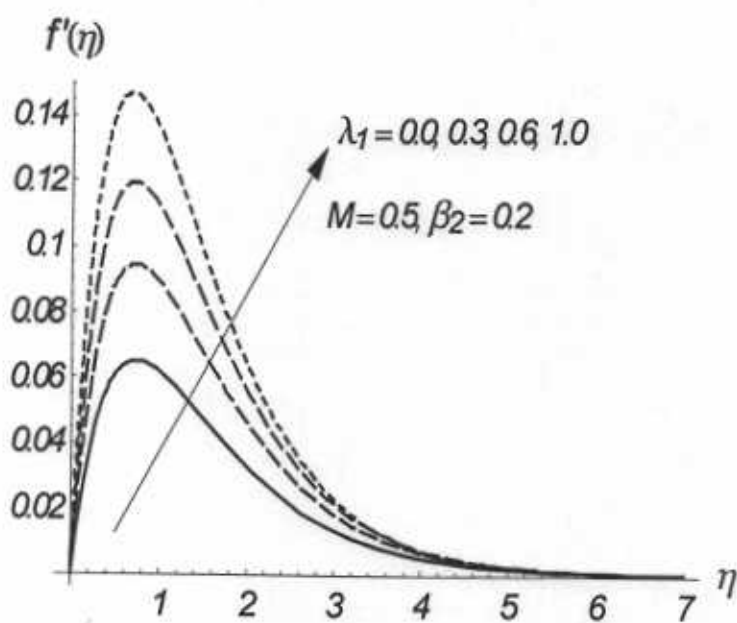


Fig. 9.5. Variation of radial velocity $f'(\eta)$ for different values of λ_1 .

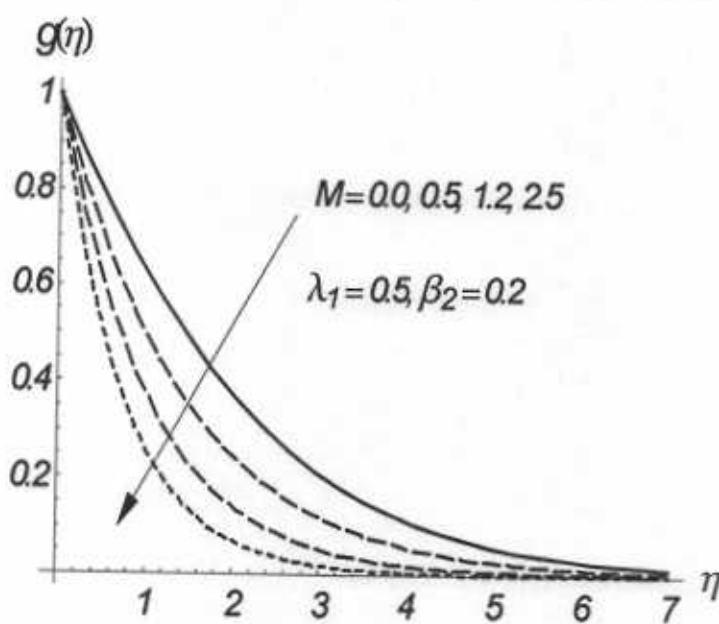


Fig. 9.6. Variation of azimuthal velocity $g(\eta)$ for different values of M .

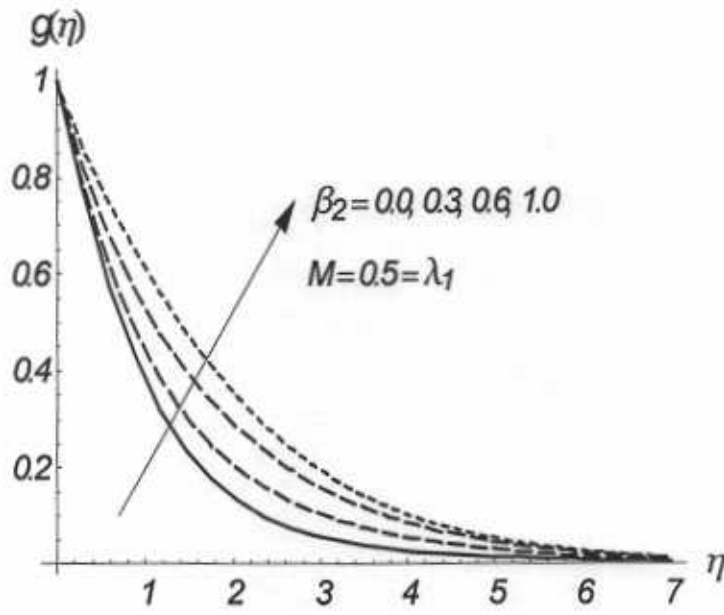


Fig. 9.7. Variation of azimuthal velocity $g(\eta)$ for different values of β_2 .

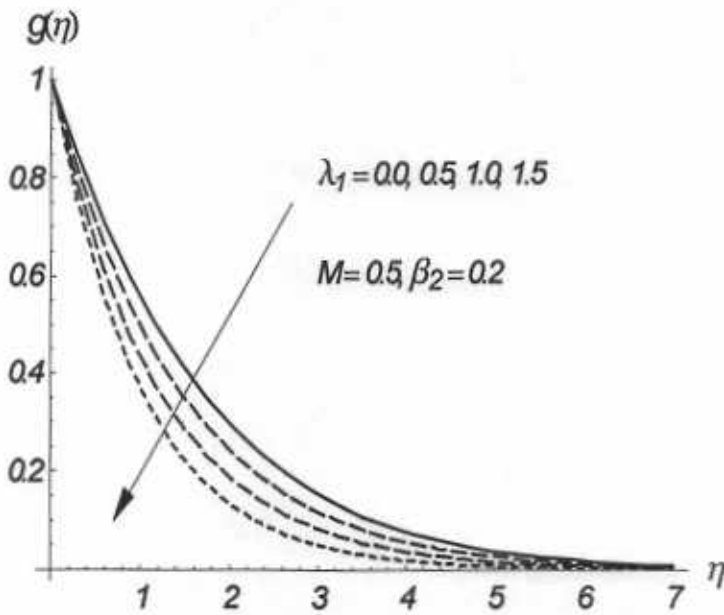


Fig. 9.8. Variation of azimuthal velocity $g(\eta)$ for different values of λ_1 .

Table 9.2: Numerical values of skin friction coefficients for different values of physical parameter.

M	λ_1	β_2	$(\frac{Re_r}{2})^{1/2} C_f$	$(\frac{Re_r}{2})^{1/2} C_g$
0.0	1.0	0.25	1.01735	-1.27135
	1.0		-0.01336	-1.09247
	2.0		-0.72170	-1.00951
	2.5		-0.98025	-0.99714
2.0	0.0		-1.06066	-1.41421
	0.7		-0.78815	-1.09225
	1.5		-0.64475	-0.90213
	1.0	0.0	0.41359	-0.99478
		0.25	-0.72123	-0.78113
		0.5	-1.89795	-0.56231

9.5 Final remarks

The study of MHD flow of Jeffery fluid due to rotating disk is presented. The governing problems are solved analytically using HAM. The main points are given below.

- Dimensionless radial velocity $f'(\eta)$ decreases when M and β_2 are increased but it increases with the increase of λ_1 .
- Boundary layer thickness associated with dimensionless radial velocity $f'(\eta)$ decreases when M and β_2 increase but it increases by increasing λ_1 .
- Dimensionless azimuthal velocity $g(\eta)$ decreases with an increase in M and λ_1 whereas it increases with an increase in β .
- Boundary layer thickness for an azimuthal velocity $g(\eta)$ decreases with an increase in M and λ_1 whereas it increases for positive values of β_2 .
- Skin friction coefficient C_f in the radial direction is a decreasing function of M and β_2 but it increases by increasing λ_1 .

- Skin friction coefficient C_g in azimuthal direction increases when M , λ_1 and β_2 are increased.

Chapter 10

Unsteady three-dimensional flow of second grade fluid over a stretching surface

The three-dimensional unsteady flow of stretching surface is investigated. Constitutive relationships of second grade fluid are utilized in the problem formulation. Nonlinear partial differential equations are reduced into a system of ordinary differential equations by using the similarity transformations. The homotopy analysis method (HAM) has been implemented for the series solutions. Graphs are displayed for the effects of different parameters on the velocity field.

10.1 Mathematical analysis

Let us consider the unsteady three-dimensional flow of a second grade fluid over a stretching surface. The fluid is bounded by the non-conducting surface situated at $z = 0$. An incompressible fluid occupies the region $z > 0$. The equations governing the boundary layer flow are

$$\frac{\partial u}{\partial x} + \frac{\partial v}{\partial y} + \frac{\partial w}{\partial z} = 0, \quad (10.1)$$

$$\rho \left(\frac{\partial u}{\partial t} + u \frac{\partial u}{\partial x} + v \frac{\partial u}{\partial y} + w \frac{\partial u}{\partial z} \right) = \mu \frac{\partial^2 u}{\partial z^2} + \alpha_1 \left(\begin{array}{l} u \frac{\partial^3 u}{\partial z \partial z^2} + v \frac{\partial^3 u}{\partial y \partial z^2} + w \frac{\partial^3 u}{\partial z^3} \\ - \frac{\partial u}{\partial z} \frac{\partial^2 w}{\partial z^2} + \frac{\partial u}{\partial x} \frac{\partial^2 u}{\partial z^2} + \frac{\partial^2 v}{\partial z \partial x} \frac{\partial v}{\partial z} \\ + \frac{\partial v}{\partial x} \frac{\partial^2 v}{\partial z^2} - \frac{\partial u}{\partial z} \frac{\partial^2 v}{\partial y \partial z} + \frac{\partial^3 u}{\partial t \partial z^2} \end{array} \right), \quad (10.2)$$

$$\rho \left(\frac{\partial v}{\partial t} + u \frac{\partial v}{\partial x} + v \frac{\partial v}{\partial y} + w \frac{\partial v}{\partial z} \right) = \mu \frac{\partial^2 v}{\partial z^2} + \alpha_1 \left(\begin{array}{l} u \frac{\partial^3 v}{\partial x \partial z^2} + v \frac{\partial^3 v}{\partial y \partial z^2} + w \frac{\partial^3 v}{\partial z^3} \\ - \frac{\partial v}{\partial z} \frac{\partial^2 w}{\partial z^2} + \frac{\partial u}{\partial y} \frac{\partial^2 u}{\partial z^2} + \frac{\partial^2 v}{\partial z^2} \frac{\partial v}{\partial y} \\ + \frac{\partial u}{\partial z} \frac{\partial^2 u}{\partial y \partial z} - \frac{\partial v}{\partial z} \frac{\partial^2 u}{\partial x \partial z} + \frac{\partial^3 v}{\partial t \partial z^2} \end{array} \right). \quad (10.3)$$

The subjected boundary conditions are given by

$$\begin{aligned} u &= \frac{ax}{1-\alpha t}, \quad v = \frac{bx}{1-\alpha t}, \quad w = 0 \quad \text{at } z = 0, \\ u &\rightarrow 0, \quad v \rightarrow 0, \quad \frac{\partial u}{\partial z} \rightarrow 0, \quad \frac{\partial v}{\partial z} \rightarrow 0 \quad \text{as } z \rightarrow \infty, \end{aligned} \quad (10.4)$$

where u , v and w as the velocities parallel to the x , y and z directions respectively, ρ indicates the fluid density, μ the dynamic viscosity, α_1 the second grade parameter and the constants $a > 0$, $b > 0$ and $\alpha t < 1$. We now define

$$\begin{aligned} \eta &= \sqrt{\frac{a}{\nu(1-\alpha t)}} z, \quad u = \frac{ax}{1-\alpha t} f'(\eta), \quad v = \frac{ay}{1-\alpha t} g'(\eta), \\ w &= -\sqrt{\frac{av}{1-\alpha t}} \{f(\eta) + g(\eta)\}. \end{aligned} \quad (10.5)$$

All the quantities appearing in Eqs. (10.2) – (10.3) have been computed using Chain rule through Eq. (10.5). It is noticed that Eq. (10.1) is identically satisfied and Eqs. (10.2) and (10.3) become

$$f''' - f'^2 + (f+g)f'' - \zeta(f' + \frac{\eta}{2}f'') + \alpha^* \left[\begin{array}{l} f''^2 + 2f'f''' - (f+g)f^{iv} \\ + \zeta(2f''' + \frac{\eta}{2}f^{iv}) \end{array} \right] = 0, \quad (10.6)$$

$$g''' - g'^2 + (f+g)g'' - \zeta(g' + \frac{\eta}{2}g'') + \alpha^* \left[\begin{array}{l} g''^2 + 2g'g''' - (f+g)g^{iv} \\ + \zeta(2g''' + \frac{\eta}{2}g^{iv}) \end{array} \right] = 0. \quad (10.7)$$

Now the boundary conditions through Eqs. (10.4) and (10.5) give

$$f(0) + g(0) = 0, \quad f'(0) = 1, \quad f'(\infty) = 0, \quad g'(0) = c, \quad g'(\infty) = 0, \quad (10.8)$$

where ζ is the time dependent parameter, α^* is the dimensionless second grade parameter and c is the ratio parameter. These are given by

$$\zeta = c/a, \quad \alpha^* = \frac{a\alpha_1}{\mu(1 - \alpha t)}, \quad c = b/a. \quad (10.9)$$

10.2 Series solutions

10.2.1 Zeroth-order deformation problems

The velocity distributions $f(\eta)$ and $g(\eta)$ in the set of base functions

$$\left\{ \eta^k \exp(-n\eta) \mid k \geq 0, n \geq 0 \right\}, \quad (10.10)$$

are given by

$$f(\eta) = a_{0,0}^0 + \sum_{n=1}^{\infty} \sum_{k=1}^{\infty} a_{m,n}^k \eta^k \exp(-n\eta), \quad (10.11)$$

$$g(\eta) = A_{0,0}^0 + \sum_{n=1}^{\infty} \sum_{k=1}^{\infty} A_{m,n}^k \eta^k \exp(-n\eta), \quad (10.12)$$

where as the initial guesses are

$$f_0(\eta) = 1 - \exp(-\eta), \quad (10.13)$$

$$g_0(\eta) = c(1 - \exp(-\eta)). \quad (10.14)$$

The linear operators and their associated properties are

$$\mathcal{L}_f = \frac{d^3 f}{d\eta^3} - \frac{df}{d\eta}, \quad (10.15)$$

$$\mathcal{L}_g = \frac{d^3 g}{d\eta^3} - \frac{dg}{d\eta}, \quad (10.16)$$

$$\mathcal{L}_f [C_1 + C_2 \exp(\eta) + C_3 \exp(-\eta)] = 0, \quad (10.17)$$

$$\mathcal{L}_g [C_4 + C_5 \exp(\eta) + C_6 \exp(-\eta)] = 0, \quad (10.18)$$

where $C_1 - C_6$ are the constants and $a_{m,n}^k$ and $A_{m,n}^k$ are the coefficients.

The problems corresponding to the zeroth order deformation can be written as

$$(1-p)\mathcal{L}[\bar{f}(\eta, p) - f_0(\eta)] = p\hbar_f \mathcal{N}_f[\bar{f}(\eta, p), \bar{g}(\eta, p)], \quad (10.19)$$

$$(1-p)\mathcal{L}[\bar{g}(\eta, p) - g_0(\eta)] = p\hbar_g \mathcal{N}_g[\bar{f}(\eta, p), \bar{g}(\eta, p)], \quad (10.20)$$

$$\begin{aligned} \bar{f}(0, p) &= 0, \quad \bar{f}'(0, p) = 1, \quad \bar{g}(0, p) = 0, \quad \bar{g}'(0, p) = p, \\ \bar{f}'(\infty, p) &= 0, \quad \bar{g}'(\infty, p) = 0, \end{aligned} \quad (10.21)$$

$$\begin{aligned} \mathcal{N}_f[\bar{f}(\eta, p), \bar{g}(\eta, p)] &= \frac{\partial^3 \bar{f}}{\partial \eta^3} - \left(\frac{\partial \bar{f}}{\partial \eta}\right)^2 + \{\bar{f}(\eta, p) + \bar{g}(\eta, p)\} \frac{\partial^2 \bar{f}}{\partial \eta^2} \\ &\quad - \zeta \left\{ \bar{f}'(\eta, p) + \frac{\eta}{2} \bar{f}''(\eta, p) \right\} + \alpha^* \left[\begin{aligned} &\bar{f}''^2(\eta, p) + 2\bar{f}'(\eta, p)\bar{f}'''(\eta, p) \\ &- \{\bar{f}(\eta, p) + \bar{g}(\eta, p)\} \bar{f}^{iv}(\eta, p) \\ &+ A \{2\bar{f}'''(\eta, p) + \frac{\eta}{2} \bar{f}^{iv}(\eta, p)\} \end{aligned} \right], \end{aligned} \quad (10.22)$$

$$\begin{aligned} \mathcal{N}_g[\bar{f}(\eta, p), \bar{g}(\eta, p)] &= \frac{\partial^3 \bar{g}}{\partial \eta^3} - \left(\frac{\partial \bar{g}}{\partial \eta}\right)^2 + \{\bar{f}(\eta, p) + \bar{g}(\eta, p)\} \frac{\partial^2 \bar{g}}{\partial \eta^2} \\ &\quad - \zeta \left\{ \bar{g}'(\eta, p) + \frac{\eta}{2} \bar{g}''(\eta, p) \right\} + \alpha^* \left[\begin{aligned} &\bar{g}''^2(\eta, p) + 2\bar{g}'(\eta, p)\bar{g}'''(\eta, p) \\ &- \{\bar{f}(\eta, p) + \bar{g}(\eta, p)\} \bar{g}^{iv}(\eta, p) \\ &+ A \{2\bar{g}'''(\eta, p) + \frac{\eta}{2} \bar{g}^{iv}(\eta, p)\} \end{aligned} \right]. \end{aligned} \quad (10.23)$$

Here \hbar_f and \hbar_g show the auxiliary non-zero parameters and $p \in [0, 1]$ indicates an embedding parameter. For $p = 0$ and $p = 1$ we have

$$\begin{aligned} \bar{f}(\eta, 0) &= f_0(\eta), & \bar{f}(\eta, 1) &= f(\eta), \\ \bar{g}(\eta, 0) &= g_0(\eta), & \bar{g}(\eta, 1) &= g(\eta), \end{aligned} \quad (10.24)$$

and the initial guesses $f_0(\eta)$ and $g_0(\eta)$ approach to the final solutions $f(\eta)$ and $g(\eta)$ when p

varies from 0 to 1. In view of Taylor's expression

$$\bar{f}(\eta, p) = f_0(\eta) + \sum_{m=1}^{\infty} f_m(\eta) p^m, \quad (10.25)$$

$$\bar{g}(\eta, p) = g_0(\eta) + \sum_{m=1}^{\infty} g_m(\eta) p^m, \quad (10.26)$$

$$f_m(\eta) = \frac{1}{m!} \left. \frac{\partial^m \bar{f}(\eta, p)}{\partial p^m} \right|_{p=0}, \quad g_m(\eta) = \frac{1}{m!} \left. \frac{\partial^m \bar{g}(\eta, p)}{\partial p^m} \right|_{p=0}, \quad (10.27)$$

and the convergence of series (10.25) and (10.26) depends upon \hbar_f and \hbar_g . The \hbar_f and \hbar_g are chosen in such a way that the series (10.25) and (10.26) converge for $p = 1$. Hence

$$f(\eta) = f_0(\eta) + \sum_{m=1}^{\infty} f_m(\eta), \quad (10.28)$$

$$g(\eta) = g_0(\eta) + \sum_{m=1}^{\infty} g_m(\eta), \quad (10.29)$$

10.2.2 *m*th order deformation problems

The problems corresponding to the *m*th order deformations are

$$\mathcal{L}_f [f_m(\eta) - \chi_m f_{m-1}(\eta)] = \hbar_f \mathcal{R}_{f,m}(\eta), \quad (10.30)$$

$$\mathcal{L}_g [g_m(\eta) - \chi_m g_{m-1}(\eta)] = \hbar_g \mathcal{R}_{g,m}(\eta), \quad (10.31)$$

$$f_m(0) + g_m(0) = f'_m(0) = f'_m(\infty) = g'_m(0) = g'_m(\infty) = 0, \quad (10.32)$$

$$\begin{aligned} \mathcal{R}_m^f(\eta) = & f_{m-1}''' + \sum_{k=0}^{m-1} [(f_{m-1-k} + g_{m-1-k}) f_k'' - f_{m-1-k}' f_k'] - \zeta (f_{m-1}' + \frac{\eta}{2} f_{m-1}'') \\ & + \alpha^* \left[\sum_{k=0}^{m-1} \{ f_{m-1-k}'' f_k'' + 2 f_{m-1-k}' f_k''' - (f_{m-1-k} + g_{m-1-k}) f_k^{iv} \} \right. \\ & \left. + \zeta (2 f_{m-1}''' + \frac{\eta}{2} f_{m-1}^{iv}) \right] \end{aligned} \quad (10.33)$$

$$\begin{aligned} \mathcal{R}_m^g(\eta) = & g_{m-1}''' + \sum_{k=0}^{m-1} [(f_{m-1-k} + g_{m-1-k}) g_k'' - g_{m-1-k}' g_k'] - \zeta (g_{m-1}' + \frac{\eta}{2} g_{m-1}'') \\ & + \alpha^* \left[\sum_{k=0}^{m-1} \{ g_{m-1-k}'' g_k'' + 2 g_{m-1-k}' g_k''' - (f_{m-1-k} + g_{m-1-k}) g_k^{iv} \} \right. \\ & \left. + \zeta (2 g_{m-1}''' + \frac{\eta}{2} g_{m-1}^{iv}) \right] \end{aligned} \quad (10.34)$$

$$\chi_m = \begin{cases} 0, & m \leq 1 \\ 1, & m > 1 \end{cases} \quad (10.35)$$

Using MATHEMATICA the resulting problems for $m = 1, 2, 3, \dots$ have been solved successfully.

It is worth mentioning to point out that present problem for $\zeta = 0 = \alpha^*$ reduces to the problem of a viscous fluid. Exact numerical solution for this viscous fluid problem is computed by Ariel [41]. The present attempt extends the analysis of Ariel [41] from viscous to second grade fluid. The considered fluid model has preference in the sense that it can easily describes the normal stress effects. This consideration hikes the order of differential system. Further the governing equations are more complicated and nonlinear. Such complexities appear due to viscoelastic properties of second grade fluid. Another difference occurs in the boundary conditions. Ariel [41] considered the steady case of stretching surface whereas unsteady stretched flow is taken into account in the present analysis.

10.3 Convergence of the series solutions

It is noted that the convergence of solution depends on \hbar_f and \hbar_g . Figs. 10.1 and 10.2 help for the allowed values of \hbar_f and \hbar_g in the convergent solutions. This Fig. shows that admissible values are $-1.0 \leq (\hbar_f, \hbar_g) \leq -0.25$. Table 10.1 is presented to access that how much order of approximation is necessary for a convergent solution. It is noticed that 20th order approximations are sufficient. Table 10.2 presents the comparison of the present HAM results with the

results found by Ariel [41] for the case of viscous fluid. An excellent agreement is found between the results.

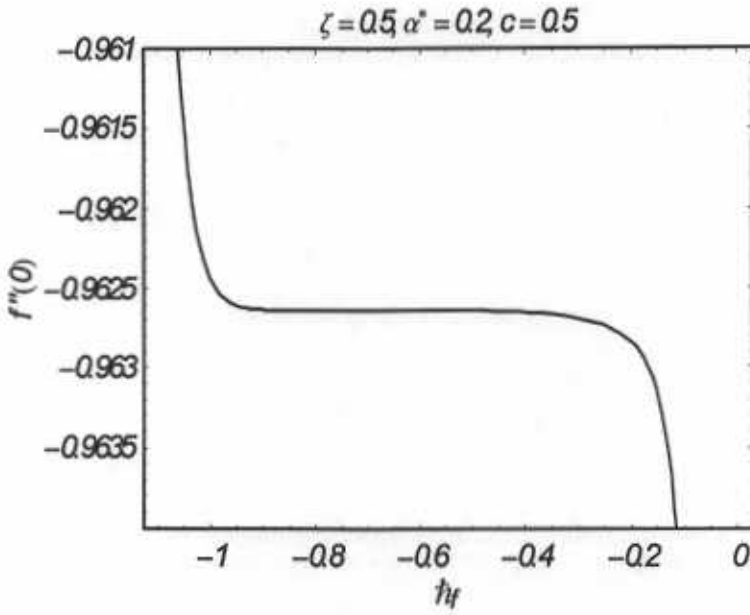


Fig. 10.1 : h curves of $f''(0)$ at the 15th order of approximation.

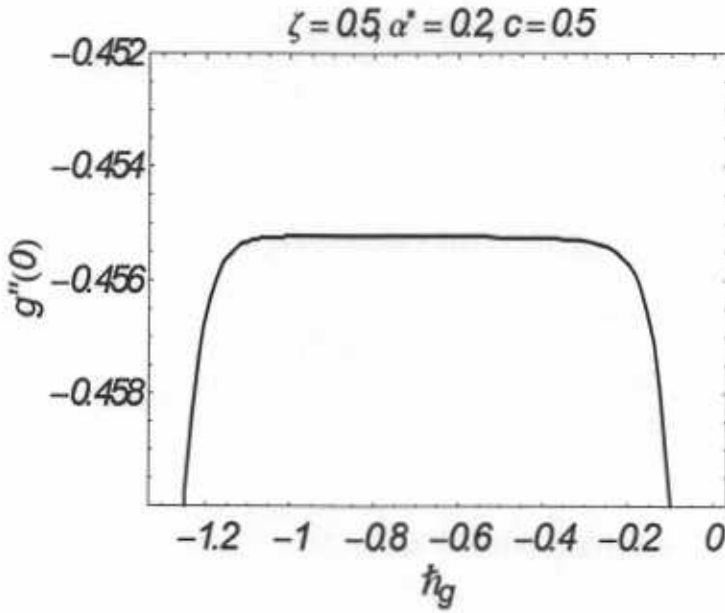


Fig. 10.2 : h curves of $g''(0)$ at the 15th order of approximation.

Table 10.1: Convergence of the HAM solutions for different order of approximations when $c = 0.5$, $\alpha^* = 0.2$ and $\zeta = 0.5$.

order of approximation	$-f''(0)$	$-g''(0)$
1	0.953333	0.453333
2	0.965036	0.455542
5	0.455542	0.455301
10	0.455301	0.455231
15	0.962639	0.455227
20	0.962639	0.455226
25	0.962639	0.455226
30	0.962639	0.455226
40	0.962639	0.455226
50	0.962639	0.455226

10.4 Results and discussion

In this section behavior of certain parameters of interest on the velocity components f' and g' has been analyzed. Figs. (10.3) – (10.8) are plotted for this interest. The variations of ζ on f' and g' are shown in the Figs. 10.3 and 10.4. These Figs. show that f' , g' and the associated boundary layer thickness are increasing function of ζ . It is also noted that the results for three-dimensional case are similar to those for two-dimensional and axisymmetric cases in a qualitative sense whereas the magnitude for three-dimensional case is larger. It is because of the fact that an extra agent has been introduced in such case in terms of bidirectional stretching. The effects of second grade parameter α^* on f' and g' are displayed in the Figs. 10.5 and 10.6. Fig. 10.5 elucidates that f' and associate boundary layer is increasing function of α^* and similar results are obtained for the second component of the velocity i.e. g' as shown in Fig. 10.6. Fig. 10.7 illustrates the variation of the ratio parameter c on f' . This Fig. indicates that velocity field f' and boundary layer thickness decreases with an increase in c . Fig. 10.8 analyzes the effects of c on g' . This Fig. shows that velocity component g' increases with an increase in c .

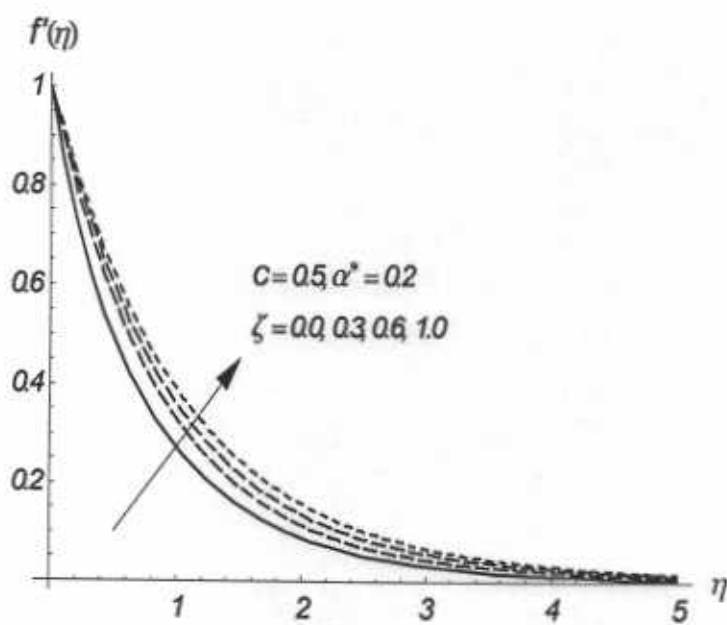


Fig. 10.3 : Influence of ζ on f' .

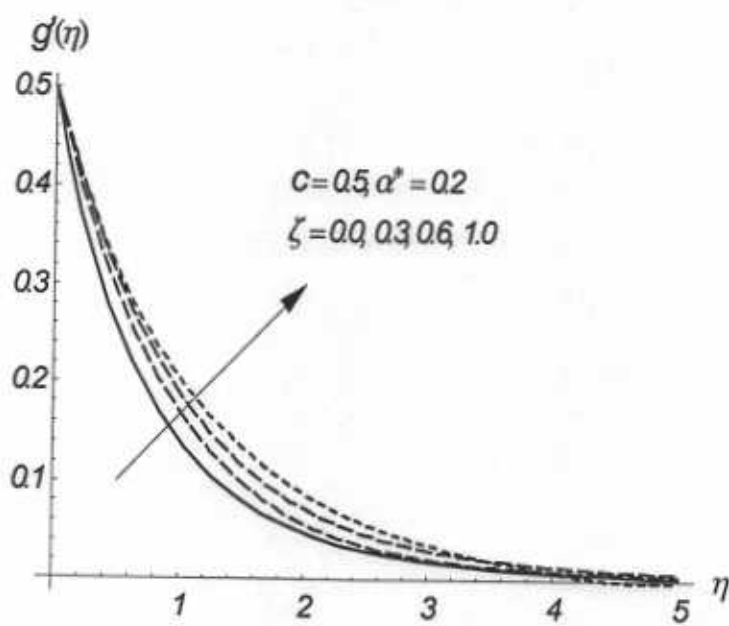


Fig. 10.4 : Influence of ζ on g' .

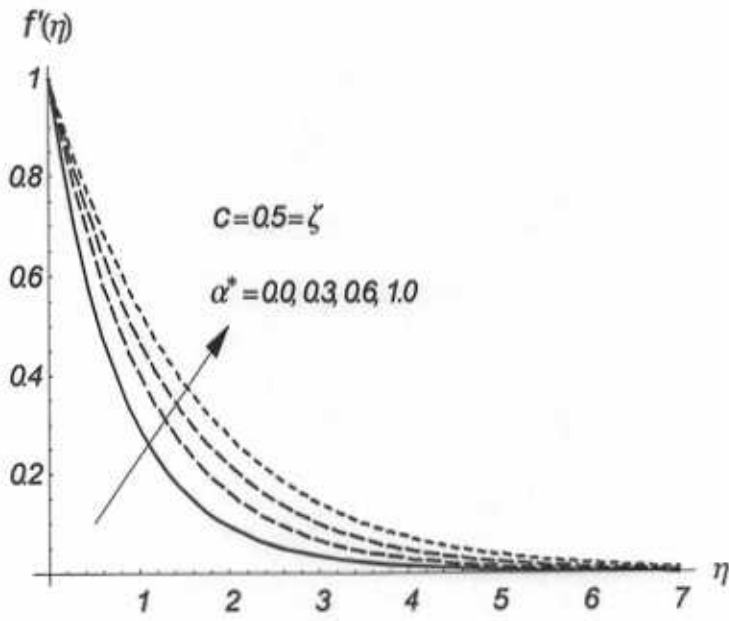


Fig. 10.5 : Influence of α^* on f' .

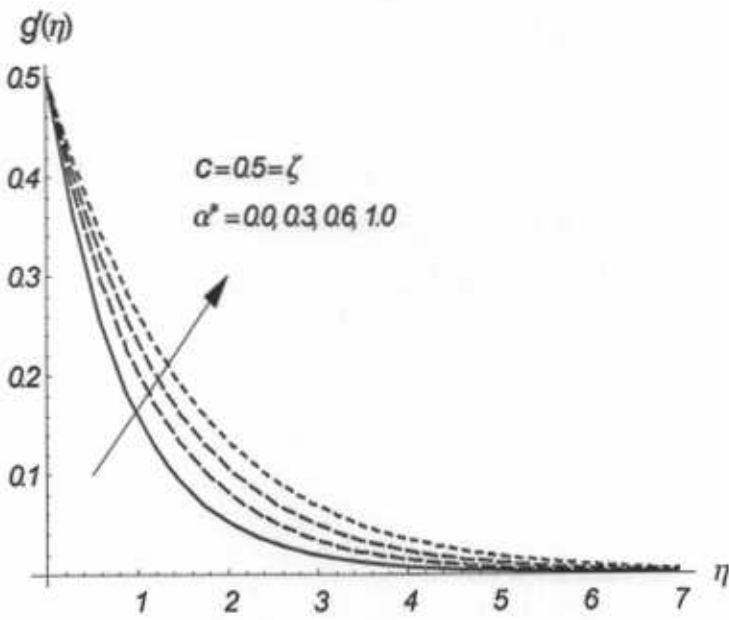


Fig. 10.6 : Influence of α^* on g' .

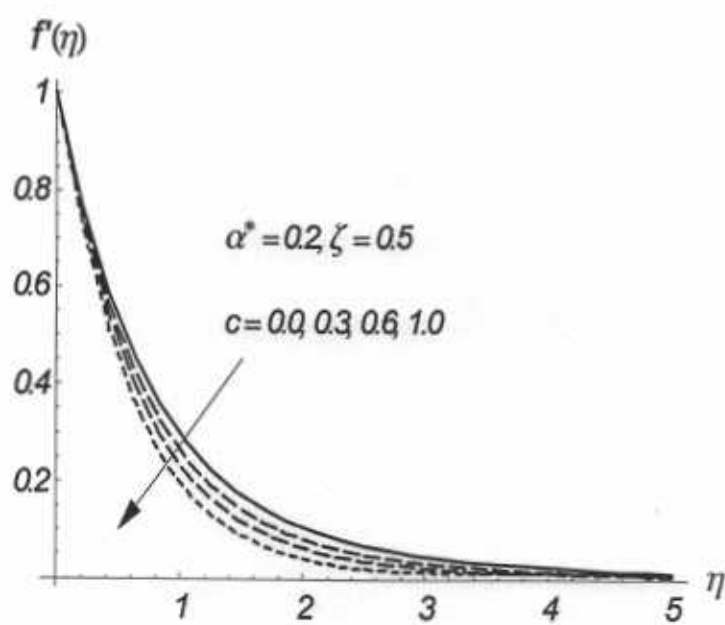


Fig. 10.7 : Influence of c on f' .

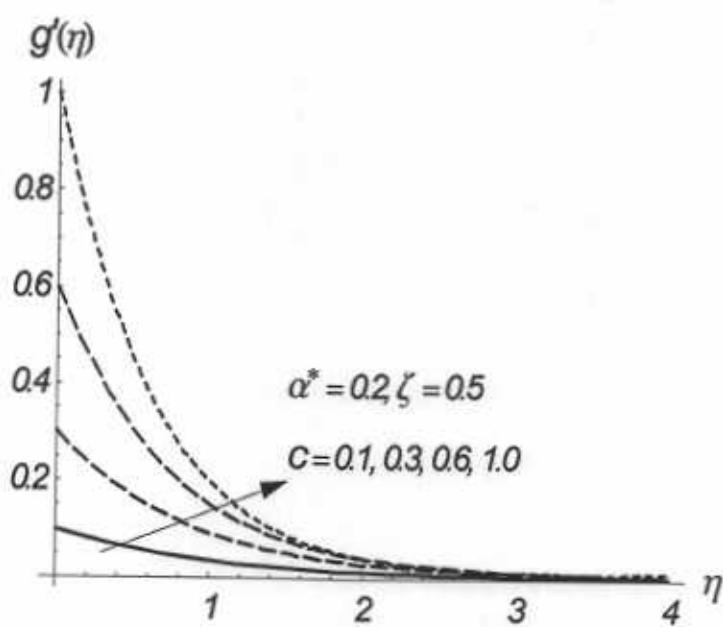


Fig. 10.8 : Influence of c on g' .

Table 10.2: Illustrating the variation of $-f''(0)$ and $-g''(0)$ with c when $\alpha^* = 0 = \zeta$, using HAM, HPM (Ariel [41]) and exact solution (Ariel [41]).

c	$-f''(0)$			$-g''(0)$		
	HAM	HPM [41]	Exact [41]	HAM	HPM [41]	Exact [41]
0.0	1	1	1	0	0	0
0.2	1.039495	1.034587	1.039495	0.148736	0.158231	0.148736
0.5	1.093095	1.088662	1.093095	0.465204	0.476290	0.465204
0.8	1.142488	1.142879	1.142488	0.866682	0.874551	0.866682
1.0	1.173720	1.178511	1.173720	1.173720	1.178511	1.173720

10.5 Conclusions

Unsteady three-dimensional flow of a second grade fluid has been analyzed. The main outcomes are listed below.

- Velocity fields f' and g' are increasing functions of time-dependent parameter ζ .
- Second grade parameter α^* enhances the flow.
- Velocity field f' decreases when c is increased.
- Velocity component g' increases rapidly near the stretching wall.
- The magnitude of velocities for unsteady case ($\zeta > 0$) is larger when compared with the steady-state case ($\zeta = 0$).

Chapter 11

Mass transfer effects in an unsteady three-dimensional flow of couple stress fluid

The unsteady three-dimensional flow of couple stress fluid over a stretched surface is investigated in this chapter. Analysis has been performed in the presence of mass transfer and chemical reaction. Nonlinear flow analysis is computed by a homotopic approach. Plots are presented and analyzed for the various parameters of interest. A comparative study with the existing solutions in a limiting sense is made.

11.1 Mathematical analysis

Consider the three-dimensional unsteady flow of an incompressible couple stress fluid over a surface at $z = 0$. The motion in fluid is created by stretching of a surface. In usual notations, the continuity, momentum and concentration equations for the boundary layer flow can be expressed as

$$\frac{\partial u}{\partial x} + \frac{\partial v}{\partial y} + \frac{\partial w}{\partial z} = 0, \quad (11.1)$$

$$\frac{\partial u}{\partial t} + u \frac{\partial u}{\partial x} + v \frac{\partial u}{\partial y} + w \frac{\partial u}{\partial z} = \nu \frac{\partial^2 u}{\partial z^2} - \nu' \frac{\partial^4 u}{\partial z^4}, \quad (11.2)$$

$$\frac{\partial v}{\partial t} + u \frac{\partial v}{\partial x} + v \frac{\partial v}{\partial y} + w \frac{\partial v}{\partial z} = \nu \frac{\partial^2 v}{\partial z^2} - \nu' \frac{\partial^4 v}{\partial z^4}, \quad (11.3)$$

$$\frac{\partial C}{\partial t} + u \frac{\partial C}{\partial x} + v \frac{\partial C}{\partial y} + w \frac{\partial C}{\partial z} = D \frac{\partial^2 C}{\partial z^2} - K(t)C, \quad (11.4)$$

subject to the boundary conditions

$$\begin{aligned} u &= \frac{ax}{1-\alpha t}, \quad v = \frac{by}{1-\alpha t}, \quad w = 0, \quad C = C_w \quad \text{at } z = 0, \\ u &\rightarrow 0, \quad v \rightarrow 0, \quad \frac{\partial u}{\partial z} \rightarrow 0, \quad \frac{\partial v}{\partial z} \rightarrow 0, \quad C \rightarrow C_\infty \quad \text{as } z \rightarrow \infty. \end{aligned} \quad (11.5)$$

Here u , v and w are the velocities in the x , y and z directions, respectively, $\nu = \mu/\rho$ the kinematic viscosity, $\nu' = n/\rho$ the couple stress viscosity, ρ the density of fluid, C the concentration of species, D the coefficients of diffusing species, $K(t) = K_1/(1-\alpha t)$ the reaction rate, C_w the concentration at the surface, C_∞ the concentration far away from the sheet, T_w the surface temperature and T_∞ the temperature far away from the surface.

The following transformations

$$\begin{aligned} \eta &= \sqrt{\frac{a}{\nu(1-\alpha t)}} z, \quad u = \frac{ax}{1-\alpha t} f'(\eta), \quad v = \frac{ay}{1-\alpha t} g'(\eta), \quad w = -\sqrt{\frac{a\nu'}{1-\alpha t}} \{f(\eta) + g(\eta)\}, \\ \phi(\eta) &= \frac{C - C_\infty}{C_w - C_\infty}, \quad C_w - C_\infty = \frac{ex}{1-\alpha t} \end{aligned} \quad (11.6)$$

identically satisfy the continuity equation (11.1). However Eqs. (11.2)–(11.6) take the following forms

$$f''' - f'^2 + (f+g)f'' - \zeta(f' + \frac{\eta}{2}f'') - Kf^v = 0, \quad (11.7)$$

$$g''' - g'^2 + (f+g)g'' - \zeta(g' + \frac{\eta}{2}g'') - Kg^v = 0, \quad (11.8)$$

$$\phi'' + Sc(f+g)\phi' - Sc\zeta(\phi + \frac{\eta}{2}\phi') - Sc\gamma\phi - Sc\phi f' = 0, \quad (11.9)$$

$$\begin{aligned} f(0) + g(0) &= 0, \quad f'(0) = 1, \quad g'(0) = c, \quad \phi(0) = 1, \\ f'(\infty) &= 0, \quad g'(\infty) = 0, \quad \phi(\infty) \rightarrow 0, \end{aligned} \quad (11.10)$$

in which $\zeta = \alpha/a$ is the time dependent parameter, $K = \nu'a/\nu^2(1 - \alpha t)$ the couple stress parameter, prime for the differentiation with respect to η and the constants $a > 0$ and $b > 0$. The stretching ratio c , Schmidt number Sc , chemical reaction parameter γ are as follows:

$$c = b/a, Sc = \frac{\nu}{D}, \gamma = \frac{K_1}{a}. \quad (11.11)$$

We point out that the two-dimensional ($g = 0$) case has been recovered for $c = 0$. For $c = 1$, we obtain axisymmetric case i.e. ($f = g$) and for ($\zeta = 0$) the system of Eqs. (11.7) – (11.9) reduce to the steady situation.

11.2 Series solutions

11.2.1 Zeroth-order deformation problems

For the development of the homotopy solutions, the functions $f(\eta)$, $g(\eta)$ and $\phi(\eta)$ in the set of base functions

$$\left\{ \eta^k \exp(-n\eta) \mid k \geq 0, n \geq 0 \right\} \quad (11.12)$$

can be introduced as follows:

$$f(\eta) = a_{0,0}^0 + \sum_{n=1}^{\infty} \sum_{k=1}^{\infty} a_{m,n}^k \eta^k \exp(-n\eta), \quad (11.13)$$

$$g(\eta) = A_{0,0}^0 + \sum_{n=1}^{\infty} \sum_{k=1}^{\infty} A_{m,n}^k \eta^k \exp(-n\eta), \quad (11.14)$$

$$\phi(\eta) = \sum_{n=0}^{\infty} \sum_{k=0}^{\infty} c_{m,n}^k \eta^k \exp(-n\eta), \quad (11.15)$$

with the following initial guesses and auxiliary linear operators

$$f_0(\eta) = 1 - \exp(-\eta), \quad g_0(\eta) = c(1 - \exp(-\eta)), \quad \phi_0(\eta) = \exp(-\eta), \quad (11.16)$$

$$\mathcal{L}_f = \frac{d^3 f}{d\eta^3} - \frac{df}{d\eta}, \quad \mathcal{L}_g = \frac{d^3 g}{d\eta^3} - \frac{dg}{d\eta}, \quad \mathcal{L}_\phi = \frac{d^2 \phi}{d\eta^2} - \phi. \quad (11.17)$$

Obviously the linear operators have the following properties

$$\mathcal{L}_f [C_1 + C_2 \exp(\eta) + C_3 \exp(-\eta)] = 0, \quad (11.18)$$

$$\mathcal{L}_g [C_4 + C_5 \exp(\eta) + C_6 \exp(-\eta)] = 0, \quad (11.19)$$

$$\mathcal{L}_\phi [C_7 \exp(\eta) + C_8 \exp(-\eta)] = 0, \quad (11.20)$$

where $C_1 - C_8$ are the constants and $a_{m,n}^k$, $A_{m,n}^k$ and $c_{m,n}^k$ are the coefficients. The problems at the zeroth order can be expressed as

$$(1-p)\mathcal{L}_f [\bar{f}(\eta, p) - f_0(\eta)] = p\hbar_f \mathcal{N}_f [\bar{f}(\eta, p), \bar{g}(\eta, p)], \quad (11.21)$$

$$(1-p)\mathcal{L}_g [\bar{g}(\eta, p) - g_0(\eta)] = p\hbar_g \mathcal{N}_g [\bar{f}(\eta, p), \bar{g}(\eta, p)], \quad (11.22)$$

$$(1-p)\mathcal{L}_\phi [\bar{\phi}(\eta, p) - \phi_0(\eta)] = p\hbar_\phi \mathcal{N}_\phi [\bar{f}(\eta, p), \bar{g}(\eta, p), \bar{\phi}(\eta, p)], \quad (11.23)$$

$$\begin{aligned} \bar{f}(0, p) + \bar{g}(0, p) &= 0, \quad \bar{f}'(0, p) = 1, \quad \bar{g}'(0, p) = c, \\ \bar{f}'(\infty, p) &= 0, \quad \bar{f}''(\infty, p) = 0, \quad \bar{g}'(\infty, p) = 0, \quad \bar{g}''(\infty, p) = 0, \\ \bar{\phi}(0; p) &= 1, \quad \bar{\phi}(\infty; p) = 0 \end{aligned} \quad (11.24)$$

$$\begin{aligned} \mathcal{N}_f [\bar{f}(\eta, p), \bar{g}(\eta, p)] &= \frac{\partial^3 \bar{f}}{\partial \eta^3} - \left(\frac{\partial \bar{f}}{\partial \eta} \right)^2 + \{ \bar{f}(\eta, p) + \bar{g}(\eta, p) \} \frac{\partial^2 \bar{f}}{\partial \eta^2} - K \bar{f}^v(\eta, p) \\ &\quad - \zeta \left(\frac{\partial \bar{f}}{\partial \eta} + \frac{\eta}{2} \frac{\partial^2 \bar{f}}{\partial \eta^2} \right), \end{aligned} \quad (11.25)$$

$$\begin{aligned} \mathcal{N}_g [\bar{f}(\eta, p), \bar{g}(\eta, p)] &= \frac{\partial^3 \bar{g}}{\partial \eta^3} - \left(\frac{\partial \bar{g}}{\partial \eta} \right)^2 + \{ \bar{f}(\eta, p) + \bar{g}(\eta, p) \} \frac{\partial^2 \bar{g}}{\partial \eta^2} \\ &\quad - \zeta \left(\frac{\partial \bar{g}}{\partial \eta} + \frac{\eta}{2} \frac{\partial^2 \bar{g}}{\partial \eta^2} \right) - K \bar{g}^v(\eta, p), \end{aligned} \quad (11.26)$$

$$\begin{aligned} \mathcal{N}_\phi [\bar{f}(\eta, p), \bar{g}(\eta, p), \bar{\phi}(\eta, p)] &= \frac{\partial^2 \bar{\phi}(\eta, p)}{\partial \eta^2} + Sc (\bar{f}(\eta, p) + \bar{g}(\eta, p)) \frac{\partial \bar{\phi}(\eta, p)}{\partial \eta} \\ &\quad - Sc \zeta (\bar{\phi}(\eta, p) + \frac{\eta}{2} \bar{\phi}'(\eta, p)) - Sc \gamma \bar{\phi}(\eta, p) - Sc \bar{\phi}(\eta, p) \bar{f}'(\eta, p), \end{aligned} \quad (11.27)$$

where \hbar_f , \hbar_g and \hbar_ϕ are the auxiliary non-zero parameters and $p \in [0, 1]$ is an embedding parameter. When $p = 0$ and $p = 1$, we obtain

$$\bar{f}(\eta, 0) = f_0(\eta), \quad \bar{f}(\eta, 1) = f(\eta), \quad (11.28)$$

$$\bar{g}(\eta, 0) = g_0(\eta), \quad \bar{g}(\eta, 1) = g(\eta), \quad (11.29)$$

$$\bar{\phi}(\eta; 0) = \phi_0(\eta), \quad \bar{\phi}(\eta; 1) = \phi(\eta). \quad (11.30)$$

Through Taylor series expansion one obtains

$$\bar{f}(\eta, p) = f_0(\eta) + \sum_{m=1}^{\infty} f_m(\eta) p^m, \quad (11.31)$$

$$\bar{g}(\eta, p) = g_0(\eta) + \sum_{m=1}^{\infty} g_m(\eta) p^m, \quad (11.32)$$

$$\bar{\phi}(\eta; p) = \phi_0(\eta) + \sum_{m=1}^{\infty} \phi_m(\eta) p^m, \quad (11.33)$$

with

$$f_m(\eta) = \left. \frac{1}{m!} \frac{\partial^m \bar{f}(\eta, p)}{\partial p^m} \right|_{p=0}, \quad (11.34)$$

$$g_m(\eta) = \left. \frac{1}{m!} \frac{\partial^m \bar{g}(\eta, p)}{\partial p^m} \right|_{p=0}, \quad (11.35)$$

$$\phi_m(\eta) = \left. \frac{1}{m!} \frac{\partial^m \bar{\phi}(\eta; p)}{\partial p^m} \right|_{p=0}. \quad (11.36)$$

The convergence of series (11.31) – (11.33) depends upon the auxiliary parameters \hbar_f , \hbar_g and \hbar_ϕ . The values of \hbar_f , \hbar_g and \hbar_ϕ have been selected in the manner that the series (11.31) – (11.33) converge at $p = 1$. Hence

$$f(\eta) = f_0(\eta) + \sum_{m=1}^{\infty} f_m(\eta), \quad (11.37)$$

$$g(\eta) = g_0(\eta) + \sum_{m=1}^{\infty} g_m(\eta), \quad (11.38)$$

$$\phi(\eta) = \phi_0(\eta) + \sum_{m=1}^{\infty} \phi_m(\eta). \quad (11.39)$$

11.2.2 *m*th order deformation problems

Here the problems are given by

$$\mathcal{L}_f [f_m(\eta) - \chi_m f_{m-1}(\eta)] = \hbar_f \mathcal{R}_{f,m}(\eta), \quad (11.40)$$

$$\mathcal{L}_g [g_m(\eta) - \chi_m g_{m-1}(\eta)] = \hbar_f \mathcal{R}_{g,m}(\eta), \quad (11.41)$$

$$\mathcal{L}_\phi [\phi_m(\eta) - \chi_m \phi_{m-1}(\eta)] = \hbar_\phi \mathcal{R}_m^\phi(\eta), \quad (11.42)$$

$$\begin{aligned} f_m(0) + g_m(0) = f'_m(0) = f'_m(\infty) = g'_m(0) = g'_m(\infty) = 0, \\ \phi_m(0) = 0, \quad \phi_m(\infty) = 0, \end{aligned} \quad (11.43)$$

$$\begin{aligned} \mathcal{R}_m^f(\eta) = & f_{m-1}''' - \zeta(f'_{m-1} + \frac{\eta}{2} f''_{m-1}) - K f_{m-1}^v \\ & + \sum_{k=0}^{m-1} [(f_{m-1-k} + g_{m-1-k}) f_k'' - f'_{m-1-k} f_k'], \end{aligned} \quad (11.44)$$

$$\begin{aligned} \mathcal{R}_m^g(\eta) = & g_{m-1}''' - \zeta(g'_{m-1} + \frac{\eta}{2} g''_{m-1}) - K g_{m-1}^v \\ & + \sum_{k=0}^{m-1} [(f_{m-1-k} + g_{m-1-k}) g_k'' - g'_{m-1-k} g_k'], \end{aligned} \quad (11.45)$$

$$\begin{aligned} \mathcal{R}_m^\phi(\eta) = & \phi_{m-1}'' - Sc\gamma\phi_{m-1} - Sc\zeta(\phi_{m-1} + \frac{\eta}{2}\phi'_{m-1}) + \\ & Sc \sum_{k=0}^{m-1} [(f_{m-1-k} + g_{m-1-k}) \phi_k' - \phi_{m-1-k} f_k'], \end{aligned} \quad (11.46)$$

$$\chi_m = \begin{cases} 0, & m \leq 1 \\ 1, & m > 1 \end{cases}. \quad (11.47)$$

The equations (11.40) – (11.42) have been solved one after the other in the order $m = 1, 2, 3, \dots$ by employing Mathematica.

11.3 Convergence of the HAM solution

In this section our aim is to ensure the convergence of the obtained series solutions. Thus Figs. (11.1) and (11.2) have been plotted for the admissible values of h_f , h_g and h_ϕ regarding convergence of the solutions (11.37) – (11.39). Ultimate the admissible values have been noticed in the ranges $-1.25 \leq (h_f, h_g) \leq -0.25$ and $-1.0 \leq h_\phi \leq -0.5$. Further $h_f = -0.7 = h_g = h_\phi$ one has the better solution. Table 11.1 is presented to find that how much order of approximations are necessary for a convergent solution. It is noticed that 15th order approximations are sufficient for the velocity fields whereas 25th order of approximation are required for the concentration field. Table 11.2 provides a comparative study for viscous flow. It is found that HAM solution in a limiting case of present study has a good agreement with the exact and HPM solutions provided in ref. [41].

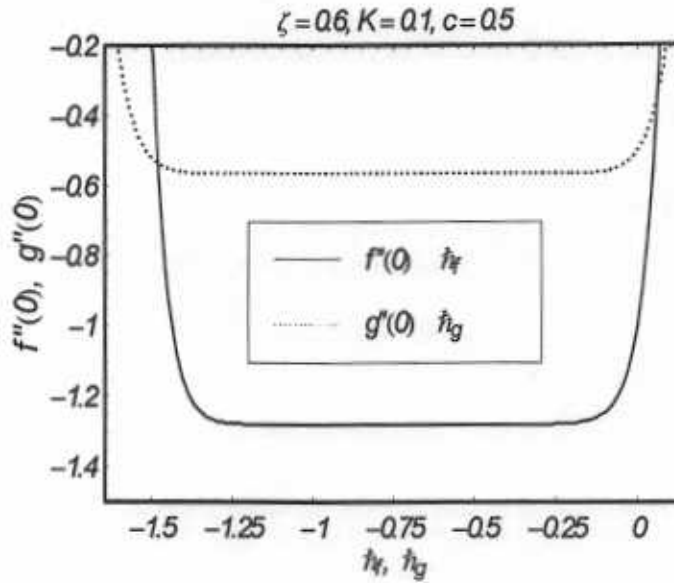


Fig. 11.1 : h curves of $f''(0)$ and $g''(0)$ at the 15th order of approximation.

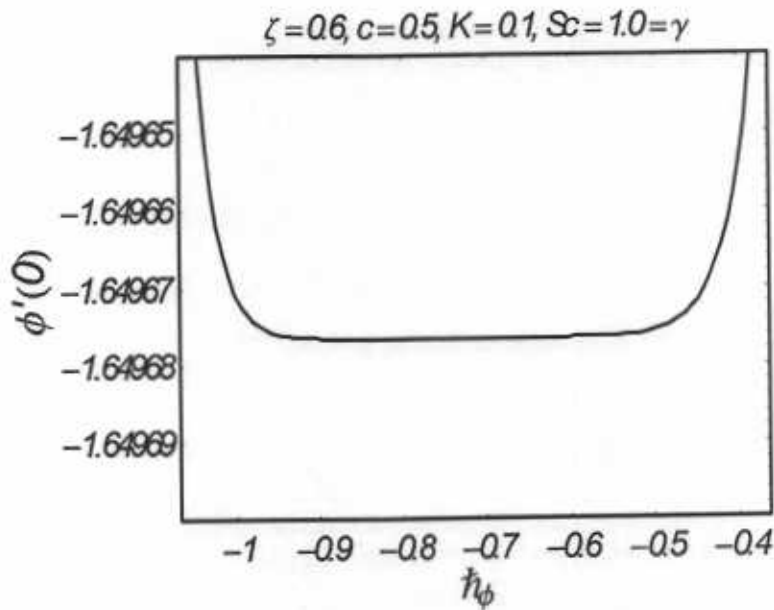


Fig. 11.2 : h curves of $\phi'(0)$ at the 15th order of approximation.

Table 11.1: Convergence of the HAM solutions for different order of approximations when $c = 0.5, A = 0.6, K = 0.5, Sc = \gamma = 1$

order of approximation	$-f''(0)$	$-g''(0)$	$-\phi'(0)$
1	1.21933333	0.55133333	1.5658333
2	1.26218363	0.56192793	1.6216753
5	1.27716191	0.56371964	1.6491773
10	1.27749261	0.56359020	1.6496750
15	1.27749261	0.56358705	1.6496764
20	1.27749258	0.56358694	1.6496764
25	1.27749257	0.56358692	1.6496764
30	1.27749257	0.56358692	1.6496764
40	1.27749257	0.56358692	1.6496764
50	1.27749257	0.56358692	1.6496764

11.4 Results and discussion

Computations for the effects of different parameters on velocity and concentration fields have been carried out and Figs (11.3) – (11.8) have been displayed. The variations of K on f' and g' are presented in the Figs. (11.3) and (11.4). It is observed the f' and g' are decreasing functions of the couple stress parameter K . It is noted that couple stress parameter is dependent upon the couple stress viscosity n and this couple stress viscosity acts as a retarding agent which makes the fluid more denser resulting into a decrease in the velocity of the fluid. The variations of K , γ and Sc on the concentration field ϕ are portrayed in the Figs. (11.5) – (11.8). Effect of K on ϕ has been shown in Fig. 11.5. This Fig. shows that ϕ is an increasing function of K . The concentration boundary layer also increases with an increase in K . Fig. 11.6 predicts the effects of destructive ($\gamma > 0$) chemical reactions on ϕ . It is noticed that ϕ decreases in case of destructive ($\gamma > 0$) chemical reaction. Fig. 11.7 explains the variation of generative ($\gamma < 0$) chemical reaction on the concentration field ϕ . It is noted that generative ($\gamma < 0$) chemical reaction causes an increase in the concentration. It is also noted that the magnitude of ϕ is larger in case of generative chemical reaction ($\gamma < 0$) in comparison to the case of destructive chemical reaction ($\gamma > 0$). Physically for generative case, chemical reaction γ takes place without creating much disturbance whereas disorder in the case of destructive chemical reaction is much larger. Due to this fact molecular motion in the case of ($\gamma > 0$) is quite larger which finally results into an increase in the mass transport phenomenon. Finally Fig. 11.8 plots the effects of Schmidt number Sc on the concentration field. This Fig. elucidates that concentration field ϕ decreases with an increase in Sc . From the definition of Schmidt number given in Eq. (11.11), it is clearly observed that Sc is inversely proportional to the diffusion coefficient D . Therefore larger values of Sc correspond to a decrease in the concentration field.

Table 11.2: Variation of $-f''(0)$ and $-g''(0)$ with c when $A = 0 = K$ using HAM, HPM (Ariel [41]) and exact solutions (Ariel [41])

c	$-f''(0)$			$-g''(0)$		
	HAM	HPM [41]	Exact [41]	HAM	HPM [41]	Exact [41]
0.0	1	1	1	0	0	0
0.2	1.039495	1.034587	1.039495	0.148736	0.158231	0.148736
0.4	1.075788	1.070529	1.075788	0.349208	0.360599	0.349208
0.6	1.109946	1.106797	1.109946	0.590528	0.600833	0.590528
0.8	1.142488	1.142879	1.142488	0.866682	0.874551	0.866682
1.0	1.173720	1.178511	1.173720	1.173720	1.178511	1.173720

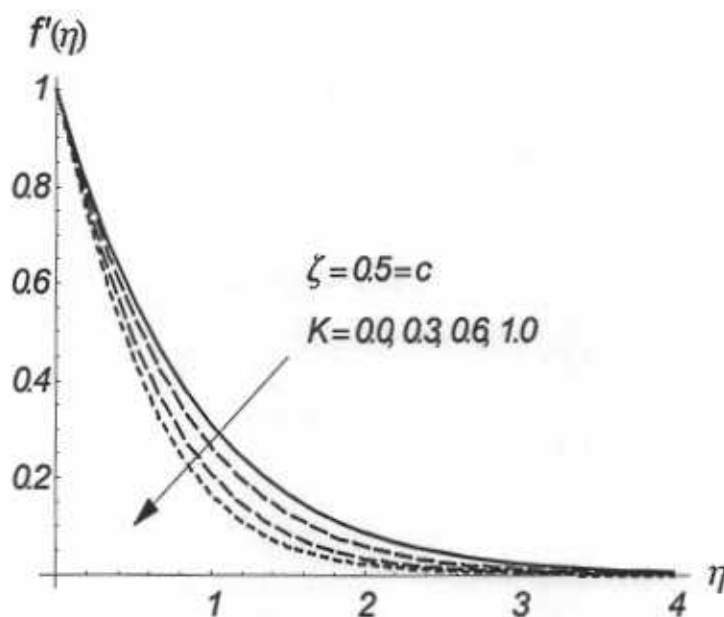


Fig. 11.3 : Influence of K on f' .

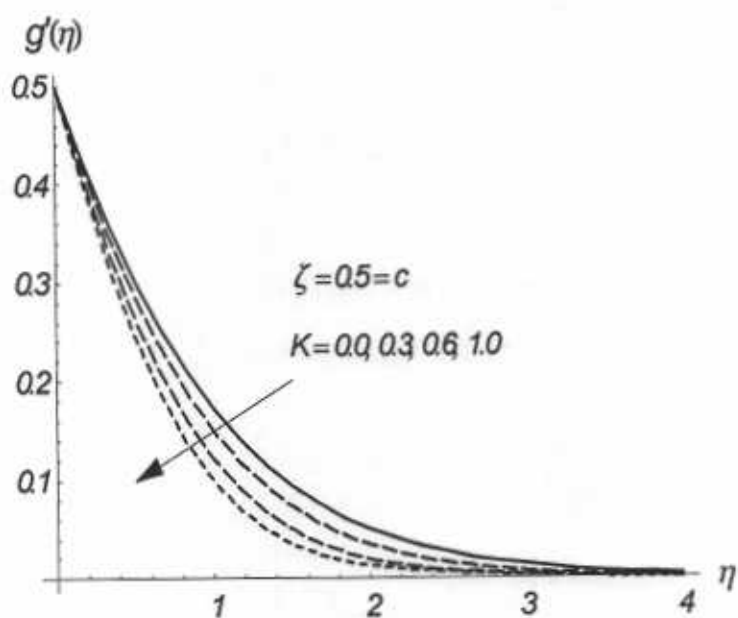


Fig. 11.4 : Influence of K on g' .

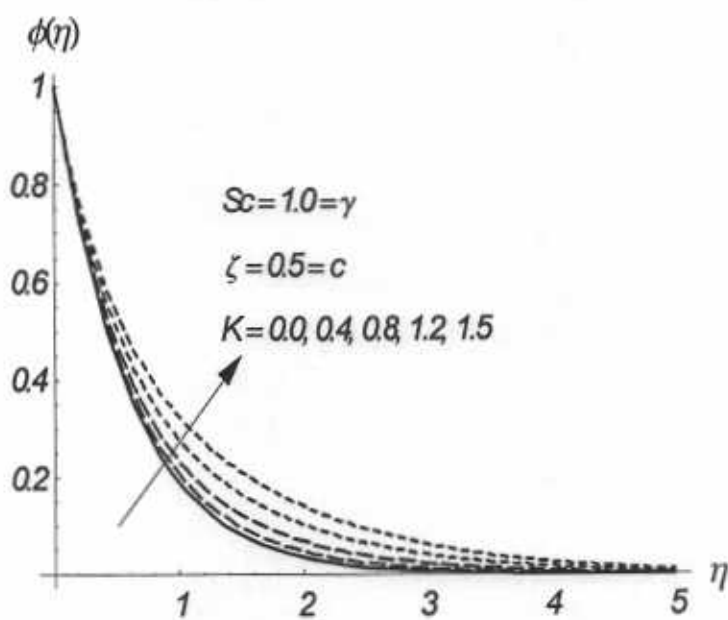


Fig. 11.5 : Influence of K on ϕ .

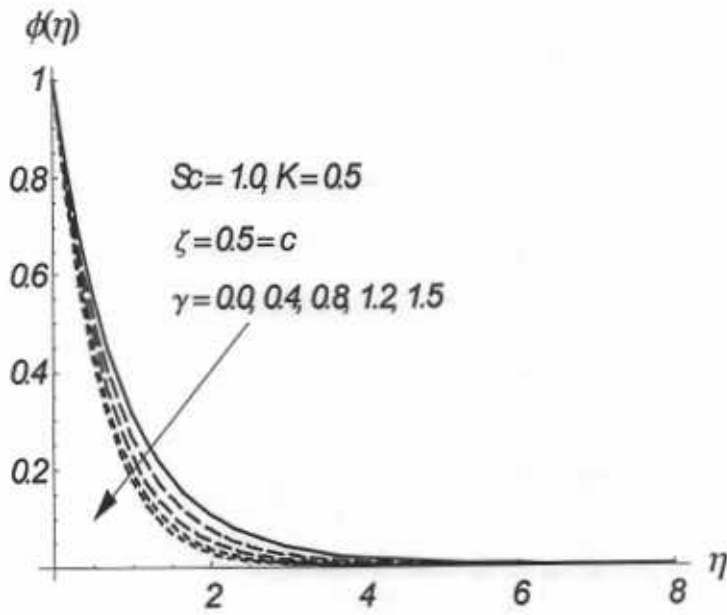


Fig. 11.6 : Influence of $\gamma > 0$ on ϕ .

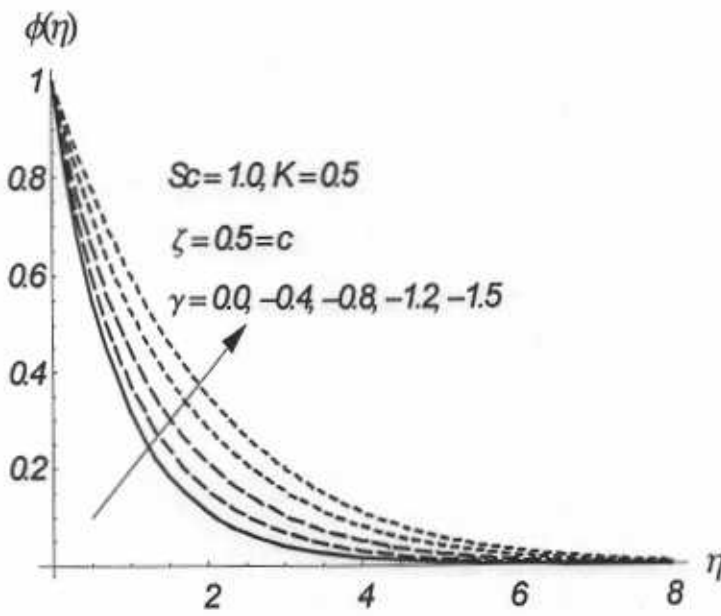


Fig. 11.7 : Influence of $\gamma < 0$ on ϕ .

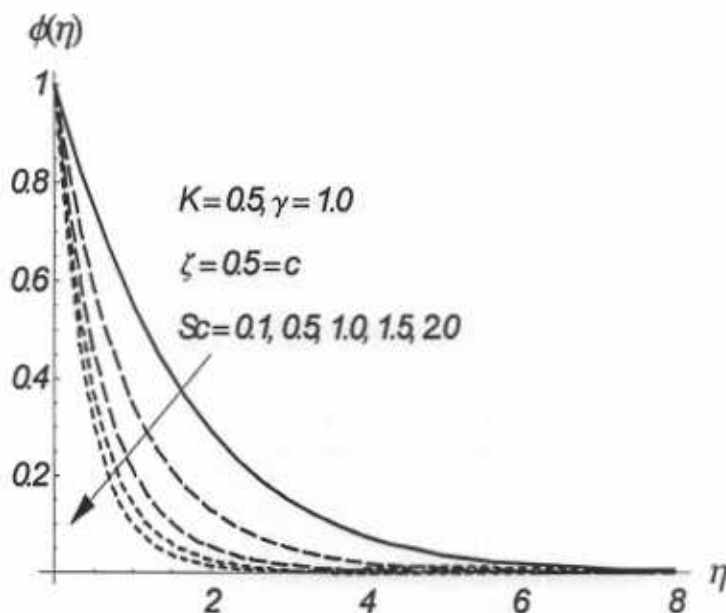


Fig. 11.8 : Influence of Sc on ϕ .

11.5 Concluding remarks

Effects of mass transfer on the unsteady three-dimensional flow of couple stress fluid over a stretching sheet is investigated. Analysis is performed in the presence of chemical reaction. The main observations are listed below.

- Velocity field and boundary layer thickness are decreasing functions of K .
- Variations of K on the velocity field for the axisymmetric, two- and three-dimensional flow cases are qualitatively similar.
- The effects of K on f' and g' are similar.
- Influence of K on the velocity and concentration fields are opposite.
- Concentration field ϕ is a decreasing function of Schmidt number Sc .
- The concentration field ϕ has opposite results for destructive ($\gamma > 0$) and generative ($\gamma < 0$) chemical reactions.

Chapter 12

Soret and Dufours effects in three-dimensional flow of viscoelastic fluid

This chapter presents the Soret and Dufour effects on three-dimensional boundary layer flow of viscoelastic fluid over a stretching surface. The governing partial differential equations are transformed into a dimensionless coupled system of non-linear ordinary differential equations and then solved by the homotopy analysis method (HAM). Graphs are plotted to analyze the variation of different parameters of interest for the velocity, concentration and temperature fields.

12.1 Mathematical analysis

We consider the three-dimensional flow of an incompressible viscoelastic fluid over a stretching surface at $z = 0$. The motion in fluid is created by a non-conducting stretching surface. The heat and mass transfer characteristics are considered when both Soret and Dufour effects are present. The continuity, momentum, concentration and energy equations for the present boundary layer flow are reduced to the following equations:

$$\frac{\partial u}{\partial x} + \frac{\partial v}{\partial y} + \frac{\partial w}{\partial z} = 0, \quad (12.1)$$

$$u \frac{\partial u}{\partial x} + v \frac{\partial u}{\partial y} + w \frac{\partial u}{\partial z} = \nu \frac{\partial^2 u}{\partial z^2} - k \left[- \left(\frac{\partial u}{\partial x} \frac{\partial^2 u}{\partial x^2} + \frac{\partial u}{\partial z} \frac{\partial^2 w}{\partial z^2} + 2 \frac{\partial u}{\partial z} \frac{\partial^2 u}{\partial x \partial z} + 2 \frac{\partial w}{\partial z} \frac{\partial^2 v}{\partial z^2} \right) \right], \quad (12.2)$$

$$u \frac{\partial v}{\partial x} + v \frac{\partial v}{\partial y} + w \frac{\partial v}{\partial z} = \nu \frac{\partial^2 v}{\partial z^2} - k \left[- \left(\frac{\partial v}{\partial y} \frac{\partial^2 v}{\partial y^2} + \frac{\partial v}{\partial z} \frac{\partial^2 w}{\partial z^2} + 2 \frac{\partial v}{\partial z} \frac{\partial^2 v}{\partial y \partial z} + 2 \frac{\partial w}{\partial z} \frac{\partial^2 v}{\partial z^2} \right) \right], \quad (12.3)$$

$$u \frac{\partial C}{\partial x} + v \frac{\partial C}{\partial y} + w \frac{\partial C}{\partial z} = D \frac{\partial^2 C}{\partial z^2} - K_1 C + \frac{Dk_T}{T_m} \frac{\partial^2 T}{\partial z^2}, \quad (12.4)$$

$$u \frac{\partial T}{\partial x} + v \frac{\partial T}{\partial y} + w \frac{\partial T}{\partial z} = \alpha_m \frac{\partial^2 T}{\partial z^2} + \frac{Dk_T}{C_s C_p} \frac{\partial^2 C}{\partial z^2} \quad (12.5)$$

in which u , v and w are the velocities in the x , y and z directions, respectively, ν the kinematic viscosity, k the material fluid parameter, C the concentration of species, D the coefficients of diffusing species, K_1 the reaction rate, k_T the thermal-diffusion, T the temperature, C_p the specific heat, C_s the concentration susceptibility, α_m the thermal diffusivity and T_m the fluid mean temperature.

The boundary conditions for the present situation can be written as

$$\begin{aligned} u &= u_w(x) = ax, \quad v = v_w(y) = by, \quad w = 0, \quad T = T_w, \quad C = C_w \quad \text{at } z = 0, \\ u &\rightarrow 0, \quad v \rightarrow 0, \quad \frac{\partial u}{\partial z} \rightarrow 0, \quad \frac{\partial v}{\partial z} \rightarrow 0, \quad T \rightarrow T_\infty, \quad C \rightarrow C_\infty \quad \text{as } z \rightarrow \infty, \end{aligned} \quad (12.6)$$

where C_w denotes the concentration at the surface, C_∞ is the concentration far away from the sheet, T_w is the surface temperature and T_∞ is the temperature far away from the surface.

Using

$$\begin{aligned} \eta &= \sqrt{\frac{a}{\nu}} z, \quad u = axf'(\eta), \quad v = ayg'(\eta), \quad w = -\sqrt{a\nu} \{f(\eta) + g(\eta)\}, \\ \theta(\eta) &= \frac{T - T_\infty}{T_w - T_\infty}, \quad \phi(\eta) = \frac{C - C_\infty}{C_w - C_\infty} \end{aligned} \quad (12.7)$$

the continuity equation (12.1) is identically satisfied and Eqs. (12.2) – (12.6) take the following

forms

$$f''' - f'^2 + (f + g)f'' + K_0 [(f + g)f^{iv} + (f'' - g'')f'' - 2(f' + g')f'''] = 0, \quad (12.8)$$

$$g''' - g'^2 + (f + g)g'' + K_0 [(f + g)g^{iv} + (f'' - g'')g'' - 2(f' + g')g'''] = 0, \quad (12.9)$$

$$\phi'' + Sc(f + g)\phi' - Sc\gamma\phi + ScS_r\theta'' = 0, \quad (12.10)$$

$$\theta'' + Pr(f + g)\theta' + PrD_f\phi'' = 0, \quad (12.11)$$

$$\begin{aligned} f(0) + g(0) &= 0, \quad f'(0) = 1, \quad g'(0) = c, \quad \phi(0) = 1, \quad \theta(0) = 1, \\ f'(\infty) &= 0, \quad g'(\infty) = 0, \quad \phi(\infty) \rightarrow 0, \quad \theta(\infty) \rightarrow 0, \end{aligned} \quad (12.12)$$

where $K_0 = ka/\nu$ is the dimensionless viscoelastic parameter, prime is the differentiation with respect to η and the constants $a > 0$ and $b > 0$. Furthermore the ratio c , Schmidt number Sc , chemical reaction parameter γ , Prandtl number Pr , Dufour number D_f and Soret number S_r are defined by

$$\begin{aligned} c &= b/a, \quad Sc = \frac{\nu}{D}, \quad \gamma = \frac{K_1}{a}, \quad Pr = \nu/\alpha_m, \\ Df &= \frac{Dk_T(C_w - C_\infty)}{C_s C_p (T_w - T_\infty)\nu}, \quad Sr = \frac{Dk_T(T_w - T_\infty)}{T_m \nu (C_w - C_\infty)}. \end{aligned} \quad (12.13)$$

Note that the two-dimensional ($g = 0$) case is obtained when $c = 0$. For $c = 1$, one finds an axisymmetric case i.e. ($f = g$).

The local Nusselt (Nu_x) and local Sherwood (Sh) numbers can be written as

$$Nu = \frac{xq_w}{k(T_w - T_\infty)}, \quad Sh = \frac{xj_w}{D(C_w - C_\infty)} \quad (12.14)$$

with

$$q_w = -k \left(\frac{\partial T}{\partial z} \right)_{z=0}, \quad j_w = -D \left(\frac{\partial C}{\partial z} \right)_{z=0}, \quad (12.15)$$

where q_w and j_w respectively denote the heat and mass fluxes.

Equation (12.14) in dimensionless form becomes

$$Nu_x / Re_x^{1/2} = -\theta'(0), \quad Sh / Re_x^{1/2} = -\phi'(0) \quad (12.16)$$

where $Re_x = u_w x / \nu$ is the local Reynolds number.

12.2 Series solutions

12.2.1 Zeroth-order deformation problems

In order to obtain the HAM solution, the velocity distributions $f(\eta)$, $g(\eta)$, $\phi(\eta)$ and $\theta(\eta)$ in the set of base functions

$$\{\eta^k \exp(-n\eta) \mid k \geq 0, n \geq 0\} \quad (12.17)$$

can be expressed as

$$f(\eta) = a_{0,0}^0 + \sum_{n=1}^{\infty} \sum_{k=1}^{\infty} a_{m,n}^k \eta^k \exp(-n\eta), \quad (12.18)$$

$$g(\eta) = A_{0,0}^0 + \sum_{n=1}^{\infty} \sum_{k=1}^{\infty} A_{m,n}^k \eta^k \exp(-n\eta), \quad (12.19)$$

$$\phi(\eta) = \sum_{n=0}^{\infty} \sum_{k=0}^{\infty} c_{m,n}^k \eta^k \exp(-n\eta), \quad (12.20)$$

$$\theta(\eta) = \sum_{n=0}^{\infty} \sum_{k=0}^{\infty} b_{m,n}^k \eta^k \exp(-n\eta) \quad (12.21)$$

subject to following initial guesses

$$f_0(\eta) = 1 - \exp(-\eta), \quad (12.22)$$

$$g_0(\eta) = c(1 - \exp(-\eta)), \quad (12.23)$$

$$\phi_0(\eta) = \exp(-\eta), \quad (12.24)$$

$$\theta_0(\eta) = \exp(-\eta), \quad (12.25)$$

and the linear operators

$$\mathcal{L}_f = \frac{d^3 f}{d\eta^3} - \frac{df}{d\eta}, \quad (12.26)$$

$$\mathcal{L}_g = \frac{d^3 g}{d\eta^3} - \frac{dg}{d\eta}, \quad (12.27)$$

$$\mathcal{L}_\phi = \frac{d^2 \phi}{d\eta^2} - \phi, \quad (12.28)$$

$$\mathcal{L}_\theta = \frac{d^2 \theta}{d\eta^2} - \theta, \quad (12.29)$$

with

$$\mathcal{L}_f [C_1 + C_2 \exp(\eta) + C_3 \exp(-\eta)] = 0, \quad (12.30)$$

$$\mathcal{L}_g [C_4 + C_5 \exp(\eta) + C_6 \exp(-\eta)] = 0, \quad (12.31)$$

$$\mathcal{L}_\phi [C_7 \exp(\eta) + C_8 \exp(-\eta)] = 0, \quad (12.32)$$

$$\mathcal{L}_\theta [C_9 \exp(\eta) + C_{10} \exp(-\eta)] = 0, \quad (12.33)$$

where $C_1 - C_{10}$ are the constants and $a_{m,n}^k$, $A_{m,n}^k$, $c_{m,n}^k$ and $b_{m,n}^k$ are the coefficients.

The problems at the zeroth order are

$$(1-p)\mathcal{L} [\bar{f}(\eta, p) - f_0(\eta)] = p\hbar_f \mathcal{N}_f [\bar{f}(\eta, p), \bar{g}(\eta, p)], \quad (12.34)$$

$$(1-p)\mathcal{L} [\bar{g}(\eta, p) - g_0(\eta)] = p\hbar_g \mathcal{N}_g [\bar{f}(\eta, p), \bar{g}(\eta, p)], \quad (12.35)$$

$$(1-p)\mathcal{L}_\phi [\bar{\phi}(\eta, p) - \phi_0(\eta)] = p\hbar_\phi \mathcal{N}_\phi [\bar{f}(\eta, p), \bar{\phi}(\eta, p)], \quad (12.36)$$

$$(1-p)\mathcal{L}_\theta [\bar{\theta}(\eta, p) - \theta_0(\eta)] = p\hbar_\theta \mathcal{N}_\theta [\bar{f}(\eta, p), \bar{\theta}(\eta, p)], \quad (12.37)$$

$$\begin{aligned} \bar{f}(0, p) + \bar{g}(0, p) &= 0, \quad \bar{f}'(0, p) = 1, \quad \bar{g}'(0, p) = c, \\ \bar{f}'(\infty, p) &= 0, \quad \bar{g}'(\infty, p) = 0, \\ \bar{\phi}(0; p) &= 1, \quad \bar{\phi}(\infty; p) = 0, \quad \bar{\theta}(0; p) = 1, \quad \bar{\theta}(\infty; p) = 0, \end{aligned} \quad (12.38)$$

$$\begin{aligned} \mathcal{N}_f[\bar{f}(\eta, p), \bar{g}(\eta, p)] &= \frac{\partial^3 \bar{f}}{\partial \eta^3} - \left(\frac{\partial \bar{f}}{\partial \eta} \right)^2 + \{\bar{f}(\eta, p) + \bar{g}(\eta, p)\} \frac{\partial^2 \bar{f}}{\partial \eta^2} \\ &+ K_0 \left[\begin{array}{l} \{\bar{f}(\eta, p) + \bar{g}(\eta, p)\} \bar{f}^{iv}(\eta, p) \\ + \{\bar{f}''(\eta, p) - \bar{g}''(\eta, p)\} \bar{f}''(\eta, p) \\ - 2\{(\bar{f}'(\eta, p) + \bar{g}'(\eta, p)) \bar{f}'''(\eta, p)\} \end{array} \right], \end{aligned} \quad (12.39)$$

$$\begin{aligned} \mathcal{N}_g[\bar{f}(\eta, p), \bar{g}(\eta, p)] &= \frac{\partial^3 \bar{g}}{\partial \eta^3} - \left(\frac{\partial \bar{g}}{\partial \eta} \right)^2 + \{\bar{f}(\eta, p) + \bar{g}(\eta, p)\} \frac{\partial^2 \bar{g}}{\partial \eta^2} \\ &+ K_0 \left[\begin{array}{l} \{\bar{f}(\eta, p) + \bar{g}(\eta, p)\} \bar{g}^{iv}(\eta, p) \\ + \{\bar{f}''(\eta, p) - \bar{g}''(\eta, p)\} \bar{g}''(\eta, p) \\ - 2\{(\bar{f}'(\eta, p) + \bar{g}'(\eta, p)) \bar{g}'''(\eta, p)\} \end{array} \right], \end{aligned} \quad (12.40)$$

$$\begin{aligned} \mathcal{N}_\phi[\bar{f}(\eta; p), \bar{g}(\eta, p), \bar{\phi}(\eta; p), \bar{\theta}(\eta; p)] &= \frac{\partial^2 \bar{\phi}(\eta; p)}{\partial \eta^2} - Sc_\gamma \bar{\phi}(\eta; p) + Sc S_r \frac{\partial^2 \bar{\phi}(\eta, p)}{\partial \eta^2} \\ &+ Sc (\bar{f}(\eta, p) + \bar{g}(\eta, p)) \frac{\partial \bar{\phi}(\eta; p)}{\partial \eta}, \end{aligned} \quad (12.41)$$

$$\begin{aligned} \mathcal{N}_\theta[\bar{f}(\eta; p), \bar{g}(\eta, p), \bar{\phi}(\eta; p), \bar{\theta}(\eta; p)] &= \frac{\partial^2 \bar{\theta}(\eta; p)}{\partial \eta^2} + Pr D_f \frac{\partial^2 \bar{\phi}(\eta, p)}{\partial \eta^2} \\ &+ Pr (\bar{f}(\eta, p) + \bar{g}(\eta, p)) \frac{\partial \bar{\theta}(\eta; p)}{\partial \eta}. \end{aligned} \quad (12.42)$$

In above equations h_f , h_g , h_ϕ and h_θ are the auxiliary non-zero parameters and $p \in [0, 1]$ is an embedding parameter. For $p = 0$ and $p = 1$, we have

$$\bar{f}(\eta, 0) = f_0(\eta), \quad \bar{f}(\eta, 1) = f(\eta), \quad (12.43)$$

$$\bar{g}(\eta, 0) = g_0(\eta), \quad \bar{g}(\eta, 1) = g(\eta). \quad (12.44)$$

$$\bar{\phi}(\eta; 0) = \phi_0(\eta), \quad \bar{\phi}(\eta; 1) = \phi(\eta), \quad (12.45)$$

$$\bar{\theta}(\eta; 0) = \theta_0(\eta), \quad \bar{\theta}(\eta; 1) = \theta(\eta), \quad (12.46)$$

Expanding $\bar{f}(\eta, 0)$, $\bar{g}(\eta, 0)$, $\bar{\phi}(\eta; 0)$ and $\bar{\theta}(\eta; 0)$ in Taylor's theorem with respect to p we have

$$\bar{f}(\eta, p) = f_0(\eta) + \sum_{m=1}^{\infty} f_m(\eta)p^m, \quad (12.47)$$

$$\bar{g}(\eta, p) = g_0(\eta) + \sum_{m=1}^{\infty} g_m(\eta)p^m, \quad (12.48)$$

$$\bar{\phi}(\eta; p) = \phi_0(\eta) + \sum_{m=1}^{\infty} \phi_m(\eta)p^m, \quad (12.49)$$

$$\bar{\theta}(\eta; p) = \theta_0(\eta) + \sum_{m=1}^{\infty} \theta_m(\eta)p^m, \quad (12.50)$$

where

$$f_m(\eta) = \left. \frac{1}{m!} \frac{\partial^m \bar{f}(\eta, p)}{\partial p^m} \right|_{p=0}, \quad g_m(\eta) = \left. \frac{1}{m!} \frac{\partial^m \bar{g}(\eta, p)}{\partial p^m} \right|_{p=0}, \quad (12.51)$$

$$\phi_m(\eta) = \left. \frac{1}{m!} \frac{\partial^m \bar{\phi}(\eta; p)}{\partial p^m} \right|_{p=0}, \quad \theta_m(\eta) = \left. \frac{1}{m!} \frac{\partial^m \bar{\theta}(\eta; p)}{\partial p^m} \right|_{p=0}. \quad (12.52)$$

Note that the convergence of series (12.47) – (12.50) depends upon the auxiliary parameters h_f , h_g , h_ϕ and h_θ . The values of h_f , h_g , h_ϕ and h_θ are chosen in such a way that the series (12.47) – (12.50) converge at $p = 1$. Therefore, Eqs. (12.47) – (12.50) take the form

$$f(\eta) = f_0(\eta) + \sum_{m=1}^{\infty} f_m(\eta), \quad (12.53)$$

$$g(\eta) = g_0(\eta) + \sum_{m=1}^{\infty} g_m(\eta), \quad (12.54)$$

$$\phi(\eta) = \phi_0(\eta) + \sum_{m=1}^{\infty} \phi_m(\eta), \quad (12.55)$$

$$\theta(\eta) = \theta_0(\eta) + \sum_{m=1}^{\infty} \theta_m(\eta). \quad (12.56)$$

12.2.2 m th order deformation problems

The m th order deformation problems are

$$\mathcal{L}_f [f_m(\eta) - \chi_m f_{m-1}(\eta)] = \hbar_f \mathcal{R}_{f,m}(\eta), \quad (12.57)$$

$$\mathcal{L}_g [g_m(\eta) - \chi_m g_{m-1}(\eta)] = \hbar_g \mathcal{R}_{g,m}(\eta), \quad (12.58)$$

$$\mathcal{L}_\phi [\phi_m(\eta) - \chi_m \phi_{m-1}(\eta)] = \hbar_\phi \mathcal{R}_m^\phi(\eta), \quad (12.59)$$

$$\mathcal{L}_\theta [\theta_m(\eta) - \chi_m \theta_{m-1}(\eta)] = \hbar_\theta \mathcal{R}_m^\theta(\eta), \quad (12.60)$$

$$\begin{aligned} f_m(0) = f'_m(0) = f''_m(0) = f'''_m(0) = g_m(0) = g'_m(0) = g''_m(0) = g'''_m(0) = 0, \\ \phi_m(0) = 0, \phi_m(\infty) = 0, \theta_m(0) = 0, \theta_m(\infty) = 0, \end{aligned} \quad (12.61)$$

$$\mathcal{R}_m^f(\eta) = f'''_{m-1} + \sum_{k=0}^{m-1} \left[\begin{aligned} & (f_{m-1-k} + g_{m-1-k}) f''_k - f'_{m-1-k} f'_k \\ & + K_0 \left\{ \begin{aligned} & (f_{m-1-k} + g_{m-1-k}) f_k^{iv} \\ & + (f''_{m-1-k} - g''_{m-1-k}) f''_k \\ & - 2(f'_{m-1-k} + g'_{m-1-k}) f'''_k \end{aligned} \right\} \end{aligned} \right], \quad (12.62)$$

$$\mathcal{R}_m^g(\eta) = g'''_{m-1} + \sum_{k=0}^{m-1} \left[\begin{aligned} & (f_{m-1-k} + g_{m-1-k}) g''_k - g'_{m-1-k} g'_k \\ & + K_0 \left\{ \begin{aligned} & (f_{m-1-k} + g_{m-1-k}) g_k^{iv} \\ & + (f''_{m-1-k} - g''_{m-1-k}) g''_k \\ & - 2(f'_{m-1-k} + g'_{m-1-k}) g'''_k \end{aligned} \right\} \end{aligned} \right], \quad (12.63)$$

$$\mathcal{R}_m^\phi(\eta) = \phi''_{m-1} + Sc \sum_{k=0}^{m-1} [f_{m-1-k} + g_{m-1-k}] \phi'_k - Sc\gamma\phi_{m-1} + ScS_r\theta''_{m-1}, \quad (12.64)$$

$$\mathcal{R}_m^\theta(\eta) = \theta''_{m-1} + Pr \sum_{k=0}^{m-1} [f_{m-1-k} + g_{m-1-k}] \theta'_k + Pr D_f \phi''_{m-1}, \quad (12.65)$$

$$\chi_m = \begin{cases} 0, & m \leq 1 \\ 1, & m > 1 \end{cases}. \quad (12.66)$$

Using MATHEMATICA, it is easy to solve the Eqs. (12.57) – (12.60) one after the other in the order $m = 1, 2, 3, \dots$

12.3 Convergence of the developed solution

The aim of this section is to find the convergent solution. Thus Figs. (12.1) and (12.2) are prepared in order to obtain the admissible values of \hbar_f , \hbar_g , \hbar_ϕ and \hbar_θ for the convergence of the solutions (12.53) – (12.56). The admissible values are $-1.8 \leq (\hbar_f, \hbar_g) \leq -0.4$ and $-1.2 \leq (\hbar_\phi, \hbar_\theta) \leq -0.3$. In Figs. (12.3 – 12.6) the \hbar -curves for the residual errors of f , g , ϕ and θ are plotted in order to get the meaning ranges for \hbar_f , \hbar_g , \hbar_ϕ and \hbar_θ . We analyzed that through proper choice of the values of auxiliary parameters \hbar_f , \hbar_g , \hbar_ϕ and \hbar_θ from this range we will get the correct result upto 6th decimal place. It is observed that $\hbar_f = \hbar_g = \hbar_\phi = \hbar_\theta = -1.0$ give the better solution. Table 12.1 is presented to find that how much order of approximations are necessary for a convergent solution. It is noticed that 15th order approximations are sufficient for the velocity fields whereas 25th order of approximation are required for the concentration and temperature fields. Table 12.2 provides a comparative study for viscous flow. It is found that HAM solution in a limiting case of present study has a good agreement with the exact and HPM solutions provided in ref. [41].

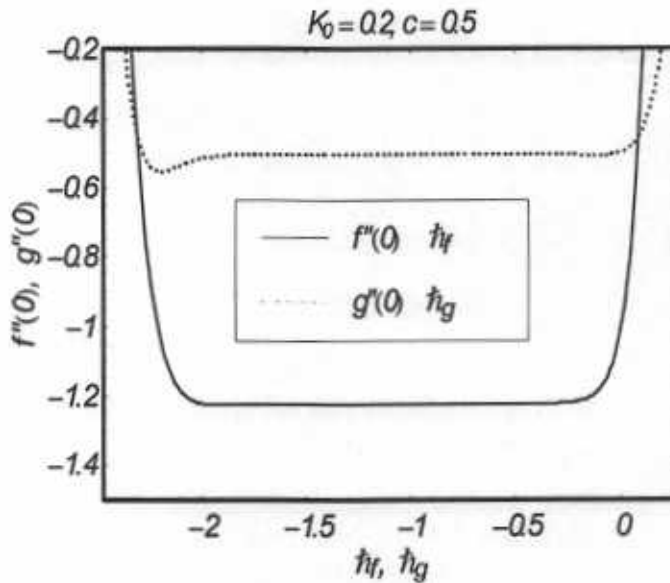


Fig. 12.1 : \hbar curves of $f''(0)$ and $g''(0)$ at the 15th order of approximation.

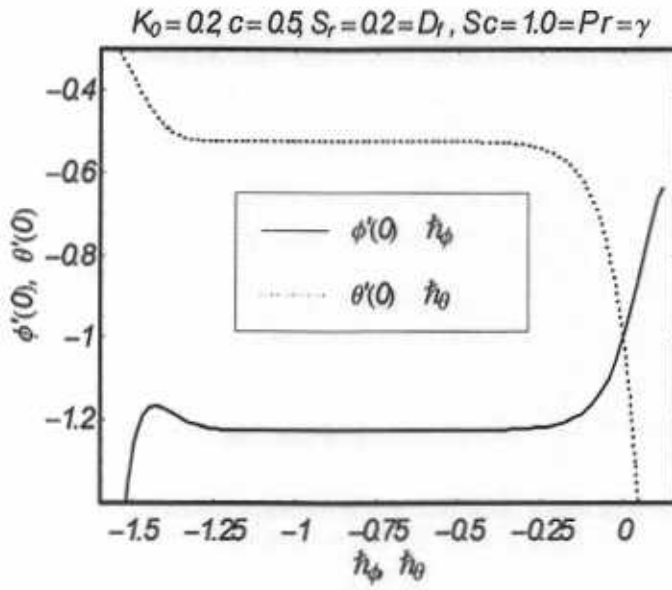


Fig. 12.2 : h curves of $\phi''(0)$ and $\theta''(0)$ at the 15th order of approximation.

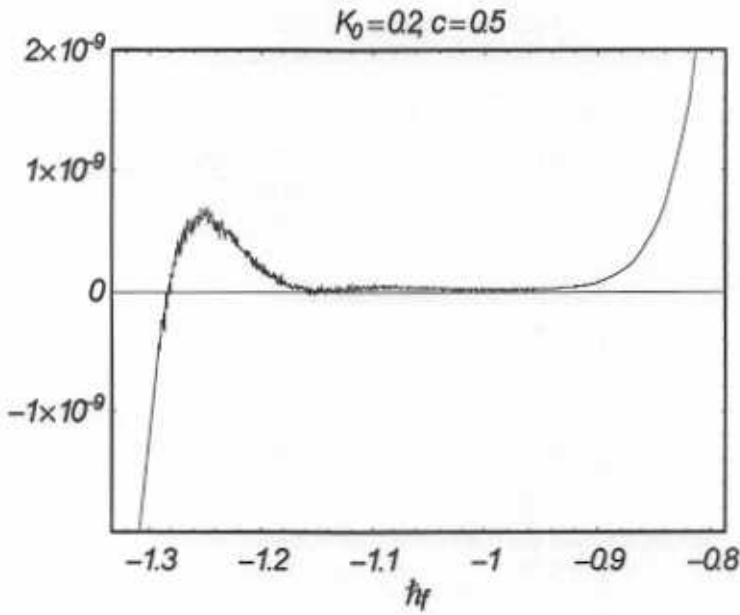


Fig. 12.3 : h curve for residual error in $f(\eta)$ at the 15th order of approximation.

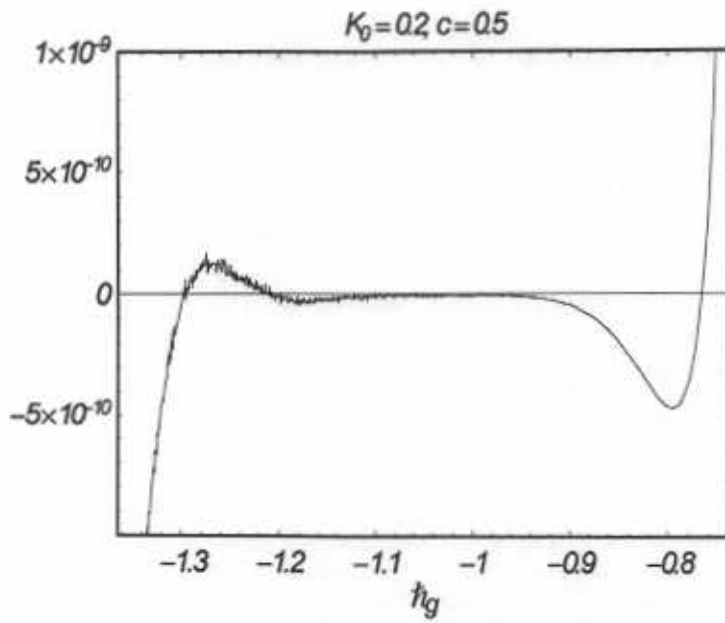


Fig. 12.4 : h curve for residual error in $g(\eta)$ at the 15th order of approximation.

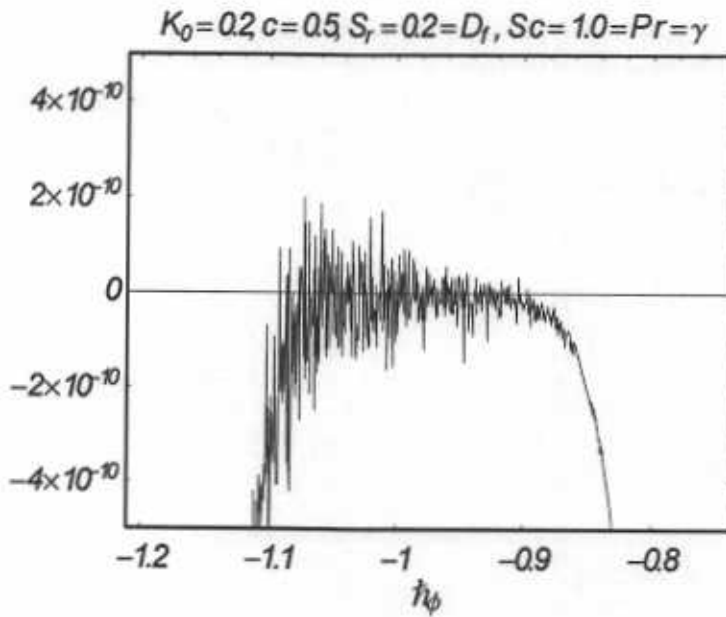


Fig. 12.5 : h curve for residual error in $\phi(\eta)$ at the 15th order of approximation.

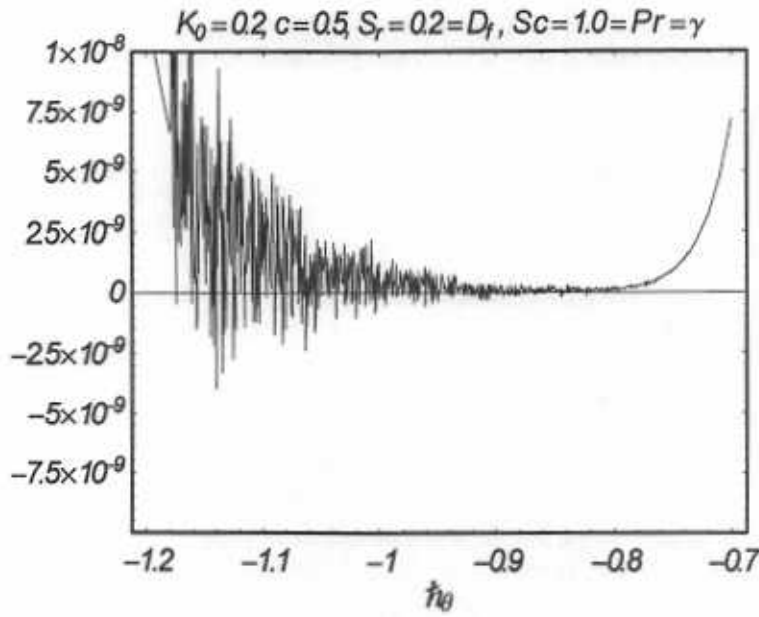


Fig. 12.6 : h curve for residual error in $\theta(\eta)$ at the 15th order of approximation.

Table 12.1: Convergence of the HAM solutions for different order of approximations when $c = 0.5$, $K_0 = 0.1$, $D_f = S_r = 0.2$, $Pr = 1 = Sc = \gamma$.

order of approximation	$-f''(0)$	$-g''(0)$	$-\phi'(0)$	$-\theta'(0)$
1	1.191667	0.512500	1.150000	0.650000
2	1.220035	0.510017	1.222639	0.580972
5	1.222892	0.505508	1.226159	0.527799
10	1.222923	0.505349	1.225311	0.524501
15	1.222923	0.505349	1.225473	0.524381
20	1.222923	0.505349	1.225456	0.524388
25	1.222923	0.505349	1.225458	0.524384
30	1.222923	0.505349	1.225458	0.524384
40	1.222923	0.505349	1.225458	0.524384
50	1.222923	0.505349	1.225458	0.524384

Table 12.2: Illustrating the variation of $-f''(0)$ and $-g''(0)$ with c when $K_0 = 0$ using HAM, HPM (Ariel [41]) and exact solutions (Ariel [41])

c	$-f''(0)$			$-g''(0)$		
	HAM	HPM [41]	Exact [41]	HAM	HPM [41]	Exact [41]
0.0	1	1	1	0	0	0
0.2	1.039495	1.034587	1.039495	0.148736	0.158231	0.148736
0.4	1.075788	1.070529	1.075788	0.349208	0.360599	0.349208
0.6	1.109946	1.106797	1.109946	0.590528	0.600833	0.590528
0.8	1.142488	1.142879	1.142488	0.866682	0.874551	0.866682
1.0	1.173720	1.178511	1.173720	1.173720	1.178511	1.173720

12.4 Results and discussion

In this section the effect of different parameters on velocity, concentration and temperature fields is analyzed. For this purpose Figs 12.7 – 12.16 have been plotted. The variations of K_0 on f' and g' are portrayed in the Figs. 12.7 and 12.8. These Figs. depict that f' , g' and their associated boundary layer are decreasing function of K_0 . The variations of K_0 , Sc , γ , D_f and S_r on the concentration field ϕ are shown in the Figs. 12.9 – 12.13. Fig. 12.9 describes the influence of K_0 on the concentration field ϕ . It is seen that ϕ is an increasing function of K_0 . Fig. 12.10 gives the variation of Schmidt number Sc on ϕ . The concentration field ϕ and concentration boundary layer are decreasing functions of Sc . Figs. 12.11 and 12.12 explain the variations of generative ($\gamma < 0$) and destructive ($\gamma > 0$) chemical reactions on ϕ . It is noticed that ϕ is an increasing function of generative ($\gamma < 0$) chemical reaction whereas ϕ decreases in case of destructive ($\gamma > 0$) chemical reaction. The magnitude of ϕ is larger in case of generative chemical reaction ($\gamma < 0$) when compared with the case of destructive chemical reaction ($\gamma > 0$). Fig. 12.13 discusses the effects of D_f and S_r on ϕ . This Fig. reports that the concentration field increases by increasing the Soret number S_r and decreasing the Dufours number D_f in such a way that their product remains constant. The variations of Pr , K_0 , D_f and S_r on the temperature field θ are shown in the Figs. 12.14 – 12.16. Fig. 12.14 elucidates the variation of Prandtl number Pr on the temperature field θ . Here θ decreases when Pr is increased. It is quite obvious that increasing the Prandtl number Pr corresponds

to the weaker thermal diffusivity and hence the boundary layer decreases. Fig. 12.15 depicts that temperature increases due to increase in K_0 . Since the velocity field decreases due to an increase in viscoelastic parameter which represents that this parameters reduces the molecular movement. Thus due to decrease in molecular movement, the temperature profile decreases. Simultaneous effects of S_r and D_f are portrayed in Fig. 12.16. It is noticed that temperature profile decreases by increasing the Soret number S_r and decreasing the Dufours number D_f by keeping their product constant.

Table 12.3 shows the values of the local Sherwood number $Re_x^{-1/2} Sh$ and the local Nusselt number $Re_x^{-1/2} Nu_x$ for c, K_0, D_f, S_r, Pr, Sc and γ . Here magnitude of local Sherwood number increases for large values of c, D_f, Sc and γ whereas it decreases with an increase in K_0, S_r and Pr . The magnitude of local Nusselt number increases for large values of c, S_r and Pr . Such magnitude decreases for large values of K_0, D_f, Sc and γ .

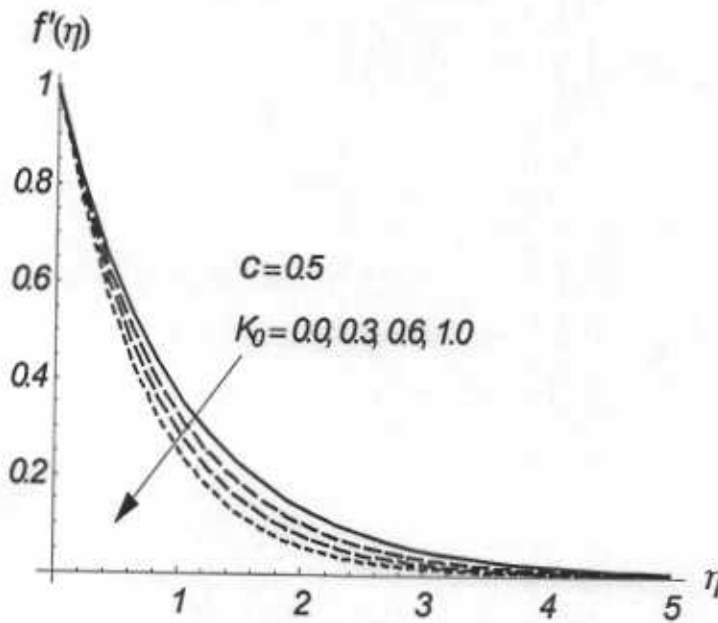


Fig. 12.7 : Influence of K_0 on f' .

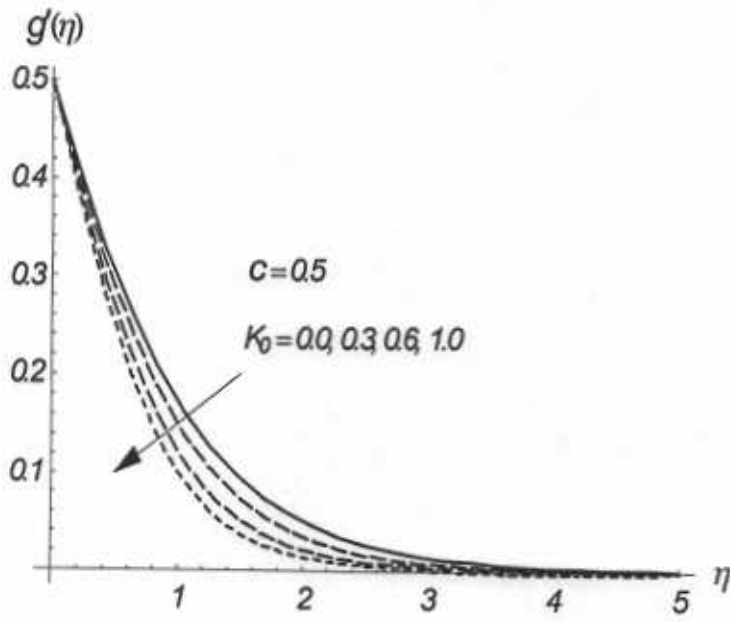


Fig. 12.8 : Influence of K_0 on g' .

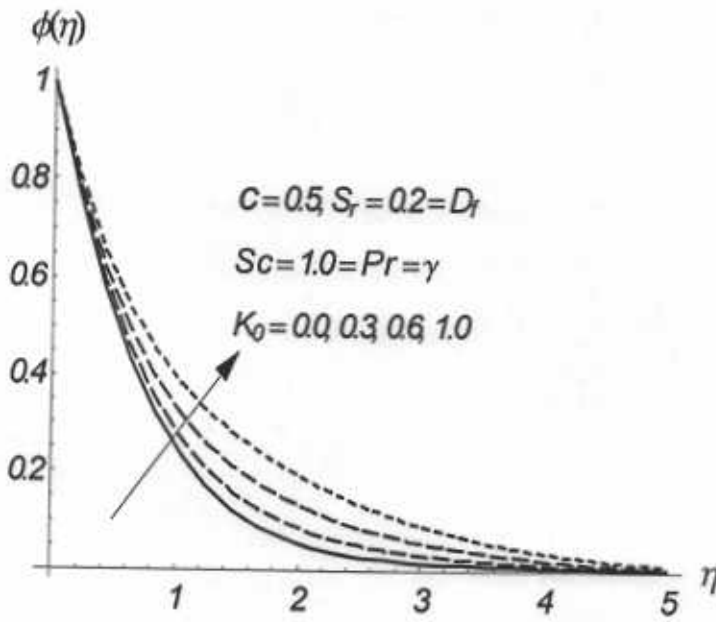


Fig. 12.9 : Influence of K_0 on ϕ .

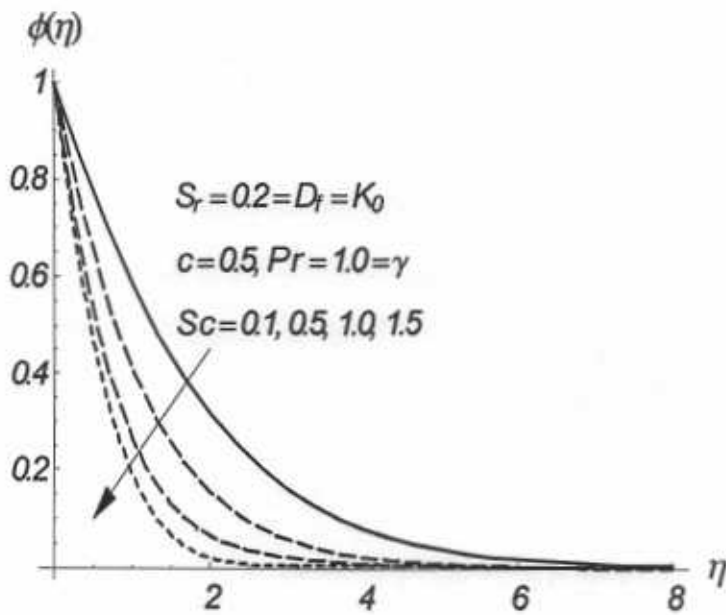


Fig. 12.10 : Influence of Sc on ϕ .

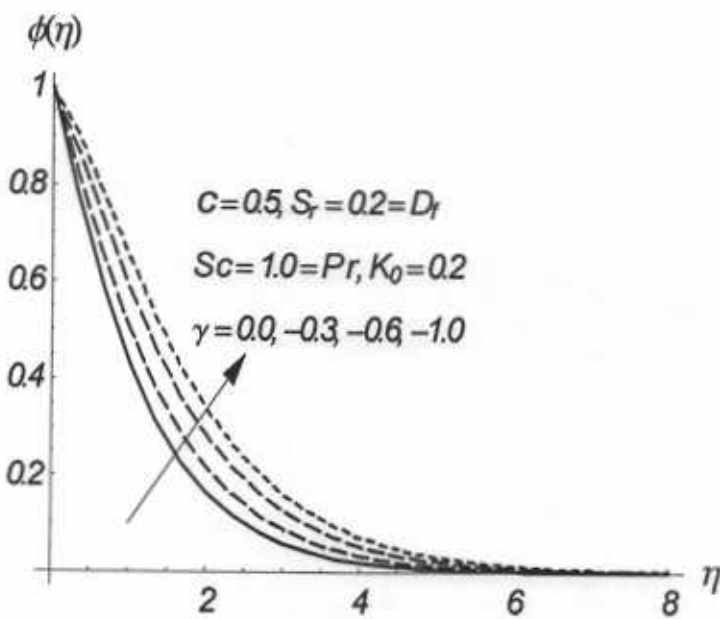


Fig. 12.11 : Influence of $\gamma < 0$ on ϕ .

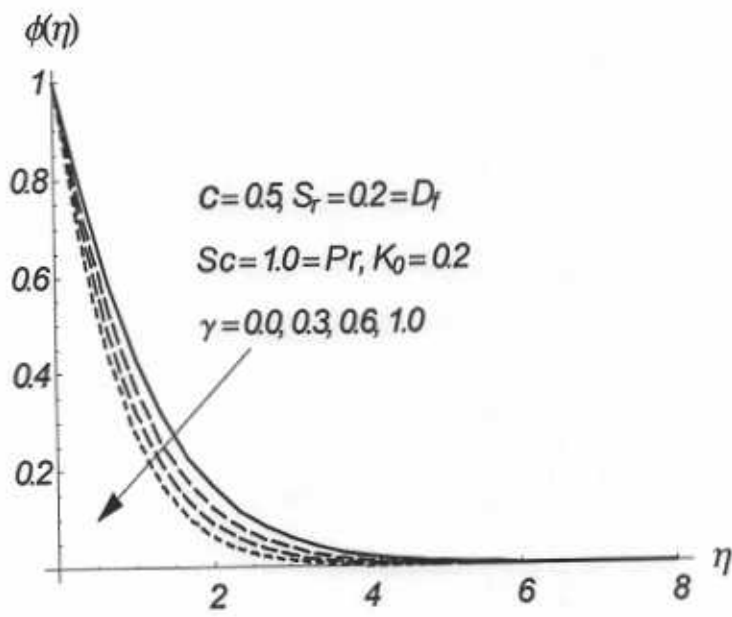


Fig. 12.12 : Influence of $\gamma > 0$ on ϕ .

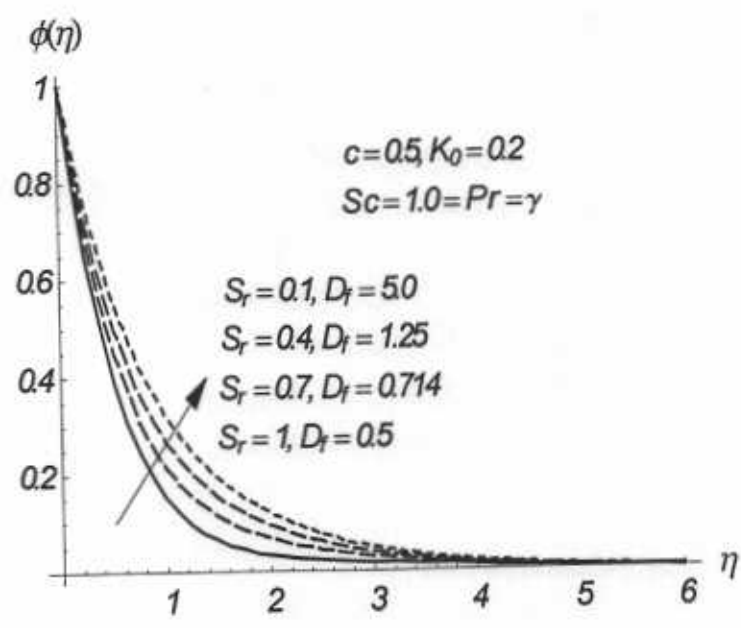


Fig. 12.13 : Influence of S_r and D_f on ϕ .

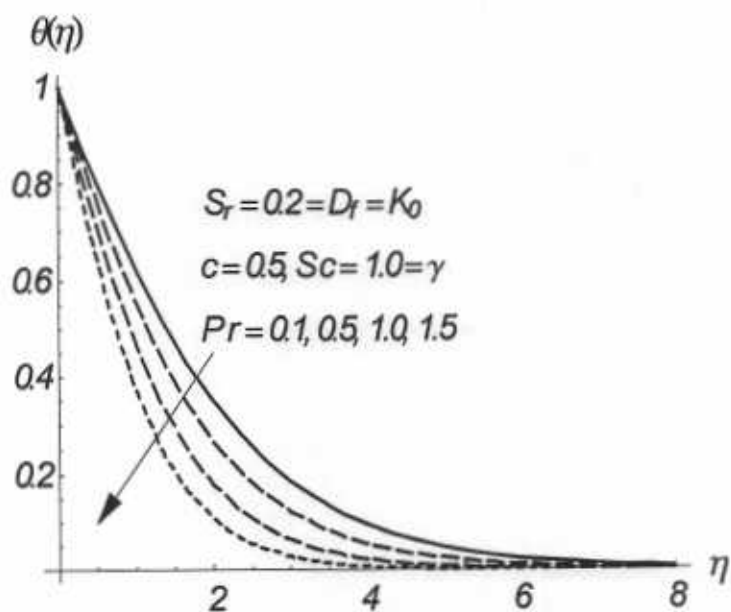


Fig. 12.14 : Influence of Pr on θ .

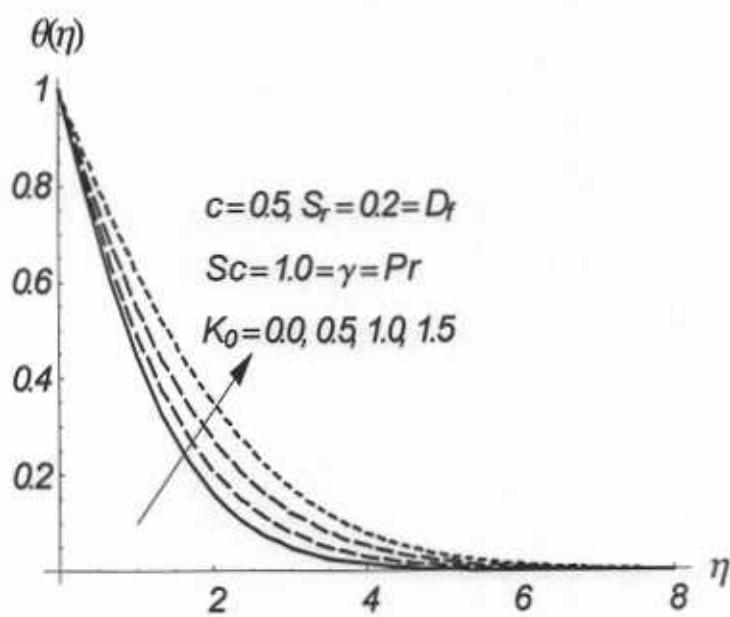


Fig. 12.15 : Influence of K_0 on θ .

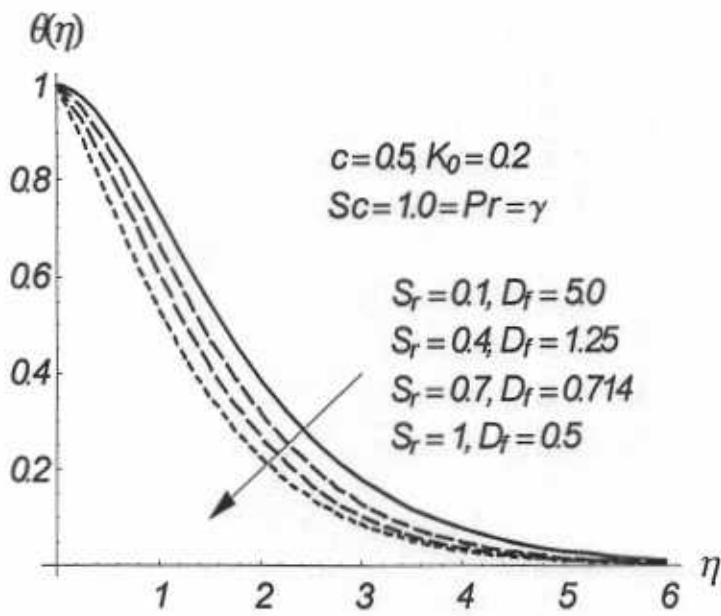


Fig. 12.16 : Influence of S_r and D_f on θ .

Table 12.3: Values of local Sherwood number $Re_x^{-1/2} Sh$ and the local Nusselt number $Re_x^{-1/2} Nu_x$ for some values of c, D_f, S_r, Pr, Sc and γ .

c	K_0	Pr	Sc	γ	D_f	S_r	$-\phi'(0)$	$-\theta'(0)$
0.0	0.1	1.0	1.0	1.0	0.2	0.2	1.164161	0.388584
	0.5						1.225458	0.524384
	1.0						1.275686	0.618866
0.5	0.1						1.231664	0.551137
	0.1						1.225458	0.524384
	0.2						1.217281	0.488017
	0.1	0.1					1.250315	0.144251
		0.7					1.235753	0.413403
		1.5					1.208899	0.674969
		1.0	0.1				0.350485	0.664485
			0.7				1.006065	0.561584
			1.5				1.474819	0.479377
			1.0	0.0			0.626315	0.626315
				0.7			1.083542	0.549192
				1.5			1.429336	0.488321
				1.0	0.1	0.2	1.211815	0.619107
					0.2	0.1	1.238280	0.522684
					0.3	0.07	1.246881	0.426519
					0.2	0.1	1.238280	0.522684
					0.1	0.2	1.211815	0.619107
					0.07	0.3	1.186135	0.648117

12.5 Concluding remarks

The present study describes the Soret and Dufour effects in three-dimensional boundary layer flow of viscoelastic fluid over a stretching surface. The presented analysis shows that solution upto 10th order of approximations is enough for velocity fields whereas solution for concentration

and temperature fields are convergent at 20th order of approximation (Table 12.1). The main observations are listed below.

- Influence of K_0 on velocity fields is qualitatively similar in two-dimensional, three-dimensional and axisymmetric flow cases.
- Influence of K_0 on velocity field is quite opposite to that of concentration field.
- Soret number Sr and Dufour number D_f show opposite behavior for temperature and concentration field
- Variations of Prandtl number Pr on θ and Schmidt number Sc on ϕ are similar
- The concentration field ϕ is opposite for destructive ($\gamma > 0$) and generative ($\gamma < 0$) chemical reactions.

Bibliography

- [1] K. R. Rajagopal, T. Y. Na and A. S. Gupta, Flow of a viscoelastic fluid over a stretching surface, *Rheologica Acta*, 23 (1984) 213 – 215.
- [2] B. Pak, Y. I. Cho and S. U. S. Choi, Separation and reattachment of non-newtonian fluid flows in a sudden expansion pipe *J. Non-Newtonian Fluid Mech.*, 37 (1990) 175 – 199.
- [3] T. J. Lockett, S. M. Richardson and W. J. Worraker, The stability of inelastic non-Newtonian fluids in Couette flow between concentric cylinders: a finite-element study, *J. Non-Newtonian Fluid Mech.*, 43 (1992) 165 – 177.
- [4] G. Pontrelli, Flow of a fluid of second grade over a stretching sheet, *Int. J. Non-Linear Mech.*, 30 (1995) 287 – 293.
- [5] I. A. Hassanien, A. A. Abdullah and R. S. R. Gorla, Flow and heat transfer in a power-law fluid over a nonisothermal stretching sheet, *Math. Comp. Mod.*, 28 (1998) 105 – 116.
- [6] C. Fetecau, The Rayleigh–Stokes problem for an edge in an Oldroyd-B fluid, *Comptes Rendus Mathematique*, 335 (2002) 979 – 984.
- [7] C. Fetecau and C. Fetecau, Decay of a potential vortex in a Maxwell fluid, *Int. J. Non-Linear Mech.*, 38 (2003) 985 – 990.
- [8] C. Fetecau and C. Fetecau, Decay of a potential vortex in an Oldroyd-B fluid, *Int. J. Engng. Sci.*, 43 (2005) 340 – 351.
- [9] C. Fetecau, C. Fetecau, M. Khan and D. Vieru, Decay of a potential vortex in a generalized Oldroyd-B fluid, *Appl. Math. Comp.*, 205 (2008) 497 – 506.

- [10] M. Jamil and C. Fetecau, Some exact solutions for rotating flows of a generalized Burgers' fluid in cylindrical domains, *J. Non-Newtonian Fluid Mech.*, 165 (2010) 1700 – 1712.
- [11] M. Jamil, C. Fetecau and M. Imran, Unsteady helical flows of Oldroyd-B fluids, *Comm. Nonlinear Sci. Numer. Simulat.*, 16 (2011) 1378 – 1386.
- [12] C. Fetecau, M. Nazar and C. Fetecau, Unsteady flow of an Oldroyd-B fluid generated by a constantly accelerating plate between two side walls perpendicular to the plate, *Int. J. Non-Linear Mech.*, 44 (2009) 1039 – 1047.
- [13] W. C. Tan, W. Pan and M. Xu, A note on unsteady flows of a viscoelastic fluid with the fractional Maxwell model between two parallel plates, *Int. J. Non-Linear Mech.*, 38 (2003) 645 – 650.
- [14] W. C. Tan and T. Masuoka, Stokes' first problem for a second grade fluid in a porous half-space with heated boundary, *Int. J. Non-Linear Mech.*, 40 (2005) 515 – 522.
- [15] W. C. Tan and T. Masuoka, Stability analysis of a Maxwell fluid in a porous medium heated from below, *Phys. Lett. A*, 360 (2007) 454 – 460.
- [16] S. Wang and W. C. Tan, Stability analysis of solet-driven double-diffusive convection of Maxwell fluid in a porous medium, *Int. J. Heat Fluid Flow*, 32 (2011) 88 – 94.
- [17] J. Kang, C. Fu and W. C. Tan, Thermal convective instability of viscoelastic fluids in a rotating porous layer heated from below, *J. Non-Newtonian Fluid Mech.*, 166 (2011) 93 – 101.
- [18] K. Vajravelu and D. Rollins, Hydromagnetic flow of a second grade fluid over a stretching sheet, *Appl. Math. Comp.*, 148 (2004) 783 – 791.
- [19] K. Vajravelu, S. Sreenadh and G. V. Reddy, Helical flow of a power-law fluid in a thin annulus with permeable walls, *Int. J. Non-Linear Mech.*, 41 (2006) 761 – 765.
- [20] K. Vajravelu, S. Sreenadh and P. Lakshminarayana, The influence of heat transfer on peristaltic transport of a Jeffrey fluid in a vertical porous stratum, *Comm. Nonlinear Sci. Numer. Simulat.*, 16 (2011) 3107 – 3125.

- [21] K. Vajravelu, S. Sreenadh, K. Rajanikanth and C. Lee, Peristaltic transport of a Williamson fluid in asymmetric channels with permeable walls, *Nonlinear Analysis: Real World Applications*, 13 (2012) 2804 – 2822.
- [22] K. Vajravelu, K. V. Prasad and C. O. Ng, Unsteady flow and heat transfer in a thin film of Ostwald–de Waele liquid over a stretching surface, *Comm. Nonlinear Sci. Numer. Simulat.*, 17 (2012) 4163 – 4173.
- [23] B. Raftari and K. Vajravelu, Homotopy analysis method for MHD viscoelastic fluid flow and heat transfer in a channel with a stretching wall, *Comm. Nonlinear Sci. Numer. Simulat.*, 17 (2012) 4149 – 4162.
- [24] H. Xu and S. J. Liao, Series solutions of unsteady magnetohydrodynamic flows of non-Newtonian fluids caused by an impulsively stretching plate, *J. Non-Newtonian Fluid Mech.*, 129 (2005) 46 – 55.
- [25] C. H. Chen, Effects of magnetic field and suction/injection on convection heat transfer of non-Newtonian power-law fluids past a power-law stretched sheet with surface heat flux, *Int. J. Therm. Sci.*, 47 (2008) 954 – 961.
- [26] T. Hayat, N. Ahmad and N. Ali, Effects of an endoscope and magnetic field on the peristalsis involving Jeffrey fluid, *Comm. Nonlinear Sci. Numer. Simulat.*, 13 (2008) 1581 – 1591.
- [27] T. Hayat and M. Awais, Simultaneous effects of heat and mass transfer on time-dependent flow over a stretching surface, *Int. J. Numer. Meth. Fluids*, 67 (2011) 1341 – 1357.
- [28] T. Hayat, M. Awais, S. Asghar, and S. Obaidat, Unsteady Flow of Third Grade Fluid With Soret and Dufour Effects, *ASME, J. Heat Transfer*, 134 (2012) 062001.
- [29] T. Hayat, M. Awais and A. Alsaedi, Newtonian heating and magnetohydrodynamic effects in flow of a Jeffery fluid over a radially stretching surface, 7 (2012) 2838 – 2844.
- [30] T. Hayat, M. Awais, M. Qasim and A. A. Hendi, Effects of mass transfer on the stagnation point flow of an upper-convected Maxwell (UCM) fluid, *Int. J. Heat Mass Transfer*, 54 (2011) 3777 – 3782.

- [31] R. L. Fosdick and B. Straughan, Catastrophic instabilities and related results in a fluid of third grade, *Int. J. Nonlinear Mech.*, 16 (1981) 191 – 198.
- [32] B. Straughan, Energy stability in the Benard problem for a fluid of second grade, *Z. Angew. Math. Phys.*, 34 (1983) 502 – 509.
- [33] B. Straughan, The backward in time problem for a fluid of third grade, *Ricerche di Matematica*, 36 (1987) 289 – 293.
- [34] B. Straughan, Sharp global nonlinear stability for temperature dependent viscosity convection, *Proc. Roy. Soc. London*, 458 (2002) 1773 – 1782.
- [35] B. Straughan, *Explosive instabilities in mechanisms*, Springer ISBN 3540635890, (1998).
- [36] F. Franchi and B. Straughan, Convection stability and uniqueness for a fluid of third grade, *Int. J. Nonlinear Mech.*, 23 (1988) 377 – 384.
- [37] F. Franchi and B. Straughan, Stability and nonexistence results in the generalized theory of fluid of second grade, *J. Math. Anal. Appl.*, 180 (1993) 122 – 137.
- [38] L. J. Crane, Flow past a stretching plate, *Z. Angew. Math. Phys.* 21 (1970) 645 – 647.
- [39] C. Y. Wang, The three dimensional flow due to a stretching flat surface, *Phys. Fluids*, 27 (1984) 1915 – 1917.
- [40] C. D. S. Devi, H. S. Takhar and G. Nath, Unsteady three-dimensional boundary layer flow due to stretching surface, *Int. J. Heat Mass Transfer*, 29 (1986) 1996 – 1999.
- [41] P. D. Ariel, Three-dimensional flow past a stretching sheet and the homotopy perturbation method, *Comp. Math. App.*, 54 (2007) 920 – 925.
- [42] T. Hayat and T. Javed, On analytic solution for generalized three-dimensional MHD flow over a porous stretching sheet, *Phys. Lett. A*, 370 (2007) 243 – 250.
- [43] K. Singh, Three-dimensional flow of a viscous fluid with heat and mass transfer, *Int. Comm. Heat Mass Transfer*, 32 (2005) 1420 – 1429.

- [44] H. Xu, S. J. Liao and I. Pop, Series solutions of unsteady free convection flow in the stagnation-point region of a three-dimensional body, *Int. J. Therm. Sci.*, 47 (2008) 600 – 608.
- [45] T. Hayat, M. Sajid and I. Pop, Three-dimensional flow over a stretching surface in a viscoelastic fluid, *Nonlinear Analysis: Real World Applications*, 9 (2008) 1811 – 1822.
- [46] T. Hayat, M. Mustafa and M. Sajid, On mass transfer in three-dimensional flow of a viscoelastic fluid, *Numer. Meth. Partial Diff. Eq.*, 27 (2011) 915 – 936.
- [47] K. Ahmad, R. Nazar, A. Ishaq and I. Pop, Unsteady three-dimensional boundary layer flow due to a stretching surface in a micropolar fluid, *Int. J. Numer. Meth. Fluids*, 68 (2012) 1561 – 1573.
- [48] T. Hayat, M. Qasim and Z. Abbas, Homotopy solution for the unsteady three-dimensional MHD flow and mass transfer in a porous space, *Comm. Nonlinear Sci. Numer. Simulat.*, 15 (2010) 2375 – 2387.
- [49] A. K. Borkakoti and A. Bharali, Hydromagnetic flow and heat transfer between two horizontal plates, *Quart. Appl. Math.*, 41 (1983) 461 – 467.
- [50] K. Vajravelu and B. V. R. Kumar, Analytical and numerical solutions of a coupled nonlinear system arising in a three-dimensional rotating flow, *Int. J. Nonlinear Mech.*, 39 (2004) 13 – 24.
- [51] T. Hayat, Z. Abbas, T. Javed and M. Sajid, Three-dimensional rotating flow induced by a shrinking sheet for suction, *Chaos, Solitons & Fractals*, 39 (2009) 1615 – 1626.
- [52] A. Mehmood and A. Ali, Analytic homotopy solution of generalized three-dimensional channel flow due to uniform stretching of the plate, *Acta Mechanica Sinica*, 23 (2007) 503 – 510.
- [53] G. Domairry and A. Aziz, Approximate analysis of MHD squeeze flow between two parallel disks with suction or injection by homotopy perturbation method, *Math. Prob. Eng.* doi: 10.1155/2009/603916.

- [54] J. C. Misra, G. C. Shit and H. J. Rath, Flow and heat transfer of a MHD viscoelastic fluid in a channel with stretching walls: Some applications to haemodynamics, *Computers Fluids*, 37 (2008) 1 – 11.
- [55] T. Hayat, S. Irum, T. Javed and S. Asghar, An analytic solution for shrinking flow of second grade fluid in a rotating frame, *Comm. Nonlinear Sci. Numer. Simulat.*, 15 (2010) 2932 – 2941.
- [56] A. Mehmood and A. Ali, Heat transfer analysis of three-dimensional flow in a channel of lower stretching wall, *J. Taiwan Institute Chemical Engineers*, 41 (2010) 29 – 34.
- [57] S. Munawar, A. Mehmood and A. Ali, Three-dimensional squeezing flow in a rotating channel of lower stretching porous wall, *Comp. Math. Appl.*, In Press, 2012.
- [58] A. Qayyum, M. Awais, A. Alsaedi and T. Hayat, Unsteady squeezing flow of Jeffery fluid between two parallel disks, *Chin. Phys. Lett.*, 26 (2012) 034701.
- [59] M. Mustafa, T. Hayat and S. Obaidat, On heat and mass transfer in the unsteady squeezing flow between parallel disks, *Meccanica*, DOI: 10.1007/s11012-012-9536-3.
- [60] T. Hayat, M. Awais and A. A. Hendi, Three-dimensional rotating flow between two porous walls with slip and heat transfer, *Int. Comm. Heat Mass Transfer*, 39 (2012) 551 – 555.
- [61] S. J. Liao, *Beyond Perturbation, Introduction to Homotopy Analysis Method*, Chapman & Hall/CRC Press, Boca Raton (2003).
- [62] S. J. Liao, Notes on the homotopy analysis method: Some definitions and theorems, *Comm. Nonlinear Sci. Numer. Simulat.*, 14 (2009) 983 – 997.
- [63] J. Cheng, S. J. Liao, R. N. Mohapatra and K. Vajravelu, Series solutions of nano boundary layer flows by means of the homotopy analysis method, *J. Math. Anal. Appl.*, 343 (2008) 233 – 245.
- [64] N. Konsar and S. J. Liao, Unsteady non-similarity boundary layer flows caused by an impulsively stretching flat sheet, *NonLinear Analysis: Real World Applications*, 12 (2011) 333 – 342.

- [65] R. A. V. Gorder and K. Vajravelu, On the selection of auxiliary functions, operators, and convergence control parameters in the application of the Homotopy Analysis Method to nonlinear differential equations: A general approach, *Comm. Nonlinear Sci. Numer. Simulat.*, 14 (2009) 4078 – 4089.
- [66] Y. Tan and S. Abbasbandy, Homotopy analysis method for quadratic Riccati differential equation, *Comm. Nonlinear Sci. Numer. Simulat.*, 13 (2008) 539 – 546.
- [67] S. Abbasbandy, Soliton solutions for the Fitzhugh–Nagumo equation with the homotopy analysis method, *Appl. Math. Mod.*, 32 (2008) 2706 – 2714.
- [68] S. Abbasbandy and T. Hayat, Solution of the MHD Falkner–Skan flow by homotopy analysis method, *Comm. Nonlinear Sci. Numer. Simulat.*, 14 (2009) 3591 – 3598.
- [69] S. Abbasbandy, Homotopy analysis method for the Kawahara equation, *Nonlinear Analysis: Real World Applications*, 11 (2010) 307 – 312.
- [70] S. Abbasbandy and A. Shirzadi, A new application of the homotopy analysis method: Solving the Sturm–Liouville problems, *Comm. Nonlinear Sci. Numer. Simulat.*, 16 (2011) 112 – 126.
- [71] M. M. Rashidi, G. Domairry and S. Dinarvand, Approximate solutions for the Burger and regularized long wave equations by means of the homotopy analysis method, *Comm. Nonlinear Sci. Numer. Simulat.*, 14 (2009) 708 – 717.
- [72] M. M. Rashidi and S. Dinarvand, Purely analytic approximate solutions for steady three-dimensional problem of condensation film on inclined rotating disk by homotopy analysis method, *Nonlinear Analysis: Real World Applications*, 10 (2009) 2346 – 2356.
- [73] S. Dinarvand and M. M. Rashidi, A reliable treatment of a homotopy analysis method for two-dimensional viscous flow in a rectangular domain bounded by two moving porous walls, *Nonlinear Analysis: Real World Applications*, 11 (2010) 1502 – 1512.
- [74] M. M. Rashidi and S. A. M. Pour, Analytic approximate solutions for unsteady boundary-layer flow and heat transfer due to a stretching sheet by homotopy analysis method, *Nonlinear Analysis: Modelling and Control*, 15 (2010) 83 – 95.

- [75] A. A. Joneidi, G. Domairry and M. Babaelahi, Homotopy Analysis Method to Walter's B fluid in a vertical channel with porous wall, *Meccanica*, 45 (2010) 857 – 868.
- [76] B. Yao and J. Chen, Series solution to the Falkner–Skan equation with stretching boundary, *Appl. Math. Comp.*, 208 (2009) 156 – 164.
- [77] A. S. Bataineh, M. S. M. Noorani and I. Hashim, Approximate analytical solutions of systems of PDEs by homotopy analysis method, *Comp. Math. Appl.* 55 (2008) 2913 – 2923.
- [78] T. Hayat, M. Awais and M. Sajid, Mass transfer effects on the unsteady flow of UCM fluid over a stretching sheet, *Int. J. Modern Physics-B*, 25 (2011) 2863 – 2878.
- [79] T. Hayat, M. Mustafa and S. Obaidat, Soret and Dufour effects on the stagnation-point flow of a micropolar fluid toward a stretching sheet, *ASME J. Fluid Engng.* 133 (2011) 021202.
- [80] S. Nadeem, M. Hussain and M. Naz, MHD stagnation flow of a micropolar fluid through a porous medium, *Meccanica*, 45 (2010) 869 – 880.
- [81] T. Hayat and M. Awais, Three-dimensional flow of an upper-convected Maxwell (UCM) fluid, *Int. J. Numer. Meth. Fluid*, 66 (2011) 875 – 884.
- [82] T. Hayat, M. Mustafa and A. A. hendi, Time-dependent three-dimensional flow and mass transfer of elastico-viscous fluid over unsteady stretching surface, *Appl. Math. Mech.*, 32 (2011) 167 – 178.
- [83] N. Bachok, A. Ishak and I. Pop, Unsteady three-dimensional boundary layer flow due to a permeable shrinking surface, *Appl. Math. Mech.*, 31 (2010) 1421 – 1428.
- [84] J. Harris, *Rheology and non-Newtonian flow*, Longman Inc., New York, 1977.